SHORT AND LONG-TERM PERFORMANCE OF ECO-EFFICIENT CONCRETE MIXTURES

Mayra Tagliaferri de Grazia

Thesis submitted to the University of Ottawa

in partial Fulfillment of the requirements for the

Doctor of Philosophy

Department of Civil Engineering

Faculty of Engineering
University of Ottawa

Abstract

Concrete is the most widely used construction material worldwide, yet, it presents major sustainability drawbacks due to the CO_2 released during the manufacturing of its main constituent, cement. Several approaches are used to improve concrete's eco-efficiency and reduce the binder intensity index, a metric used to measure the eco-efficiency of concrete, to a value below that of conventional concrete mixtures (i.e., 10 $kg/m^3.MPa^{-1}$ for 25-40 MPa mixtures). Particle Packing Models (PPM) is consequently an approach that can be used to enhance system packing density, reducing cement content while increasing hardened state properties and durability (i.e., reducing porosity). However, packed mixtures normally present issues in the fresh state while their hardened state performance is not fully comprehended. Therefore, this Ph.D. project proposes a new mix-design method called PPM-MP approach to develop eco-efficient mixtures. First, a detailed laboratory investigation was conducted on mixtures developed using the proposed approach in order to understand their fresh and hardened state performance. Concrete samples containing distinct ranges of cement content (320, 250, 200, 150 kg/m^3) and slump (180, 90, and 20 +/- 20 mm) were fabricated and a wide range of fresh state tests (pH, temperature, fresh density, air content, slump and rheology over time) and hardened state tests (apparent porosity, surface electrical resistivity, compressive strength, and modulus of elasticity) were performed over time. Then, its performance against the alkali-silica reaction (ASR) induced expansion and deterioration, which is one of the leading and most damaging distress mechanisms issues in durability, was evaluated. In this section of the project, four sustainable concrete mixtures developed with varying cement content (e.g., 325, 250, 200, and 150 kg/m^3) were developed and compared to a control mixture containing 420 kg/m^3 of cement content. The mixtures were tested over a year under Concrete prism test (CPT) setup, which is the current method used to evaluate concrete ASR and using three different non-boosted

test setups (i.e., Wrapped - W, Soaked - S, and Encapsulated - E). Moreover, two distinct types of highly reactive aggregates (e.g., Springhill Greywacke coarse aggregate and Texas Polymictic sand) were selected. Microscopic analysis was used to better understand the impact of ASR on sustainable mixtures, as well as the differences in ASR-damage and crack propagation under different test protocols. The results show the feasibility of producing an eco-efficient mixture in a more efficient manner which may contribute to the Net Zero Concrete targets. The proposed PPM-MP approach improves the sustainability of concrete mixtures and can be used for specific projects requiring 28-day compressive strength ranging from 18 to 45 MPa and slumps (180, 90, and 20 +/- 20 mm).

Keywords: *Eco-efficient concrete, rheology, low cement content, particle packing models, mobility parameters, durability and long-term performance, alkali-aggregate reaction (ASR), laboratory test methods, microscopic characterization, crack propagation, damage rating index (DRI).*

This thesis is dedicated to Gustavo Adami, my husband, for supporting me throughout this journey. My love thanks for your patience.

"*If you don't make mistakes, you're not working on hard enough problems. And that's a mistake.*"

— Frank Wilczek

Acknowledgements

First, I would like to express my gratitude to my husband, Gustavo Adami, for believing in my strength since the beginning of this journey, for your endless help, for your continuous support, for working with me on my schedules, and for taking care of our family daily. It is an honour to have you in my life.

The support of my parents, Adalberto and Silvia, and my sister Thays, for being my guide even far from home and for all their sacrifices. To my father for making me passionate about engineering, for teaching me how to become a hard worker and for supporting me to pursue my dreams regardless of distance. My mother for all the years she worked hard to encourage me to reach my full potential. My sister for being my role model and my inspiration.

To Dr. Leandro Sanchez, who led me on distinct opportunities that allow me to learn several skills for my career and life and for sharing his passion for concrete technology. Thank you for giving me the opportunity to continue studying the feasibility of producing eco-efficient concrete mixtures and I hope we can see the industry using PPM with a high amount of limestone fillers. I would also like to thank Dr. Ammar Yahia for his guidance and amazing contributions to this research. To the members of my dissertation committee, Dr. Aali R. Alizadeh Dr. Beatriz Martin-Perez, Dr. Douglas Hooton, and Dr. Reza Fathifazl, for kindly offering their time to improve this research.

I would like to acknowledge and express my deepest appreciation to the lab technician at University of Ottawa, Muslim Majeed, who waited for me several times before closing the lab, and Gamal Elnabelsy for all the morning talks and inspiration, I am very thankful for all lessons and your support during my Master and Ph.D.

To my µStructure colleagues and friends who contributed to the Ph.D. experience, help with daily tasks and sieved ten tons of aggregates, shared their experience, and provided me with amazing concrete batching days, I will definitely miss it. Special thanks to Derick Asirvatham for all our brainstorming sessions, lab activities and wonderful batching days of 8+ hours, really miss these good times working together. To Gonzalo Lozano, Hian Freitas, and Hugo Deda for the great discussions and teamwork experience. Special thanks to Cassandra Trottier for all the inspirations and great work collaborations, for sharing her working ethics, and for setting amazing standards in our research group, you are my example as a woman in engineering, it was a privilege to learn and

work with you; I am really proud of our accomplishments to date and I am looking forward for the future.

To Marilia Salustiano, Gabriela Puente, Caroline Chagas, Isabela Papalardo and my friends who were essential for my creative idleness and especially for all the support during COVID-19 pandemic.

To Corey Guertin-Normoyle who believed in my potential from the application to the Vanier scholarship until the completion of this project, it is a privilege to work with you. Tamisa Santos, who was also one of the references on my Vanier scholarship application and who provided me with unconditional support throughout my Ph.D., I am also thanked for her assistance with AutoCAD and 3D images during my Master's and Ph.D. To Gisela Hernandes Gomes, my undergraduate professor, whose passion for research and teaching inspired me to follow in her footsteps and pursue a career in academia, thank you for your encouragement and support in pursuing my Master's and Ph.D. in Canada, as well as your assistance with scholarship applications. Special thanks to Ana Milena Rebellon (Lehigh Hanson Inc.) for all the great shared experiences about concrete eco-efficiency and GWP.

I would like to extremely thank Natural Sciences and Engineering Research Council of Canada (NSERC) for the funding they provided through the prestigious Vanier CGS scholarship and Ontario Student Assistance Program for the Ontario Graduate Scholarship (OGS).

Last, I want to express my gratitude to God for giving me the chance to finish my Ph.D. in Civil Engineering at the University of Ottawa, especially during the COVID-19.

Table of Contents

List of Tables

List of Figures

List of Symbols/Abbreviations

ΔP	Pressure Variation
μ	Fluid Viscosity
ACI	American Concrete Institute
a_i	Apparent Volume of the i^{th} Size Particle in a Monodisperse System
AP	Apparent Porosity
ASR	Alkali Silica Reaction
AV	Apparent Viscosity
BC	Binder Content
bi	Binder Intensity
c	Coarse
ci_{cs}	CO_2 Intensity Index
C_2S	Dicalcium Silicate
C_3A	Tricalcium Aluminate
$CaCO_3$	Limestone
CaO	Lime
CO_2	Carbon Dioxide
CPFT	Cumulative (Volume) Percent Finer Than D_p
C-S-H	Calcium Silicate Hydrate
D_L	Larger Particle Diameter
D_{max}	Maximum Aggregate Size
D_{min}	Minimum Aggregate Size
D_P	Particle Diameter
D_S	Smallest Particle Diameter
f	Fines
f'_c	Concrete Compressive Strength
f_r	Relationship between Compressive Strength and Cement Content
g	Aggregate Volume in a Unit Volume of Concrete
g*	Packing Density of the Aggregate
H_2O	Water Vapour
HA	Hysteresis Area
He	Helium Gas
HRWRA	High-Range Water-Reducing Admixtures
IF	Inert Fillers
IPS	*Interparticle Spacing*
k_1	Darcian Permeability Constant
K_1, K_2, K_3, K_4, K_5, K_6	Empirical Constants
k_2	non-Darcian Permeability Constant
k_B	Viscosity Constant of Bingham
k_{HB}	Viscosity Constant of Herschel-Bulkley
L	Specimen Thickness
LCC	Low Cement Content
m	Aggregate to Cement Ratio
MCO	Mortar Content Optimization

m_d	Dry Mass
m_i	Immersed Mass
MPT	*Maximum Paste Thickness*
MPT_{coarse}	Maximum Distance between the Coarse Aggregates
m_w	Wet Mass
n	Number of Particle Sizes
n	Flow Behaviour Factor
N_2	Nitrogen Gas
NMS	Nominal Maximum Size
$Ø_p$	Packing Density
$Ø_{p1}$	Packing Density of Large Particles
$Ø_{p2}$	Packing Density of Small Particles
P	Performance Requirement
PC	Portland Cement
PF	Packing Factor
P_{of}	Pore Fraction
P_{ofc}	Pore of Aggregate Fraction Assuming the Densest Packing
PPMs	Particle Packing Models
PSD	Particle Size Distribution
PUNDIT	Portable Ultrasound Non-Destructive Digital Indicating Tester
q	Distribution Coefficient
SCC	Self-Consolidating Concrete
SCMs	Supplementary Cementitious Materials
SSA	Specific Surface Area
TP	Total Porosity
UPV	Ultrasonic Pulse Velocity
V_1	Fraction of Small Particles Solid Volume
V_2	Fraction of Large Particles Solid Volume
V_a	Apparent Volume
V_{ai}	Apparent Volume of the Mixture with n Particle Sizes
v_s	Speed of Air-Percolation
Vs	Volume Fraction Solids
VSA	Volume Surface Area
VSA_c	Calculated Volume Surface Area of Aggregate Fraction
V_{sc}	Volumetric Aggregate Solid Fraction
V_{solid}	Solid Volume
V_{total}	Total Volume (Solids and Pores)
w/c	Water to Cement Ratio
w/f	Water to Fines Ratio
x_i	Mass Fraction of i^{th} Size Particle
γ	Rotation
ρ	Fluid Density
ρ_{rel}	Relative Density
τ	Torque
τ_o	Yield Torque
ρ_{part}	Particle Density

Foreword

This Ph.D. thesis presents the findings and analysis of an extensive investigation conducted by the author in the laboratory. The primary goal of this thesis is to assist the progress towards sustainable concrete production by providing tools to aid in the design and mix-proportioning of eco-efficient concrete on a performance-basis. The outcomes demonstrate the feasibility of producing a more eco-efficient mixture contributing to the Net Zero Concrete targets, while maintaining the required performance in the fresh and hardened states as well as their durability aspects.

This thesis is divided into a number of chapters, including five scientific papers covering distinct but complementary topics to assist in the overall understanding of the need to consider sustainability and amount of cement as a design parameter when developing concrete. It consists of a paper-based Ph.D. thesis in which Chapter One highlights the importance of the development of eco-efficient concrete mixtures to reduce carbon footprint emitted during concrete production, the research objectives, and a explanation of the scientific papers. Chapter Two provides a detailed review of the literature on producing eco-efficient concrete using particle packing models, as well as the importance of using mobility parameters to better understand their fresh state behaviour. The importance of durability and long-term performance, especially against Alkali-Silica Reaction - ASR), of eco-friendly concrete will be discussed as proof of their ability to be an alternative for the construction industry. Then, Chapter Three presents the main experimental programme. In Chapters Four through Eight, the scientific papers are presented. Finally, presentation of the future works and recommendations are presented in Chapter Nine and Ten.

Chapter One: Introduction

1.1 Synopsis

Concrete environmental impact has risen concerns over the past decades. Concrete production is responsible for more than 7% of global carbon dioxide (CO_2) emissions, wherein more than 92% is emitted during ordinary Portland cement (OPC) production [1–4]. The increased development of cities and infrastructure resulted in substantial growth of concrete, and thus in OPC demand. In 2012, the global industry produced approximately 3.8 billion tons of OPC, but after only six years, the production has raised to 300 million tons [5,6]. Although standards are pressing several industries to reduce CO_2 emissions, forecasts indicate that global cement demand will continue to grow considerably in the next years. Moreover, the countries that are considered the largest global cement producers coincide with major global CO_2 emitters [7,8], highlighting the need to produce eco-efficient concrete mixtures. In general, one ton of OPC produces approximately one ton of CO_2 [9–11], hence, one of the best methods to improve concrete eco-efficiency is through reducing OPC content. The three main approaches presented in the literature to reduce the carbon footprint of concrete are shown hereafter: 1) enhancement of OPC production; 2) reducing OPC content in concrete mixtures by using SCMs (Supplementary Cementitious Materials) and/or limestone fillers (LF) as a partial replacement; and 3) optimizing OPC efficiency in concrete mixtures through the use of advanced mix-design techniques (e.g. particle packing models – PPMs and/or mobility parameters – MP) [12–14]. The former approach is presented by distinct studies in which enhancement of production processes and also thermal energy efficiency are investigated to reduce the CO_2 emitted during cement production [2,3,13,15]. In terms of civil engineering, the use of eco-friendly materials (approach 2) with PPMs (approach 3) are the main methods available to produce

a more sustainable concrete mixture. SCMs are considered outstanding OPC replacements since they often improve concrete performance, durability, and sustainability; however, their availability does not increase at the same rate as OPC demand [12]. Moreover, previous studies show that the combination of PPMs and limestone fillers can result in a cement reduction of more than 50% [14,16,17]. However, conventional concrete mixtures, which account for 90% of global production, are manufactured with more than 350 kg/m^3 of OPC to achieve a compressive strength between 25 and 35 MPa [18]. Although it is well understood that OPC is responsible for the formation of calcium silicate hydrate (C-S-H) and thus the strength of concrete mixtures, there is a widespread misconception in the concrete industry that associates the amount of OPC with concrete strength. Damineli et al. [19] proposed a binder intensity (bi) index to correlate the amount of OPC required to develop one unit of concrete property, for instance, the compressive strength. This study demonstrated that conventional concrete mixtures (i.e., 20-40 MPa) are often designed with moderate to high OPC contents, requiring further eco-efficiency improvement. The vast majority of concrete produced worldwide contains OPC contents ranging from 350 to 500 kg/m³ [19], which agrees with the ACI 302 [20] recommendation of a minimum of 335 kg/m³ for de-icer exposures. Additionally, only 2% of the concrete mixtures commonly used worldwide present OPC contents equal to or lower than 250 kg/m³ of concrete [19]. The above strategies to reduce cement content are widely known, yet eco-efficient concrete is currently not used for important structural applications due to several concerns about the selection of the w/c, the prediction of the slump and compressive strength. Besides the short-term performance, the durability aspects of these concrete mixtures must also be evaluated. Yet very few data are available enveloping mix-design methods to produce eco-efficient materials while accounting for their durability.

1.2 Research objectives

The main objectives of this project are:

- Develop conventional eco-efficient (i.e., < 45 MPa) concrete mixtures using the proposed PPM-MP approach and incorporating limestone fillers, which can be used as a performance-based design method accounting for concrete eco-efficiency while maintaining the main fresh and hardened state performance, such as slump and compressive strength. In this context, this work was focused on short-term performance assessment that can be divided into fresh and hardened state properties. The fresh properties included slump, rheology, temperature, pH, and air content, whereas the hardened properties were assessed through compressive strength, porosity, electrical resistivity, and modulus of elasticity.
- Evaluate the long-term performance (i.e., durability aspects) of low cement/ low alkali mixtures developed through PPM-MP approach against one of the most harmful deterioration mechanisms affecting critical concrete infrastructure in Canada and worldwide: alkali-silica reaction (ASR). The mixtures incorporate highly reactive aggregates and specimens are exposed to accelerated standardized CPT procedure to evaluate the induced expansion, crack development and features of these mixtures. Additionally, the efficacy of three different laboratory test setups (i.e., wrapped – W, soaked – S, and encapsulated – E) without the addition of alkalis into the concrete mixtures to evaluate ASR-development of low alkali systems in comparison to the standardized CPT procedure (i.e., with the addition of alkalis to the concrete mixture) was also investigated. Microscopic tests were performed to evaluate the influence of the alkali boost on the ASR-kinetics and distress features.

1.3 Core of the Ph.D. Thesis – Scientific Papers

This thesis is considered a starting point towards the production of eco-efficient concrete mixtures, developed with low cement content through the PPM-MP approach. The research presents a general overview of distinct eco-efficient mixtures and their performance in the fresh and hardened state as well as their durability aspects, specially alkali aggregate reaction. Figure 4.1 presents a summary of the Ph.D. thesis structure with the scientific rationale of each paper developed. Paper I was developed to further understand the concrete industry's main sustainability challenges, particularly those related to CO_2 emissions from cement content and the options for achieving Concrete Net Zero by 2050. Moreover, the literature shows distinct Particle Packing Models (PPMs) that can be applied to reduce cement content, and thus increase the sustainability of concrete. However, due to a lack of procedures on how to mix-proportion an eco-friendly concrete with the required fresh and hardened state properties, eco-efficient concrete is currently not used for important structural applications. To address the gaps presented, the scientific papers Paper II and III propose a new mix-design approach named the PPM-MP model and investigate the short-term performance of sustainable mixtures. Charts and models are also included to assist with the selection of the water-to-cement ratio (w/c) for the required compressive strength and slump, as well as to assist in understanding the compressive strength development of the designed concrete. Additionally, sustainability indicators, such as Global Warming Potential (GWP), CO_2 intensity index, and binder intensity index are presented to assist in determining the level of sustainability of the concrete designed. Finally, to start understanding the advantages and disadvantages of the long-term performance of sustainable concrete, Papers IV and V are developed appraising their performance against one of the most harmful deterioration mechanisms: alkali-silica reaction (ASR). Paper IV

evaluates low cement/alkali concrete affected by ASR using the standardized CPT protocol, whereas Paper V compares it to advanced ASR test methods.

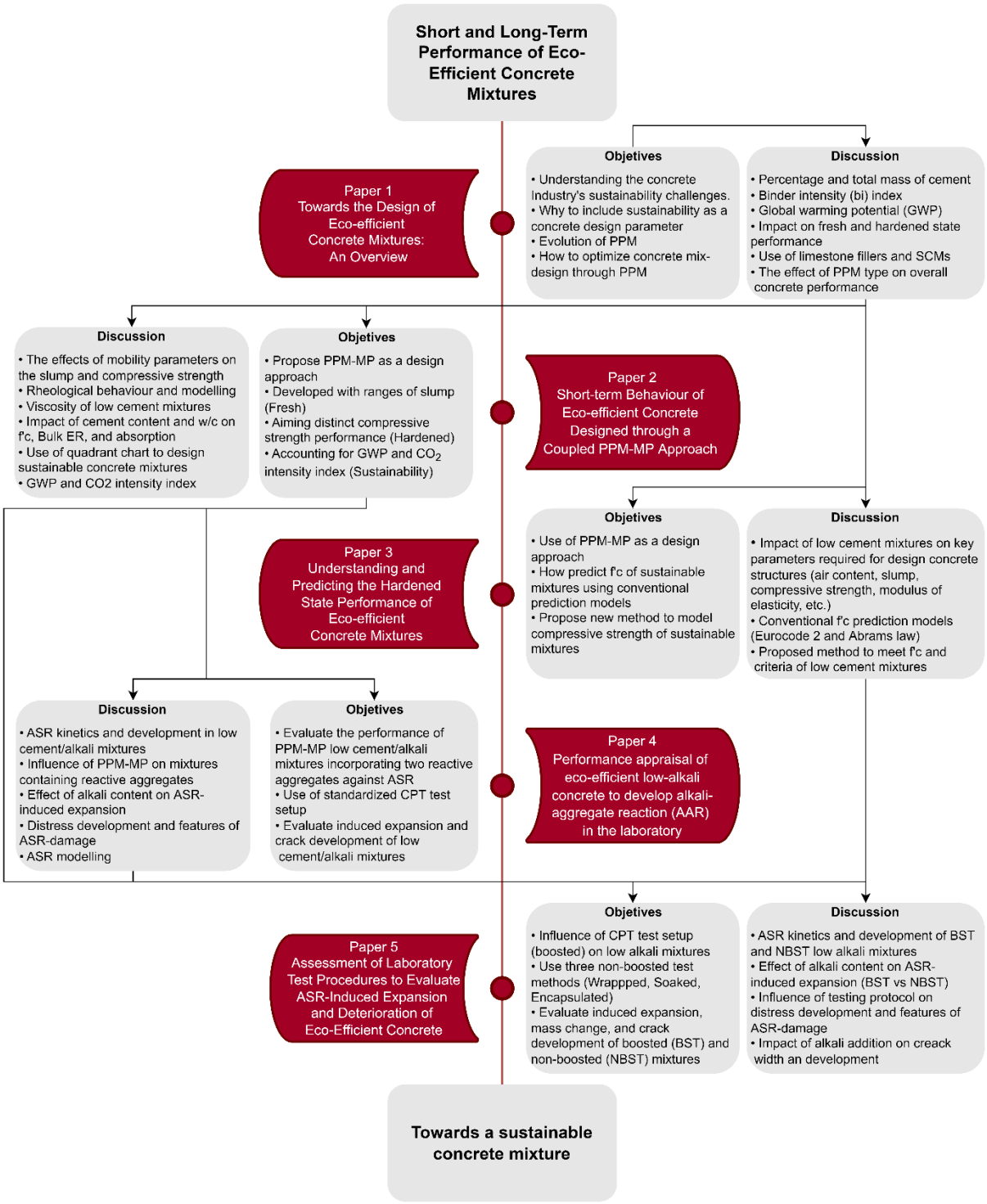

Figure 1.1. Structure of Ph.D. Thesis - Scientific Rationale.

1.4 References

[1] M. Limbachiya, S.C. Bostanci, H. Kew, Suitability of BS EN 197-1 CEM II and CEM V cement for production of low carbon concrete, Constr. Build. Mater. 71 (2014) 397–405.

[2] J. Di Filippo, J. Karpman, J.R. Deshazo, J. Di Filippo, J. Karpman, J.R. Deshazo, The impacts of policies to reduce CO2 emissions within the concrete supply chain, Cem. Concr. Compos. 101 (2019) 67–82. doi:10.1016/j.cemconcomp.2018.08.003.

[3] W. Schakel, C.R. Hung, L.-A. Tokheim, A. Hammer Strømman, E. Worrell, A. Ramírez, Impact of fuel selection on the environmental performance of post-combustion calcium looping applied to a cement plant, Appl. Energy. 210 (2017) 75–87. doi:10.1016/j.apenergy.2017.10.123.

[4] H.F. Campos, N.S. Klein, J. Marques Filho, Proposed mix design method for sustainable high-strength concrete using particle packing optimization, J. Clean. Prod. 265 (2020) 1–15. doi:10.1016/j.jclepro.2020.121907.

[5] Statista, Cement production globally and in the U.S. from 2010 to 2017 (in million metric tons), (2017). https://www.statista.com/statistics/219343/cement-production-worldwide/ (accessed March 28, 2018).

[6] U.S. and world cement production 2018, Statista. (2018). https://www.statista.com/statistics/219343/cement-production-worldwide/ (accessed October 11, 2019).

[7] Statista, Major Countries in Worldwide Cement Production from 2011 to 2017, (2017). https://www.statista.com/statistics/267364/world-cement-production-by-country/ (accessed March 28, 2018).

[8] Statista, Largest producers of CO2 emissions worldwide in 2016, based on their share of global CO2 emissions, (2018). https://www.statista.com/statistics/271748/the-largest-emitters-of-co2-in-the-world/ (accessed March 8, 2018).

[9] M.C. Gonçalves, F. Margarido, Materials for Construction and Civil Engineering : Science, Processing, And Design, Springer International Publishing, 2015.

[10] A. Hasanbeigi, L. Price, E. Lin, Emerging Energy-Efficiency and CO2 Emission-Reduction Technologies for Cement and Concrete Production: A Technical Review, Renew. Sustain. Energy Rev. 16 (2012) 6220–6238.

[11] T.R. Naik, M. Asce, S.S. Singb, M.M. Hossain, Permeability of high-strength concrete containing low cement factor, J. Energy Eng. 122 (1996) 21–39.

[12] M. Noël, L. Sanchez, G. Fathifazl, Recent Advances in Sustainable Concrete for Structural Applications, in: Sustain. Constr. Mater. Technol. 4, 2016: p. 10.

[13] U.N. Environment, K.L. Scrivener, V.M. John, E.M. Gartner, Eco-efficient cements: Potential economically viable solutions for a low-CO2 cement-based materials industry, Cem. Concr. Res. 114 (2018). doi:10.1016/j.cemconres.2018.03.015.

[14] M. T. de Grazia, L. F. M. Sanchez, R. C. O. Romano, R. G. Pileggi, M.T. de Grazia, L. Sanchez, R.C.O. Romano, R.G. Pileggi, M. T. de Grazia, L. F. M. Sanchez, R. C. O. Romano, R. G. Pileggi, Investigation of the use of continuous particle packing models (PPMs) on the fresh and hardened properties of low-cement concrete (LCC) systems, Constr. Build. Mater. 195 (2019) 524–536. doi:10.1016/j.conbuildmat.2018.11.051.

[15] S. Licht, H. Wu, C. Hettige, B. Wang, J. Asercion, J. Lau, J. Stuart, STEP cement: Solar Thermal Electrochemical Production of CaO without CO2 emission, Chem. Commun. 48 (2012) 6019–6021. doi:10.1039/c2cc31341c.

[16] S.A.A.M. Fennis, J.C. Walraven, Using particle packing technology for sustainable concrete mixture design, Heron. 57 (2012) 73–101.

[17] M. Grazia, L.F.M. Sanchez, R. Romano, R.G. Pileggi, M.T. de Grazia, L.F.M. Sanchez, R. Romano, R.G. Pileggi, M. T. de Grazia, L. F. M. Sanchez, R. C. O. Romano, R. G. Pileggi, Evaluation of the Fresh and Hardened State Properties of Low-Cement Content (LCC) Systems, Mag. Concr. Res. 72 (2018) 1–14. doi:10.1680/jmacr.18.00271.

[18] S.H. Kosmatka, B. Kerkhoff, W.C. Panarese, Designing and Proportioning Normal Concrete Mixtures, in: Des. Control Concr. Mix., Portland Cement Association, 2002: pp. 151–172.

[19] B.L. Damineli, F.M. Kemeid, P.S. Aguiar, V.M. John, Measuring the eco-efficiency of cement use, Cem. Concr. Compos. 32 (2010) 555–562.

[20] ACI Committee 302, Guide for Concrete Floor and Slab Construction - ACI 302.1R-04, 2004.

Chapter Two: Literature Review

2.1 Eco-efficient concrete mixtures

Recent studies have been focusing on methodologies to produce eco-efficient concrete mixtures [1,2]. Figure 2.1 shows a summary of the kg CO_2e (carbon dioxide equivalent) per cubic meter of concrete produced after investigating CO_2 (carbon dioxide) emission in the concrete supply chain using a 40 MPa conventional concrete mix-design with 328 kg/m^3 of OPC and 1242, 781, and 190 kg/m^3 of coarse and fine aggregate and water content, respectively.

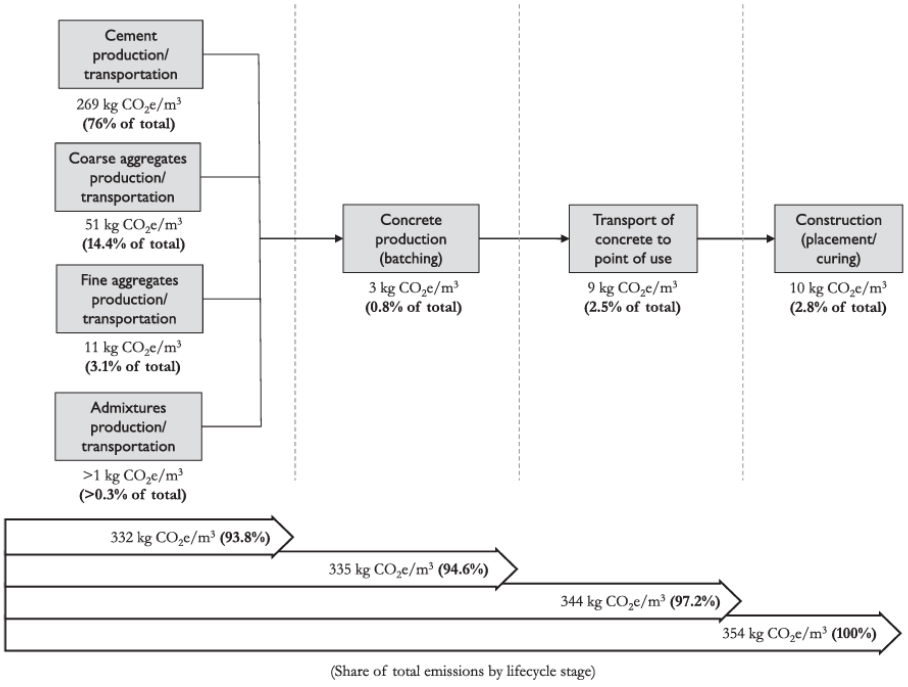

Figure 2.1: Lifecycle analysis of concrete mixture developed with 40 MPa [1].

Moreover, it exhibits the percentage of CO_2 emissions during four major steps in the production of 40 MPa concrete: 1) raw material production and transportation, 2) concrete production, 3) concrete transportation, and 4) concrete placement. The former phase accounts for 93.8% of the emission (332 kg CO_2e/m^3), wherein OPC (ordinary Portland cement) production and transportation accounts

for approximately 82% of the total emission of the raw material phase. Therefore, more than three-quarters of emission resulting from conventional concrete mixtures productions is governed by OPC.

To increase concrete sustainability, OPC can be partially replaced by supplementary cementitious materials (SCMs) or inert fillers (e.g., limestone fillers). SCMs are considered more eco-efficient than OPC since many are waste materials and/or industrial by-products [1,3,4]. Figure 2.2 shows that, from 2000 to 2013, 15% of CO_2 emissions were reduced due to the production of blended cement [5]. Fly ash, silica fume, and granulated blast furnace slag (GBFS) are the most commonly used SCMs worldwide [6–8]**.** Although OPC can be replaced by up to 80% by GBFS, 70% by fly-ash, and 10% by silica fume, conventional concrete mixtures normally replace SCMs with only 20% of OPC, owing to local unavailability [1,9].

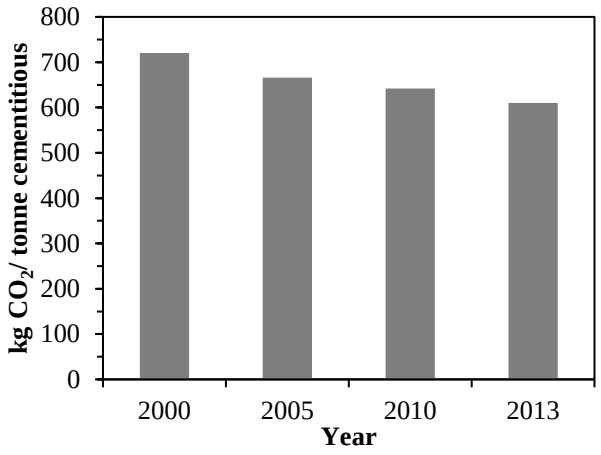

Figure 2.2: CO_2 emissions of blended cement Adapted from [5].

Although most of the SCMs produced are already used in the construction industry, their production does not keep up with the increased OPC demand. As seen in Figure 2.3, filler and calcined clay are the only materials available to be used as partial substitutes for OPC that overcome its production.

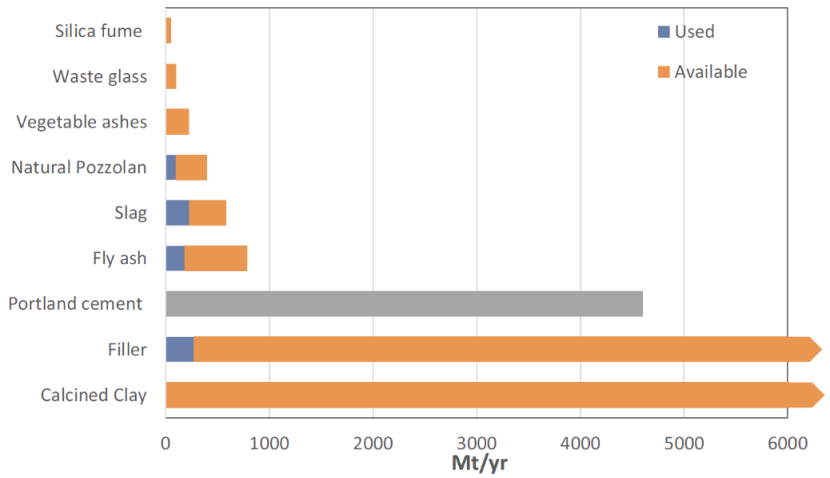

Figure 2.3: Amount (used and available) of substitutes for OPC [9].

Although several types of inert fillers may be used, limestone filler (LF) is the most common one due to its availability worldwide, economy, volumetric stability within the cement paste, improvement in the fresh state due to its shape and its ability to be produced in different particle size distributions - PSD [10–15]. The average replacement ratio of limestone fillers is around 20%; nevertheless, the limit of 35% is acceptable in some standards (i.e. in Europe and South Africa) [10,11,16,17]. However, previous studies have shown promising results with higher replacement levels (up to 50%) [18–20]. Lothenbach et al. (2008) [21] assessed the impact of limestone fillers on the hydration of OPC and emphasizes that their fine PSD is one of the main strength contributors enhancing the cement hydration rather than the influence of limestone fillers on the system's chemistry or physical packing. Furthermore, two other phenomena are frequently associated with the addition of fillers: the filler effect and the dilution effect [12,14,22–26]. The filler effect, which is studied since the 1990s [27–29], occurs due to the use of particles finer than OPC which accelerates cement hydration due to the formation of nucleation sites [26]. Yet, the beneficial effect of limestone filler effect may be diminished when specimens combined fillers with distinct

materials, such as with pozzolan (PL) or with a higher volumetric concentration of aggregates (FL-2), as seen in Figure 2.4 [27]

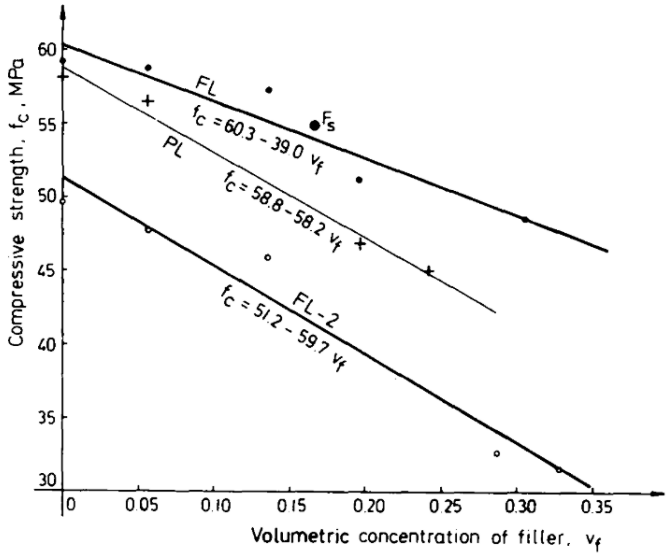

Figure 2.4: Filler effect of specimens containing limestone filler (FL), pozzolan and limestone filler (PL), and limestone filler with a higher volume of aggregate [27].

The dilution effect, defined as an increase in water content per unit mass of cement particles (i.e., an increase in water-to-cement ratio; w/c), can have a positive impact (accelerating cement hydration at early ages) or a negative impact (reducing compressive strength due to increase of porosity caused by an increase in w/c) [11,16,19,21,23,24,30]

Aside from the importance of reducing cement content, assessing concrete eco-efficiency is also critical. The global warming potential (GWP) is a measure of how much energy one tonne of a gas will absorb over a given time period in comparison to one tonne of carbon dioxide emissions (CO_2). In terms of concrete production, GWP can be translated into the total CO_2 emissions (in mass) per unit volume of concrete (Equation 2.1).

$$GWP = \sum_{i=1}^{n} m_i . g_i \quad \text{Equation 2.1}$$

where m_i is the mass of concrete ingredient (i) per unit volume of concrete and g_i is the CO_{2eq} per unit mass of concrete ingredient (i).

Distinct life cycle assessment (LCA) software, such as GreenConcrete LCA tool, Ecoinvent 3, and SimaPro, provide databases containing the GWP (i.e., kg CO_{2eq}/kg of material) of each concrete ingredient used to calculate the total GWP of concrete from cradle to grave. Table 2.1 shows an example of some concrete ingredients' GWP, highlighting the significantly higher CO_2 emission of cement production when compared to other ingredients.

Table 2.1. GWP in kg CO_2 emissions (CO_2eq) for raw materials, adapted from [31]

Raw materials (kg)					
CEM I	**Superplasticizer**	**Fly Ash**	**Water**	**Fine Aggregate**	**Coarse Aggregate**
0.9	0.00188	0.00392	0.00013	0.0014	0.0282

To appraise concrete eco-efficiency, Damineli et al. (2010) proposed the use of two indicators: binder intensity (bi) and CO_2 intensity (ci). The binder intensity index correlates the amount of binder required to develop one unit of concrete property, for instance, the compressive strength (Equation 2.2).

$$bi = \frac{BC}{P} \quad \text{Equation 2.2}$$

where bi is the binder intensity index, BC is the binder content (kg/m^3), and P is the performance requirement (e.g., compressive strength – MPa).

The CO_2 intensity index ($ci_{cs;}$ Equation 2.3) calculates the amount of GWP required to produce one unit of any concrete property [32]. Since 28-day compressive strength is the most important one, it is the most applied in the CO_2 intensity index.

$$ci_{cs} = \frac{GWP}{f'_c} \qquad \text{Equation 2.3}$$

where ci_{cs} is the CO_2 intensity index (kg/m^{-3}. MPa^{-1}), GWP is the global warming potential of the concrete investigated (CO_{2eq}/kg), and f'_c is the concrete compressive strength (MPa).

Using these two indices, Damineli et al. (2010) evaluated the eco-efficiency of concrete produced worldwide by selecting 156 random concrete mix-designs used for different applications from 1988 to 2009, resulting in a total of 1585 data points, as displayed in Figure 2.5 and Figure 2.6.

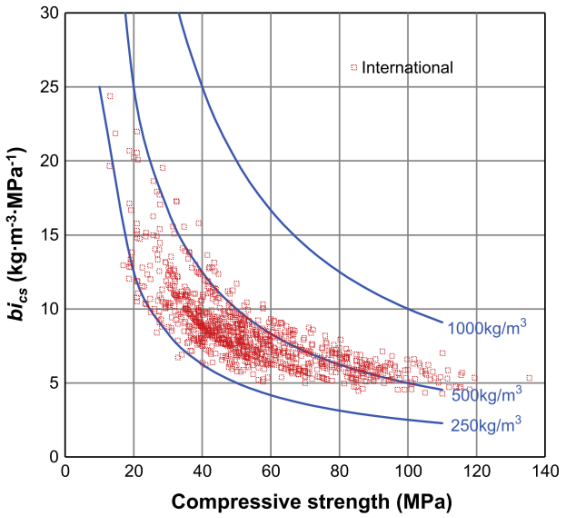

Figure 2.5: Relationship between binder intensity and compressive strength at 28-days [32].

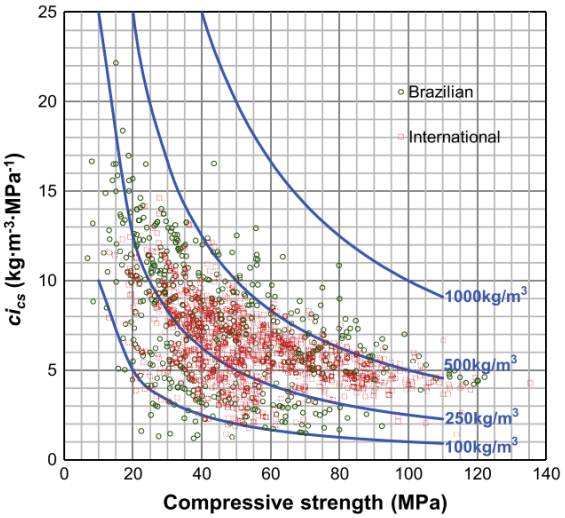

Figure 2.6: Relationship between CO_2 index and compressive strength at 28-days [32].

High-strength concrete (i.e., > 40 MPa) presents lower bi factors and are considered more eco-efficient, whereas conventional concrete mixtures (i.e., 20-40 MPa) are often designed with considerably high OPC contents. It results in bi values of around 10 $kg.m^{-3}.MPa^{-1}$, which clearly demonstrates the need for techniques to improve their eco-efficiency. Additionally, the majority of concrete produced worldwide presents OPC contents ranging from 350 to 500 kg/m^3. Regarding the CO_2 intensity index, Figure 2.6 displays a similar trend to that of the binder intensity index. Moreover, it was concluded that it is possible to produce concrete mixtures with an CO_2 intensity index as low as 4.3 kg/m^{-3}. MPa^{-1} without replacing OPC, yet conventional concrete mixtures produced worldwide yielded ci_{cs} values of around 10 kg/m^{-3}. MPa^{-1}.

Furthermore, Wallevik et al. [33] developed a classification of concrete eco-efficiency based on its carbon footprint, as displayed in

Table 2.2, in which mixtures developed with OPC content of 250 kg/m^3 or less are classified as low-carbon concrete (LCC) [33].

Table 2.2. Low Carbon Concrete Classes as per [33].

Classification	Carbon footprint (kg CO_{2eq}/kg)
Semi-LCC	≤ 300
LCC_{250}	≤ 250
LCC_{200}	≤ 200
LCC_{150}	≤ 150
EcoCrete	≤ 125
EcoCrete Xtreme	≤ 105

2.2 Particle packing model

Another approach that can be applied to produce eco-efficient mixtures is the use of advanced mix-design techniques. The particle size distribution (PSD) of concrete matrix can be optimized through particle packing models (PPMs). In 1892, Féret analyzed for the first time the influence of aggregate packing on concrete hardened state [18,34]. Although several PPMs were created, all of them aim to reduce the system porosity while increasing the packing density. PPMs can generally be classified into two types: discrete and continuous. Discrete models consider multimodal distributions containing "n" discrete size classes of particles (also known as gap-graded particles). Moreover, it is assumed that each class of particle will be rearranged to achieve the maximum packing density possible [18,35]. Conversely, continuous models are numerical procedures developed considering that particles have continuous size distribution (i.e. no gaps throughout the whole PSD) [18,35]. Previous studies have suggested that real aggregate blends are better represented by continuous models [20,36]. The first continuous PPM was created by Fuller in 1907 [18,35,37,38], whereas the first discrete model was created by Furnas in 1929 for binary systems and in 1931 for multimodal models [18,34,35,38]. The PPM science was then enhanced based on Fuller (continuous) and Furnas (discrete) [18,34,35,37–39].

Discrete models can be further divided into three more categories: binary (Furnas), ternary (Toufar and modified Toufar), and multimodal (Furnas and De Larrard) [35,37]. De Larrard has developed three mix-designs approaches: Linear Packing Density Model (LPDM), Solid Suspension Model (SSM), and Compressive Packing Model (CPM); yet CPM is considered the most recent and updated discrete method and it is considerably used in the literature to produce eco-efficient concrete mixtures. Conversely, CPM is a complicated mathematical model, in which software must be used to develop the mix-design, reducing its practicality in the construction industry [40].

Additionally, there are three types of continuous models: Fuller, Andreasen, and Alfred (also known as modified Andreasen). Similar to CPM, the Andreasen's modified model is the most recent continuous PPM developed and can be calculated through Equation 2.4.

$$CPFT = 100 * \left(\frac{{D_P}^q - {D_S}^q}{{D_L}^q - {D_S}^q}\right) \quad \text{Equation 2.4}$$

where D is the particle size in question, CFPT is the cumulative percent finer than D, D_L and D_S is the largest and smallest particle size in the system, respectively, and q is a distribution factor.

The optimum packing of a system can be achieved when the distribution factor is selected as 0.37 [18,38]. However, studies show that due to the low porosity, these mixtures developed with a q-factor of 0.37 present fresh state issues [20,41]. Conversely, a q-factor of 0.22 is recommended for high-flowability mixtures. Figure 2.7 shows the comparison between the Alfred model designed with a q-factor of 0.37 and 0.22. One may notice that the former presents a lower amount of powder, which results in a lower amount of cement required in the mixture. As a result, the lower porosity combined with the lower cement content justifies the flowability reduction when compared to a mixture developed with a q-factor of 0.22.

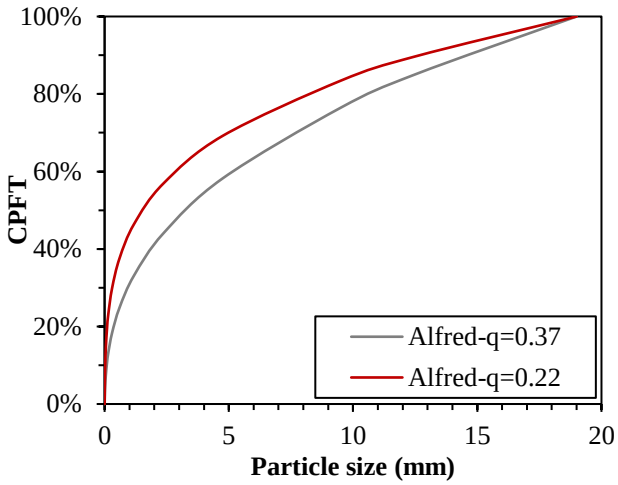

Figure 2.7. Comparison between Alfred model developed with q-factors of 0.37 and 0.22.

Moreover, previous studies [20,42] showed that eco-efficient mixtures with cement content lower than 250 kg/m^3 can be produced; however, w/c between 0.56 and 2.13 was selected, which is not common in the concrete industry.

Continuous PPMs are focused on CPFT, therefore, a model published by Westman and Hugill in 1930 may be used as a complementary equation to calculate the system porosity [38]. Figure 2.8 shows the Westman and Hugill algorithm applied to Alfred Model, highlighting the difference in porosity between systems with q-factors of 0.37 and 0.22.

2.3 Mobility parameters

Mobility parameters can also be used as complementary methods of PPMs to help the prediction of fresh-state properties. There are two types of mobility parameters (Figure 2.9): 1) interparticle separation distance (IPS) and 2) maximum paste thickness (MPT) [19,20,24,43]. IPS is considered as the average distance between two adjacent particles that are smaller than 125 µm, which are normally separated by water (Equation 2.5) [19,20,24,38,44].

$$IPS = \frac{2}{VSA}\left[\frac{1}{V_s} - \frac{1}{(1 - P_{of})}\right]$$ Equation 2.5

Where: IPS is the interparticle spacing, VSA is the calculated volume surface area per cubic centimetre of powder, V_s is the volume fraction of fine solids (particles smaller than 125 μm), and P_{of} is the pore fraction assuming the densest packing of the fine particles.

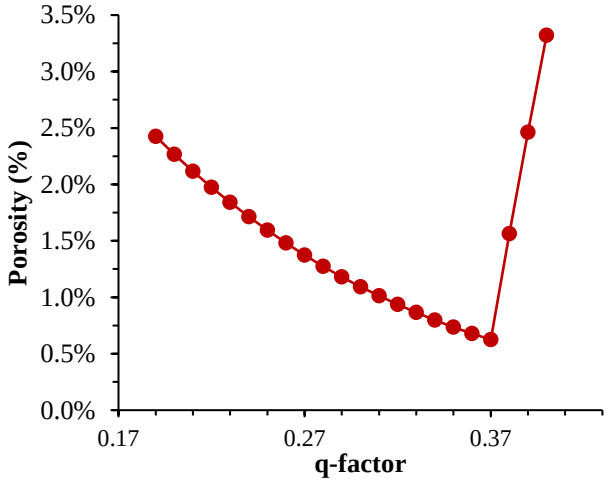

Figure 2.8. Relationship between dry material porosity and Alfred model q-factor.

Similar to IPS, MPT measures the maximum distance amongst particles greater than 125 μm (Equation 2.6). MPT is also known to have a direct correlation to cement paste thickness around aggregate particles [19,20,24,43].

$$MPT = \frac{2}{VSA_c}\left[\frac{1}{V_{sc}} - \frac{1}{(1 - P_{ofc})}\right]$$ Equation 2.6

where MPT is the distance between aggregates, VSA_c is the calculated volume surface area of aggregate (particles greater than 125 μm) fraction, V_{sc} is the volumetric aggregate solid fraction, and P_{ofc} is the pore of aggregate fraction assuming the densest packing.

a) b)

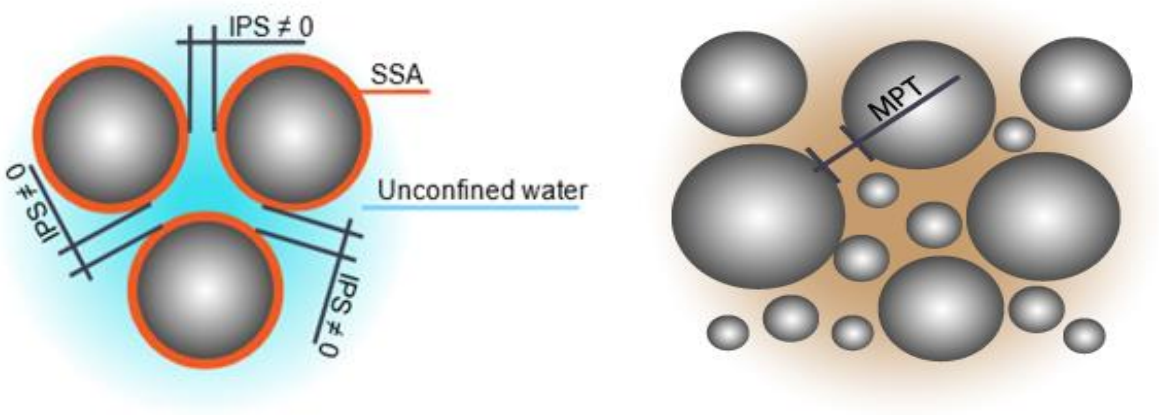

Figure 2.9. Mobility parameters a) interparticle separation distance (IPS) and b) maximum paste thickness (MPT).

Mobility parameters present two main contributions to PPM. First, mobility parameters account for particle shape that is not considered in PPMs. Both mobility parameters are computed as a function of the particles' volume surface area, which is calculated by the multiplication of the specific surface area by the particle density (Equation 2.7).

$$VSA = SSA * \rho_{part} \quad \text{Equation 2.7}$$

where VSA is the volume surface area (m^2/cm^3), SSA is the specific surface area (m^2/g), and ρ_{part} is the particle density (g/cm^3).

Moreover, mobility parameters can be used to further understand the fresh state behaviour of cement-based materials. It has been found that the lower the IPS and MPT, the lower the flowability of granular systems (i.e., higher viscosity and particle collisions). Conversely, high IPS and MPT yield less viscous, more flowable mixes [19,20,23,41,45,46]. However, cement-based materials may also include gravitational forces as the dominant regime or surface forces as the dominant regime [47]. When the former occurs, the MPT governs the flowability behaviour as the gravitational forces are dominant in mixtures with high aggregate volumes. Similarly, the surface force is dominant

when powder volumes govern, which is represented by IPS. Moreover, several studies have shown that mobility parameters have a direct relationship to distinct rheological parameters (i.e., yield stress, final torque, viscosity, etc.) [19,20,23,41,45,46]. Yet, further studies are required to present the optimum IPS and MPT value for an eco-efficient mixture for a required flowability.

2.4 Short-term performance of sustainable concrete developed through PPM

Kumar and Santhanam (2003) [37] used the Alfred PPM to mix-proportion three types of eco-friendly concrete using q-factors of 0.26, 0.27, and 0.22, respectively: high strength concrete (HSC), high-performance concrete (HPC), and self-compacting concrete (SCC). The high-strength eco-friendly concrete was developed with 270, 55, and 30 kg/m^3 of OPC, quartz filler, and micro silica, respectively. Moreover, HPC contains only OPC (360 kg/m^3) and micro silica (42 kg/m^3), whereas SCC has OPC (320 kg/m^3) and fly ash (220 kg/m^3). With the aid of high amount of superplasticizer, HSC and HPC achieved slump of 100 mm; however, a viscosity modifier was also added to SCC to achieve a slump flow of 690 mm. Interestingly, despite having a lower water-to-binder ratio (w/b - 0.33), SCC achieved a lower 28-day compressive strength (41 MPa). At 28 days, HSC and HPC mixtures with similar q-factors (thus packing density) and w/b of 0.40 and 0.36 achieved 83 and 78 MPa, respectively.

Wenqiang et al. (2018) [48] selected a combination of PPM (CPM and 3PM) coupled with experimental work to develop twelve eco-efficient self-compacting concrete mixtures by varying the sand-to-aggregate ratio (from 45% to 55%). The mixtures investigated incorporate 308 kg/m^3 of OPC and limestone fillers ranging from 53 to 212 kg/m^3, corresponding to powder additions ranging from 20 L/m^3 to 80 L/m^3. Interestingly, mixtures with 20 L/m^3 of limestone powders and 3.61 kg/m^3 of superplasticizer achieved slump flows between 480 and 560 mm (Figure 2.10). The increase of

limestone filler content and superplasticizers resulted in a slump flow of up to 700 mm. In terms of compressive strength, the mixtures ranged from 30 to 48 MPa. Furthermore, regardless of the percentage of limestone filler, mixtures with a high sand ratio (0.55%) yielded lower compressive strengths.

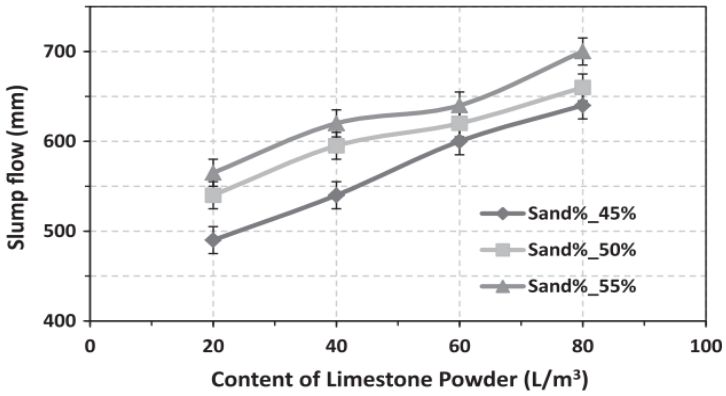

Figure 2.10. Slump flow of concrete mixtures investigated [48].

Esmaeikhanian et al. [49] also developed thirteen eco-efficient self-compacting concrete using Alfred model and incorporating limestone filler, silica fume, and/or fly ash. The cement content ranged from 196 to 271 kg/m^3, while the total powder content ranged from 280 to 310 kg/m^3. Although all the mixtures contained superplasticizer, some of them also required a stabilizer and an air-entraining agent. Slump flow range of 560-640 mm and a compressive strength range of 25-30 MPa was achieved. The mixtures' eco-efficiency was also appraised using binder intensity CO_2 intensity indicators. In general, $c_{i,cs}$ ranged from 5.7-9.1 kg/m^3.MPa^{-1}, whereas bi varied between 9 and 13 kg/m^3.MPa^{-1}.

Ali et al., 2020 [50] investigated over 20 different mixtures proportioned with Fuller-Thompson distribution moduli (q) ranging from 0.4 to 0.5 and distinct volumetric sand-to-total aggregate ratios, achieving an OPC content of 232 kg/m^3, combined with fly ash (62 kg/m^3) and silica fume (15

kg/m^3). Although the same binder content (total of 309 kg/m^3) and w/b (0.60) were selected for these mixtures, the compressive strength varied from 28 to 35 MPa and the slump flow ranged from 605 to 770 mm. The mixtures achieved outstanding eco-efficiency indicators, as such $c_{i,cs}$ (from 5.7 to 6.6 kg/m^3.MPa^{-1}) and bi (from 8.4 to 10 kg/m^3.MPa^{-1}).

2.5 Durability aspects: alkali aggregate reaction

The previous section presented methods for developing eco-efficient concrete. Besides a suitable fresh and hardened state properties, a proper mix-design approach must proportion a mixture with adequate durability-related characteristics. A wide range of durability-related problems is known to affect concrete structures in Canada and worldwide such as alkali-aggregate reaction (AAR), delayed ettringite formation (DEF), external sulphate attack (ESA), freezing and thawing cycles (FT) and scaling (SCA), carbonation, and steel corrosion. However, this research will focus on the first one (alkali-aggregate reaction) due to the concern caused by reactive aggregates in North America.

Alkali-aggregate reaction (AAR), with the first dated case in the 1940s in California (USA), is one of the most well-known internal swelling reactions (ISR) that affects concrete infrastructure [51,52]. AAR is generally divided into two main reactions: alkali-silica reaction (ASR) and alkali-carbonate reaction (ACR). ASR is the most common AAR reaction worldwide. It occurs in the presence of alkali hydroxides (i.e., NaOH and KOH - from cement paste), metastable silica minerals (from some fine and coarse aggregates), and high moisture conditions [51–53]. This chemical reaction generates an expansive product called ASR-gel that induces tensile pressures within the reacting aggregate material(s) and the adjacent cement paste while moisture uptake. As a result, the material slowly loses its integrity (mechanical and durability properties) due to the microcracks created due to the

ASR-gel. Conversely, ACR is a mechanism less understood compared to ASR. Previous research [54,55] classify it as a type of ASR, while [52,56–58] present ACR as a completely different distress mechanism. Although ASR is the most common type of AAR, ACR can be found when reactive dolomite is used as concrete aggregates. ACR occurs due to one or more reasons: a) hydraulic pressures (movement of water and alkali ions); b) alkali ions and water adsorption; and c) rearrangement and generation of new products (dedolomitization process (Equation 2.8) – formation of brucite and calcite) [52,59].

$$CaMg(CO_3)_2 + 2(Na,K)OH \rightarrow Mg(OH)_2 + CaCO_3 + (Na,K)_2CO_3$$

Dolomite Alkali Hydroxide Brucite Calcite Alkali Carbonates Equation 2.8

Moreover, the alkali carbonates generated in the dedolomitization process can further react with portlandite presented in the cement paste, formatting secondary calcite and regenerating alkali hydroxides as shown in Equation 2.9 [52,59].

$$(Na, K)_2CO_3 + Ca(OH)_2 \rightarrow CaCO_3 + 2(Na, K)OH$$

Alkali-Carbonate Portlandite Secondary Calcite Alkali Hydroxide Equation 2.9

The AAR damage in concrete structures can be qualitatively identified through the crack pattern (Figure 2.11) that can be first seen as soon as 2 years or up to more than 25 years.

However, the damage will depend on three main factors: 1) alkali content, 2) reactive aggregate type, and 3) moisture availability. The moisture availability and the reactive aggregate type cannot be fully controlled as in some areas non-reactive aggregates are limited or even not available. Moreover, the transportation costs of non-reactive aggregates affect greatly the concrete costs. Thus,

in certain cases, the use of reactive aggregate is the only option and the one with a lower environmental impact. Therefore, controlling the alkali content is the best option to mitigate or inhibit AAR expansion.

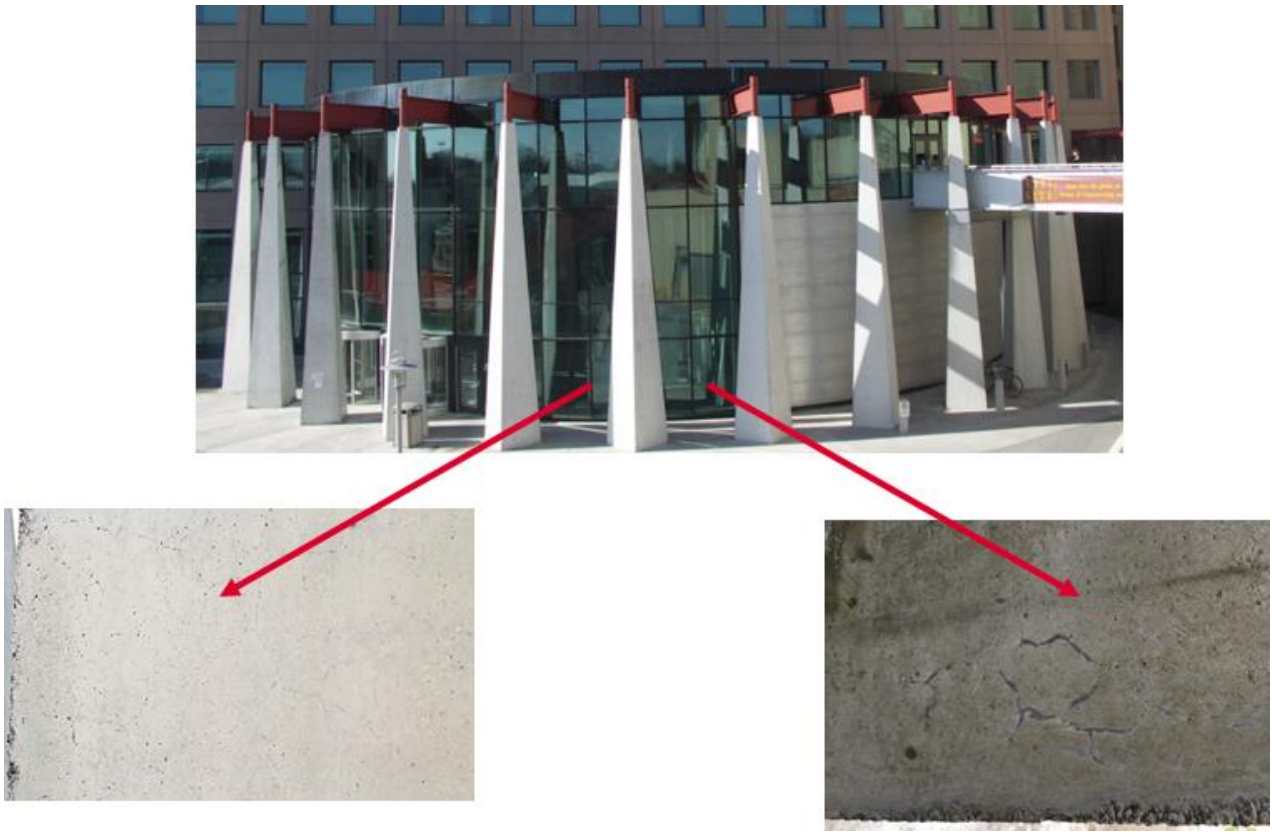

Figure 2.11. ASR crack pattern visualized at University of Ottawa SITE building.

The alkali hydroxides are present in the concrete pore solution due to the high alkali content of cement. Thus, lower cement contents or lower alkali system due to SCM's dilution can be used to reduce the system alkali hydroxides. According to CSA A23.2-27A recommendations, ASR-development can be mitigated when the system's total alkali content contributed by the Portland cement is less than the values presented in Table 2.3.

Table 2.3. System's total alkali content (kg/m^3) contributed by the Portland cement as per CSA A23.2-27A.

Prevention level	System's total alkali content (kg/m^3) contributed by the OPC
–	–
Mild – W	3.0
Moderate – X	2.4
Strong – Y	1.8
Very Strong – Z	1.2

However, as previously mentioned, the SCMs availability worldwide is not enough to match the demand for OPC. Therefore, reducing cement content is the main option to produce eco-efficient concrete mixtures with low alkali hydroxides. Several studies show that ASR can be mitigated with the use of SCM [52,60–62], yet just a few studies focus on use of low alkali systems without SCMs [63–66].

2.6 Effect of alkali content of concrete on Alkali-Silica Reaction (ASR)

Fournier et al. (2009) [67] evaluated the influence of ASR-induced development in concrete mixtures incorporating a variety of reactive fine and coarse aggregates and two alkali loadings (boosted and non-boosted). Mixtures with boosted alkalis have their equivalent alkalis in the cement (Na_2O_e) raised to 1.25 kg/m^3 (i.e., total alkali content of 5.25 kg/m^3) as per the CPT standard (ASTM C 1293), while non-boosted mixtures contain 0.90% of Na_2O_e (i.e., total alkali content of 3.78 kg/m^3). Regardless of the aggregate reactivity, the boosted mixtures resulted in greater expansions over time due to the higher alkali content of the system. Yet, the aggregate type and nature have a significant impact on the expansion development of concrete containing varying amounts of alkalis, as shown in Figure 2.12 [68].

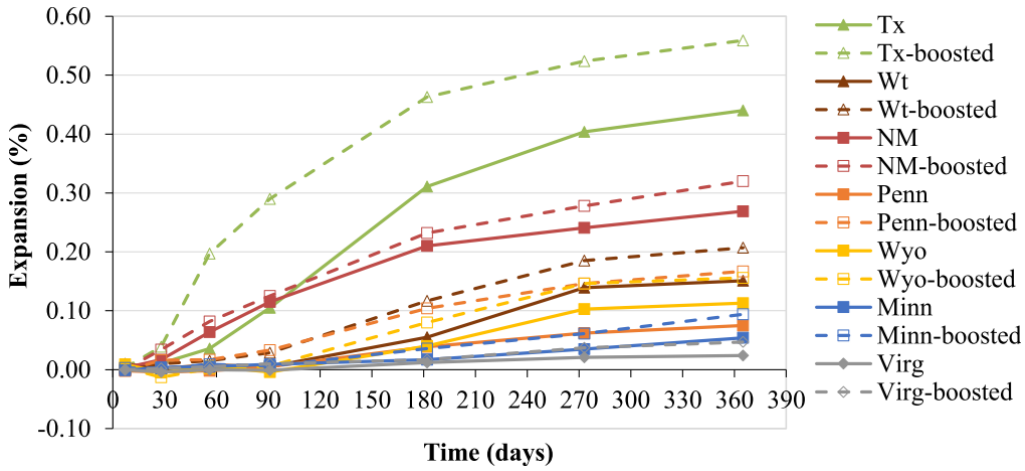

Figure 2.12. Concrete mixtures developed with 3.78 (non-boosted) and 5.25 kg/m^3 (boosted) of alkali content.

For instance, concrete incorporating Texas sand (Tx) resulted in expansions above 0.40% for boosted and non-boosted mixtures. Moreover, mixtures incorporating New Mexico reactive aggregate achieved around 0.30% expansion after one year regardless of the addition of alkalis. The other reactive aggregates reached final expansions lower than 0.20% when developed at 3.78 and 5.25 kg/m^3 alkali content. When reactive aggregates with varying reactive potentials (i.e., ultra-high/very high, high, and moderate/marginal) were selected, mixtures developed with an alkali content of 3.78 kg/m^3 (non-boosted) achieved 18%, 27%, and 43% lower expansions, respectively, than conventional CPT mixtures (boosted mixtures) [67].

To evaluate ASR-evolution under laboratory test conditions, de Grazia et al. [68] proposed a modified version of Larive's model (Equation 2.10). Aside from the aggregate type and nature, this equation also accounts for three other factors, such as temperature, total alkali content, and relative humidity, which are significant contributors to ASR-development and must be considered to describe laboratory ASR-induced expansion more precisely. In this study, the ultimate expansion (ε_∞, or expansion at infinity), an average τl and τc coefficients were calibrated (Table 2.4) based on

mixtures developed by Sanchez et al. (2017) [57], which incorporate reactive aggregates with distinct damage degrees ranging from marginal to ultra-high.

$$\varepsilon(t,\theta) = \xi(t)\varepsilon^{\infty}$$

$$= \frac{1 - e^{-\frac{t}{\tau_c\, k_{c,T}\, k_{c,RH}\, k_{c,\%A} k_{c,E}}}}{1 + e^{-\frac{(t-\tau_l\, k_{L,T}\, k_{L,RH}\, k_{L,\%A} k_{L,E})}{\tau_c\, k_{c,T}\, k_{c,RH}\, k_{c,\%A} k_{c,E}}}} \times \left(k_{Inf,T}\, k_{Inf,RH}\, k_{Inf,E}\, k_{Inf,\%A}\right)\varepsilon^{\infty} \quad \text{Equation 2.10}$$

where t is elapsed time; $\varepsilon\ (t)$ is the expansion at a given elapsed time; ε^{∞} is the maximum expansion at infinity (or ultimate expansion); τ_c is the characteristic time (as a function of the aggregates type and nature/reactivity); τ_l is the latency time (as a function of the aggregate type and nature/reactivity); $k_{C,T}, k_{C,RH}, k_{C,E}, k_{C,\%A}$ are the temperature, humidity, exposure and alkali content coefficients impacting the characteristic time; $k_{L,T}, k_{L,RH}, k_{L,E}, k_{L,\%A}$ are the temperature, humidity, exposure and alkali content coefficients impacting the latency time; $k_{inf,T}, k_{inf,RH}, k_{inf,E}, k_{inf,\%A}$ is the temperature, humidity, exposure and alkali content coefficients, respectively, influencing the maximum expansion.

Table 2.4. Aggregate's type and nature/reactivity coefficients [68].

	Damage degree	**ʊc**	**ʊl**	ε^{∞} **(%)**
ACR	Ultra High	49	0	0.70
ASR - Fine and Coarse	Ultra High	42	103	0.60
ASR - Fine	Ultra High	71	0	0.65
	High	38	157	0.26
ASR Coarse	High	50	44	0.23
	Moderate	45	165	0.15
	Marginal	43	168	0.08

Then, to describe the influence of the alkali content on AAR-induced development, the alkali content coefficients (Table 2.5) were calibrated based on previous data presented by Fournier et al. (2009) [67], as shown in Figure 2.13.

Table 2.5. Alkali content coefficients obtained for different types of reactive aggregates and two alkali contents [68].

		unboosted - 3.78 kg/m^3			boosted - 5.25 kg/m^3		
		$K_{\%a\text{-}tc}$ ($k_{C,\%A}$)	$K_{\%a\text{-}tl}$ ($k_{L,\%A}$)	$K_{\%a\text{-}exp}$ ($k_{inf,\%A}$)	$K_{\%a\text{-}tc}$ ($k_{C,\%A}$)	$K_{\%a\text{-}tl}$ ($k_{L,\%A}$)	$K_{\%a\text{-}exp}$ ($k_{inf,\%A}$)
ASR - Fine	Ultra High	2.82	1.00	0.98	1.19	1.00	0.88
	High	3.03	1.80	1.00	1.86	1.15	0.91
ASR Coarse	High	2.77	0.83	1.50	2.05	0.79	1.47
	Moderate	4.08	2.40	1.64	2.98	1.22	1.61
	Marginal	6.95	4.94	4.37	4.61	2.38	2.21

Einarsdottir and Hooton [66] also appraised low-alkali binder concrete mixtures ranging from 1.68 kg/m^3 for 50% OPC +50% SCM mixtures to 3.35 kg/m^3 for 100% OPC mixtures. The low-alkali mixtures were compared to medium-alkali (ranging from 2.62 to 5.23 kg/m^3) and high-alkali (ranging from 3.03 to 6.06 kg/m^3) mixtures. After two years of testing, mixtures developed with 100% Portland cement (alkali content ranging from 3.35 to 6.06 kg/m^3) leached 25-50% of their alkalis, whereas low-, medium- and high-alkali mixtures (where Portland cement was replaced with 15% to 50% SCMs) leached between 18% and 32%, as shown in Figure 2.14.

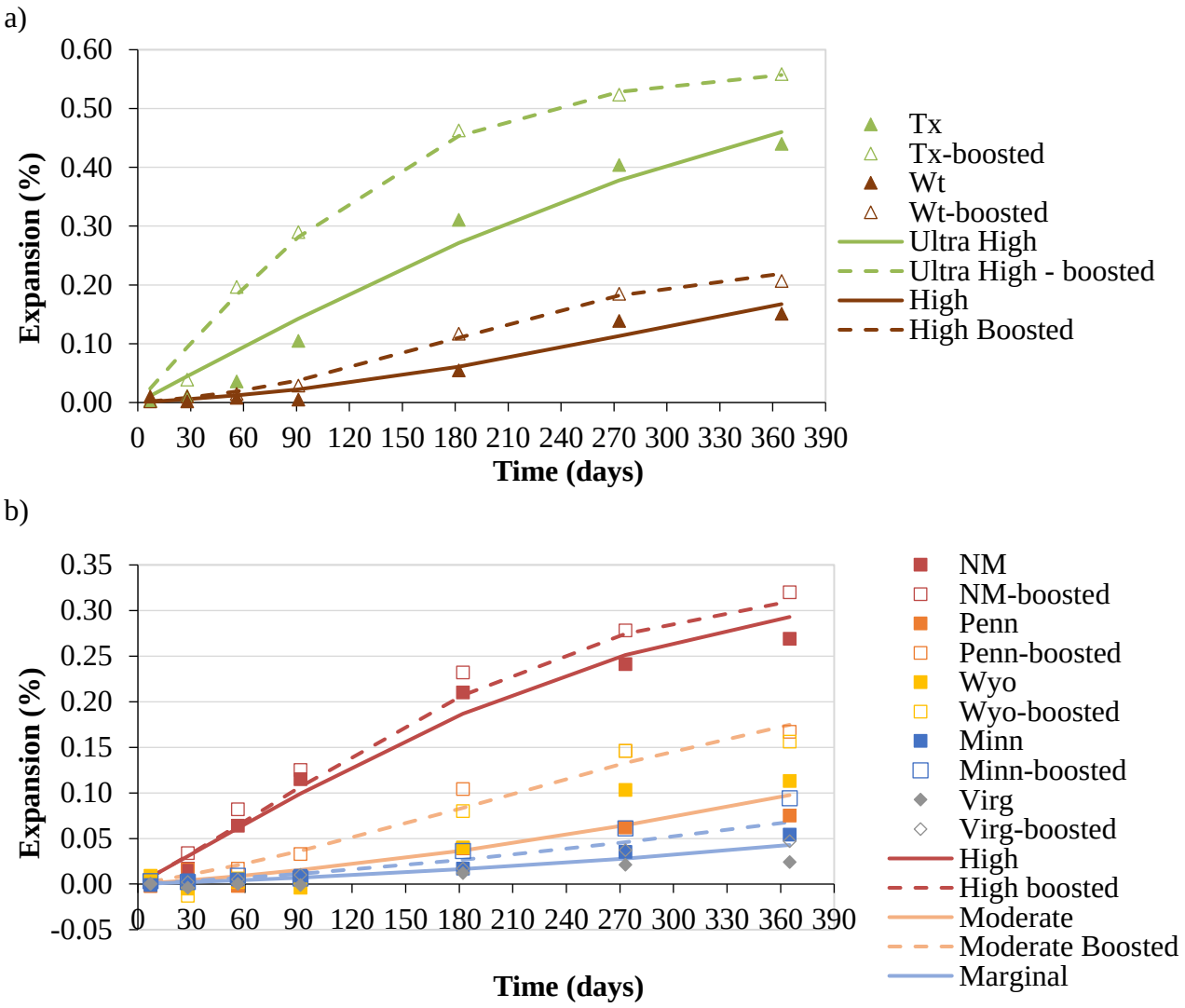

Figure 2.13. Concrete mixtures developed with 3.78 and 5.25 kg/m^3 of alkali content and a) reactive fine aggregate and b) reactive coarse aggregate [68].

Then, the alkali leaching of CPT mixtures boosted to 40% above of the alkali content from the cement was investigated after two years test, as displayed in Figure 2.15. Even though the six control mixtures were developed with different alkali content cement, they were boosted to a total of 5.25 kg/m^3 alkalis in the system. The alkali content of the systems was 6.06, 5.23, and 3.35 kg/m^3 for the high alkali, medium alkali, and low alkali mixtures, respectively. In this case, the leaching during 2 years of CPT conditions ranged from 15 to 50%.

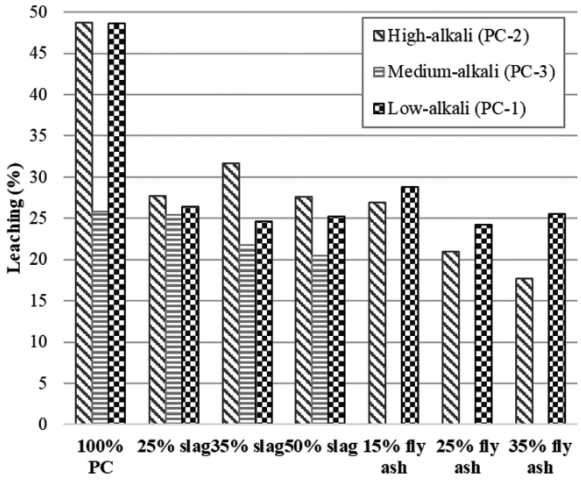

Figure 2.14. Leaching after two years from CPT specimens incorporating Sudbury reactive aggregate and various OPC and SCMs combinations [66].

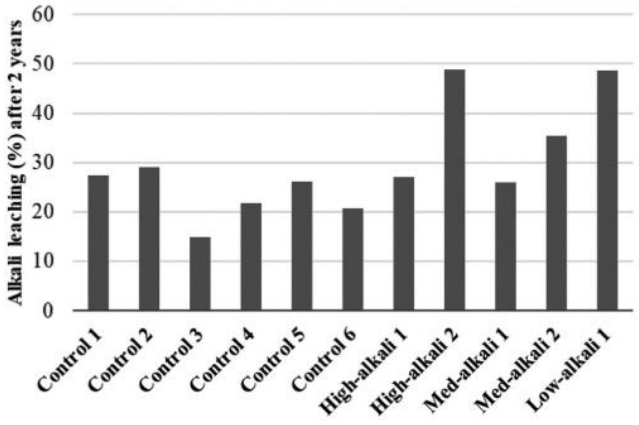

Figure 2.15. Leaching after 2 years in CPT from concrete mixtures made with 100% OPC [66].

Thus, boosting concrete mixtures with additional alkalis is recommended, especially for low-alkali mixtures, which may exhibit "false" acceptable expansion in laboratory tests due to leaching while exhibiting deleterious expansion in the field when conditions limit the occurrence of leaching. In

addition to alkali boosting, Einarsdottir and Hooton [66] suggested that each specimen may be stored covered by a plastic bag that protects 2/3 of its height (from top to bottom) to improve CPT method and minimize leaching in low alkali systems.

2.7 Laboratory test methods to accelerate ASR-kinetics

Numerous test procedures and practices are currently standardized to identify the potential reactivity of aggregates in concrete or the potential for expansion due to ASR, for instance, the accelerated mortar bar test - AMBT (ASTM C1260/CSA A23.2-25A), concrete prism test - CPT (ASTM C1293/ CSA A23.2-14A), petrographic analysis (ASTM C295/CSA A23.2-15A), and chemical test for ACR reactivity (ASTM C586). To minimize the impact on the expansion values, concrete mixtures fabricated to be tested under CPT conditions must be boosted to 40% of the cement alkalis, which is equivalent to the total alkali leaching that will occur during a 1-year test for OPC mixtures [66,69]. Although CPT is the most reliable standardized test for assessing the potential for ASR-expansion, it is controversial due to excessive alkali leaching [64,66,69]. To avoid the leaching issues presented in CPT, other non-standardized test setups are presented in the literature (e.g., wrapped method, soaked method, concrete cylinder test - CCT). The wrapped method consists of wrapping the concrete specimens in wet cloth as displayed in Figure 2.16.

Previous studies evaluated using 1.5M OH^- or 0.15M OH^- solution, which is equivalent to pH of 14.2 and 13.2, respectively [71,72]. Low alkali content concrete specimens were evaluated under two conditions: 1) wrapped test at 38^{o}C and 2) wrapped test at 60^{o}C. Since the wrapping pH is higher than the concrete one, at 38^{o}C specimens show greater expansion, yet, at 60^{o}C almost no expansion was observed. It was concluded that further tests must be conducted to better understand the wrapped method. Then, Kawabata et al. [70] proposed the Alkali-Wrapped Concrete Prism Test (AW-CPT)

to also avoid the leaching issues presented in CPT method. Similar to the wrapped method, concrete specimens are wrapped with a wet cloth, but in this case, the alkali concentration must mimic the pore solution pH.

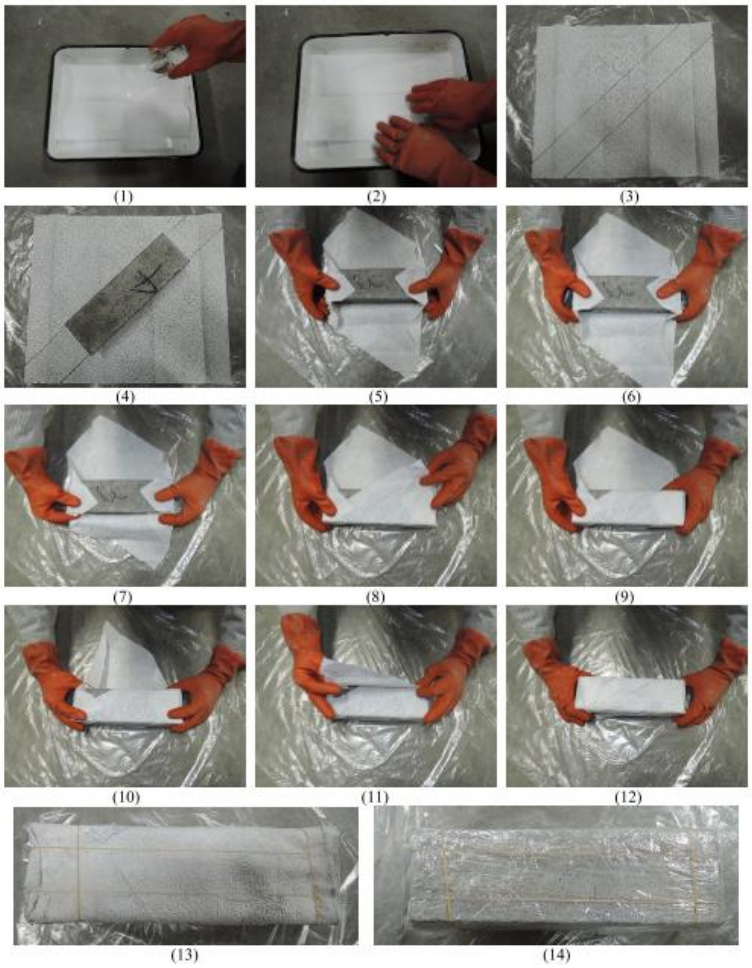

Figure 2.16. Wrapping procedure for AW-CPT [70].

It was proposed to use Equation 2.11 to calculate the concrete pore solution hydroxide ion concentration. It was concluded that compared to the CPT method, the alkali leaching and drying were significantly reduced. However, the alkali content of concrete mixtures was increased by 20% due to the transfer of alkalis from the wrap to the concrete pores. It may be explained by the water

uptake during the cement hydration, which reduces at later ages. Moreover, it was concluded that at 60ºC and with high alkali boosting, the ASR gel was extruded out without significantly expanding the specimen. Temperatures below 40ºC were recommended for ASR gel to exert tensile pressure in the concrete matrix. Although promising results were shown, further validation is still required for this test method [73].

$$[OH^-] = \frac{0386\ x\ Na_2O_{eq}}{w/c} \qquad \text{Equation 2.11}$$

Another method proposed by several authors is the soaked method, where concrete specimens are soaked in NaOH solution at 38ºC. A previous study evaluated the amount of alkali released by the aggregates when specimens are soaked in 0.7 NaOH solution and 0.7 KOH solution [74]. It was concluded that 0.7 M solution is closer to the pore solution than samples soaked in water or lime-saturated solution, which resulted in higher alkali release as it is a more aggressive solution. Although it overcomes the issues faced by CPT method, it is recommended to assess the maximum expansion capacity of the material as it presents faster kinetics and a higher ultimate expansion compared to a conventional method. Gao et al. [75] also study the immersed method with three different NaOH storage concentrations (i.e., 0.77, 1.00, and 1.25 mol/l). It is worth noting that the samples were boosted (NaOH solutions were added to the water during batching) to match the pore solution to the storage solution concentration. It was concluded that when samples were stored with abundant alkalis, the alkali concentration does not affect the expansion. Moreover, it was recommended to use smaller samples to accelerate the test procedure, that is, to achieve the final expansion in a shorter time.

A concrete cylinder test (CCT) was proposed by Naranjo in 2012 [70,73], where a cylinder is used to insulate the concrete specimen from alkali leaching. Since the specimen is shorter than the cylinder, the water pond can be placed on top of the concrete. Figure 2.17 displays an example of CCT setup. Moreover, filter paper must be installed along the cylinder to allow water to be transferred to the concrete lateral surface. It was concluded that the concrete cylinder test shortens the test duration to assess the AAR evolution.

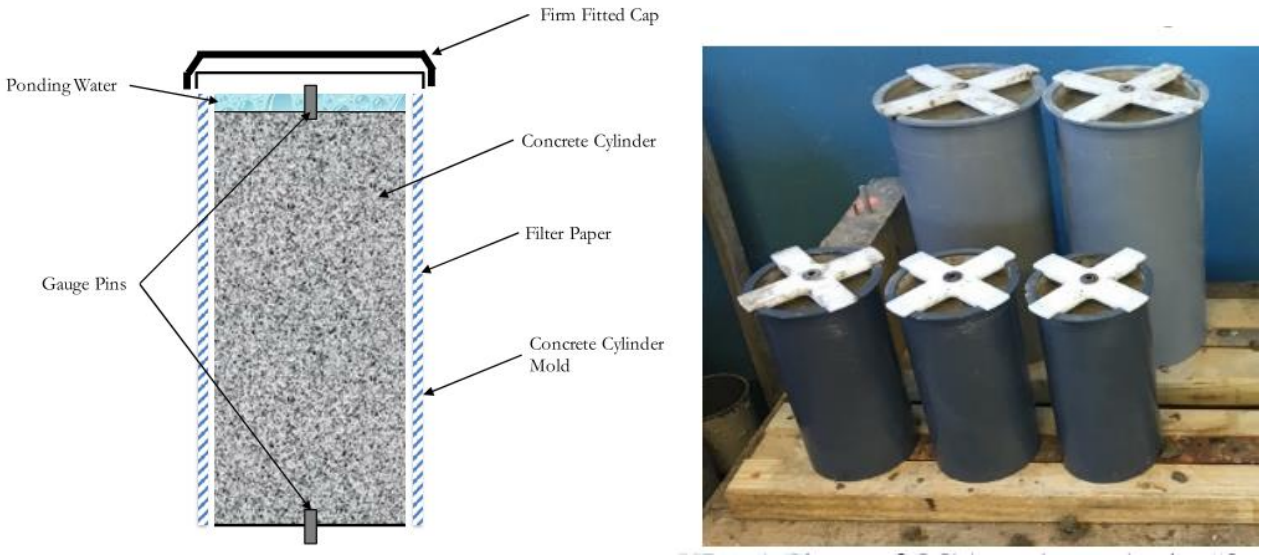

Figure 2.17. CCT setup and specimens.

2.8 Current gaps and improvement opportunities

The construction industry is committed to concrete net zero by 2050 [76,77]. Therefore, one of the largest issues this sector is currently experiencing is related to material sustainability, as concrete is usually developed with a high amount of cement, which is the main source of carbon dioxide (CO_2) emissions [1,2], as previously discussed in the literature review.

In the last century, many efforts have been made to incorporate distinct materials as a partial replacement of cement, especially SCMs and fillers; yet mix-design techniques are still limited to

concrete fresh and hardened state performance combined with durability aspects. The reluctance towards a methodology that accounts for material sustainability, or even, has eco-efficiency as the governing factor, leads the world to its main battle: to combat CO_2 emissions.

In the last 20 years, PPMs have been applied to aid the development of more sustainable concrete mixtures [4,20,37,48–50,78]. Nonetheless, sustainability commitments aim to reduce 30% of the concrete industry's 1990 carbon emissions by 2030; therefore, all the efforts made until now are insufficient to win the CO_2 battle, highlighting the importance of creating a standard mix-design procedure focused on reducing CO_2 emissions. However, before developing a procedure for that, the following questions should be answered.

- Which material can surpass cement production? Every year, approximately 6,000 million tonnes of filler are produced, making it one of the few materials that outnumber Portland cement production.
- When reducing Portland cement content in a concrete mixture, is it possible to develop mixtures with distinct fresh-state behaviour? Based on CSA recommendations and the ACI design method, concrete mix-designs are currently developed based on three slumps ranges: 50-75mm, 75-100 mm, and 150-175 mm.
- What is the effect of fillers and low cement content on the hardened and durability aspects of concrete mixtures? New parameters must be developed to predict these performances of mixtures developed with low cement content and high limestone filler addition, as conventional Abrams law may be insufficient to fully comprehend eco-efficient mixtures.
- How can concrete durability impact the overall sustainability of a structure? While it is crucial to produce sustainable materials with performances that are comparable or superior

to conventional concrete mixtures in fresh and hardened states, durability characteristics are also a decisive factor that will validate the materials eco-efficiency and their viability for use in the future. If the materials' durability has lower performance, the service life of the construction will be shortened, resulting in more waste from demolition and higher maintenance costs.

- What is the effect of reducing concrete's cement/alkali content on one of the most common distress mechanisms: Alkali aggregate reaction (ASR)? Standards recommend the use of supplementary cementing materials (SCMs) to limit the total alkali content, concrete alkali content can be reduced even without the addition of SCMs if an advanced mix-design technique is chosen.
- How can ASR-expansion and damage generation be appraised on eco-efficient mixtures? Despite the fact that the concrete Prism Test (CPT) [79] is the most commonly used standard test method to quantify ASR expansion over accelerated test configuration, is it the ideal test setup to investigate eco-efficient concrete manufactured with low cement content?

2.9 References

[1] J. Di Filippo, J. Karpman, J.R. Deshazo, J. Di Filippo, J. Karpman, J.R. Deshazo, The impacts of policies to reduce CO2 emissions within the concrete supply chain, Cem. Concr. Compos. 101 (2019) 67–82. https://doi.org/10.1016/j.cemconcomp.2018.08.003.

[2] L.K. Turner, F.G. Collins, Carbon dioxide equivalent (CO2-e) emissions: A comparison between geopolymer and OPC cement concrete, Constr. Build. Mater. 43 (2013) 125–130. https://doi.org/10.1016/j.conbuildmat.2013.01.023.

[3] S. Ruan, C. Unluer, Influence of supplementary cementitious materials on the performance and environmental impacts of reactive magnesia cement concrete, J. Clean. Prod. 159 (2017) 62–73. https://doi.org/10.1016/j.jclepro.2017.05.044.

[4] P.R. de Matos, R.D. Sakata, L.R. Prudêncio, Eco-efficient low binder high-performance self-compacting concretes, Constr. Build. Mater. 225 (2019) 941–955. https://doi.org/10.1016/j.conbuildmat.2019.07.254.

[5] M. Sonebi, Y. Ammar, P. Diederich, Sustainability of cement, concrete and cement replacement materials in construction, in: J.M. Khatib (Ed.), Sustain. Constr. Mater., Elsevier, 2016: pp. 371–396. https://doi.org/10.1016/b978-0-08-100370-1.00015-9.

[6] M. Thomas, Supplementary cementing materials in concrete, CRC Press Taylor & Francis Group, 2013. https://doi.org/10.1201/b14493.

[7] F. Pacheco Torgal, S. Miraldo, J.A. Labrincha, J. De Brito, An overview on concrete carbonation in the context of eco-efficient construction: Evaluation, use of SCMs and/or RAC, Constr. Build. Mater. 36 (2012) 141–150. https://doi.org/10.1016/j.conbuildmat.2012.04.066.

[8] S.A. Miller, V.M. John, S.A. Pacca, A. Horvath, Carbon dioxide reduction potential in the global cement industry by 2050, Cem. Concr. Res. 114 (2018) 115–124. https://doi.org/10.1016/j.cemconres.2017.08.026.

[9] K.L. Scrivener, V.M. John, E. Gartner, Eco-efficient cements : Potential economically viable solutions for a low-CO 2 cement-based materials industry, Cem. Concr. Res. 114 (2018) 2–26. https://doi.org/10.1016/j.cemconres.2018.03.015.

[10] S.H. Kang, Y. Jeong, K.H. Tan, J. Moon, High-volume use of limestone in ultra-high performance fiber-reinforced concrete for reducing cement content and autogenous shrinkage, Constr. Build. Mater. 213 (2019) 292–305. https://doi.org/10.1016/j.conbuildmat.2019.04.091.

[11] U.N. Environment, K.L. Scrivener, V.M. John, E.M. Gartner, Eco-efficient cements: Potential economically viable solutions for a low-CO2 cement-based materials industry, Cem. Concr. Res. 114 (2018). https://doi.org/10.1016/j.cemconres.2018.03.015.

[12] Y. Knop, A. Peled, Packing density modeling of blended cement with limestone having different particle sizes, Constr. Build. Mater. 102 (2016) 44–50.

[13] J.L. Gallias, R. Kara-Ali, J.P. Bigas, The effect of fine mineral admixtures on water requirement of cement pastes, Cem. Concr. Res. . 30 (2000) 1543–1549. https://doi.org/10.1016/S0008-8846(00)00380-X.

[14] Y. Knop, A. Peled, Setting behavior of blended cement with limestone: influence of particle size and content, Mater. Struct. 49 (2016) 439–452.

[15] T. Oey, A. Kumar, J.W. Bullard, N. Neithalath, G. Sant, The filler effect: The influence of filler content and surface area on cementitious reaction rates, J. Am. Ceram. Soc. 96 (2013) 1978–1990. https://doi.org/10.1111/jace.12264.

[16] V.M. John, B.L. Damineli, M. Quattrone, R.G. Pileggi, Fillers in cementitious materials — Experience, recent advances and future potential, Cem. Concr. Res. 114 (2018) 65–78. https://doi.org/10.1016/j.cemconres.2017.09.013.

[17] V. Bonavetti, H. Donza, G. Menéndez, O. Cabrera, E.F. Irassar, Limestone filler cement in low w/c concrete: A rational use of energy, Cem. Concr. Res. 33 (2003) 865–871. https://doi.org/10.1016/S0008-8846(02)01087-6.

[18] S.A.A.M. Fennis, J.C. Walraven, Using particle packing technology for sustainable concrete mixture design, Heron. 57 (2012) 73–101.

[19] M. Grazia, L.F.M. Sanchez, R. Romano, R.G. Pileggi, M.T. de Grazia, L.F.M. Sanchez, R. Romano, R.G. Pileggi, M. T. de Grazia, L. F. M. Sanchez, R. C. O. Romano, R. G. Pileggi, Evaluation of the Fresh and Hardened State Properties of Low-Cement Content (LCC) Systems, Mag. Concr. Res. 72 (2018) 1–14. https://doi.org/10.1680/jmacr.18.00271.

[20] M. T. de Grazia, L. F. M. Sanchez, R. C. O. Romano, R. G. Pileggi, M.T. de Grazia, L. Sanchez, R.C.O. Romano, R.G. Pileggi, M. T. de Grazia, L. F. M. Sanchez, R. C. O. Romano, R. G. Pileggi, Investigation of the use of continuous particle packing models (PPMs) on the fresh and hardened properties of low-cement concrete (LCC) systems, Constr. Build. Mater. 195 (2019) 524–536. https://doi.org/10.1016/j.conbuildmat.2018.11.051.

[21] B. Lothenbach, G. Le Saout, E. Gallucci, K. Scrivener, Influence of limestone on the hydration of Portland cements, Cem. Concr. Res. 38 (2008) 848–860. https://doi.org/10.1016/j.cemconres.2008.01.002.

[22] B.L. Damineli, V.M. John, B. Lagerblad, R.G. Pileggi, Viscosity prediction of cement-filler suspensions using interference model: A route for binder efficiency enhancement, Cem. Concr. Res. 84 (2016) 8–19.

[23] C. Varhen, I. Dilonardo, C. Romano, R.G. Pileggi, A. Figueiredo, Effect of the substitution of cement by limestone filler on the rheological behaviour and shrinkage of microconcretes, Constr. Build. Mater. 125 (2016) 375–386.

[24] H.R. Shadkam, S. Dadsetan, M. Tadayon, L.F.M. Sanchez, A. Zakeri, An investigation of the effects of limestone powder and Viscosity Modifying Agent in durability related parameters of self-consolidating concrete (SCC), Constr. Build. Mater. 156 (2017) 152–160.

[25] K.D. Ingram, K.E. Daugherty, A Review of Limestone Additions to Portland Cement and Concrete, Cem. Concr. Compos. 13 (1991) 165–170.

[26] B. Lothenbach, K. Scrivener, R.D. Hooton, Supplementary cementitious materials, Cem. Concr. Res. 41 (2011) 217–229.

[27] P. Krstulovi¢, N. Kamenk, K. Popovi¢, A new approach in evaluation of filler effect in cement effect on strength and workabiliity of mortar and concrete, Cem. Concr. Res. 24 (1994) 721–727.

[28] R.C.O. Romano, H. Schreurs, V.M. John, R.G. Pileggi, Influence of the dispersion process in the silica fume properties, Cerâmica. 54 (2008) 456–461.

[29] A.K. Castro, V.C. Pandolfelli, Review: Concepts of particle dispersion and packing for special concretes production, 18 Cerâmica. 55 (2009) 18–32.

[30] T.E. Oey, A. Kumar, J.W. Bullard, N. Neithalath, G. Sant, The Filler Effect: The Influence of Filler Content and Surface Area on Cementitious Reaction Rates, J. Am. Ceram. Soc. 96 (2013) 1978–1990. https://doi.org/10.1111/jace.12264.

[31] R. Kurad, J.D. Silvestre, J. de Brito, H. Ahmed, Effect of incorporation of high volume of recycled concrete aggregates and fly ash on the strength and global warming potential of concrete, J. Clean. Prod. 166 (2017) 485–502. https://doi.org/10.1016/j.jclepro.2017.07.236.

[32] B.L. Damineli, F.M. Kemeid, P.S. Aguiar, V.M. John, Measuring the eco-efficiency of cement use, Cem. Concr. Compos. 32 (2010) 555–562.

[33] O.H. Wallevik, W.I. Mansour, F.H. Yazbeck, T.I. Kristjansson, EcoCrete-Xtreme: Extreme performance of a sustainable concrete, Proc. Int. Symp. Eco-Crete. (2014) 3–10.

[34] P. Goltermann, V. Johansen, L. Palbøl, Packing of Aggregates : An Alternative Tool to Determine the Optimal Aggregate Mix, ACI Mater. J. (1997) 435–442.

[35] M.N. Mangulkar, S.S. Jamkar, Review of particle packing theories used for concrete mix proportioning, Int. J. Sci. Eng. Res. 4 (2013) 143–148.

[36] R. Yu, P. Spiesz, H.J.H. Brouwers, Mix design and properties assessment of Ultra-High Performance Fibre Reinforced Concrete (UHPFRC), Cem. Concr. Res. 56 (2014) 29–39. https://doi.org/10.1016/j.cemconres.2013.11.002.

[37] S. Kumar, M. Santhanam, S. Kunar, M. Santhanam, Particle packing theories and their application in concrete mixture proportioning : A review, Indian Concr. J. 77 (2003) 1324–1331.

[38] J.E. Funk, D.R. Dinger, Predictive process control of crowded particulate suspensions, 1st ed., New York, 1994. https://doi.org/10.1007/978-1-4615-3118-0.

[39] I. Mehdipour, K.H. Khayat, Understanding the role of particle packing characteristics in rheo-physical properties of cementitious suspensions : A literature review, Constr. Build. Mater. 161 (2018) 340–353.

[40] S.A.A.M. Fennis, J.C. Walraven, J.A. den Uijl, Compaction-interaction packing model: regarding the effect of fillers in concrete mixture design, Mater. Struct. 46 (2013) 463–478. https://doi.org/10.1617/s11527-012-9910-6.

[41] I.R. Oliveira, A.R. Studart, R.G. Pileggi, V.C. Pandolfelli, Dispersão e Empacotamento de Partículas, Fazendo Arte Editorial, São Paulo, 2000.

[42] M.T. de Grazia, L.F.M. Sanchez, R.G. Pileggi, Evaluation of the fresh and hardened state properties of low cement content systems, Mag. Concr. Res. 72 (2018) 232–245.

[43] F. De Larrard, A. Belloc, The influence of aggregate on the compressive strength of normal and high-strength concrete, ACI Mater. J. 94 (1997) 417–426.

[44] R.C.D.O. Romano, D. Dos, R. Torres, R.G. Pileggi, Impact of aggregate grading and air-entrainment on the properties of fresh and hardened mortars, Constr. Build. Mater. 82 (2015) 219–226.

[45] A.P. Silva, A.M. Segadães, T.C. Devezas, MPT influence on the rheological behaviour of self-flow refractory castables, Mater. Sci. Forum. 587–588 (2008) 133–137. https://doi.org/10.4028/www.scientific.net/msf.587-588.133.

[46] P. Bonadia, A. Studart, R. Pileggi, V. Pandolfelli, Aplicação do conceito de distância de separação interagregado (MPT) a concretos refratários de alta alumina, (1999).

[47] M.D.M. Innocentini, R.G. Pileggi, F.T. Ramal, V.C. Pandolfelli, Permeability and drying behavior of PSD-designed refractory castables, Am. Ceram. Soc. Bull. 82 (2003).

[48] W. Zuo, J. Liu, Q. Tian, W. Xu, W. She, P. Feng, C. Miao, Optimum design of low-binder Self-Compacting Concrete based on particle packing theories, Constr. Build. Mater. 163 (2018) 938–948. https://doi.org/10.1016/j.conbuildmat.2017.12.167.

[49] B. Esmaeilkhanian, K.H. Khayat, O.H. Wallevik, Mix design approach for low-powder self-consolidating concrete: Eco-SCC-content optimization and performance, Mater. Struct. 50 (2017) 18. https://doi.org/10.1617/s11527-017-0993-y.

[50] Z.S. Ali, M. Hosseinpoor, A. Yahia, New aggregate grading models for low-binder self-consolidating and semi-self-consolidating concrete (Eco-SCC and Eco-semi-SCC), Constr. Build. Mater. 265 (2020) 120314. https://doi.org/10.1016/j.conbuildmat.2020.120314.

[51] J. Lindgård, Ö. Andiç-Çakir, I. Fernandes, T.F. Rønning, M.D.A. Thomas, Alkali-silica reactions (ASR): Literature review on parameters influencing laboratory performance testing, Cem. Concr. Res. 42 (2012) 223–243. https://doi.org/10.1016/j.cemconres.2011.10.004.

[52] B. Fournier, M.-A. Bérubé, Alkali–aggregate reaction in concrete: a review of basic concepts and engineering implications, Can. J. Civ. Eng. 27 (2000) 167–191.

[53] M. Rashidi, M.C.L. Knapp, A. Hashemi, J.Y. Kim, K.M. Donnell, R. Zoughi, L.J. Jacobs, K.E. Kurtis, Detecting alkali-silica reaction: A multi-physics approach, Cem. Concr. Compos. 73 (2016) 123–135. https://doi.org/10.1016/j.cemconcomp.2016.07.001.

[54] T. Katayama, The so-called alkali-carbonate reaction (ACR) — Its mineralogical and geochemical details, with special reference to ASR, Cem. Concr. Res. 40 (2009) 643–675. https://doi.org/10.1016/j.cemconres.2009.09.020.

[55] T. Katayama, P.E. Grattan-Bellew, Petrography of the Kingston experimental sidewalk at age 22 years--ASR as the cause of deleteriously expansive, socalled alkali-carbonate reaction, in: Proc. 14th Int. Conf. Alkali-Aggregate React. Concr. Austin, Texas, USA, 2012: p. 10.

[56] M. Beyene, A. Snyder, R.J. Lee, M. Blaszkiewicz, Alkali Silica Reaction (ASR) as a root cause of distress in a concrete made from Alkali Carbonate Reaction (ACR) potentially susceptible aggregates, Cem. Concr. Res. 51 (2013) 85–95. https://doi.org/10.1016/j.cemconres.2013.04.014.

[57] L. Sanchez, B. Fournier, M. Jolin, D. Mitchell, J. Bastien, Overall assessment of Alkali-Aggregate Reaction (AAR) in concretes presenting different strengths and incorporating a wide range of reactive aggregate types and natures, Cem. Concr. Res. 93 (2017) 17–31. https://doi.org/10.1016/j.cemconres.2016.12.001.

[58] D.J. De Souza, L.F.M. Sanchez, M.T. De Grazia, Evaluation of a direct shear test setup to quantify AAR-induced expansion and damage in concrete, Constr. Build. Mater. 229 (2019). https://doi.org/10.1016/j.conbuildmat.2019.116806.

[59] T. Prinčič, P. Štukovnik, S. Pejovnik, G. De Schutter, V.B. Bosiljkov, Observations on dedolomitization of carbonate concrete aggregates, implications for ACR and expansion, Cem. Concr. Res. 54 (2013) 151–160. https://doi.org/10.1016/j.cemconres.2013.09.005.

[60] B. Fournier, R. Chevrier, A. Bilodeau, P.-C. Nkinamubanzi, N. Bouzoubaa, Comparative Field and Laboratory Investigations on the Use of Supplementary Cementing Materials (SCMs) to Control Alkali-Silica Reaction (ASR) In Concrete, 15th Int. Conf. Alkali-Aggregate React. (ICAAR. (2016).

[61] M.H. Shehata, M.D.A. Thomas, Use of ternary blends containing silica fume and f ly ash to suppress expansion due to alkali-silica reaction in concrete, Cem. Concr. Reserach. 32 (2002) 341–349. https://doi.org/10.1016/S0008-8846(01)00680-9.

[62] CSA A23.2-27A, Standard pratice to identify degree of alkali-reactivity of aggregates and to indentify measures to avoid deleterious expasion in concrete, CSA International, Mississauga, Ontario (Canada), 2009.

[63] W. Yujiang, A.E. Deng, M. Ae, T. Mingshu, Alkali release from aggregate and the effect on AAR expansion, Mater. Struct. 41 (2008) 159–171. https://doi.org/10.1617/s11527-007-9227-z.

[64] M.-A. Berube, J. Frenette, Testing Concrete for AAR in NaOH and NaCl solutions at 38°C and 80°C, Cem. Concr. Compos. 16 (1994) 189–198.

[65] S.U. Einarsdóttir, Modifications to Laboratory Test Methods to Evaluate the Beneficial Effects of Low-Alkali Binders on the Alkali-Silica Reaction Modifications to Laboratory Test Methods to Evaluate the Beneficial Effects of Low-Alkali Binders on the Alkali-Silica Reaction, University of Toronto, 2017.

[66] S.U. Einarsdottir, R. Douglas Hooton, Modifications to ASTM C1293 that allow testing of low-Alkali binder systems, ACI Mater. J. 115 (2018) 739–747. https://doi.org/10.14359/51702350.

[67] B. Fournier, J.H. Ideker, K.J. Folliard, M.D.A. Thomas, P.C. Nkinamubanzi, R. Chevrier, Effect of environmental conditions on expansion in concrete due to alkali-silica reaction (ASR), Mater. Charact. 60 (2009) 669–679. https://doi.org/10.1016/j.matchar.2008.12.018.

[68] M. T. de Grazia, N. Goshayeshi, R. Gorga, L. F.M. Sanchez, A.C. Santos, D.J. Souza, Comprehensive semi-empirical approach to describe alkali aggregate reaction (AAR) induced expansion in the laboratory, J. Build. Eng. 40 (2021). https://doi.org/10.1016/j.jobe.2021.102298.

[69] ASTM C1293, Standard Test Method for Determination of Length Change of Concrete Due to Alkali-Silica Reaction, West Conshohocken, 2018. https://doi.org/10.1520/C1293-18.

[70] Y. Kawabata, K. Yamada, Y. Sagawa, S. Ogawa, Alkali-Wrapped Concrete Prism Test (AW-CPT) - New testing protocol toward a performance test against alkali-silica reaction, J. Adv. Concr. Technol. 16 (2018) 441–460. https://doi.org/10.3151/jact.16.441.

[71] J. Lindgård, E.J. Sellevold, M.D.A. Thomas, B. Pedersen, H. Justnes, F. Rønning, Alkali-silica reaction (ASR)-performance testing: Influence of specimen pre-treatment, exposure conditions and prism size on concrete porosity, moisture state and transport properties, Cem. Concr. Res. 53 (2013) 145–167. https://doi.org/10.1016/j.cemconres.2013.05.020.

[72] J. Lindgård, M.D.A. Thomas, E.J. Sellevold, B. Pedersen, Ö. Andiç-Çakır, H. Justnes, T.F. Rønning, Alkali-silica reaction (ASR)-performance testing: Influence of specimen pre-treatment, exposure conditions and prism size on alkali leaching and prism expansion, Cem. Concr. Res. 53 (2013) 68–90. https://doi.org/10.1016/j.cemconres.2013.05.017.

[73] S. Stacey, K.J. Folliard, T. Drimalas, M.D.A.A. Thomas, An Accelerated and More Accurate Test Method To ASTM C1293: the Concrete Cylinder Test, 15th Int. Conf. Alkali-Aggregate React. (2016) 11p.

[74] M.-A. Bérubé, J. Duchesne, J.F. Dorion, M. Rivest, Laboratory assessment of alkali contribution by aggregates to concrete and application to concrete structures affected by alkali-silica reactivity, Cem. Concr. Res. 32 (2002) 1215–1227.

[75] X.X. Gao, S. Multon, M. Cyr, A. Sellier, Optimising an expansion test for the assessment of alkali-silica reaction in concrete structures, Mater. Struct. 44 (2011) 1641–1653. https://doi.org/10.1617/s11527-011-9724-y.

[76] Global Cement and Concrete Association, Our path to net zero, (2022). https://gccassociation.org/concretefuture/our-path-to-net-zero/ (accessed March 17, 2022).

[77] Joint statement: Canada's Cement Industry and the Government of Canada announce a partnership to establish Canada as a global leader in low-carbon cement and to achieve net-zero carbon concrete - Innovation, Science and Economic Development Canada, (n.d.). https://www.ic.gc.ca/eic/site/icgc.nsf/eng/07730.html (accessed March 17, 2022).

[78] M. Anson-Cartwright, Optimization of aggregate gradation combinations to improve concrete sustainability and durability, MASc Thesis, University of Toronto, 2011.

[79] ASTM C1293, Determination of Length Change of Concrete Due to Alkali-Silica Reaction, 2015. https://doi.org/10.1520/C1293-18.2.

Chapter Three: Research Program

This study proposes the use of a PPMs-MP approach to enhance the short- and long-term performance of concrete mixtures. In terms of short-term performance, the correct use of PPMs may enhance the granular skeleton of concrete, reducing its overall porosity and improving the material sustainability, while MP enhances its fresh state behaviour. Moreover, in Canada, concrete mix-designs are governed by durability aspects rather than strength (i.e., the selection of water-to-cement ratio - w/c - is more conservative than the targeted strength), increasing concrete sustainability while maintaining the required slump and compressive strength values is typically difficult. Porosity, which is also affected by w/c, is another key property to ensure the durability and long-term performance of granular mixtures such as concrete, regardless of the deterioration mechanism involved. However, there is still a lack of studies providing information on the performance of highly packed eco-efficient concrete against alkali-aggregate reaction (ASR), a common durability-related mechanisms found in Canada and worldwide.

Based on North American standard recommendations (e.g., CSA and ACI), concrete mix-design is selected based on the slump (Table 3.1), the suggested water content for non-air entrained mixtures with a maximum aggregate size (e.g., Table 3.1), and exposure class (Table 3.2).

Class exposures C, F, and N correspond to concrete exposed to chloride, freezing and thawing, and non-exposure to chloride neither freezing and thawing cycles, respectively. It is worth noting that concrete resistance to freezing and thawing deterioration process is out of the scope of this research, hence, the air content recommendation is not presented in Table 3.2.

Table 3.1: Different slump range recommendations.

Slump Range (mm)	Water Content for Non-Air Entrained Concrete with Maximum Aggregate Size 20 mm (kg/m^3)
25 to 50	190
75 to 100	205
150 to 175	216

Although Table 3.2 can be used as guidance for the maximum w/c to develop eco-efficient concrete mixtures when the cement content is reduced the w/c must be increased to maintain the minimum flow requirements. Hence, highly packed eco-efficient concrete developed with PPM, does not follow the conventional Abrams law which would allow standards to specify the maximum w/c for the required performance against durability. Therefore, further studies are required to fully understand the relationship between compressive strength and w/c on eco-efficient mixtures and how they can be classified according to the exposure class table as per CSA A23.1 [1], highlighting the importance of Papers II and III of this Ph.D., which provide charts to increase the sustainability of concrete mixtures for any required fresh and hardened state performance, assisting the selection of w/c, and provides models to predict compressive strength of the sustainable mixtures developed.

Table 3.2: Concrete exposure class and their requirements.

Class of exposure	Maximum w/c	Minimum 28-Day Compressive Strength (MPa)
C-1	0.40	35
C-2	0.45	32
C-3	0.50	30
C-4	0.55	25
F-1	0.50	30
F-2	0.55	25
N	For structural design	For structural design

Once the fresh and short-term hardened state performance of eco-efficient concrete is modelled and understood (Paper II and III), there will be still a need to check their suitability against a deterioration mechanism (e.g., ASR). As such, Paper IV and Paper V investigate the long-term performances of

eco-efficient mixtures selected based on key mix-design features: 1) sustainability (e.g., cement content) and 2) mechanical behaviour (w/c and compressive strength).

3.1 Topic 1: Develop eco-efficient concrete mixtures with PPM-MP approach

To address the short-term performance of eco-efficient concrete mixtures, a comprehensive evaluation of distinct types of low cement content is proposed in this phase. A total of 288 cylinders were developed within twelve concrete mixtures with a proposed PPM-MP approach containing distinct ranges of cement content (e.g., 320, 250, 200, 150 kg/m^3). Moreover, three groups of fresh-state and mechanical performance were investigated: slumps of 180, 90, and 20 +/- 20 mm and compressive strengths ranging from 18 to 45 MPa, which are the most common ones recommended as per ACI 211-1 [2] and CSA A23.1 [1]. To better understand the impact of the w/c (classified as high – H, medium – M, and low – L) on the compressive strength of low cement concrete, three w/c were selected for each type of cement content. A summary of the eco-efficient mixtures developed is presented in Figure 3.1.

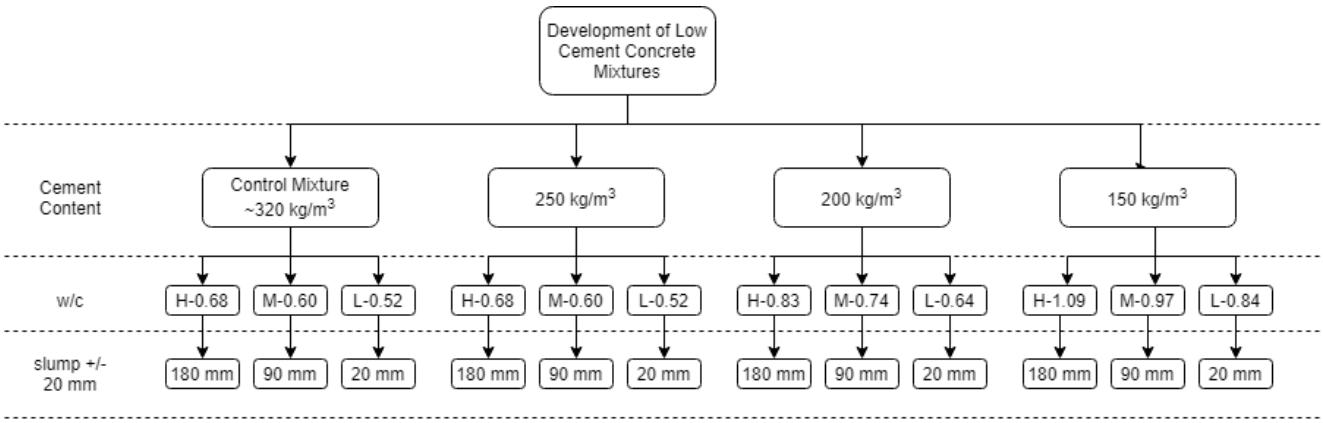

Figure 3.1. Summary of the twelve eco-efficient concrete mixtures.

3.2 Topic 2: Long-term performance of the eco-efficient mixtures

Topic 1 proved the feasibility of producing eco-efficient concrete mixtures through PPM-MP approach and with distinct rheological and mechanical performance; however, the long-term performance must be appraised to confirm the ability to use low cement concrete in the construction industry. Alkali silica reaction (ASR) is the distress mechanism selected to be investigated in Topic 2, as Canada is one of the countries with more reactive aggregates, emphasizing the need of studying the long-term performance of eco-efficient concrete with reactive aggregates. Since these mixtures can be classified as low alkali systems, the possibility of using reactive aggregate at least partially without significant expansion (i.e., damage) may contribute to the Canadian concrete industry. Figure 3.2 shows the summary of the eco-efficient mixtures pre-selected from Topic 1 based on their compressive strength to appraise the long-term performance. A total of 384 cylinders were cast to appraise the ASR of a reactive coarse aggregate, whereas 144 cylinders were manufactured to assess the ASR development of a reactive fine aggregate.

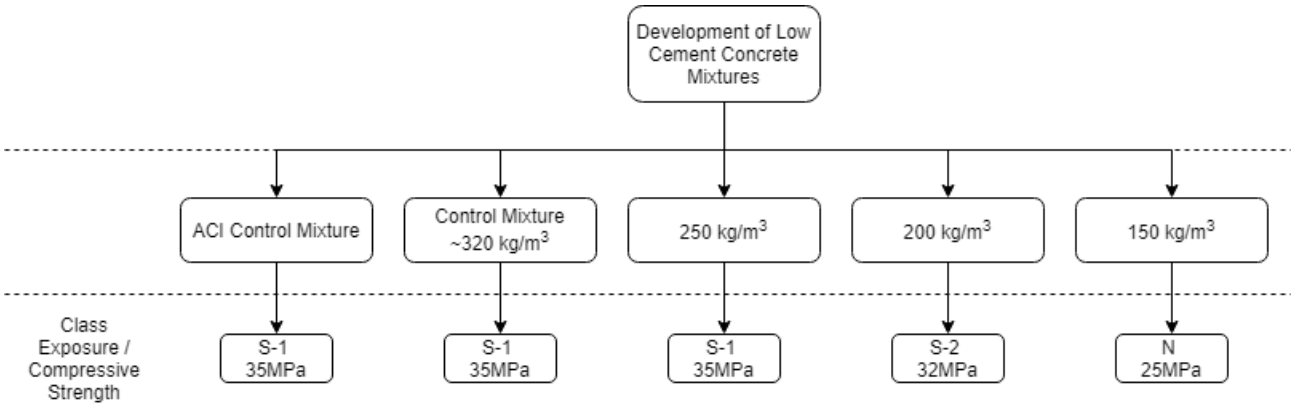

Figure 3.2. Summary of long-term performance eco-efficient concrete mixtures.

3.3 Techniques to evaluate concrete fresh state performance

3.3.1 Slump and rheology over time

The fresh state performance of twelve mixtures appraised in Topic 1 was evaluated through slump and rheology tests over time (i.e., 0, 15, and 30 minutes). Concrete's slump was measured using a conventional slump cone as per CSA A23.1 [1] and the slump loss was calculated by Equation 3.1.

$$Slump\ Loss\ (\%) = \frac{(S_i - S_t)}{S_i} * 100 \qquad \text{Equation 3.1}$$

where S_i is the initial slump and S_t is the slump measured at a time (t).

The rheology test was performed using a planetary rheometer (IBB - Figure 3.3a) with an H-shape impeller (100 mm height and 130 mm length) and a bowl with a diameter of 360 mm and 250 mm height [3].

a) b)

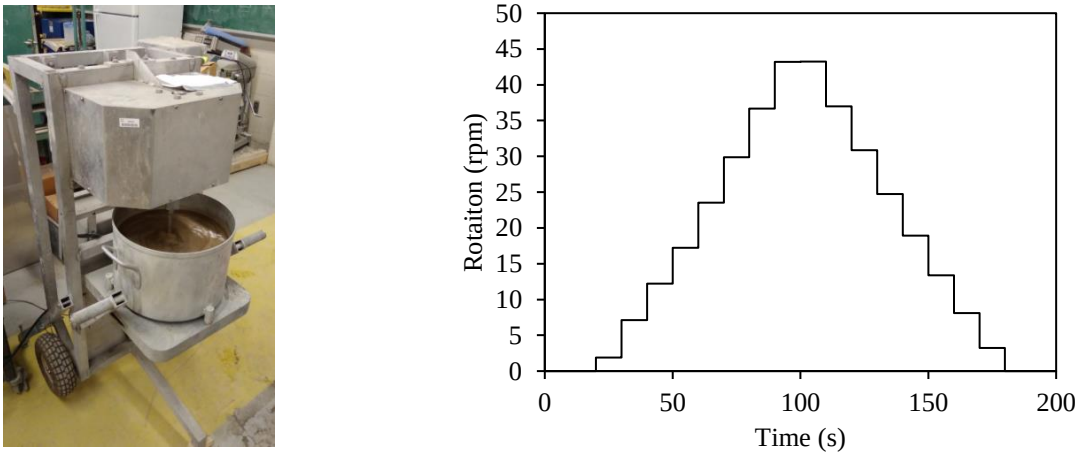

Figure 3.3. a) IBB rheometer and b) test programme used for analyzing the rheology cycle.

Moreover, this rheometer is recommended to appraise concrete mixtures with slumps ranging from 40 mm to 300 mm [4]. This rheometer contains a pre-programmed cycle that increases the shear rate

up to 0.7 s^{-1}, then it decreases at the same stepwise maintaining the rotation for roughly 10 seconds at each step (180 seconds per cycle - Figure 3.3b). First, a complete cycle was applied as a pre-shear regime. Then the flow curves were determined after applying the second cycle on each mixture appraised. Although the IBB rheometer has two Bingham output parameters (i.e., G – yield stress in N.m, and H – plastic viscosity in N.m.s), it is known that not all concrete mixtures display a Bingham behaviour; therefore, to better investigate the mixture rheological behaviour, the IBB dataset was retrieved and the flow curves were plotted [3,4]. It is worth highlighting that the IBB rheometer results are not presented in fundamental units (e.g., yield stress - Pa and plastic viscosity - Pa.s) [3,4].

3.4 Techniques to evaluate concrete hardened state performance

3.4.1 Electrical resistivity

Two types of electrical resistivity (i.e., bulk and surface ER) were performed at 3, 7, 14, and 28 days on all samples. Uniaxial electrical resistivity (ER) test, which is also known as bulk ER, was performed according to ASTM C1760 [5]. Three concrete cylinders of each mixture were placed between two electrodes. It is worth noting that a wet sponge is placed between the concrete-electrode interface to ensure a proper electrical connection. The resistance (R) is displayed in the equipment and then electrical resistivity (ρ) can be calculated by multiplying the geometric factor and the resistance (Equation 3.2). The geometrical k-factor was calculated through Equation 3.3. In this work, the average k value of 4.15 cm was calculated based on the cylinders' dimensions.

$$\rho = k * R \qquad \text{Equation 3.2}$$

where k is concrete geometric factor, R is concrete resistance, and ρ is concrete electrical resistivity.

$$k = \frac{A}{\mathrm{L}}$$ Equation 3.3

where k is concrete geometric factor, A is concrete sample transactional area, and L is concrete sample length.

The four-probe (Wenner-array) technique was used to perform the surface ER. A commercial device was selected that automatically displays the surface ER (i.e., measured through four equipment probes).

3.4.2 Porosity

Water porosity and water absorption tests were performed to compare the different properties of each concrete mixture. It was determined based on Archimedes immersion method [6]. After 7-, 14- and 28-days curing, one cylinder of each mixture was cut to obtain three samples of approximately 100 mm diameter and 65mm height. The samples were placed in an oven at 60°C, to avoid the decomposition of concrete products caused by excessive temperature, for approximately 4 days. When the difference between two successive dry mass values was less than 0.3%, the specimen's dry mass (m_d) was determined. First, tests were conducted and it was concluded that a 0.3% change in mass results in an apparent porosity difference of less than 10%. Then, samples were immersed in water and subjected to vacuum ensuring water penetration. After 24 hours of immersion, the immersed (m_i) and wet (m_w) mass values were determined. The apparent porosity (AP) was calculated by Equation 3.4, while the apparent water absorption (WA) was calculated by Equation 3.5.

$$\text{AP}\ (\%) = \frac{m_w - m_i}{m_w - m_d} * 100\% \qquad \text{Equation 3.4}$$

where m_w is the wet mass, m_i is the immersed mass, and m_d is the dry mass.

$$\text{WA}\ (\%) = \frac{m_w - m_d}{m_d} * 100\% \qquad \text{Equation 3.5}$$

where m_w is the wet mass and m_d is the dry mass.

3.4.3 Ultrasonic pulse velocity

Another non-destructive test performed at 3, 7, 14, and 28 days on all samples is the Ultrasonic Pulse Velocity (UPV), which was measured as per ASTM C597 [7]. The concrete dynamic modulus of elasticity (E) was calculated by Equation 3.6.

$$E = \left(\frac{t}{L}\right)^2 \rho * \frac{(1+\mu)(1-2\mu)}{(1-\mu)} \qquad \text{Equation 3.6}$$

where *t* is the time for a constant wavelength to traverse the length of the cylinder, *L* is the length of the cylinder, ρ is the density of the concrete, and μ is the dynamic Poisson's ratio (0.2 mm/mm).

3.4.4 Compressive strength and modulus of elasticity

Compressive strength testing was performed at 3, 7, 14, and 28 days on all mixtures as per ASTM C 39 [8]. Furthermore, the static modulus of elasticity was conducted at 28 days on three samples from each mixture.

3.5 Techniques to develop alkali aggregate reaction

The expansion results for low alkali systems are more affected by leaching than conventional concrete mixtures [9]. In this project, four test methods (i.e., CPT, Encapsulated, Soaked, and

Wrapped) were used to analyze AAR development. CPT is the only one where the mixtures were boosted with 40% of cement alkali, whereas the other three non-boosted methods consist of maintaining the mixtures in contact with 0.4 M of NaOH to avoid leaching. It is worth noting that 0.4 M of NaOH was selected trying to mimic the cement paste pore solution as presented in previous studies [10–12]. After casting, samples were demoulded, and studs were installed in the first 24 hours. Then, zero reading of length, mass and surface ER was performed. After 48-52 hours of casting, specimens were placed in the storage conditions mentioned hereafter.

3.5.1 Concrete prism test

The first test is the standardized (CSA A23.2-14A, ASTM C1293) concrete prism test (CPT) where specimens must be stored at 100% relativity humidity (R.H.) and 38^{o}C [13,14]. However, this method is known to be subjected to excessive leaching of the alkalis, thus leading to lower expansion [9,13,15]. To minimize the impact on the expansion values, concrete mixtures fabricated to be tested under CPT conditions must be boosted to 40% of the cement alkalis, which is approximately equivalent to the total alkali leaching that will occur during a 1-year test [9,13].

3.5.2 Wrapped method

The wrapped method was also used to evaluate concrete ASR expansion of three concrete mixtures. Similar to the method developed by [16,17], concrete specimens were wrapped in wet non-woven cloth soaked in the 0.4 M NaOH solution and covered with polyethylene-low density resin (also known as plastic film) and exposed to a temperature of 38^{o}C. To mimic the concrete pore solution a solution of 0.4 M of NaOH was selected as presented in previous studies [10–12].

3.5.3 Soaked method

Similar to previous studies [18,19], specimens were fully submerged in a 0.4 M NaOH solution in sealed 22-litre plastic pails and stored at 38^{o}C. To ensure that all surfaces of the specimens were in contact with the solution, plastic racks were placed at the bottom of the buckets.

3.5.4 Encapsulated method

Based on the CCT method [20,21], concrete specimens of five mixtures were placed inside plastic bags with 50 ml of 0.4 M NaOH solution and stored at 38^{o}C. Minimum air was kept inside the plastic bags, and they were compressed with an elastic band to ensure the solution is in contact with the specimen.

3.6 Techniques to evaluate damage in concrete

3.6.1 Damage rating index (DRI)

The Damage Rating Index (DRI) is a semi-quantitative microscopic tool developed to assess the damage and its extent in conventional concrete using a stereomicroscope (about 15-16x magnification) [22,23]. Concrete cylinders were cut axially in half using a masonry saw equipped with a notched diamond blade, followed by successive grinding and polishing using a mechanical rotating steel wheel, upon which magnetic grinding and polishing disks are attached whose grits are 30, 60, 140, 280 (80-100 µm), 600 (20-40 µm), 1200 (10-20 µm) and 3000 (4-8 µm). The petrographic distress features (i.e., cracks) are counted in squares drawn with 1 cm^2 on the surface of a polished concrete section. Weighting factors, as per Villeneuve and Fournier [24] - Table 3.3, were applied to balance the importance of each type of crack based on the distress mechanism appraised.

The final DRI number is the weighted value normalized to a concrete surface of 100 cm^2 for

comparative purposes. In summary, the greater the DRI number, the higher the damage to the material. Moreover, the extended version of the DRI (i.e., without applying weighting factors) was used to evaluate the crack propagation and distribution within a concrete specimen [25,26].

Table 3.3. DRI weighing factors for ASR-affected concrete [24]**.**

Petrographic Features	Weighing Factor
Closed Cracks in Aggregate (CCA)	0.25
Opened Cracks in Aggregates (OCA)	2
Crack With Reaction Product in Coarse Aggregate (OCAG)	2
Coarse Aggregate Debonded (CAD)	3
Disaggregate/Corroded Aggregate Particle (DAP)	2
Cracks in Cement Paste (CCP)	3
Cracks with Reaction Product in Cement Paste (CCPG)	3

3.7 References

[1] CSA A23.1:19 / CSA A23.2:19, Concrete materials and methods of concrete construction / Test Methods and standard practices for concrete, Mississauga, ON, 2019.

[2] ACI Committee 211, Standard Practice for Selecting Proportions for Normal Heavyweight , and Mass Concrete (ACI 211 . 1-91) Reapproved 2002, 2004.

[3] P. Banfill, D. Beaupré, F. Chapdelaine, F. de Larrard, P. Domone, L. Nachbaur, T. Sedran, O. Wallevik, J.E. Wallevik, Comparison of concrete rheometers: international tests at LCPC (NISTIR 6819), Nantes, France, 2000.

[4] C. Ferraris, L. Brower, Comparison of Concrete Rheometers: International Tests at MB, (2003) 116.

[5] ASTM C1760, Standard Test Method for Bulk Electrical Conductivity of Hardened Concrete, (2012) 1–5. https://doi.org/10.1520/C1760-12.2.

[6] R.C.D.O. Romano, D. Dos, R. Torres, R.G. Pileggi, Impact of aggregate grading and air-entrainment on the properties of fresh and hardened mortars, Constr. Build. Mater. 82 (2015) 219–226.

[7] ASTM International, ASTM C597 Standard Test Method for Pulse Velocity Through Concrete, ASTM Int. (2016) 4. https://doi.org/10.1520/C0597-16.2.

[8] ASTM C39, Standard Test Method for Compressive Strength of Cylindrical Concrete Specimens, 1999.

[9] S.U. Einarsdottir, R. Douglas Hooton, Modifications to ASTM C1293 that allow testing of low-Alkali binder systems, ACI Mater. J. 115 (2018) 739–747. https://doi.org/10.14359/51702350.

[10] A. Leemann, B. Lothenbach, C. Thalmann, Influence of superplasticizers on pore solution composition and on expansion of concrete due to alkali-silica reaction, Constr. Build. Mater. 25 (2011) 344–350. https://doi.org/10.1016/j.conbuildmat.2010.06.019.

[11] A. Leemann, B. Lothenbach, The influence of potassium-sodium ratio in cement on concrete expansion due to alkali-aggregate reaction, Cem. Concr. Res. 38 (2008) 1162–1168. https://doi.org/10.1016/j.cemconres.2008.05.004.

[12] U. Costa, T. Mangialardi, A.E. Paolini, Minimizing alkali leaching in the concrete prism expansion test at 38 °C, Constr. Build. Mater. 146 (2017) 547–554. https://doi.org/10.1016/j.conbuildmat.2017.04.116.

[13] ASTM C1293, Standard Test Method for Determination of Length Change of Concrete Due to Alkali-Silica Reaction, West Conshohocken, 2018. https://doi.org/10.1520/C1293-18.

[14] C. A23.2-14A, A23.1-14/A23.2-14, Potential expansivity of aggregates (procedure for length change due to alkali-aggregate reaction in concrete prisms at 38 oC), 2014.

[15] M.-A. Berube, J. Frenette, Testing Concrete for AAR in NaOH and NaCl solutions at 38°C and 80°C, Cem. Concr. Compos. 16 (1994) 189–198.

[16] J. Lindgård, E.J. Sellevold, M.D.A. Thomas, B. Pedersen, H. Justnes, F. Rønning, Alkali-silica reaction (ASR)-performance testing: Influence of specimen pre-treatment, exposure conditions and prism size on concrete porosity, moisture state and transport properties, Cem. Concr. Res. 53 (2013) 145–167. https://doi.org/10.1016/j.cemconres.2013.05.020.

[17] J. Lindgård, M.D.A. Thomas, E.J. Sellevold, B. Pedersen, Ö. Andiç-Çakır, H. Justnes, T.F. Rønning, Alkali-silica reaction (ASR)-performance testing: Influence of specimen pre-treatment, exposure conditions and prism size on alkali leaching and prism expansion, Cem. Concr. Res. 53 (2013) 68–90. https://doi.org/10.1016/j.cemconres.2013.05.017.

[18] M.-A. Bérubé, J. Duchesne, J.F. Dorion, M. Rivest, Laboratory assessment of alkali contribution by aggregates to concrete and application to concrete structures affected by alkali-silica reactivity, Cem. Concr. Res. 32 (2002) 1215–1227.

[19] X.X. Gao, S. Multon, M. Cyr, A. Sellier, Optimising an expansion test for the assessment of alkali-silica reaction in concrete structures, Mater. Struct. 44 (2011) 1641–1653. https://doi.org/10.1617/s11527-011-9724-y.

[20] Y. Kawabata, K. Yamada, Y. Sagawa, S. Ogawa, Alkali-Wrapped Concrete Prism Test (AW-CPT) - New testing protocol toward a performance test against alkali-silica reaction, J. Adv. Concr. Technol. 16 (2018) 441–460. https://doi.org/10.3151/jact.16.441.

[21] S. Stacey, K.J. Folliard, T. Drimalas, M.D.A.A. Thomas, An Accelerated and More Accurate Test Method To ASTM C1293: the Concrete Cylinder Test, 15th Int. Conf. Alkali-Aggregate React. (2016) 11p.

[22] L. Sanchez, B. Fournier, M. Jolin, D. Mitchell, J. Bastien, Overall assessment of Alkali-Aggregate Reaction (AAR) in concretes presenting different strengths and incorporating a wide range of reactive aggregate types and natures, Cem. Concr. Res. 93 (2017) 17–31. https://doi.org/10.1016/j.cemconres.2016.12.001.

[23] L.F.M.L.. Sanchez, B.. Fournier, M.. Jolin, J. Duchesne, Reliable quantification of AAR damage through assessment of the Damage Rating Index (DRI), Cem. Concr. Res. 67 (2015) 74–92. https://doi.org/10.1016/j.cemconres.2014.08.002.

[24] V. Villeneuve, B. Fournier, Determination of the damage in concrete affected by ASR–the damage rating index (DRI), in: 14th Int. Conf. Alkali-Aggregate React. Concr., Austin (Texas), 2012: p. electronic.

[25] C. Trottier, R. Ziapour, A. Zahedi, L. Sanchez, F. Locati, Microscopic characterization of alkali-silica reaction (ASR) affected recycled concrete mixtures induced by reactive coarse and fine aggregates, Cem. Concr. Res. 144 (2021) 106426. https://doi.org/10.1016/j.cemconres.2021.106426.

[26] C. Trottier, A. Zahedi, R. Ziapour, L. Sanchez, F. Locati, Microscopic assessment of recycled concrete aggregate (RCA) mixtures affected by alkali-silica reaction (ASR), Constr. Build. Mater. 269 (2021). https://doi.org/10.1016/j.conbuildmat.2020.121250.

Chapter Four: Towards the Design of Eco-efficient Concrete Mixtures: An Overview

De Grazia, M. T.[a], Sanchez, L. F. M.[b], Yahia A.[c]

[a] Ph.D. Candidate – University of Ottawa, Department of Civil Engineering, ON, Canada.

[b] Associate Professor – University of Ottawa, Department of Civil Engineering, ON, Canada.

[c] Full Professor - Université de Sherbrooke, Department of Civil and Building Engineering, QC, Canada.

Abstract

Sustainability is one of the major issues faced by the concrete industry due to the high CO_2 emissions caused by cement production. Although most of the conventional mix-design approaches account for requirements in the fresh and hardened states, along with durability criteria, sustainability is a new key parameter that must be evaluated in concrete production. This paper focuses on disseminating the environmental concerns related to cement, highlighting the importance of using alternative materials as its partial replacement. Moreover, advanced mix-design techniques must be used to further enhance concrete eco-efficiency; hence, an overview of the different types of particle packing models (PPMs) is presented. Combining PPM with limestone fillers as an alternative ready-to-apply method to produce eco-efficient mixtures is then proposed enabling concrete future competitiveness as a sustainable material. Finally, a brief discussion on the fresh and hardened performance of sustainable concrete along with its global warming impact is conducted.

Keywords: *Cement Sustainable Impact, Concrete Eco-efficiency, Alternative Materials, Particle Packing Models, Discrete Models, Continuous Models*

4.1 Introduction

Concrete mixtures are tailored to achieve specific fresh and hardened properties based on the construction requirements. The conventional and standardized mix-design methods, including the ACI and British methods, usually used in the construction industry are based on experimental, analytical, or semi-experimental approaches. For example, in the ACI method, the proportion of concrete ingredients is selected according to the absolute volume of concrete [1]. To proportion a conventional concrete, several characteristics of the components must be predetermined, including material's specific gravities, water absorption, aggregate finesses modulus, coarse aggregate dry rodded bulk density, and maximum particle size. Moreover, the targeted compressive strength and exposure conditions dictate the selection of water-to-cement ratio (w/c) and category of air-void characteristics for durability requirements. Furthermore, the fine and coarse aggregate particle-size distributions (PSD) must be within standard limits. Although it is known that these are the basic properties of the concrete's components, aggregates and powders may also present significant variations in their morphological characteristics, including shape, specific surface area (SSA), packing density, etc. [2–6]. These properties not only affect concrete fresh state behaviour but can also increase the voids between the aggregate particles compromising the concrete hardened and durability aspects [3,7–9] as well as the required paste volume to achieve a given workability.

4.1.1 Problem statement and objectives

Although sustainability is one of the biggest challenges that the civil engineering industry is facing nowadays, high amount of cement, which is the main carbon dioxide (CO_2) emitter [10,11], is used to fill the voids between these aggregates and achieve the required fresh, hardened, and durability properties. Concrete sector is currently with a total CO_2 emission in excess of 2.5 Gt due to cement

production [12]. To overcome these environmental challenges, cement is commonly partially replaced by supplementary cementing materials (SCMs), including fly ash, blast furnace slag, and silica fume [4,10,13,14]. However, their use affects overall physical characteristics of concrete due to differences in morphological characteristics including particle shape, SSA, packing density, and PSD [3,4]. These properties affect significantly concrete workability resulting in complex rheology, distinct compatibility with admixtures, and limitations on applications [4,15]. Besides the issues faced on fresh state, they also presented the lack of early-strength development which may delay the early-age compressive strength. On the other hand, fillers can also be used as cement replacement without affecting negatively concrete workability while increasing the system packing, hence reducing system porosity and improving hardened and long-term performances [16–18].

Global commitments are targeting concrete net zero by 2050. Based on the Global Cement and Concrete Association [12], seven main actions are required to achieve this goal, including 1) savings in clinker production (11% - 430Mt CO_2), 2) efficiency in concrete production (11% - 430Mt CO_2), 3) savings in cement and binders (9% - 350Mt CO_2), 4) decarbonization (5% - 190Mt CO_2), 5) CO_2 sink: recarbonation (6% - 240Mt CO_2), 6) carbon capture and utilization/storage (36% - 1370Mt CO_2), and 7) efficiency in design and construction (22% - 840Mt CO_2). This paper presents solutions for items two and three that correspond to 20% of the total goal. The main objective of this study is to provide a comprehensive understanding of the cement environmental constraints and show the importance of using alternative materials, especially limestone fillers, as a partial replacement for cement. Moreover, to overcome the challenges caused by conventional mix-design, a summary of the existing types of particle packing models (PPMs) and a discussion on different mix-design procedures available in the literature focusing on developing low cement content concrete is discussed [14,19–25].

4.2 Environmental constraints

Concrete mixtures may be considered an eco-friendly material when the standard ingredients (i.e., aggregates and cement) are replaced by low-environmental impact materials that generate lower CO_2 during their production and processing, including recycled materials. There are several examples in the literature of sustainable concrete where fine and/or coarse aggregates are substituted by recycled concrete aggregates, rubber, etc. [26–35]. Nevertheless, cement production accounts for 85% of the CO_2 emitted during raw material production and more than three-quarters of the total concrete's CO_2 emission of concrete from its production to its placement, hence it is considered the concrete component with the lowest sustainable aspect [10,11]. Global Cement and Concrete Association is committed with several countries to achieve Net Zero Concrete by 2050 [36,37]. Yet, sustainability commitments are targeting a reduction of 30% of the concrete industry's 1990 carbon emissions, which may result in a minimum reduction of 15MTs in greenhouse gases (GHG) by 2030. In this context, the following sections will explain the issues related to cement production and alternative methods to reduce carbon footprint.

4.2.1 Cement production

The optimization of a mixture design of concrete targets the three main concrete concerns, including 1) fresh state properties, 2) hardened state properties, and 3) structure durability. However, its sustainability must also be considered due to concerns regarding carbon footprint and climate change (Figure 4.1) [10]. Concrete production is a responsible source of CO_2 accounting for more than 7% of global emissions, wherein ordinary Portland cement (OPC) production accounts for almost 6.5% of the annual CO_2 emission [10,38,39]. Studies have shown that one ton of OPC produces approximately one ton of CO_2 [40–42]. Moreover, the amount of CO_2 emitted during OPC

production depends on the ratio between clinker and OPC, which is responsible for more than 50% of the total CO_2 released.

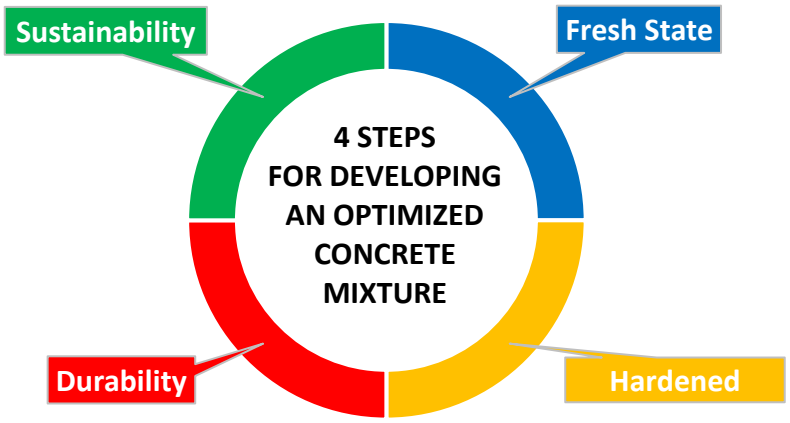

Figure 4.1. Important factors for developing optimized concrete mixture.

Thus, a ton of clinker is responsible for releasing approximately 540 kilograms of CO_2 during the calcination process, where limestone ($CaCO_3$) is transformed into lime (CaO) [10,41]. To achieve the required temperature (1400-1500 °C), fuel is burned in the kilns allowing calcination. As a result, the thermal energy needed for the calcination process is responsible for the other 50% of CO_2 emissions during cement production. Statistics show that the top five cement producers countries have been unchanged (1: China, 2: India, 3: United States (US), 4: Turkey, 5: Vietnam) for more than five years, as shown in Table 4.1 [43–45]. China represents approximately 58% of the global OPC industry, while India and the United States account for 7% and 2%, respectively. In 2012, the global industry produced around 3.8 billion tons of OPC, but in 2018 the production reached 4.1 billion tons [45,46]. Despite being less discussed, it is important to assess the cement production per capita to better analyze the cement need per country. In this context, the cement production in tons

per capita is lower in India and the United States (second and third top cement producers) than in Turkey and Vietnam (fourth and fifth top cement producers).

Table 4.1. Cement production in million metric tons worldwide [43–45]

Cement production in million metric tons						
Year	**China**	**India**	**United States**	**Turkey**	**Vietnam**	**World**
2018	2370	290	89	84	80	4100
2017	2320	290	87	81	79	4050
2016	2410	290	86	77	70	4100
2015	2350	270	83	77	61	4100
2014	2480	260	83	75	61	4180
2013	2420	280	77	71	58	4080
2012	2210	270	75	64	60	3800
Cement production tons per capita[1]						
Year	**China**	**India**	**United States**	**Turkey**	**Vietnam**	**World**
2018	1.70	0.21	0.27	1.02	0.84	0.54
2017	1.67	0.22	0.27	0.99	0.83	0.54
2016	1.75	0.22	0.27	0.96	0.75	0.55
2015	1.71	0.21	0.26	0.98	0.66	0.56
2014	1.82	0.20	0.26	0.97	0.66	0.58
2013	1.78	0.22	0.24	0.94	0.64	0.57
2012	1.64	0.21	0.24	0.86	0.67	0.54

[1]World and country population was retrieved from [47] to calculate cement production tons per capita.

Linking the data quoted above with statistics regarding CO_2 production, one may notice that the largest global cement producers coincide with major global CO_2 emitters [44,48], as can be observed in Figure 4.2. Although the production and transportation of coarse aggregate also represent a high portion (14.4%) of CO_2 release [10], a small reduction of 15% of cement content may denote a reduction of more than 10% in CO_2 emission during the production of conventional concrete (350-400 kg/m^3 of cement and over than 900 kg/m^3 of coarse aggregate).

Different studies focusing on practices that may be used to reduce the energy required for cement production have been published [10,39,49,50]. However, a cement drop of more than 50%

[22,25,51] has been reported when cement is replaced by eco-friendly materials and non-standardized mix-design methods are used [25,50,52].

a) b)

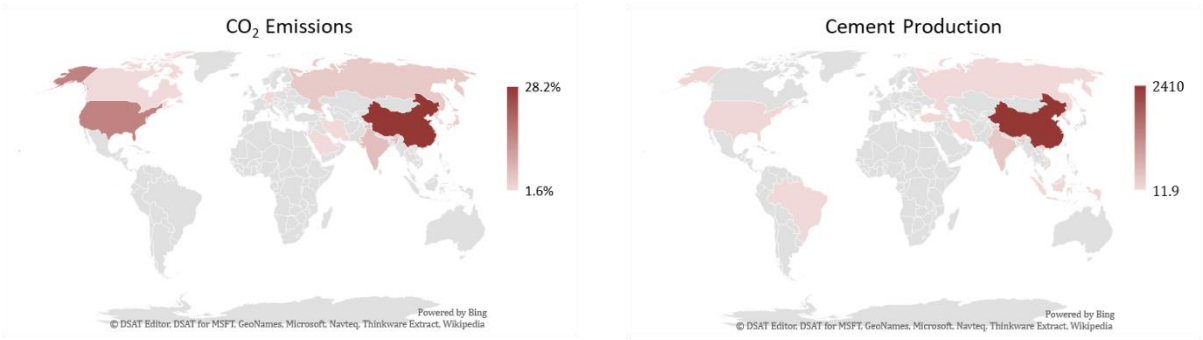

Figure 4.2. Map of the global share of CO2 emissions and cement production in million metric tons from the top 10 producers in 2016 (graph developed with data from [44,48]**).**

4.3 Alternative approaches to producing sustainable concrete

4.3.1 Supplementary cementitious materials - SCMs

Alternative eco-friendly binders (SCMs) started to be developed and largely employed to reduce cement environmental impact [13] in the last few years. Fly ash, silica fume, and granulated blast furnace slag (GBFS) are the three most commonly used SCMs [31,53,54]. SCMs and/or industrial by-products contribute to the reduction of CO_2 emissions since no further process is required for their production [10,13,14]. However, some materials (i.e., GGBS) require grinding. For each ton of GGBS produced, approximately 0.07 tons of CO_2 is released [55], yet this is very sustainable compared to cement. As can be observed in Figure 4.3, the reduction of CO_2 emissions due to the production of blended cement [56] is displayed. From 2000 to 2013, the decrease was approximately 15%. Nevertheless, the most significant drop occurred in 2005, when the CO_2 release reduced by 7.5% in 5 years.

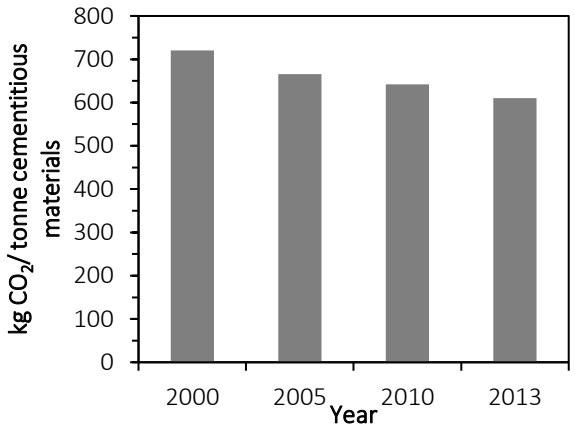

Figure 4.3. CO_2 emissions of blended cement (Adapted from [56]**).**

Besides pre-blended cement, direct substituting cement by SCMs can also lower the carbon footprint. Standards around the world allow a higher replacement for GBFS and fly ash than silica fume (Table 4.2). Therefore, considering the cement production in 2018 and the maximum percent of replacement allowed by CSA [57], the world production of GBFS and fly ash should exceed 2,870 and 2,050 million metric tons per year, respectively. The amount of GBFS and fly ash required represent more than 11 and 2.5 times, respectively, of their production in 2010 (Table 4.3). Thus, although SCMs are considered outstanding cement replacements due to their performance, durability, sustainability, and economic aspects [10,13,14,31,55,58], their availability does not increase at the same rate as cement demand [50,59,60].

Table 4.2. Percentage limits of blended hydraulic cement (Adapted from [57,61]**).**

Material	Fly ash	GBFS	Silica Fume	Ternary and quaternary blended
Maximum component based on common cement produced in Europe	35	35	10	-
CSA Component percent limits (%)	50	70	15	60[1]

[1]In a ternary blend containing silica fume and slag, the maximum supplementary cementing materials content shall be increased to 70%.

Table 4.3. Estimated Slag and Fly Ash production in million metric tons worldwide.

Year	Slag	Fly Ash
2005	~210 [62,63]	~500 [64]
2010	~250 [63,65]	~750 [64,66,67]

4.3.2 Limestone fillers

Inert fillers are other key materials that may be used to enhance concrete mixtures. Although a high range of inert fillers may be used, limestone fillers (LF) are the most used ones [50] due to their availability worldwide, economy, volumetric stability within the cement paste, improvement in the fresh state due to the spherical shape, and its production in different PSD [50,68–73]. In terms of production and availability, approximately 6,000 million tons of filler are produced yearly [50], being one of the only products that exceed Portland cement production. Based on previous studies, the average replacement ratio is around 20%; nevertheless, the limit of 35% is acceptable in some standards (i.e. in Europe and South Africa) [16,50,68,74].

Another important advantage of limestone fillers is their production with PSD similar to cement PSD. As can be observed in Figure 4.4, two distinct cement PSD available in North America are compared with seven different fillers. One may notice that the fillers presented in green shades (Fillers 4, 5, and 6) contain PSD comparable to cement 1 and 2. The darker green presents the least equivalent cement PSD, while the lighter green contains almost exactly the same PSD as cement 2. These types of filler can be called "*replacement filler*" [25,51].

On the other hand, LFs with PSD lower than cement (presented in colours different than green - Figure 4.4) are also available in the market and can be called "*performance filler*". Finer LF enhances concrete mechanical properties due to its filler effect, raise of nucleation sites, growth of hydration kinetics, and increase in packing density [72,73,75,76]. However, it is worth noting that

the higher the SSA of a material, the higher its water demand [18,70]. Therefore, the fresh state performance and the water required for the desired consistency may be affected especially when the "*performance filler"*, which contains d_{50} <10 µm, is not diluted. Thus, LF must be carefully selected to avoid negatively impacting the concrete performance, while enhancing its ecological aspect.

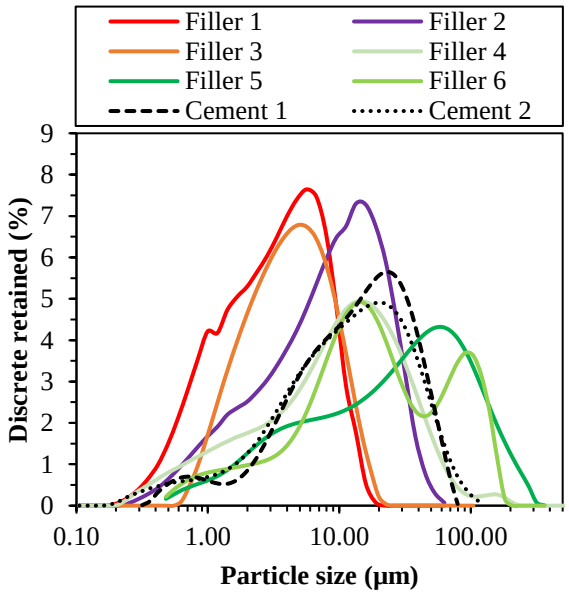

Figure 4.4. Different PSD of limestone fillers.

Thus, the main reasons to use LF as a replacement for cement are highlighted hereafter:

- By-products from aggregate quarries and thus constitute an economic and sustainable alternative to civil construction [69,77];
- Considerable ecological benefits due to the reduction of CO_2 emission compared to OPC production [69,78];
- Availability with distinct PSD and containing spherical particles which improve the fresh-state performance [50,68–72].

- Improvement of the rheological performance of cementitious materials (i.e. cement paste, mortar and concrete made by OPC) – known as dilution effect – reduction of OPC particles with the addition of LF at constant water content [16,69,71];
- Enhancement of the microstructure of concrete by reducing porosity and shrinkage. Moreover, they may improve durability-related properties of the material, especially the ones linked to transport mechanisms [78,79];
- Enrichment of the hydration process, especially at early ages, due to the increase of nucleation sites for hydration products and the raise in the amount of space available for hydration products precipitation [72,75,76].

Although there are numerous advantages to concrete's short-term behaviour, more research is needed to determine the effect of limestone filler on concrete durability when a its PSD is accounted for mix-proportioning the concrete. Some studies [80] concluded that using limestone fillers as a direct replacement for OPC increases the carbonation rate when compared to concrete with the same w/c, whereas other investigations found no significant effect on concrete carbonation resistance when up to 15% [81] and 35% [82] limestone filler were used. However, the use of limestone filler may improve other aspects of durability, such as alkali aggregate reaction due to decrease of system's alkali content or freeze/thaw and corrosion resistance when system's permeability is reduced [83].

4.3.3 Particle packing models - PPMs

Although IF and/or SCMs may be used as a partial replacement for OPC, further reduction of OPC may be achieved by enhancing the system's PSD. PPMs are analytical/mathematical techniques developed to optimize the gradation of the skeleton aiming to minimize the porosity of different

materials, such as ceramics, concrete, and asphalt [8,20,84–87]. Packing density ($Ø_p$) is defined by the solid volume that fills the total volume, as defined in Equation 4.1, being inversely proportional to the voids fraction.

$$Ø_p = \frac{V_{solid}}{V_{total}} \quad \text{Equation 4.1}$$

Although PPMs may be divided into discrete and continuous models, the overall main objective is to densifier the material microstructure [22,86]. The higher the packing density, the lower the amount of voids between fine and coarse aggregates, which are filled by paste (≤ 125 μm, i.e., binder, fillers, and water). Albeit satisfying fresh and hardened state properties can be achieved with conventional mix-design techniques, PPMs may be used to improve concrete eco-efficiency, while enhancing matrix packing and reducing the required amount of paste to achieve a given workability.

The science of particle packing started in the late 19th, when Féret in 1892 studied the influence of aggregate packing on concrete hardened state [22,88]. However, only in the 1900s PPMs start to be developed. The first continuous PPMs was created by Fuller in 1907 [19,20,22,87], whereas the first discrete model was created by Furnas between 1929 (i.e. binary) and 1931 (multimodal models) [19,22,87,88]. Based on these both pioneers of PPMs, this science was enhanced over the years and the literature presents several types of PPMs summarized in Figure 4.5 [19,20,22,87–89].

4.3.3.1 Furnas

The discrete packing theory proposed by Furnas considers the optimum packing of two materials (finer material – 2 and coarser material – 1) [19,20,22,90]. Based on this research, two possibilities must be considered: a) Fine material dominant (Figure 4.6a): Volume fraction of fine (Vf_2) greater

than Vf_1 and b) Coarse material dominant (Figure 4.6b): Vf_1 greater than Vf_2 [19,20,22,90]. For the latter case, the partial volume of the coarse (V_1) is equal to the residual packing density of the coarser particles ($Ø_{p1}$), since the particles will be rearranged to their maximum particle and the voids volume produced will be enough to allow adding the fine material without changing the coarse particle place.

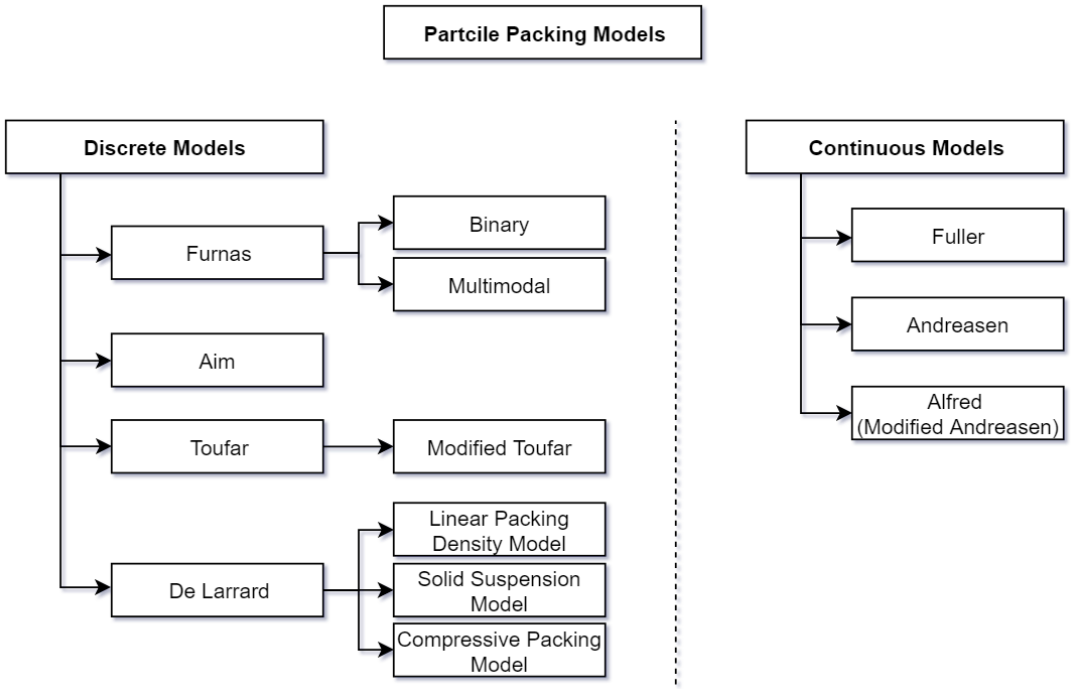

Figure 4.5. Particle packing models available in the literature.

The system packing density ($Ø_{p\text{-}s}$) can be described as the sum of the maximum packing density of the coarser particle ($Ø_{p1}$) and the partial volume of the finer particle (V_2), as described in Equation 4.2 [86,91,92].

$$Ø_{p-s1} = V_1 + V_2 = Ø_{p1} + V_2 = \frac{Ø_{p1}}{1 - Vf_2} \qquad \text{Equation 4.2}$$

where Vf_2 is the volume fraction of large particles (ratio between the V_2 and the total volume of particles).

a) b)

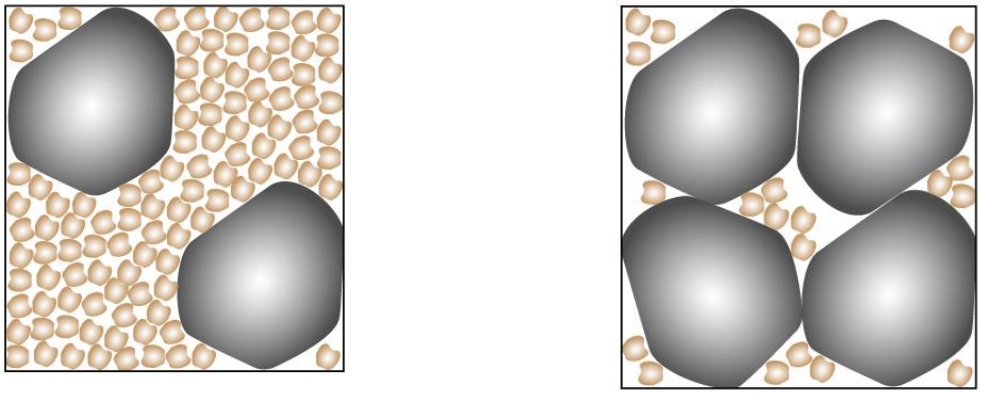

Figure 4.6. Binary systems, including a) Fine material dominant and b) Coarse material dominant.

Conversely, when the volume of fine material is dominant, the coarse particles are added into a system that is already filled by small particles occupying the entire volume (i.e., 100%). As a result, the coarse partial volume is equal to its contribution to the system packing density. Whereas, the fine particles fill up the volume not occupied by the coarser particles with their own maximum packing density (Equation 4.3) [86,91].

$$\emptyset_{p-s2} = V_1 + V_2 = V_1 + \emptyset_{p2}(1 - V_1) = \frac{1}{Vf_1 + \frac{Vf_2}{\emptyset_{p2}}} \qquad \text{Equation 4.3}$$

where $\emptyset_{p2}$ is the packing density of small particles and Vf_1 is the volume occupied by large particles in a unit volume.

However, this case of high-density packed systems may only be achieved when D_2 is significantly smaller than D_1 (i.e., smaller than the voids between the current components); otherwise, two types of system interactions may occur. First, the coarser particles may be disturbed and displaced by the fine particles resulting in increased porosity. This phenomenon is known as the “loosening effect”

and it is illustrated in Figure 4.7a [19,20]. Second, the so-called “wall effect”, may take place whenever fine particles get trapped around much coarser particles, increasing the system porosity, as illustrated in Figure 4.7a [19,20].

Kawashima et al. (2012) explained mathematically the creation of the void in a binary system of a cement paste matrix. The cement paste $Ø_p$ is primarily affected by flocculation or agglomeration of the particles (i.e., the stage where a cement particle becomes a floc of higher volume). Similarly to Furnas theory, two possible states can be considered: flocculation and dispersion. The former takes place when large particles (flocs) have the maximum $Ø_p$ and their voids are filled with smaller particles (Equation 4.2). If the volume of small particles is increased (V_2), the packing density is governed by the second state: dispersion (Equation 3) [92]. The packing density of flocculated or dispersed systems is presented in Figure 4.7b.

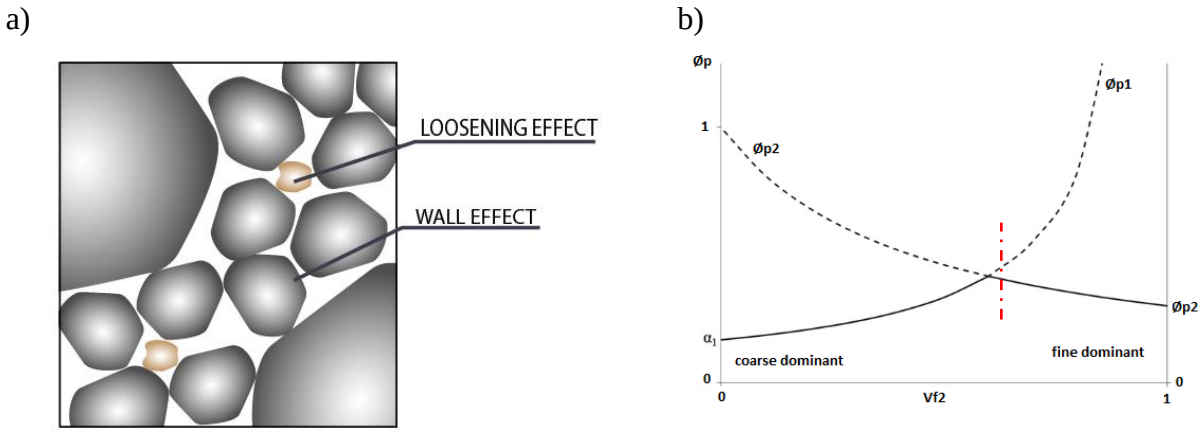

Figure 4.7. a) Wall and Loosening effect and b) Cement paste packing density as a function of small particles volume adapted from[90,92].

Furthermore, Furnas extended his discrete distribution studies to multimodal cases. Therefore, monodispersing materials with a discrete distribution represent only a fraction of a multimodal

system that forms a geometric progression, which has a similar representation to a continuous distribution with all sizes of diameter (Equation 4.4) [87,93].

$$CPFT = \left(\frac{D_p^{\log r} - D_S^{\log r}}{D_L^{\log r} - D_S^{\log r}} \right). 100 \quad \text{Equation 4.4}$$

where CPFT is the cumulate percentage finer than D_p; D_p is the particle diameter; D_S is the smallest particle diameter available in the system; D_L is the largest particle diameter available in the system; r is the ratio between the retained volume of D_p and D_{p-1} (next smaller sieve).

4.3.3.2 Aim's model

Continuing the idea of fine or coarse material dominant, Aim further developed the former equations focusing on the wall effect [88]. Therefore, this model is more recommended for a small ratio between D_2 and D_1 [88,94]. According to Aim's model, the maximum packing density (y*) may be calculated using Equation 4.5 and Equation 4.6. where the second term of p ($1+0.9*D_2/D_1$) refers to the wall effect. When the fine grain volume (Vf_2) is lower than y*, the system packing density is calculated similarly to Equation 4.2. Whereas when $Vf_2 \geq y^*$, the packing density is found by Equation 4.7

$$y^* = \frac{p}{1+p} \quad \text{Equation 4.5}$$

$$p = \frac{\emptyset_{p2}}{\emptyset_{p1}} - \left(1 + 0.9 * \frac{D_2}{D_1}\right) * \emptyset_{p2} \quad \text{Equation 4.6}$$

$$\emptyset_{p-s} = \frac{1}{\left[\frac{Vf_2}{\emptyset_{p2}} + (1 - V_2) * \left(1 + 0.9 * \frac{D_2}{D_1}\right)\right]} \quad \text{Equation 4.7}$$

However, Goltermann et al. [88] verified that Aim's model cannot predict precisely the system packing density and Toufar's model showed a better prediction of the packing degree of two or three aggregates.

4.3.3.3 Toufar

Toufar approach takes into consideration two phenomena (wall and loosening effect) that can occur when $D_1 \approx D_2$ [88,95]. It was valid for ternary or multi-component mixtures using a weighted average of binary mixtures when the diameter ratio (D_2/D_1) ranged from 0.22 to 1.0 [19,20]. Toufar and modified Toufar models are further described in [88]; however, the latter is considered more precise to predict the system packing density when compared with experimental work. Europack is a program available that calculates dry system packing density through the modified Toufar model, which optimizes aggregate proportions with another concrete material aiming at the highest packed system [96–98]. However, it is not considered a mix-proportioning method, since similar to Aim's model, it only calculates the aggregates packing degree (i.e., the ideal proportion between the aggregates); hence, further models must be considered to determine the amount of paste in the system [96]. Jones et al. [98] proved that the modified Toufar model was not adequate when optimizing the proportioning of Portland cement and limestone filler due to the low characteristic diameter ratio ($D_2/D_1 = 0.40$). Another important drawback of the model is that all particles are assumed to be spherical and the materials are monosized [23].

4.3.3.4 De Larrard

As previously stated in Figure 4.4, De Larrard has developed three mix-design approaches: Linear Packing Density Model (LPDM), Solid Suspension Model (SSM), and Compressive Packing Model

(CPM). The SSM was also developed based on LPDM; however, the virtual packing density (β) was introduced as the maximum packing density truly achievable in the dry system when the particles are added one by one [20]. The CPM is the most modern type of discrete PPM and is well-known in concrete technology due to the software BétonlabPro and RENE LCPC [97]. The main difference/upgrade from LPDM to CPM is that the first calculates the system packing through eigen packing, while CPM used the compaction K-index and the virtual packing density (β) [20,97]. Since in the real applications the particles are not placed one by one and their organization depends on the compaction type and energy applied, the K-index was introduced to enhance the prediction of the real system packing density [90,99,100]. One way to correlate both models is to consider LPDM with a compaction K-index equal to infinite [20,97]. Fennis et al. [86] concluded that CPM is not the ideal model to predict the packing density of powder mixtures and a new model called Compaction-Interaction Packing Model must be used to optimize the dry system packing density (aggregates + powders) and reduce the amount of binder required. There is still a lack of studies regarding this new model and the correlation between fresh and hardened states and the packing density [86].

4.3.4 Continuous particle packing models

The second type of PPMs is called continuous models, which are mathematical procedures developed considering particles with continuous size distribution (i.e. no gaps throughout the whole PSD) [19,20,22]. Within continuous models, three well-known approaches are found, including Fuller, Andreasen, and Alfred model (also known as modified Andreasen). In the 90s, studies show that gap-graded aggregates affect concrete compressive strength [9,19,22,94], as a result, continuous models started to be developed and are still being used nowadays. Since these models are focused

on the CPFT, a complementary algorithm published by Westman and Hugill in 1930 may be used to calculate the system's maximum packing factor [87].

4.3.4.1 Fuller

One of the first and most well-known continuous PPMs was presented by Fuller in 1907 notorious as Fuller-Thompson equation (Equation 4.8). The ideal system gradation curve, which reaches the system maximum packing density ($Ø_p$), was proposed using a distribution coefficient equal to 0.5 [19,20,22]. After further research, it was concluded that a distribution coefficient equal to 0.45 must be used for ideal curves in pavement mix-design [20].

$$CPFT = 100 * \left(\frac{D_P}{D_L}\right)^q \qquad \text{Equation 4.8}$$

where CPFT is the cumulative (volume) percent finer than D_P, D_P is the particle diameter, D_L is the larger particle diameter, and q is the distribution coefficient.

4.3.4.2 Andreasen

Studies were performed based on Fuller-Thompson equation to achieve an ideal packing through continuous PPMs. According to Andreasen, the ideal packing occurs when there is a similarity in the distribution and arrangements of the particles even when comparing particles of different sizes (Figure 4.8), the so-called granulation image [93]. Besides, Andreasen determined experimentally that the distribution coefficient should be between 0.33 and 0.50 [22,93].

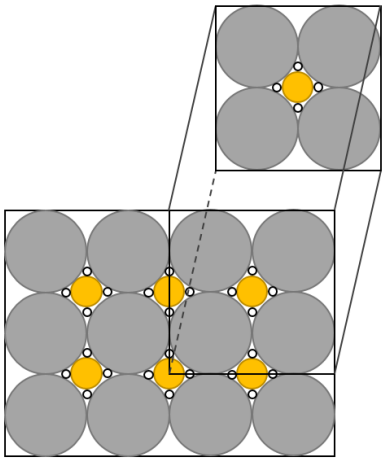

Figure 4.8. Ideal packing showed through granulation image.

4.3.4.3 Alfred

Fuller-Thompson curve presents a significant drawback due to the neglect of the smallest particle size of the PSD, which in reality is different from 0. Therefore, in 1980, Funk and Dinger enhanced Fuller-Thompson equation accounting not only for the largest particle diameter but also for the smallest particle diameter (D_S), as displayed in Equation 4.9. This model is known as Alfred model or modified Andreasen [101,102].

$$CPFT = 100 * \left(\frac{{D_P}^q - {D_S}^q}{{D_L}^q - {D_S}^q} \right) \quad \text{Equation 4.9}$$

Based on computational analysis, it was determined that the optimum packing is achieved when the distribution factor is equal to 0.37 [22,87]. Conversely, the optimum q-factor reduces concrete flowability as the concrete presents less porosity and thus OPC content. Aiming to improve concrete flowability, a q-factor of 0.22 is often suggested since it results in a higher amount of powders and a lower amount of coarse aggregates producing a suitable amount of powder to liquid ratio, helping the coarse aggregate particles slippage. The difference between the q-factors of 0.22 and 0.37 is further discussed hereafter.

4.3.4.4 Comparison of the three continuous models

Several authors have shown the importance of continuous packing model [19,20,22,93], a full analysis demonstrating the difference between the models must be performed before applying these methods in a cement-based material mix-design. A comparison between the three continuous models presented above (i.e., Fuller, Andreasen, Alfred model) is presented in Figure 4.9. It is worth noting that the maximum diameter of 19 mm was selected, which represents the maximum diameter of coarse aggregate of conventional concrete. On the other hand, when required the minimum diameter was attributed as 3 µm to represent the minimum diameter of the powder (i.e., binder and/or filler). Additionally, the particle diameter chosen for this representation follows the sieve size of ASTM C33 [103] for a standard concrete, where the CPFT was divided as shown hereafter from largest to smallest: 1) coarse aggregate of 19, 12.5, and 9.5 mm; 2) fine aggregate of 4.75, 2.36, 1.18, 0.6, 0.3, 0.15 mm; and 3) powder of 0.1, 0.05, 0.025, 0.125, 0.006, 0.003 mm. The third group (powder) was selected based on a class-size ratio of two.

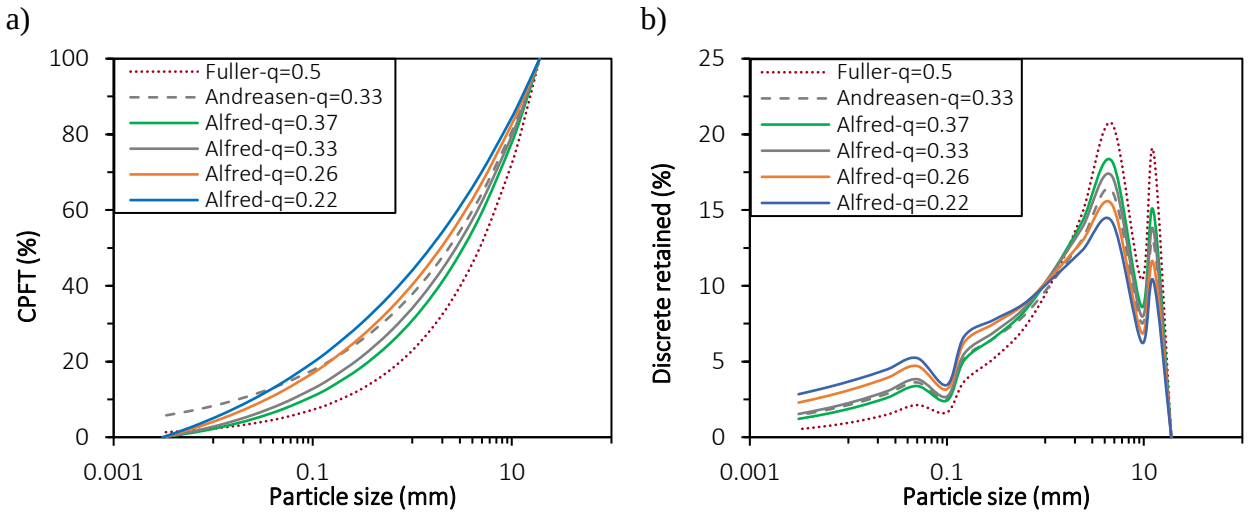

Figure 4.9. Ideal packing calculated through distinct continuous models showed in terms of a) CPFT and b) discrete percentage retained.

The dotted line represents the first continuous model – Fuller with a coefficient of distribution (q) equal to 0.5. The second model (dashed line) is the Andreasen with a q value of 0.33 calculated with the same equation and varying just the q-factor. Both models show that since the smallest diameter particle is not considered in the calculations, both present a CPFT higher than 0% for particles around 0.003 mm (3 μm), precisely 1% and 6%, respectively. Knowing that the material characterization is performed, the binder and fillers' PSDs are determined. The use of Fuller or Andreasen model leads to a notable miscalculation since it considers that the system PSD will always have 1% or 6% of material finer than 3 μm independently of the powder selection. Moreover, one may notice that both methods present a similar CPFT curve shape, while Figure 4.9b highlights a lower powder (particles < 125 μm) content, approximately 8%, on Fuller model, while Andreasen model achieves 19% for the simulation with d_{max} = 19 mm. The difference between four Alfred models with a q-factor equal to 0.22, 0.26, 0.33, and 0.37 representing models that are recommended for highly flowable mixtures (i.e., self-consolidating concrete q = 0.22) and highly-packed mixtures (q = 0.37) is shown in Figure 4.9. The first advantage of this approach is that the real minimum diameter of the system is considered in the calculations. As a result, all four curves contain a CPFT of 0% when the particle diameter reaches the minimum size. Analyzing further Figure 4.9a, one may notice that at 125 μm Alfred model q = 0.26 reached the CPFT of 19% analogous to Andreasen model with a q value of 0.33. However, while appraising Figure 4.9b, Andreasen and Alfred model with q values of 0.33 and 0.37 displayed similar discrete retained curves at 125 μm, but also extending up to 0.6 mm. As a result, one may conclude that although these mixtures achieve different percentages of powders, they may be produced for similar applications - conventional vibrated concrete. Yet, it is worth emphasizing that all these percentages must be used to calculate the final

dry-PSD of cement-based materials. The selection of materials far from the ideal curve and water-to-cement ratio keeps affecting the fresh and hardened-state properties of the produced mixture.

4.4 Mix-design procedures

One may note that continuous packing models are simpler than discrete ones and can be easily implemented without software and a large number of materials characterization tests. Therefore, to propose a ready-to-apply method to produce eco-efficient mixtures, this section will present how to calculate a concrete mix-design using Alfred model as the most novel continuous model. Besides, the main environmental benefits are presented hereafter.

4.4.1 Example of concrete mix-designs (comparison of the three continuous models)

A detailed calculation of a concrete mix-proportion is presented hereafter to better explain the difference between the three continuous methods presented in Section 6.2.2.4. Although the three distinct methods offer the percentage of dry material, a w/c must be selected to further calculate the mass required of each concrete component. The example below was based on the assumption of 0.42 w/c, which is the minimum amount of water required to complete the degree of hydration (α) based on Powers' model [104–107]. Considering the total volume of concrete components, the mass of cement may be calculated through Equation 10.

$$m_c = \frac{V_{concrete} - V_{air}}{\frac{1}{\gamma_c} + \frac{a}{\gamma_{F.A.}} + \frac{b}{\gamma_{C.A.}} + \frac{w}{c}} \qquad \text{Equation 4.10}$$

where F.A. is fine aggregate, C.A. is coarse aggregate, $V_{concrete}$ is the total volume of concrete, V_{air} is the total volume of entrapped air, γ_c is cement specific gravity, $\gamma_{F.A.}$ is fine aggregate specific gravity, $\gamma_{C.A.}$ is coarse aggregate specific gravity, a is mass ratio of F.A. and cement, and b is mass ratio of C.A. and cement.

For calculation purposes, the volume of entrapped air adopted is equal to 2%, while the cement, F.A., and C.A. specific gravities are equal to 3.12, 2.54, and 2.68, respectively. The mass proportion of the six concrete mixtures investigated in this study (Table 4.4). It is worth emphasizing that the first method (Fuller q = 0.5) was the first continuous PPM model and it is clear that a unit volume of concrete cannot be developed with only 7% (i.e. 210 kg/m^3) of cement and 9% of water (i.e. 88 kg/m^3), as shown in Figure 4.10. As mentioned before, Andreasen model presents the same issue disregarding the minimum diameter in the calculation. Nevertheless, when a q-factor of 0.33 is selected, this model results in conventional mix-design which is fairly similar to the Alfred model with a q value of 0.26. The Alfred model with q value of 0.37 introduces the mix-design with higher packing density, hence lower cement content, while q value of 0.22 is recommended for more flowable concrete mixtures (i.e., self-consolidating concrete), hence resulting in higher cement content requirement.

Table 4.4. Mix-design in kg/m^3 for different continuous PPM.

	Fuller	**Andreasen**	**Alfred**			
	q = 0.5	**q = 0.33**	**q = 0.37**	**q = 0.33**	**q = 0.26**	**q = 0.22**
Cement	210.21	434.58	300.60	345.03	431.65	485.44
F.A.	972.70	924.57	1023.14	1017.72	990.24	964.12
C.A.	1182.91	788.42	950.31	867.85	724.94	645.76
water	88.29	182.52	126.25	144.91	181.29	203.88
w/c	0.42	0.42	0.42	0.42	0.42	0.42

To develop a more eco-efficient concrete, SCMs and/or filler are used as mentioned in Section 3. Assuming cement is partially replaced by limestone filler since it is a by-product of aggregate company, concrete sustainability can be further enhanced. A limestone filler with a specific gravity of 2.70 was used as 30% of the total mass of powder (i.e., cement + filler). The usage of limestone fillers using the Alfred model with q values of 0.37, 0.26, and 0.22 is highlighted in Figure 10. The

cement content was reduced by 27% on average. Moreover, the volume of F.A. and C.A. increased by 2% and 1% on average, respectively. Therefore, one may conclude that in terms of total aggregate, the quantities are similar for mix-design with or without cement replacement. Nevertheless, special attention must be taken regarding the water content since it is significantly reduced (on average 5% in volume) since the w/c was kept constant. Therefore, for real mix-design with low cement content and a high volume of replacement filler, the w/c can be substantially higher than the conventional. Previous studies [25,51] achieved compressive strength higher than 40 MPa with w/c higher than 0.50, proving that the conventional Abrams law cannot be used to predict concrete compressive strength when advanced mix-design techniques and a high volume of limestone filler are used.

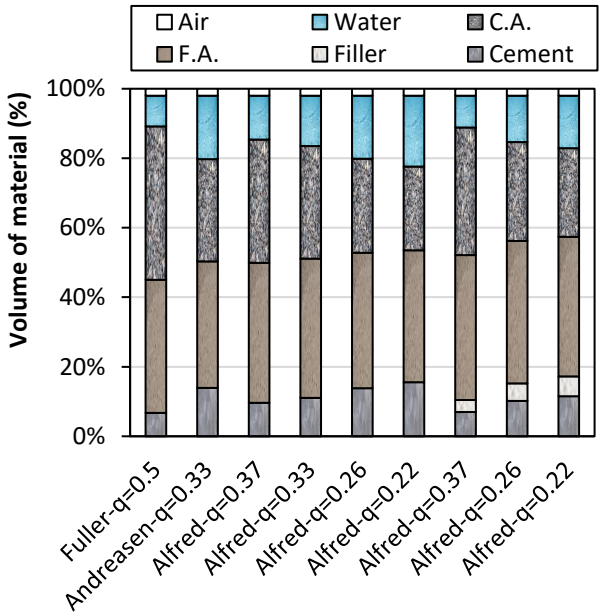

Figure 4.10.Volumetric comparison between distinct continuous PPMs with and without fillers.

4.4.2 Analyzing eco-efficient concrete mixtures

Mix-design science must be carefully applied to develop optimum concrete mix-proportions and achieve the required properties [2]. As mentioned in Section 6.2, nowadays mix-design must have a balance between suitable fresh and hardened properties, durability, economy, and sustainability. Since it is known that cement is the most expensive and least eco-friendly component of concrete, a list of studies with eco-efficient concrete (i.e., reduced cement content) will be presented hereafter.

Although standardized mix-design methods (e.g. American Concrete Institute – ACI method) are widely applied, these methods disregard important features of the mixture components (e.g. PSD) and concrete yield with a high cement content (i.e., higher than 320 kg/m^3 for nominal coarse aggregate size equal to 20 mm) [108]. A database of 71 PPM concrete mixtures, containing mixtures classified as eco-efficient available in the literature, was developed [14,20,23–25,101,102]. As can be observed in Figure 4.11a, the highly packed concrete mixtures considered eco-friendly in the literature contain at least 50% of cement mass to the total mass of powder, regardless of the type of PPM and the replacement materials (e.g., SCMs and/or fillers). Moreover, more than 93% of the mixtures were produced with cement content equal to or lower than 320 kg/m^3, as shown in Figure 4.11b. The five outlier mixtures are considered high-performance concrete (e.g., compressive strength > 50 MPa). Moreover, four out of five of them were produced by packing only the aggregate portion.

a)

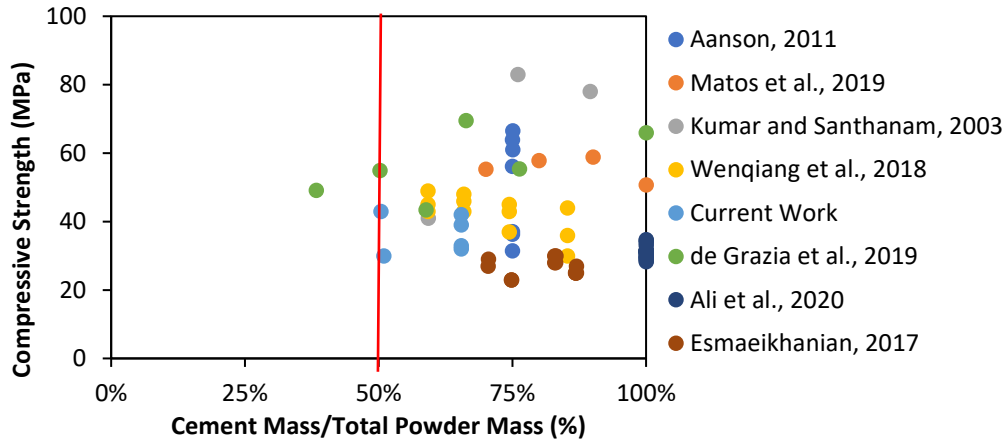

b)

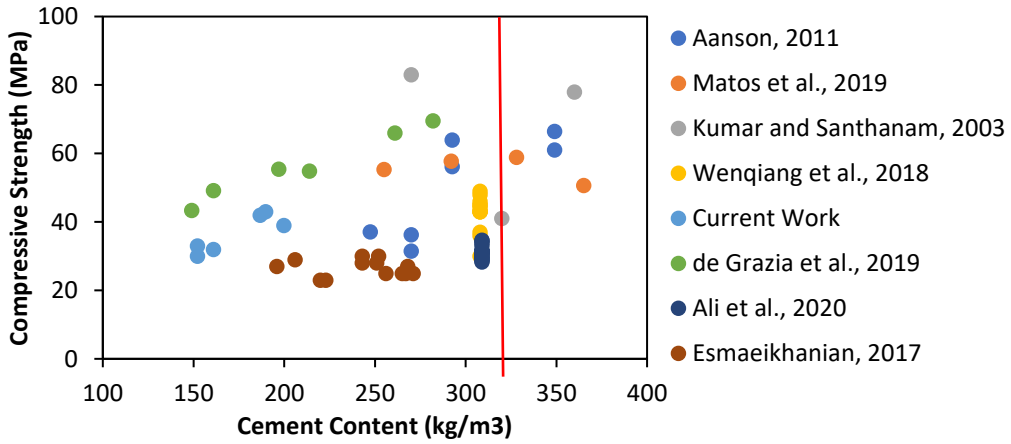

Figure 4.11. Mass of cement percentage in relation to the total amount of powders of eco-friendly mixtures.

4.4.3 Binder intensity

Compressive strength at 28-days is the main parameter for structural design. Although OPC is responsible for generating calcium silicate hydrate (C-S-H) responsible for strength development, there is a misconception in concrete industry that links the amount of OPC with concrete strength. In this context, an index correlating the amount of binder required to develop one unit of concrete property, for instance, the compressive strength is proposed [109]. They called it as binder intensity index (bi). The bi factor may be calculated through Equation 4.11, and it quantifies the eco-efficiency of concrete mixtures.

$$bi = \frac{BC}{P}$$ Equation 4.11

where bi is the binder intensity index, BC is the binder content (kg/m^3), and P is the performance requirement (e.g., compressive strength – MPa).

This calculation does not require additional information and may facilitate the analysis of the environmental effects caused by different types of concrete. This study clearly demonstrated that high strength (> 40 MPa) concrete mixtures are "naturally" more optimized since they correspond to lower bi factors compared to conventional concrete. On the other hand, conventional concrete mixes (i.e., 20-40 MPa) showed to be often designed with moderate to high OPC contents, which shows the need for techniques to improve their eco-efficiency. As can be observed in Figure 4.12a, the majority of concrete produced worldwide presents OPC contents ranging from 250 to 500 kg/m³ and the vast majority of bi found in conventional concrete are close to or higher than 10 kg.m^{-3}.MPa^{-1}. Finally, it is important to note that only roughly 2% of the concrete mixtures commonly used worldwide present OPC contents lower than 250 kg/m³ of concrete.

Based on the database analyzed in this study (Figure 4.12b and Table 4.5), around 6% of the packed eco-friendly mixtures resulted in a bi-factor above 11 kg.m^{-3}.MPa^{-1}. Analyzing only the self-consolidating concrete (SCC) mixtures, the average bi-factor and cement content were 9.2 kg.m^{-3}.MPa^{-1} and 261 kg/m^3, respectively. These mixtures can be classified as eco-efficient due to the PPM. Besides, regardless of the concrete type (i.e., vibrated or SCC), it was proven that when the newest PPM models are selected (i.e., Alfred model and CPM), bi-factor is on average lower than the other methods.

Table 4.5. Summary of SCMs, fillers content, and bi factor of the mixtures in the database.

Name	Packing Only Agg.	Method	Cement (kg/m^3)	Slag (kg/m^3)	Fly ash (kg/m^3)	Micro Silica /Silica Fume (kg/m^3)	Filler (kg/m^3)	bi ($kg.m^{-3}.MPa^{-1}$)
Aanson, 2011 [23]	Y	Modified Toufar	270	90	-	-	-	11.4
			270	90	-	-	-	9.9
			248	83	-	-	-	8.9
			349	116	-	-	-	7.0
			349	116	-	-	-	7.6
			293	98	-	-	-	6.1
			293	98	-	-	-	6.9
Matos et al., 2019 [14]	Y	Experimental Optimum Agg. Packing	365	-	-	-	-	7.2
			328	-	36	-	-	6.2
			292	-	73	-	-	6.3
			255	-	109	-	-	6.6
Kumar and Santhanam, 2003 [20]	N	Modified Andreasen	270	-	-	30	55	3.6
			360	-	-	42	-	5.2
			320	-	220	-	-	13.2
Wenqiang et al., 2018 [24]	N	CPM, 3PM and Experimental	308	-	-	-	53	7.0
			308	-	-	-	53	8.6
			308	-	-	-	53	10.3
			308	-	-	-	106	6.8
			308	-	-	-	106	7.2
			308	-	-	-	106	8.3
			308	-	-	-	159	6.4
			308	-	-	-	159	6.7
			308	-	-	-	159	7.2
			308	-	-	-	212	6.3
			308	-	-	-	212	6.8
			308	-	-	-	212	7.2
Current Work	N	Alfred	161	85	-	-	-	7.7
			152	93	-	-	53	8.2
			200	106	-	-	-	7.8
			190	116	-	-	70	7.1
			152	80	-	-	-	7.0
			187	99	-	-	-	6.8
de Grazia et al., 2019 [25]	N	Alfred	261	-	-	-	-	4.0
			197	-	-	-	61	3.6
			149	-	-	-	104	3.4
			282	-	-	-	143	4.1
			214	-	-	-	212	3.9
			161	-	-	-	259	3.3
Ali et al., 2020 [101]	N	Fuller	232	-	62	15	-	9.8
			232	-	62	15	-	10.8
			232	-	62	15	-	9.8
			232	-	62	15	-	10.5
			232	-	62	15	-	10.2
			232	-	62	15	-	8.9
			232	-	62	15	-	10.0
			232	-	62	15	-	10.4
			232	-	62	15	-	10.1
			232	-	62	15	-	9.9
			232	-	62	15	-	9.9
			232	-	62	15	-	10.3
			232	-	62	15	-	9.0
			232	-	62	15	-	9.1
			232	-	62	15	-	9.8
			232	-	62	15	-	10.0
			232	-	62	15	-	9.3

Name	Packing Only Agg.	Method	Cement (kg/m³)	Slag (kg/m³)	Fly ash (kg/m³)	Micro Silica /Silica Fume (kg/m³)	Filler (kg/m³)	bi (kg.m^{-3}.MPa^{-1})
Ali et al., 2020 [101]	N	Fuller	232	-	62	15	-	9.7
			232	-	62	15	-	10.6
			232	-	62	15	-	10.9
Esmaeikhanian, 2017 [102]	N	Alfred	268	-	-	-	40	9.9
			271	-	-	-	41	10.8
			220	-	74	-	-	12.8
			252	-	-	11	40	8.8
			251	-	-	11	40	9.4
			206	-	75	11	-	10.1
			267	-	-	-	40	10.7
			265	-	-	-	40	10.6
			223	-	75	-	-	13.0
			256	-	-	-	39	10.2
			243	-	-	11	39	8.5
			243	-	-	11	39	9.1
			196	-	71	11	-	10.3

a)

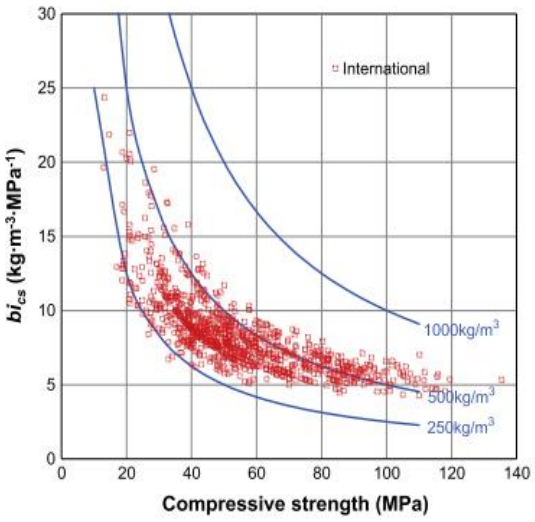

b)

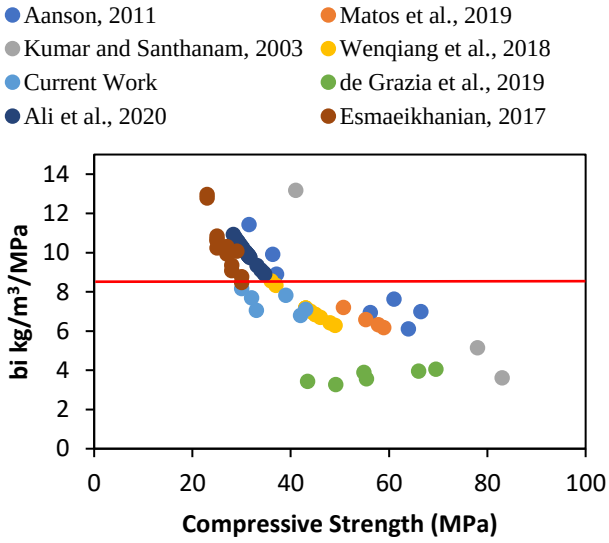

Figure 4.12. a) Relationship between binder intensity and compressive strength at 28-days international records [109] **and b) Comparison of bi-factor of PPM mixtures.**

4.5 Fresh state properties of packed concrete

The use of packing model is growing in the concrete industry; nevertheless, no clear procedure has stated the optimum w/c to achieve the required fresh and compressive strength properties, similar to

ACI method. Due to these difficulties, many authors [14,23,51] have stated that previous experimental work and/or trial and error must be performed to determine the effective water content and w/c. Anson-Cartwright et al. [23] stated that each mixture was first manufactured to check the fresh state (i.e., workability), then the samples were produced. Other authors [25,51] added admixtures (e.g., high-range and mid-range water reducers) to achieve acceptable workability or desirable slump. For conventional concrete, slump is the most common test used to appraise concrete fresh state behaviour, whereas for self-consolidating concrete (SCC) the slump-flow, V-funnel, J-ring, and L-box are the standard tests performed to evaluate its fresh state. The slump or slump flow values of the investigated mixtures are summarized in Table 4.6. Moreover, it also shows the water content and water-to-binder ratio (w/b) which are two parameters that affect concrete fresh state, whereas the cement content is presented to better evaluate the mixture's eco-efficiency. One may notice that the lower the cement content, the higher the w/b since a minimum amount of water is required to achieve the desirable fresh state properties (i.e., slump or slump flow). However, the slump or slump flow tests are not adequate methods to appraise cement-based mixtures' fresh state behaviour and workability [97]. Both are single-point tests that appraise the easiness of the material to flow under its own weight at a specific time (e.g., right after batching or removing from the truck). This property is known as consistency, which is not linked to concrete fresh state behaviour since two materials can have the same consistency (i.e., slump), but behaviour differently when they are vibrated (i.e., pumped concrete). It occurs because the concrete may present different viscosity at distinct torque applied [25,51,73,101,102,110]. [111] investigated the rheological behaviour of three highly packed mixtures mix-proportioned with the same slump, their rheological behaviours are completely different, resulting in distinct viscosity at medium and high rotation. Therefore, in other to properly evaluate concrete fresh state behaviour, a rheological analysis must be performed.

Although some studies present the rheological analysis [101,102,112], further studies are still required to fully comprehend the effect of PPM mixtures and low cement content on concrete rheological behaviour.

Table 4.6. Summary of cement and water content, w/b, and slump/slump flow of the mixtures in the database.

Name	Method	Cement (kg/m^3)	Water (kg/m^3)	w/b	slum/slump flow (mm)
Anson, 2011 [23]	Modified Toufar	270	142	0.39	230
		270	142	0.39	230
		248	130	0.39	235
		349	155	0.33	225
		349	155	0.33	235
		293	130	0.33	225
		293	130	0.33	240
Matos et al., 2019 [14]	Experimental Optimum Agg. Packing	365	175	0.48	720
		328	175	0.48	675
		292	175	0.48	725
		255	175	0.48	720
Kumar and Santhanam, 2003 [20]	Modified Andreasen	270	120	0.40	100
		360	144	0.36	100
		320	180	0.33	690
		308	177	0.57	560
		308	182	0.59	540
		308	182	0.59	695
Wenqiang et al., 2018 [24]	CPM, 3PM and Experimental	308	182	0.59	620
		308	181	0.59	600
		308	181	0.59	620
		308	181	0.59	640
		308	180	0.58	640
		308	180	0.58	660
		308	180	0.58	700
Current Work	Alfred	161	165	0.67	70
		152	165	0.67	75
		200	165	0.54	50
		190	165	0.54	85
		152	156	0.67	85
		187	154	0.54	65
de Grazia et al., 2019 [25]	Alfred	261	140	0.54	13
		197	120	0.61	11
		149	118	0.79	6
		282	152	0.54	155
		214	131	0.61	0
		161	128	0.80	0
Ali et al., 2020 [101]	Fuller	232	185	0.60	625
		232	185	0.60	650
		232	185	0.60	640
		232	185	0.60	615
		232	185	0.60	660
		232	185	0.60	640
		232	185	0.60	620
		232	185	0.60	570
		232	185	0.60	770

Name	Method	Cement (kg/m^3)	Water (kg/m^3)	w/b	slum/slump flow (mm)
Ali et al., 2020 [101]	Fuller	232	185	0.60	760
		232	185	0.60	680
		232	185	0.60	660
		232	185	0.60	730
		232	185	0.60	720
		232	185	0.60	720
		232	185	0.60	680
		232	185	0.60	660
		232	185	0.60	670
		232	185	0.60	610
		232	185	0.60	605
Esmaeikhanian, 2017 [102]	Alfred	268	199	0.74	610
		271	201	0.74	620
		220	198	0.67	640
		252	199	0.76	580
		251	198	0.76	610
		206	200	0.68	570
		267	198	0.74	590
		265	197	0.74	590
		223	201	0.67	600
		256	166	0.65	610
		243	168	0.66	600
		243	167	0.66	600
		196	166	0.60	560

Moreover, the water content ranged from 118 to 165 kg/m^3, while for SCC the amount of range from 166 to 201 kg/m^3, as can be observed in Table 4.6. However, it is worth noting that all the mixtures used different types and amounts of water reducer admixtures. Before concrete sets, water is responsible for moving the granular particles and thus has a direct impact on the overall flowability of the suspension. Therefore, one may conclude that a minimum amount of water is required to enable the material's flow in the fresh state (Damineli, 2013). It has been found that the minimum amount of water may be considered as the average distance that separates two adjacent powder particles, assuming that all the particles are not agglomerated [93]. The latter is called *Interparticle Spacing* (IPS) and can be calculated by Equation 4.12. On the other hand, the minimum amount of cement paste to enable flow in a mixture is considered as the maximum distance between two coarse aggregate adjacent particles and is called *Maximum Paste Thickness* (MPT – Equation 4.13) [78,87,93,113]. These two above parameters are called "mobility parameters" and have been demonstrated to be promising while appraising the mix-design of highly packed systems.

$$IPS = \frac{2}{VSA}\left[\frac{1}{V_s} - \frac{1}{(1 - P_{of})}\right] \quad \text{Equation 4.12}$$

where VSA is the calculated volume surface area per cubic centimetre of powder (SSA times the material density), V_s is the volume fraction of solids, P_{of} is the pore fraction assuming the densest packing that may be calculated by Westman and Hugill method.

$$MPT = \frac{2}{VSA_c}\left[\frac{1}{V_{sc}} - \frac{1}{(1 - P_{ofc})}\right] \quad \text{Equation 4.13}$$

where VSA_c is the calculated volume surface area of aggregate fraction, V_{sc} is the volumetric aggregate solid fraction, P_{ofc} is the pores of aggregate fraction assuming the densest packing that may be calculated by Westman and Hugill method. It is worth noting that PPMs consider spherical particles. Since this is not a reality, the IPS is calculated based on the VSA to account for the different particle shapes showing the benefit of working with PPM and mobility parameters to develop a sustainable concrete with required flowability.

Previous studies highlighted that the greater the IPS and MPT, the higher the flowability of the mixtures [78,114]. It occurs because of the decrease of friction among the particles without changing the water content. Moreover, these two mobility parameters are directly proportional to the concrete microstructure (e.g. permeability) [115]. Literature shows that increasing the IPS also reduces the mixing energy required to manufacture low cement concrete containing high amount of fillers. Yet, there is a lack of research presenting the real relationship between mobility parameters and rheological properties (i.e., yield stress, viscosity, minimum torque, etc.).

4.6 Hardened state properties of packed concrete

4.6.1 Modified Abrams law

Analyzing a new Abrams law is another important method to evaluate the efficiency of PPM. The conventional Abrams law, which may be used to predict concrete compressive strength based on its w/c and considering A and B parameters equal to 100 and 10, respectively, cannot be applied to PPM concrete mixtures developed to achieve a highly packed system, and new A and B factors must be proposed. Moreover, John et al. [16] concluded that when a high amount of LF is added as a partial replacement for cement, a new ratio called water-to-fines ratio (w/f) - also known as water-to-powder (w/p) - plays a more important role than the w/c. However, even though conventional Abrams law does not work for PPM mixtures, studies show that when the w/c is different among the mixtures, it is still the main factor influencing compressive strength development [25,111]. Fennis et al. [86] hypothesized that the compressive strength of highly packed mixtures may be predicted based on the distance between cement particles. Yet, no model is well proposed to predict the compressive strength of these mixtures, especially when high amount of limestone fillers is used, which further complicates the idea of w/c and w/b since LF is a semi-inert filler. Approximately 94% of the PPM mixtures yielded compressive strength higher than the one predicted in the conventional Abrams law, as shown in Figure 4.13.

The 3 out of 4 mixtures that could be predicted with the conventional Abrams law have been manufactured with the Modified Toufar considering the particle packing only in the aggregates portion. In this context, a modified Abrams law ($y = 150.7/ 10.0^{w/b}$) was proposed for the remaining mixtures, which predicted around 44% of the mixtures with reliability within +/-10%. It is important to highlight that different types of cement and concrete applications (SCC versus vibrated concrete) are analyzed together. Thus, if a project is developed with controlled materials and the same

application, all results must be within +/-10% of the proposed modified Abrams. As it can be observed in Figure 4.13, 81% of the mixtures that were above the +10% line contain filler as a partial replacement of cement, whereas the exception contains micro silica. This proves the importance of working with materials in which the PSD is lower than OPC to increase compressive strength. Moreover, one may notice that the Modified Abrams proposed based on the minimum squared error maintains B-factor equal to 10, whereas the A-factor must be increased by 50% (from 100 to 150.7). In this context, one may conclude that highly packed mixtures are more influenced by the aggregates (A-factor) than the cement (B-factor). Since mixtures containing fillers and silica fume exhibit higher packing, one may conclude the A-factor must englobe the whole system packing and not only aggregate one.

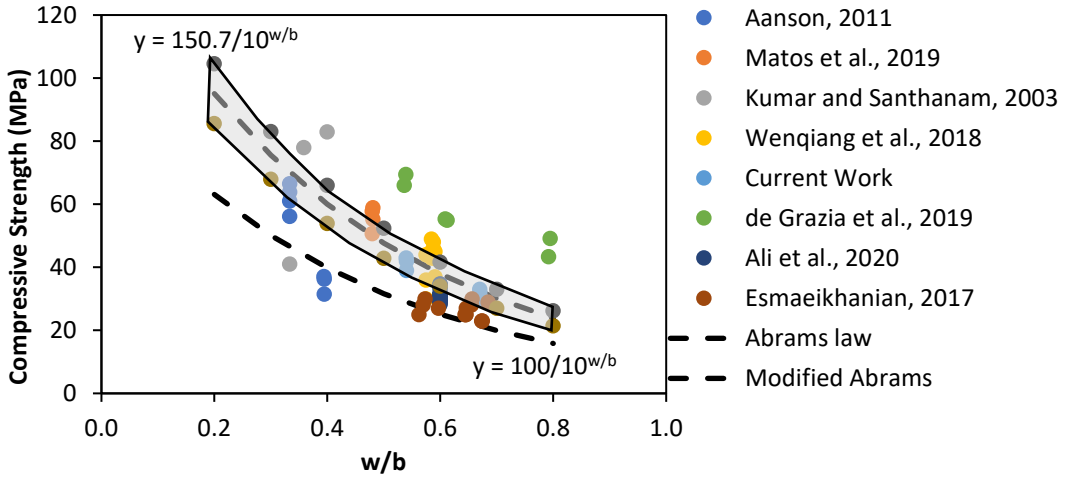

Figure 4.13. Appraisal of the efficiency of Abrams law of predicting compressive strength of eco-concrete investigated.

4.7 Global warming potential assessment

Besides the use of bi-index to appraise the eco-efficiency of concrete mixtures, their global warming potential (GWP), which corresponds to the CO_2 emissions (in mass) per unit volume of concrete, can also be calculated by Equation 4.14 [101,102].

$$\text{GWP} = \sum_{i=1}^{n} m_i . g_i \qquad \text{Equation 4.14}$$

where m_i is the mass of concrete ingredient (i) per unit volume of concrete and g_i is the e-CO_2 per unit mass of concrete ingredient (i).

Table 4.7 shows the GWP of each concrete ingredient used to calculate the GWP of each m^3 of concrete [101,102,116–118]. It is worth noting that the GWP of SCMs can vary greatly depending on the production method and region; for example, some datasets from the United States and Canada show slag, fly ash, and silica GWPs as high as 0.39, 0.15, and 0.53 kg CO_2eq/ kg of material, respectively. Similar to the approach of bi-index, the GWP was plotted against the concrete compressive of 71 eco-efficient mixtures appraised in this work, as shown in Figure 4.14. The maximum GWP (337 kg CO_2 eq/m^3 of concrete) was achieved by the mixture made with the aggregates optimized using PPM, while the minimum one (144 kg CO_2 eq/m^3 of concrete) was achieved with the Alfred model mixture which contains slag and limestone filler used as partial replacement of cement. Moreover, only one mixture which was proportioned with whole system optimization through PPM achieved GWP higher than 300 kg CO_2 eq/m^3 of concrete. Therefore, one may conclude that mixtures with GWP lower than 300 kg CO_2 eq/m^3 of concrete can be considered eco-concrete. Only 15% of the mixtures achieved GWP equal to or lower than 200 kg CO_2 eq/ m^3 of concrete. All the mixtures were proportioned using Alfred model, highlighting the efficiency of this PPM. Around 80% of these mixtures were designed with limestone fillers and/or slag as one of the cement replacements, wherein 33% contain only limestone fillers and 44% contains only slag. One may conclude that selecting either limestone filler and/or slag as a cement replacement may improve concrete sustainability.

Table 4.7. Equivalent CO_2 emissions (CO_2eq) of concrete ingredients (in kg/kg)

Ingredient	Cement	Slag	Silica Fume	Fly Ash	Limestone Filler	Fine Aggregate	Coarse Aggregate	Water
GWP (kg CO_{2eq}/ kg of material)	0.9	0.02	0.0052	0.00526	0.032	0.0029	0.0062	0.00034
Reference	[116]	[118]	[101,102]	[101]	[102]	[101,102]	[102]	[101,102]

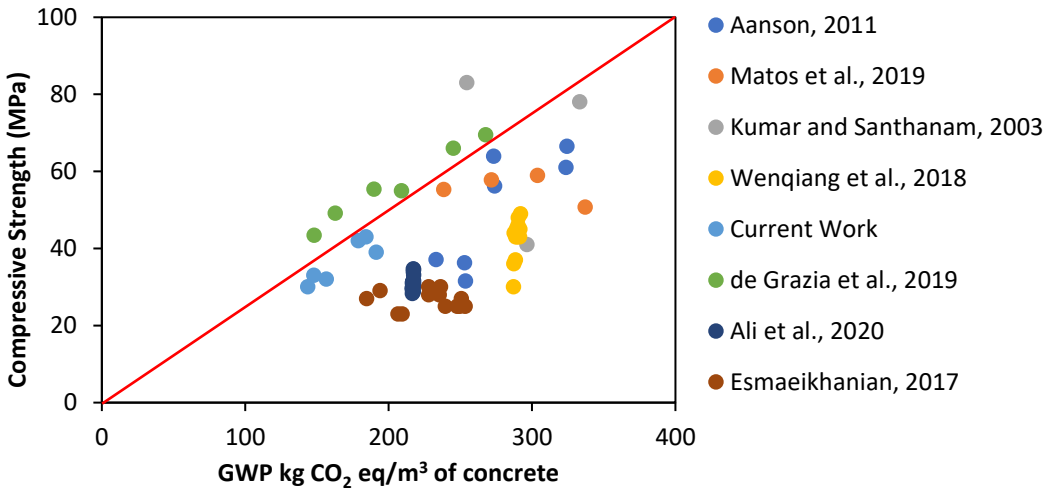

Figure 4.14. Relationship between concrete mixtures GWP and compressive strength.

4.8 Conclusions

In this study, the most advanced mix-design method used to design eco-efficient concrete mixtures is discussed. Different particle packing models (PPMs) are reviewed and discussed. Also, the importance of using alternative materials as a partial replacement for cement is highlighted. Based on the data presented in this paper, the following concluding remarks can be pointed out:

- Although conventional concrete mixtures are produced with OPC contents lower than around 320 kg/m^3, it is possible to produce concrete with a reduced amount of OPC through PPM to optimize the packing density of the skeleton with or without partial replacement of cement.

- Limestone filler is the only material largely available that has production equal to or higher than cement yearly. Moreover, LF may be produced with distinct PSD improving concrete hardened state behaviour and the fresh sate properties.
- The most used PPMs models are discussed and may be used as a reference for further work. However, continuous PPMs are as efficient as discrete models, yet easier to apply to optimize the grading and achieved proper fresh and mechanical properties.
- Concrete eco-efficiency must be considered as one of the main goals during mix-design (i.e., besides fresh, hardened, and durability aspects) and can be calculated through bi-factor.
- The use of PPM is proven to be an efficient method to produce eco-efficient mixtures. 93% of the investigated mixtures were mix-proportioned with less than 320 kg/m^3, whereas the others are high-performance concrete (i.e., > 50 MPa). Moreover, most of the investigated mixtures contain more than 50% of cement mass related to the total powder mass, highlighting that further studies are required to extend the cement content reduction.
- The lower the cement content in the mixtures, the higher w/b should be used to achieve the desirable fresh state properties. Moreover, mobility parameters (IPS and MPT) are recommended to better predict the fresh state behaviour of highly packed mixtures. However, further studies are required to highlight the correlation between mobility parameters and concrete rheological behaviour.
- Abrams law (i.e., w/c) is not enough to predict the compressive strength of highly packed mixtures. Further studies must be performed to evaluate the influence of w/p, or even develop a new method to predict the compressive strength of eco-friendly mixtures designed through PPMs. Moreover, Abrams law A-factor must englobe the whole system packing and not only aggregate.

- Although bi-index is a fast and easy method to appraise concrete eco-efficiency, GWP can further evaluate CO_2 emission due to concrete ingredients. This study can serve as a reference to assess new eco-efficient mixtures GWP.
- Concrete mixtures with GWP lower than 300 kg $CO_{2\ eq}$/m3 of concrete can be considered eco-concrete. Mixtures proportioned with Alfred model and/or either limestone filler and/or slag as a cement replacement may achieve higher levels of eco-efficiency.

4.9 Acknowledgments

The authors gratefully acknowledge the financial support that M. T. de Grazia benefits from the prestigious Vanier scholarship funded by NSERC.

4.10 References

[1] S. Gopinath, A.R. Murthy, D. Ramya, N.R. Iyer, Optimised mix design for normal strength and high performance concrete using particle packing method, Arch. Civ. Eng. 57 (2011) 357–571.

[2] M. Ahmed, S. Islam, S. Nazar, R.A. Khan, A comparative study of popular concrete mix design methods from qualitative and cost-effective point of view for extreme environment, Arab. J. Sci. Eng. 41 (2016) 1403–1412. https://doi.org/10.1007/s13369-015-1946-9.

[3] Y. Knop, A. Peled, R. Cohen, Influences of limestone particle size distributions and contents on blended cement properties, Constr. Build. Mater. 71 (2014) 26–34. https://doi.org/10.1016/j.conbuildmat.2014.08.004.

[4] O. Ahmadah, H. Bessaies-Bey, A. Yahia, N. Roussel, A new mix design method for low-environmental-impact blended cementitious materials: Optimization of the physical characteristics of powders for better rheological and mechanical properties, Cem. Concr. Compos. 128 (2022). https://doi.org/10.1016/j.cemconcomp.2022.104437.

[5] P. Estephane, E.J. Garboczi, J.W. Bullard, O.H. Wallevik, Three-dimensional shape characterization of fine sands and the influence of particle shape on the packing and workability of mortars ☆, Cem. Concr. Compos. 97 (2019) 125–142. https://doi.org/10.1016/j.cemconcomp.2018.12.018.

[6] P. Estephane, E.J. Garboczi, J.W. Bullard, O.H. Wallevik, Using fine sand shape metrics determined from X-ray microcomputed tomography to illustrate the influence of particle shape on the properties of dispersed mortars, Cem. Concr. Compos. 123 (2021) 104176. https://doi.org/10.1016/j.cemconcomp.2021.104176.

[7] T. Oey, A. Kumar, J.W. Bullard, N. Neithalath, G. Sant, The Filler Effect: The Influence of Filler Content and Surface Area on Cementitious Reaction Rates, J. Am. Ceram. Soc. 96 (2013) 1978–1990. https://doi.org/10.1111/jace.12264.

[8] M. Hunger, H.J.H. Brouwers, Flow analysis of water–powder mixtures: Application to specific surface area and shape factor, Cem. Concr. Compos. 31 (2009) 39–59.

[9] A.M. Neville, Properties of Concrete, 5th ed., Pearson Education Limited, 2011.

[10] J. Di Filippo, J. Karpman, J.R. Deshazo, J. Di Filippo, J. Karpman, J.R. Deshazo, The impacts of policies to reduce CO2 emissions within the concrete supply chain, Cem. Concr. Compos. 101 (2019) 67–82. https://doi.org/10.1016/j.cemconcomp.2018.08.003.

[11] L.K. Turner, F.G. Collins, Carbon dioxide equivalent (CO2-e) emissions: A comparison between geopolymer and OPC cement concrete, Constr. Build. Mater. 43 (2013) 125–130. https://doi.org/10.1016/j.conbuildmat.2013.01.023.

[12] S. Science, N. Series, N. Oct, Complex Visual Concept in the Pigeon Author (s): R . J . Herrnstein and D . H . Loveland Published by : American Association for the Advancement of Science Stable URL : http://www.jstor.org/stable/1714350 . Complex Visual Concept in, 146 (2014) 549–551. https://doi.org/10.3102/0034654310377210.

[13] S. Ruan, C. Unluer, Influence of supplementary cementitious materials on the performance and environmental impacts of reactive magnesia cement concrete, J. Clean. Prod. 159 (2017) 62–73. https://doi.org/10.1016/j.jclepro.2017.05.044.

[14] P.R. de Matos, R.D. Sakata, L.R. Prudêncio, Eco-efficient low binder high-performance self-compacting concretes, Constr. Build. Mater. 225 (2019) 941–955. https://doi.org/10.1016/j.conbuildmat.2019.07.254.

[15] C.F. Ferraris, K.H. Obla, R. Hill, The influence of mineral admixtures on the rheology of cement paste and concrete, Cem. Concr. Res. 31 (2001) 245–255.

[16] V.M. John, B.L. Damineli, M. Quattrone, R.G. Pileggi, Fillers in cementitious materials — Experience, recent advances and future potential, Cem. Concr. Res. 114 (2018) 65–78. https://doi.org/10.1016/j.cemconres.2017.09.013.

[17] B. Lagerblad, E. Forssberg, The function of fillers in concrete, Mater. Struct. 37 (2004) 74–81.

[18] D. Youness, A. Yahia, A. Tagnit-Hamou, Coupled rheo-physical effects of blended cementitious materials on wet packing and flow properties of inert suspensions, Constr. Build. Mater. 271 (2021) 121588. https://doi.org/10.1016/j.conbuildmat.2020.121588.

[19] M.N. Mangulkar, S.S. Jamkar, Review of particle packing theories used for concrete mix proportioning, Int. J. Sci. Eng. Res. 4 (2013) 143–148.

[20] S. Kumar, M. Santhanam, S. Kunar, M. Santhanam, Particle packing theories and their application in concrete mixture proportioning : A review, Indian Concr. J. 77 (2003) 1324–1331.

[21] A.B. Yu, R.P. Zou, N. Standish, Modifying the Linear Packing Model for Predicting the Porosity of Nonspherical Particle Mixtures, Ind. Eng. Chem. Res. 35 (1996) 3730–3741.

[22] S.A.A.M. Fennis, J.C. Walraven, Using particle packing technology for sustainable concrete mixture design, Heron. 57 (2012) 73–101.

[23] M. Anson-Cartwright, Optimization of aggregate gradation combinations to improve concrete sustainability and durability, MASc Thesis, University of Toronto, 2011.

[24] W. Zuo, J. Liu, Q. Tian, W. Xu, W. She, P. Feng, C. Miao, Optimum design of low-binder Self-Compacting Concrete based on particle packing theories, Constr. Build. Mater. 163 (2018) 938–948. https://doi.org/10.1016/j.conbuildmat.2017.12.167.

[25] M. T. de Grazia, L. F. M. Sanchez, R. C. O. Romano, R. G. Pileggi, M.T. de Grazia, L. Sanchez, R.C.O. Romano, R.G. Pileggi, M. T. de Grazia, L. F. M. Sanchez, R. C. O. Romano, R. G. Pileggi, Investigation of the use of continuous particle packing models (PPMs) on the fresh and hardened properties of low-cement concrete (LCC) systems, Constr. Build. Mater. 195 (2019) 524–536. https://doi.org/10.1016/j.conbuildmat.2018.11.051.

[26] M.K. Ismail, M.T. De Grazia, A.A.A. Hassan, Mechanical Properties of Self-Consolidating Rubberized Concrete, in: Int. Conf. Adv. Struct. Geotech. Eng., Hurghada, 2015.

[27] M.K. Ismail, M.T. De Grazia, A.A.A. Hassan, Mechanical Properties of Self-Consolidating Rubberized Concrete with Different Supplementary Cementing Materials, in: Int. Conf. Transp. Civ. Eng., London, 2015: pp. 68–74. https://doi.org/http://dx.doi.org/10.17758/UR.U0315331.

[28] M.K. Ismail, M.T. De Grazia, A.A.A. Hassan, Behaviour of Self-Consolidating Rubberized Concrete under Drop-weight Impacts, in: Kamal H. Khayat (Ed.), 8th Int. RILEM Symp. Self-Compacting Concr. - SCC 2016, RILEM Publications SARL, Washington, 2016: pp. 445–454.

[29] T. Le, G. Le Saout, E. Garcia-Diaz, D. Betrancourt, S. Rémond, Hardened behavior of mortar based on recycled aggregate: Influence of saturation state at macro- and microscopic scales, (2017).

[30] M. Hayles, L.F.M. Sanchez, M. Noël, Eco-efficient low cement recycled concrete aggregate mixtures for structural applications, (2018).

[31] F. Pacheco Torgal, S. Miraldo, J.A. Labrincha, J. De Brito, An overview on concrete carbonation in the context of eco-efficient construction: Evaluation, use of SCMs and/or RAC, Constr. Build. Mater. 36 (2012) 141–150. https://doi.org/10.1016/j.conbuildmat.2012.04.066.

[32] S. Singh, R. Nagar, V. Agrawal, A review on Properties of Sustainable Concrete using granite dust as replacement for river sand, J. Clean. Prod. 126 (2016) 74–87. https://doi.org/10.1016/j.jclepro.2016.03.114.

[33] A.K. Saha, K. Sarker, Sustainable use of ferronickel slag fine aggregate and fly ash in structural concrete: Mechanical properties and leaching study, J. Clean. Prod. 162 (2017) 438–448. https://doi.org/10.1016/j.jclepro.2017.06.035.

[34] F. Aslani, G. Ma, D. Law, Y. Wan, G. Muselin, Development of high-performance self-compacting concrete using waste recycled concrete aggregates and rubber granules, J. Clean. Prod. 182 (2018) 553–566. https://doi.org/10.1016/j.jclepro.2018.02.074.

[35] F. Pelisser, N. Zavarise, T.A. Longo, A.M. Bernardin, Concrete made with recycled tire rubber: Effect of alkaline activation and silica fume addition, J. Clean. Prod. 19 (2011) 757–763. https://doi.org/10.1016/j.jclepro.2010.11.014.

[36] Joint statement: Canada's Cement Industry and the Government of Canada announce a partnership to establish Canada as a global leader in low-carbon cement and to achieve net-zero carbon concrete - Innovation, Science and Economic Development Canada, (n.d.). https://www.ic.gc.ca/eic/site/icgc.nsf/eng/07730.html (accessed March 17, 2022).

[37] Global Cement and Concrete Association, Our path to net zero, (2022). https://gccassociation.org/concretefuture/our-path-to-net-zero/ (accessed March 17, 2022).

[38] M. Limbachiya, S.C. Bostanci, H. Kew, Suitability of BS EN 197-1 CEM II and CEM V cement for production of low carbon concrete, Constr. Build. Mater. 71 (2014) 397–405.

[39] W. Schakel, C.R. Hung, L.-A. Tokheim, A. Hammer Strømman, E. Worrell, A. Ramírez, Impact of fuel selection on the environmental performance of post-combustion calcium looping applied to a cement plant, Appl. Energy. 210 (2017) 75–87. https://doi.org/10.1016/j.apenergy.2017.10.123.

[40] M.C. Gonçalves, F. Margarido, Materials for Construction and Civil Engineering : Science, Processing, And Design, Springer International Publishing, 2015.

[41] A. Hasanbeigi, L. Price, E. Lin, Emerging Energy-Efficiency and CO2 Emission-Reduction Technologies for Cement and Concrete Production: A Technical Review, Renew. Sustain. Energy Rev. 16 (2012) 6220–6238.

[42] T.R. Naik, M. Asce, S.S. Singb, M.M. Hossain, Permeability of high-strength concrete containing low cement factor, J. Energy Eng. 122 (1996) 21–39.

[43] Statistics Canada, Production of Building Materials (Cement), (2017). http://www.statcan.gc.ca/tables-tableaux/sum-som/l01/cst01/manuf31c-eng.htm (accessed June 15, 2017).

[44] Statista, Major Countries in Worldwide Cement Production from 2011 to 2017, (2017). https://www.statista.com/statistics/267364/world-cement-production-by-country/ (accessed March 28, 2018).

[45] Statista, Cement production globally and in the U.S. from 2010 to 2017 (in million metric tons), (2017). https://www.statista.com/statistics/219343/cement-production-worldwide/ (accessed March 28, 2018).

[46] U.S. and world cement production 2018, Statista. (2018). https://www.statista.com/statistics/219343/cement-production-worldwide/ (accessed October 11, 2019).

[47] World Bank Group, Population, (2019). https://data.worldbank.org/indicator/SP.POP.TOTL (accessed February 27, 2020).

[48] Statista, Largest producers of CO2 emissions worldwide in 2016, based on their share of global CO2 emissions, (2018). https://www.statista.com/statistics/271748/the-largest-emitters-of-co2-in-the-world/ (accessed March 8, 2018).

[49] S. Licht, H. Wu, C. Hettige, B. Wang, J. Asercion, J. Lau, J. Stuart, STEP cement: Solar Thermal Electrochemical Production of CaO without CO2 emission, Chem. Commun. 48 (2012) 6019–6021. https://doi.org/10.1039/c2cc31341c.

[50] U.N. Environment, K.L. Scrivener, V.M. John, E.M. Gartner, Eco-efficient cements: Potential economically viable solutions for a low-CO2 cement-based materials industry, Cem. Concr. Res. 114 (2018). https://doi.org/10.1016/j.cemconres.2018.03.015.

[51] M. Grazia, L.F.M. Sanchez, R. Romano, R.G. Pileggi, M.T. de Grazia, L.F.M. Sanchez, R. Romano, R.G. Pileggi, M. T. de Grazia, L. F. M. Sanchez, R. C. O. Romano, R. G. Pileggi, Evaluation of the Fresh and Hardened State Properties of Low-Cement Content (LCC) Systems, Mag. Concr. Res. 72 (2018) 1–14. https://doi.org/10.1680/jmacr.18.00271.

[52] M. Noël, L. Sanchez, G. Fathifazl, Recent Advances in Sustainable Concrete for Structural Applications, in: Sustain. Constr. Mater. Technol. 4, 2016: p. 10.

[53] M. Thomas, Supplementary cementing materials in concrete, CRC Press Taylor & Francis Group, 2013. https://doi.org/10.1201/b14493.

[54] S.A. Miller, V.M. John, S.A. Pacca, A. Horvath, Carbon dioxide reduction potential in the global cement industry by 2050, Cem. Concr. Res. 114 (2018) 115–124. https://doi.org/10.1016/j.cemconres.2017.08.026.

[55] N. Bouzoubaâ, B. Fournier, Current situation with the production and use of supplementary cementitious materials (SCMs) in concrete construction in Canada, Can. J. Civ. Eng. 32 (2005) 129–143. https://doi.org/10.1139/l04-109.

[56] M. Sonebi, Y. Ammar, P. Diederich, Sustainability of cement, concrete and cement replacement materials in construction, in: J.M. Khatib (Ed.), Sustain. Constr. Mater., Elsevier, 2016: pp. 371–396. https://doi.org/10.1016/b978-0-08-100370-1.00015-9.

[57] CSA A3000-08, Cementitious materials compendium, 2018.

[58] M. C. G. Juenger, R. Siddique, Recent advances in understanding the role of supplementary cementitious materials in concrete, Cem. Concr. Res. 78 (2015) 71–80. https://doi.org/10.1016/j.cemconres.2015.03.018.

[59] J. Zachar, M. Asce, Sustainable and Economical Precast and Prestressed Concrete Using Fly Ash as a Cement Replacement, J. Mat. Civ. Eng. 23 (2011) 789–792.

[60] M.C.G. Juenger, R. Siddique, Recent advances in understanding the role of supplementary cementitious materials in concrete, Cem. Concr. Res. 78 (2015) 71–80.

[61] EN 197-1, Cement - Part 1: Composition, specifications and conformity criteria for common cements, 2000.

[62] H.G. van Oss, Iron and Steel Slag Statistics and Information - 2006, in: U.S. Geol. Surv. Miner. Commod. Summ., 2006.

[63] T. Sofilić, U. Sofilić, I. Brnardić, The Significance of Iron and Steel Slag as By-Product for Utilization in Road Construction, in: 2nd Int. Foundrymen Conf. Sustain. Dev. Foundry Mater. Technol., 2012: pp. 419–436. www.simet.hr/~foundry (accessed November 13, 2019).

[64] A.R.K. Gollakota, V. Volli, C.-M. Shu, Progressive utilisation prospects of coal fly ash: A review, Sci. Total Environ. 672 (2019).

[65] K.C. Curry, Iron and Steel Slag Statistics and Information - 2011, 2011.

[66] R.S. Blissett, N.A. Rowson, A review of the multi-component utilisation of coal fly ash, Fuel. 97 (2012). https://doi.org/10.1016/j.fuel.2012.03.024.

[67] M. Izquierdo, Q. Xavier, Leaching behaviour of elements from coal combustion fly ash: An overview, Int. J. Coal Geol. 94 (2012).

[68] S.H. Kang, Y. Jeong, K.H. Tan, J. Moon, High-volume use of limestone in ultra-high performance fiber-reinforced concrete for reducing cement content and autogenous shrinkage, Constr. Build. Mater. 213 (2019) 292–305. https://doi.org/10.1016/j.conbuildmat.2019.04.091.

[69] Y. Knop, A. Peled, Packing density modeling of blended cement with limestone having different particle sizes, Constr. Build. Mater. 102 (2016) 44–50.

[70] J.L. Gallias, R. Kara-Ali, J.P. Bigas, The effect of fine mineral admixtures on water requirement of cement pastes, Cem. Concr. Res. . 30 (2000) 1543–1549. https://doi.org/10.1016/S0008-8846(00)00380-X.

[71] Y. Knop, A. Peled, Setting behavior of blended cement with limestone: influence of particle size and content, Mater. Struct. 49 (2016) 439–452.

[72] T. Oey, A. Kumar, J.W. Bullard, N. Neithalath, G. Sant, The filler effect: The influence of filler content and surface area on cementitious reaction rates, J. Am. Ceram. Soc. 96 (2013) 1978–1990. https://doi.org/10.1111/jace.12264.

[73] D. Youness, M. Hosseinpoor, A. Yahia, A. Tagnit-Hamou, Flowability characteristics of dry supplementary cementitious materials using Carr measurements and their effect on the rheology of suspensions, Powder Technol. 378 (2021) 124–144. https://doi.org/10.1016/j.powtec.2020.09.064.

[74] V. Bonavetti, H. Donza, G. Menéndez, O. Cabrera, E.F. Irassar, Limestone filler cement in low w/c concrete: A rational use of energy, Cem. Concr. Res. 33 (2003) 865–871. https://doi.org/10.1016/S0008-8846(02)01087-6.

[75] J. Tikkanen, A. Cwirzen, V. Penttala, Effects of mineral powders on hydration process and hydration products in normal strength concrete, Constr. Build. Mater. 72 (2014) 7–14. https://doi.org/10.1016/j.conbuildmat.2014.08.066.

[76] B. Lothenbach, K. Scrivener, R.D. Hooton, Supplementary cementitious materials, Cem. Concr. Res. 41 (2011) 217–229.

[77] K.D. Ingram, K.E. Daugherty, A Review of Limestone Additions to Portland Cement and Concrete, Cem. Concr. Compos. 13 (1991) 165–170.

[78] C. Varhen, I. Dilonardo, C. Romano, R.G. Pileggi, A. Figueiredo, Effect of the substitution of cement by limestone filler on the rheological behaviour and shrinkage of microconcretes, Constr. Build. Mater. 125 (2016) 375–386.

[79] H.R. Shadkam, S. Dadsetan, M. Tadayon, L.F.M. Sanchez, A. Zakeri, An investigation of the effects of limestone powder and Viscosity Modifying Agent in durability related parameters of self-consolidating concrete (SCC), Constr. Build. Mater. 156 (2017) 152–160.

[80] Q.T. Phung, N. Maes, D. Jacques, E. Bruneel, I. Van Driessche, G. Ye, G. De Schutter, Effect of limestone fillers on microstructure and permeability due to carbonation of cement pastes under controlled CO2 pressure conditions, Constr. Build. Mater. 82 (2015) 376–390. https://doi.org/10.1016/j.conbuildmat.2015.02.093.

[81] F. Lollini, E. Redaelli, L. Bertolini, Effects of portland cement replacement with limestone on the properties of hardened concrete, Cem. Concr. Compos. 46 (2014) 32–40. https://doi.org/10.1016/j.cemconcomp.2013.10.016.

[82] S. Tsivilis, E. Chaniotakis, G. Kakali, G. Batis, An analysis of the properties of Portland limestone cements and concrete, Cem. Concr. Compos. 24 (2002) 371–378. https://doi.org/10.1016/S0958-9465(01)00089-0.

[83] D.K. Panesar, R. Zhang, Performance comparison of cement replacing materials in concrete: Limestone fillers and supplementary cementing materials – A review, Constr. Build. Mater. 251 (2020) 118866. https://doi.org/10.1016/j.conbuildmat.2020.118866.

[84] A.K.H. Kwan, K.W. Chan, V. Wong, A 3-parameter particle packing model incorporating the wedging effect, Powder Technol. 237 (2013) 172–179. https://doi.org/10.1016/j.powtec.2013.01.043.

[85] T. Baghaee Moghaddam, H. Baaj, Application of compressible packing model for optimization of asphalt concrete mix design, Constr. Build. Mater. 159 (2018) 530–539.

[86] S.A.A.M. Fennis, J.C. Walraven, J.A. den Uijl, Compaction-interaction packing model: regarding the effect of fillers in concrete mixture design, Mater. Struct. 46 (2013) 463–478. https://doi.org/10.1617/s11527-012-9910-6.

[87] D. Dinger, J. Funk, Predictive process control of crowded particulate suspensions, 1st ed., New York, 1994.

[88] P. Goltermann, V. Johansen, L. Palbøl, Packing of Aggregates : An Alternative Tool to Determine the Optimal Aggregate Mix, ACI Mater. J. (1997) 435–442.

[89] I. Mehdipour, K.H. Khayat, Understanding the role of particle packing characteristics in rheo-physical properties of cementitious suspensions : A literature review, Constr. Build. Mater. 161 (2018) 340–353.

[90] F. De Larrard, Concrete Mixture Proportioning: A Scientific Approach, Scientific Approach, E&FN SPON, London and New York, 1999.

[91] T. Stovall, F. de Larrard, M. Buil, Linear packing density model of grain mixtures, Powder Technol. 48 (1986) 1–12. https://doi.org/10.1016/0032-5910(86)80058-4.

[92] S. Kawashima, J.H. Kim, D.J. Corr, S.P. Shah, Study of the mechanisms underlying the fresh-state response of cementitious materials modified with nanoclays, Constr. Build. Mater. 36 (2012) 749–757.

[93] I.R. Oliveira, A.R. Studart, R.G. Pileggi, V.C. Pandolfelli, Dispersão e Empacotamento de Partículas, Fazendo Arte Editorial, São Paulo, 2000.

[94] H.A.C.K. Hettiarachchi, W.K. Mampearachchi, Validity of aggregate packing models in mixture design of interlocking concrete block pavers (ICBP), Road Mater. Pavement Des. 20 (2019) 462–474. https://doi.org/10.1080/14680629.2017.1393001.

[95] A.K.H. Kwan, K.W. Chan, V. Wong, A 3-parameter particle packing model incorporating the wedging effect, Powder Technol. 237 (2013) 172–179.

[96] P.N. Quiroga, D.W. Fowler, The effects of aggregates characteristics on the performance of portland cement concrete the effects of aggregates characteristics on the performance of portland cement concrete, Austin, 2004.

[97] S.A.A.M. Fennis, J.C. Walraven, Using particle packing technology for sustainable concrete mixture design, Heron. 57 (2012) 73–101.

[98] M.R. Jones, L. Zheng, M.D. Newlands, Comparison of particle packing models for proportioning concrete constituents for minimum voids ratio, Mater. Struct. 35 (2002) 301–309.

[99] F. de Larrard, T. Sedran, Mixture-proportioning of high-performance concrete, Cem. Concr. Res. 32 (2002) 1699–1704. https://doi.org/10.1016/S0008-8846(02)00861-X.

[100] M. Mangulkar, S. Jamkar, Review of Particle Packing Theories Used For Concrete Mix Proportioning, Int. J. Sci. Eng. Res. 4 (2013) 143–148.

[101] Z.S. Ali, M. Hosseinpoor, A. Yahia, New aggregate grading models for low-binder self-consolidating and semi-self-consolidating concrete (Eco-SCC and Eco-semi-SCC), Constr. Build. Mater. 265 (2020) 120314. https://doi.org/10.1016/j.conbuildmat.2020.120314.

[102] B. Esmaeilkhanian, K.H. Khayat, O.H. Wallevik, Mix design approach for low-powder self-consolidating concrete: Eco-SCC-content optimization and performance, Mater. Struct. 50 (2017) 18. https://doi.org/10.1617/s11527-017-0993-y.

[103] ASTM C33, Standard Specification for Concrete Aggregates, 2016.

[104] G. Espinoza-Hijazin, M. Lopez, Extending internal curing to concrete mixtures with W/C higher than 0.42, Constr. Build. Mater. 25 (2011) 1236–1242. https://doi.org/10.1016/j.conbuildmat.2010.09.031.

[105] M.T. Hasholt, O. Mejlhede Jensen, K. Kovler, S. Zhutovsky, Can superabsorent polymers mitigate autogenous shrinkage of internally cured concrete without compromising the strength?, Constr. Build. Mater. 31 (2012) 226–230. https://doi.org/10.1016/j.conbuildmat.2011.12.062.

[106] T.C. Powers, T.L. Brownyard, Studies of the Physical Properties of Hardened Portland Cement Paste: Part 2- Studies of Water Fixation, J. Am. Concr. Inst. 18 (1946) 248–336.

[107] K.C. Hover, The influence of water on the performance of concrete, Constr. Build. Mater. J. 25 (2011) 3003–3013. https://doi.org/10.1016/j.conbuildmat.2011.01.010.

[108] S.H. Kosmatka, B. Kerkhoff, W.C. Panarese, Designing and Proportioning Normal Concrete Mixtures, in: Des. Control Concr. Mix., Portland Cement Association, 2002: pp. 151–172.

[109] B.L. Damineli, F.M. Kemeid, P.S. Aguiar, V.M. John, Measuring the eco-efficiency of cement use, Cem. Concr. Compos. 32 (2010) 555–562.

[110] N.-D. Hoang, A.-D. Pham, Estimating Concrete Workability Based on Slump Test with Least Squares Support Vector Regression, J. Constr. Eng. 2016 (2016) 1–8. https://doi.org/10.1155/2016/5089683.

[111] M.T. de Grazia, L.F.M. Sanchez, R.G. Pileggi, Evaluation of the fresh and hardened state properties of low cement content systems, Mag. Concr. Res. 72 (2018) 232–245.

[112] M.T. De Grazia, L. Sanchez, R.C.O. Romano, R.G. Pileggi, Investigation of Alfred Model Effect on the Fresh and Hardened State Properties of Low-Cement Content (LCC) Systems, Constr. Build. Mater. Accepted (2017) 1–26.

[113] B. Damineli, Consumo de ligantes: controle reologico, empacotamento e dispersao de particulas, University of Sao Paulo, 2013.

[114] A.P. Silva, A.M. Segadães, R.A. Lopes, Castable systems designed with powders reclaimed from dismantled steel induction furnace refractory linings, Ceram. Int. 43 (2017) 5020–5031. https://doi.org/10.1016/j.ceramint.2017.01.012.

[115] M.D.M. Innocentini, R.G. Pileggi, F.T. Ramal, V.C. Pandolfelli, PSD-Designed refractory castables, Am. Ceram. Soc. Bull. 82 (2003) 9401-9406.

[116] R. Kurad, J.D. Silvestre, J. de Brito, H. Ahmed, Effect of incorporation of high volume of recycled concrete aggregates and fly ash on the strength and global warming potential of concrete, J. Clean. Prod. 166 (2017) 485–502. https://doi.org/10.1016/j.jclepro.2017.07.236.

[117] W. Nguyen, D.M. Martinez, G. Jen, J.F. Duncan, C.P. Ostertag, Interaction between global warming potential, durability, and structural properties of fiber-reinforced concrete with high waste materials inclusion, Resour. Conserv. Recycl. 169 (2021) 105453. https://doi.org/10.1016/j.resconrec.2021.105453.

[118] A. Sahraei Moghadam, F. Omidinasab, S. Moazami Goodarzi, Characterization of concrete containing RCA and GGBFS: Mechanical, microstructural and environmental properties, Constr. Build. Mater. 289 (2021) 123134. https://doi.org/10.1016/j.conbuildmat.2021.123134.

Chapter Five: Short-term Behaviour of Eco-efficient Concrete Designed through a Coupled PPM-MP Approach

De Grazia, M. T.[a], Sanchez, L. F. M.[b], Yahia, A.[c]

[a] Ph.D. Candidate – University of Ottawa, Department of Civil Engineering, ON, Canada.

[b] Associate Professor – University of Ottawa, Department of Civil Engineering, ON, Canada.

[c] Full Professor - Université de Sherbrooke, Department of Civil and Building Engineering, QC, Canada.

Abstract

A new mix-design approach, coupling Particle Packing Models (PPMs) and Mobility Parameters (MP), is proposed in this work to proportion eco-efficient mixtures incorporating limestone fillers. Twelve concrete mixtures containing distinct ranges of cement content (320, 250, 200, 150 kg/m^3), slumps (180, 90, and 20 mm) and compressive strengths (18 – 45 MPa) were developed, targeting conventional values as per ACI 211-1. Comprehensive analyses (experimental and analytical) were then conducted to investigate and describe the impact of increasing eco-efficiency on the fresh state behaviour of these mixtures. Moreover, a new parameter, the so-called interparticle spacing of cement particles (IPS_{cement}), is proposed to predict the compressive strength of sustainable mixtures. Finally, global warming potentials (GWPs) were calculated to investigate the importance of developing and optimizing low-carbon footprint mixtures. All these findings demonstrate the feasibility of producing eco-efficient mixtures for distinct applications, which contributes towards Net Zero goals of concrete construction.

Keywords: *Eco-efficient concrete, rheology, flowability characteristics, low cement content, particle packing models, mobility parameters.*

5.1 Introduction

With the rise of environmental concerns, the construction industry must focus not only on the economical and performance aspects of concrete. Although the depletion of natural aggregates is an important environmental impact faced by the concrete industry, carbon dioxide emission is considered the main issue. Ordinary Portland cement (OPC) is responsible for 92% of concrete CO_2 emissions, hence, its reduction is crucial to manufacturing an eco-friendly material [1–4]. Besides the ecological drawbacks, Portland cement is also the most expensive concrete component. Thus, its reduction may solve partially the financial challenges faced by infrastructure managers. The construction industry worldwide is committed to Global Cement and Concrete Association to reach Net Zero Concrete by 2050 [5,6]. Yet, sustainability commitments are urging action now to achieve a reduction greater than 30% in less than 10 years. Actions are required in seven main phases of concrete production, including 1) savings in clinker production, 2) efficiency in concrete production, 3) savings in cement and binders, 4) decarbonization, 5) CO_2 sink: recarbonation, 6) carbon capture and utilization/storage, and 7) efficiency in design and construction.

Conventional concrete mixtures are designed for 25-40 MPa compressive strength, yet the lack of mix-design optimization leads to high cement content usage (i.e., 350-500 kg/m^3) [7]. Portland cement can be reduced through the use of supplementary cementing materials (SCMs), such as silica fume, fly ash, blast furnace slag, natural pozzolans and/or inert fillers (IF) [8–12]. Using SCMs as a partial replacement for OPC often results in improvements in the hardened states of concrete and also durability aspects [13,14], but can pose challenges on the rheological behaviour of mixtures [8,15]. Moreover, although most of the SCMs produced are already used in Construction Industry, their production does not overcome the increased OPC demand [11].

Inert fillers may also be used to decrease the carbon footprint of concrete. Amongst them, limestone filler (LF) is the most common one due to its availability worldwide, economy, volumetrically stability within the cement paste, improvement in the fresh state due to its semi-spherical shape and its ability to be produced in different particle size distributions (PSD) [16–22]. Two types of limestone fillers can be selected to develop eco-efficient mixtures; the first, so-called "*replacement filler"* which contains PSD similar to Portland cement and it is selected to direct replace cement and reduce its content, and the second, so-called "*performance filler"* which contains PSD smaller than cement and it improves the system packing density reducing concrete's total porosity [23,24]. The average replacement ratio of limestone fillers is around 20%; nevertheless, the limit of 35% is acceptable by some standards (i.e. in Europe and South Africa) [16,17,25,26]. However, previous studies have shown promising hardened results with higher replacement levels (up to 50%), especially when using Particle Packing Models (PPM) as mix-design procedure [12,27–34]. Yet, no clear procedure has been established indicating ranges of water-to-cement (w/c) ratios to achieve required fresh and compressive strength properties of eco-efficient mixtures designed through PPMs. To overcome these difficulties, a number of authors [28,30,31] pointed out the need of conducting further experimental works to determine the effective water content, admixtures (e.g., high-range and mid-range water reducers), and w/c for distinct applications. From a fresh state perspective, slump is the most common test used to appraise the behaviour of conventional concrete (CC), whereas slump-flow, V-funnel, J-ring, and L-box are the usual standard tests performed to assess self-consolidating concrete (SCC). For concrete designed through PPMs, previous studies [12,30–34] indicate that the water-to-binder (w/b) ratio should be increased to keep the fresh state performance (either slump or slump flow) of both CC and SCC, which may have an adverse impact on the hardened state properties of the material. For that reason, numerous works in the literature

[29,35,36] emphasize a poor fresh state performance (low slump or slump flow values) of concrete mixtures optimized for hardened state and sustainability criteria. This work aims to propose a new mix-design approach, coupling particle packing models and mobility parameters, to proportion eco-efficient conventional concrete mixtures presenting proper fresh state performance and designed for structural applications.

5.2 Background

5.2.1 Methods to optimize concrete mix-design

PPMs are used to mix-proportion concrete and densify the material microstructure, where the higher the packing density, the lower the amount of powder (≤ 125 μm i.e., binder and fillers) required, increasing concrete eco-efficiency. PPMs can be divided into two main groups: a) discrete and b) continuous models [27,37]. The first discrete and continuous PPMs were created by Furnas in 1929 [27,38–40] and Fuller in 1907 [27,39,40], respectively. The PPMs science has been developed over the years based on these two pioneers [27,32,38–41]. Yet, previous studies [29,42] have suggested that real aggregate blends are better represented by continuous models as concrete contains particles of all sizes (i.e. no gaps throughout the whole PSD) [27,39]. The Alfred model or modified Andreasen is the most recent continuous PPM developed (Equation 5.1).

$$CPFT = 100 * \left(\frac{{D_P}^q - {D_S}^q}{{D_L}^q - {D_S}^q} \right) \quad \text{Equation 5.1}$$

where D is the particle size in question, CPFT is the cumulative percent finer than D, D_L and D_S is the largest and smallest diameter particle size in the system, respectively, and q is a distribution factor.

Based on Westman and Hugill porosity model [40], it was determined that the optimum packing is achieved when the distribution factor is equal to 0.37 (Figure 5.1). Conversely, the optimum q-factor reduces concrete flowability as the concrete presents less porosity and thus OPC content. Aiming to improve concrete flowability, a q-factor of 0.22 is often suggested since it results in a higher amount of fines and a lower amount of coarse aggregates producing a suitable amount of powder to liquid ratio, helping the coarse aggregate particles slippage.

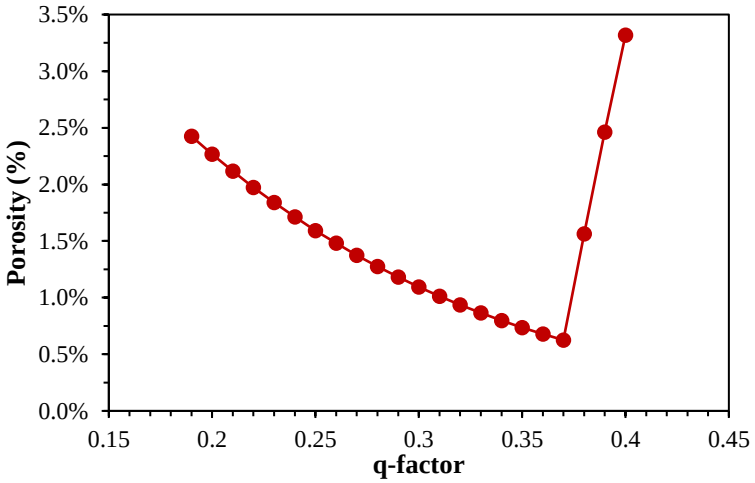

Figure 5.1. Westman and Hugill model correlation between porosity and Alfred model q-factor.

Although this q-factor range can be used as a suggestion of the flowability expected, the fresh state behaviour of packed concrete is still a concern. Mobility parameters may be used as a complementary approach with PPMs while mix-proportioning eco-efficient mixtures. Two parameters have been proposed to clarify the mobility of granular systems: the interparticle spacing (IPS; Equation 5.2) and the maximum paste thickness (MPT; Equation 5.3) [28,29,43,44]. IPS is considered as the average distance between two adjacent particles smaller than 125 μm, which are normally separated by water [28,29,40,44,45], whereas MPT measures the maximum distance amongst particles greater than 125 μm; hence, MPT has a direct correlation to cement paste thickness

around aggregate particles [28,29,43,44]. It has been found that the lower the IPS and MPT, the lower the flowability of granular systems due to particle collision, which increases the system viscosity. Conversely, high IPS and MPT yield less viscous and more flowable mixtures [28,29,46].

$$IPS = \frac{2}{VSA}\left[\frac{1}{V_s} - \frac{1}{(1 - P_{of})}\right] \quad \text{Equation 5.2}$$

where IPS is the interparticle spacing, VSA is the calculated volume surface area per cubic centimetre of powder, V_s is the volume fraction of fine solids (particles smaller than 125 μm), and P_{of} is the pore fraction assuming the densest packing of the fine particles.

$$MPT = \frac{2}{VSA_c}\left[\frac{1}{V_{sc}} - \frac{1}{(1 - P_{ofc})}\right] \quad \text{Equation 5.3}$$

where MPT is the maximum paste thickness, VSA_c is the calculated volume surface area of aggregate (particles greater than 125 μm) fraction, V_{sc} is the volumetric aggregate solid fraction, and P_{ofc} is the pore of aggregate fraction assuming the densest packing.

5.2.2 Short-term performance of sustainable mixtures

PPMs are mathematical techniques used to optimize concrete mix-proportioning and may be used to design low carbon footprint concrete (i.e., OPC content greater than 300 kg/m³) [12,29–34]. The eco-efficiency of the mixture can be further improved with the use of limestone fillers and/or SCMs; yet fillers are amongst the few products that outperform OPC production [17]. Previous research [47,48] has shown that up to 10% limestone filler can be added without affecting the hardened state properties of concrete. This happens due to two main phenomena that contribute to the strength and durability of concrete: 1) the filler effect, which reduces the system's porosity and 2) further reaction

with alumina, which forms carbo-aluminate phases [28,44,47,49,50]. Moreover, the dilution effect, defined as an increase in water content per unit mass of cement particles (i.e., an increase in w/c), can also contribute to the overall hardened state properties by accelerating cement hydration at early ages; yet, this may negatively impact the 28-day concrete compressive strength of mixtures incorporating fillers [17,25,47,49].

Kumar and Santhanam, 2003 [32] developed high-strength eco-efficient concrete mixtures containing 270, 55, and 30 kg/m^3 of OPC, quartz filler, and silica fume respectively through Alfred's model. With the aid of high amounts of superplasticizer, the authors obtained outstanding fresh and hardened state results with slump of 100 mm and 28-day compressive strength of 83 MPa. Wenqiang et al. [33] selected a combination of PPM (i.e., CPM and 3PM) coupled with experimental works to develop twelve eco-efficient self-compacting concrete mixtures. All of the mixtures incorporated 308 kg/m^3 of OPC and limestone fillers ranging from 53 to 212 kg/m^3, corresponding to limestone filler additions ranging from 14.7% to 40.7% of total powder mass. Interestingly, mixtures with 20 L/m^3 of limestone powders and 3.61 kg/m^3 of superplasticizer achieved slump flow values varying from 480 to 560 mm. The increase of limestone filler and superplasticizer contents resulted in a slump flow of up to 700 mm; the compressive strength values ranged from 30 to 48 MPa. Esmaeikhanian et al. [34] also developed thirteen eco-efficient self-compacting concrete mixtures using Alfred's model and incorporating limestone fillers, silica fume, and/or fly ash. The optimal powder composition was determined based on the rheological results of cement paste analysis to reduce water demand while maintaining the desired properties. The cement content ranged from 196 to 271 kg/m^3, while the total powder content varied from 280 to 310 kg/m^3. Although all the mixtures contained superplasticizer, some of them also required stabilizer and air-entraining agents. Slump flow between 560-640 mm and compressive strength values ranging from 25 to 30 MPa were

achieved. These investigations clearly indicate that, although through distinct approaches, eco-efficient concrete mixtures yielding proper rheological behaviour and hardened state properties can be designed via PPMs; yet there is no clear systematic procedure for developing those conventional concrete mixtures for the most common and distinct applications as presented in ACI 211-1.

5.2.3 Global warming potential assessment

It is known that cement is the main CO_2-emitting concrete component. Yet, cement production highly affects the total amount of CO_2 emission, wherein more than 50% of the total pollutants depend on the ratio between clinker and OPC. A ton of clinker is responsible for releasing approximately 540 kilograms of CO_2 during the calcination process, where limestone ($CaCO_3$) is transformed into lime (CaO) [51]. While the thermal energy needed for the calcination process is responsible for the other 50% of CO_2 emissions during OPC production. Several studies [2,3,17,52] are focusing on optimizing cement production to reduce its global warming potential (GWP), which ranges from 0.82 to 0.931 kg CO_{2eq}/kg [12,34,53–55]. According to Damineli et al. [7], most concrete mixtures produced worldwide are developed with OPC content higher than 300 kg/m³. In addition, Wallevik et al. [56] created a classification (Table 5.1) of concrete eco-efficiency based on its carbon footprint. Therefore, mixtures developed with OPC content of 250 kg/m^3 or lower can be considered low-carbon concrete (LCC) [56].

Table 5.1. Low Carbon Concrete Classes as per [56]**.**

Classification	Carbon footprint (kg CO_{2eq}/kg)
Semi-LCC	≤ 300
LCC_{250}	≤ 250
LCC_{200}	≤ 200
LCC_{150}	≤ 150
EcoCrete	≤ 125
EcoCrete Xtreme	≤ 105

Equation 5.4 can be used to quantify their global warming potential (GWP), which corresponds to the CO_2 emissions (in mass) per unit volume of concrete [12,34]. Table 5.2 shows the GWP of each concrete ingredient [12,34,53–55] that may be used combined with Equation 5.4.

$$GWP = \sum_{i=1}^{n} m_i . g_i \qquad \text{Equation 5.4}$$

where m_i is the mass of concrete ingredient (i) per unit volume of concrete and g_i is the e-CO_2 per unit mass of concrete ingredient (i).

Table 5.2. Equivalent CO_2 emissions (CO_{2eq}) of concrete ingredients (in kg/kg)

Ingredient	Cement	Limestone Filler	Fine Aggregate	Coarse Aggregate	Water	Admixtures
GWP (kg CO_{2eq}/ kg of material)	0.9	0.032	0.0029	0.0062	0.00034	0.72
Reference	[53]	[34]	[12,34]	[34]	[12,34]	[34]

Besides GWP, concrete mixtures' eco-efficiency can also be evaluated based on the CO_2 intensity index ($ci_{cs;}$ Equation 5.5), where the amount of GWP required to produce one unit of any concrete property is appraised [7]. Since 28-day compressive strength is the most important one, it is the most applied in the CO_2 intensity index.

$$ci_{cs} = \frac{GWP}{f'_c} \qquad \text{Equation 5.5}$$

where ci_{cs} is the CO_2 intensity index ($kg/m^{-3}. MPa^{-1}$), GWP is the global warming potential of the concrete investigate (CO_{2eq}/kg), and f'_c is the concrete compressive strength (MPa).

5.3 Scope of the work

This work aims to present a new method (PPM-MP approach) for developing eco-efficient concrete mixtures targeting distinct fresh state performances, such as slump of 180, 90, and 20 mm with variability of +/- 20 mm and a wide range of compressive strength (between 18 and 45 MPa), which are the most commonly selected consistency and strength values as per ACI 211-1 [57] and CSA A23.1 [58]. PPM is used to reduce system porosity and increase eco-efficiency, while MPs are used to better understand and describe the fresh state performance of low cement concrete. A total of twelve concrete mixtures were developed with a proposed PPM-MP approach containing distinct ranges of cement content (e.g., 320, 250, 200, 150 kg/m^3). To further improve the system eco-efficiency and hardened state performance, two types of limestone fillers (performance and replacement) were added. First, the optimum volumetric percentage of the performance filler was calculated to decrease the matrix porosity. Then, the replacement filler was added to achieve the target cement content. Fresh state (i.e., slump and rheology over time) and hardened state (absorption, bulk electrical resistivity, and compressive strength) tests were performed, and global warming potentials (GWPs) and CO_2 intensity index were calculated to assess the eco-friendly mixtures developed. Rheological modelling using Herschel Bulkley was finally used to calculate the true viscosity of the mixtures investigated and understand the effect of cement reduction on the rheological parameters. Additionally, a modified version of the IPS called "IPS_{cement}" is proposed to predict the compressive strength of eco-efficient highly packed mixtures developed with a high amount of limestone fillers.

5.4 Materials and methods

5.4.1 Raw materials characterization

The concrete mixtures investigated in this study were developed with a Portland cement type general use (GU), two types of limestone fillers natural sand and a granite coarse aggregate with a nominal maximum size of 19 mm. The chemical composition of the general use cement obtained by X-ray fluorescence, the mineralogical phases calculated through Bogue [59] and the physical characteristics (specific gravity and specific surface area) of concrete's components are presented in Table 5.3. The first limestone filler called "*performance-P filler*" contains particle size distribution (PSD) smaller than OPC, whereas the second one named "*replacement – R filler*" was selected due to its PSD similarity with OPC (Figure 5.2). Moreover, certain mixtures required two types of admixtures (a polycarboxylate-based high-range water reducer and a lignosulfonate-based mid-range plasticizer) to improve their flowability and achieve the target slump.

Table 5.3. Chemical composition and mineralogical phases of GU cement and Physical properties characterization.

Chemical Composition	GU cement	Mineralogical phases		Material	Specific gravity (g/cm^3)	Specific surface area (m^2/g)
CaO	61.5	C_3S	53.5	GU cement	3.17	1.17
SiO_2	19.4					
Al_2O_3	4.9	C_2S	15.5	Filler - R	2.66	1.6
Fe_2O_3	3.7			Filler - P	2.6	3.7
SO_3	3.9	C_3A	6.7	Fine Aggregate	2.74	0.92
MgO	2.4					
Na_2O	0.95	C_4AF	11.2	Coarse Aggregate	2.81	0.11
LOI	1.9					

5.4.2 Mix-design procedure – PPM-MP approach

Alfred model (also known as modified Andreasen) was selected for this work to develop eco-

efficient mixtures. When using this mathematical model and a q-factor of 0.37, the lowest system porosity of 2.8% is produced when calculated with Westman and Hungill model. Based on a previous study [29], the Alfred model can be more optimized in terms of fresh state when the target PSD curve is divided into two parts: powder portion (from D_s to D_{pwd}; µm) and aggregate portion (from D_{pwd} µm to D_l). As per the Alfred model, D_s and D_l are the smallest and the largest particle diameter available in the system, respectively. The new D_{pwd} represents the largest powder diameter considering all the powders used in the system. A representative example of the Alfred model divided into two parts is presented in Figure 5.3.

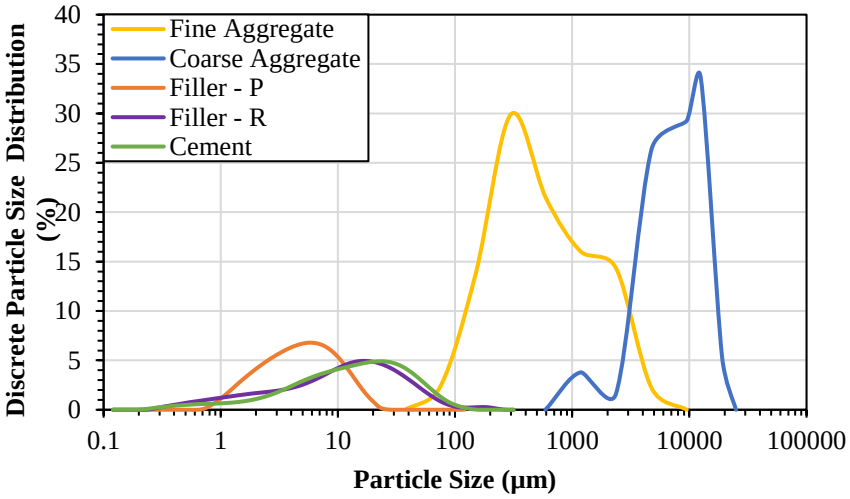

Figure 5.2. Particle size distribution of raw materials.

Following the division of the Alfred model curve, two q-factors were pre-selected to achieve the lowest system porosity. For the powder portion (from D_s to D_{pwd} µm) a q-factor of 0.34 was selected, whereas a q-factor of 0.31 ±0.1 were found to be optimum on the aggregate portion. In this work, the D_{pwd} is 80 µm which represents the largest diameter available within the powders selected (i.e., OPC, replacement and performance filler). As a result, with the selected materials characteristics and Westman and Hungill model [40], the system generated contains a dry porosity of 3.0% ±0.1. Moreover, all mixtures present the same mortar factor of 61%.

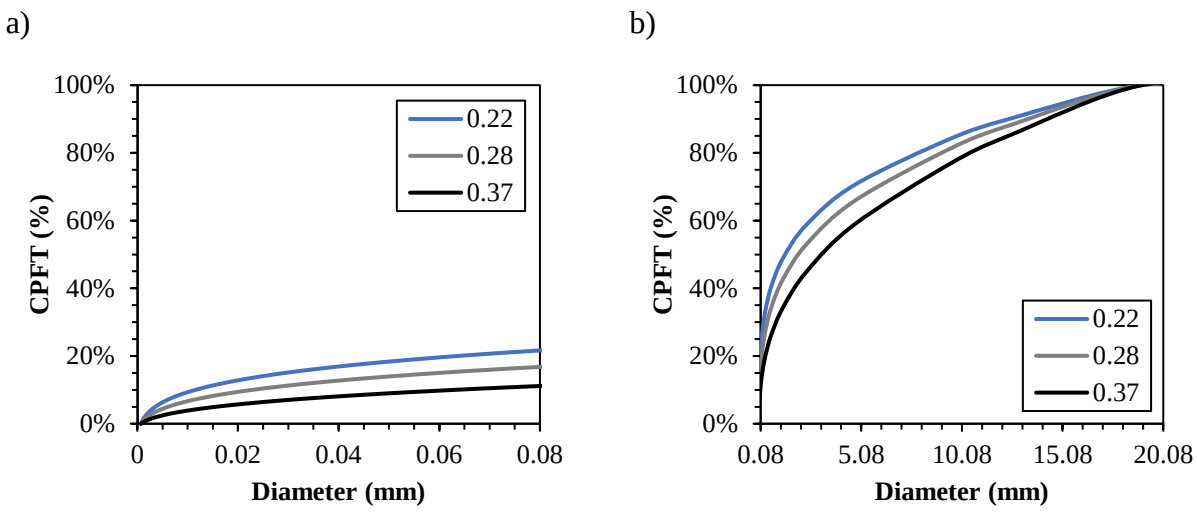

Figure 5.3. Example of Alfred model with two q-factors (broken curve) a) powder portion and b) aggregate portion.

After optimizing the mix-design based on the material characteristics, the least square method was applied and an optimum volume of "*performance filler*" of 1.9% was calculated based on the 0.34 q-factor curve of the powder portion. Three control mixtures were developed without limestone filler addition, resulting in cement content of around 320 kg/m^3, whereas the other nine mixtures were developed with performance filler. However, to evaluate the impact of limestone filler and cement content on eco-efficient mixtures, three ranges of cement content (250, 200, and 150 kg/m^3) were selected. To achieve the target cement content, "*replacement fillers"* were added which account for approximately 1.2, 3.2, and 5.1% of total concrete dry volume, respectively.

Then, the water-to-cement ratio (w/c) of 0.68, 0.60, 0.52 was selected for the control mixtures to achieve around 20, 25, 30 MPa and slumps range recommendations (i.e., 180, 90, and 20 +/- 20 mm) as per ACI 211-1 [57] and CSA A23.1 [58]. Although a similar w/c was selected for mixtures with 250 kg/m^3 of OPC, it would result in not enough free water for mixtures with 200 and 150 kg/m^3. Then the mobility parameters of each mix-design were calculated and to maintain the same mobility

parameters range, the same water-to-powder ratio (w/p, i.e., total water divided by mass of cement and fillers) was selected for the nine eco-efficient mixtures (i.e., developed with limestone filler). Accounting for the physical characteristics of the materials selected in this work, the IPS ranged from 1.06 to 0.40, whereas MPT ranged from 0.52 to 0.31. Three w/p (i.e., 0.54, 0.47, and 0.40) were selected resulting in IPS of 0.60, 0.51, 0.42 ± 0.02 μm, whereas MPT of 0.41, 0.37, 0.32 ± 0.02 μm, respectively.

5.4.3 Eco-efficient concrete mixtures

To address the short-term performance and understand the impact of cement content and limestone filler on the fresh state performance of eco-efficient concrete mixtures, four main groups were created with distinct cement contents (320, 250, 200, and 150 kg/m^3). Within each group, three w/c were selected for manufacturing eco-efficient mixtures with three targeting slumps (i.e., 180, 90, and 20 +/- 20 mm).

The mixtures were classified and divided into 4 groups based on their cement content; where Group 1 (G1) represents the control mixtures (on average 320 kg/m^3 of cement), while Group 4 (G4) represents the mixtures with the lowest cement content (150 kg/ m^3). After the group number a letter H, M or L was added to classify them as high – H, medium – M, and low – L mobility parameters. Then their names present the cement content followed by w/c. For example, mixture 2M-250-0.60 is from Group 2 (G2) and has medium water content, 250 kg/m^{-3} of cement, and w/c of 0.60. A summary of the eco-efficient mixtures developed is presented in Figure 5.4 and Table 5.4. Moreover, Table 5.5 highlights the impact of limestone fillers on the mobility parameters, where control mixtures achieved higher IPS and MPT values.

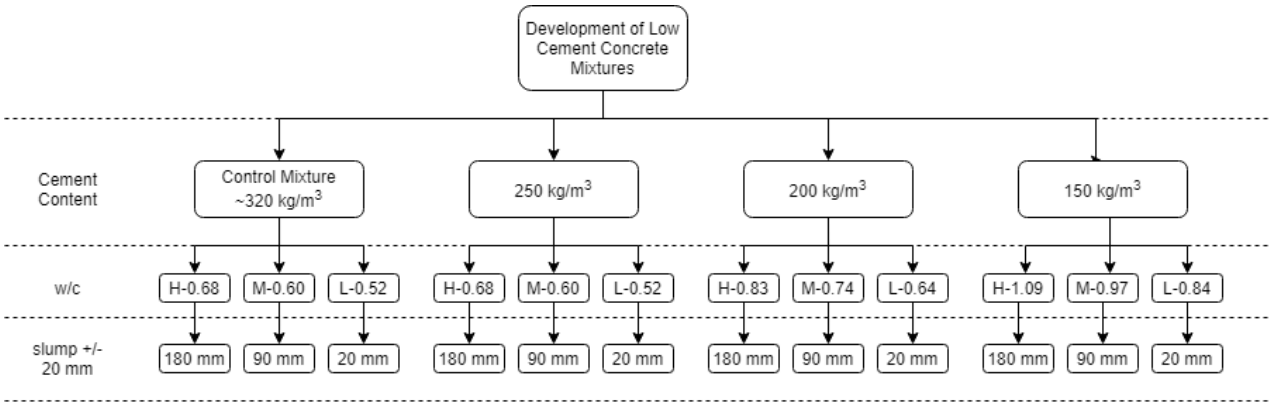

Figure 5.4. Summary of the twelve eco-efficient concrete mixtures.

Table 5.4. Mix-design of twelve eco-efficient concrete mixtures.

Mix-name	kg/m³													
		Powder		Fine Aggregate					Coarse Aggregate					
	OPC	Filler P	Filler R	150-300 mm	300-600 mm	600-1180 mm	1180-2360 mm	2360-4750 mm	4750-9500 mm	9500-12500 mm	12500-19000 mm	Water	SP	MR
1H-311-0.68	311	0	0	126	157	189	239	300	378	174	295	212	0.0	0.0
1M-319-0.60	320	0	0	130	161	194	246	307	388	178	303	192	0.0	0.0
1L-328-0.52	328	0	0	133	165	199	252	316	398	183	311	171	0.0	0.0
2H-250-0.68	250	39	25	133	165	199	252	316	398	183	311	170	1.9	1.9
2M-250-0.60	250	40	31	136	169	204	259	324	408	187	319	150	3.9	3.2
2L-250-0.52	250	41	37	140	173	209	265	332	418	192	326	130	3.9	3.9
3H-200-0.83	200	40	69	134	166	200	254	318	401	184	313	165	1.9	1.9
3M-200-0.74	200	41	74	137	169	204	259	324	409	188	319	148	3.8	3.1
3L-200-0.64	200	41	79	140	174	210	266	333	419	193	327	129	3.9	3.9
4H-150-1.09	150	40	111	138	170	204	256	319	399	182	309	163	2.4	1.2
4M-150-0.97	150	41	117	141	174	208	262	326	408	187	316	145	4.3	2.5
4L-150-0.84	150	42	122	144	178	213	268	333	417	191	323	126	3.9	3.9

Note: SP and MR stand for superplasticizer and mid-range admixtures, respectively.

Table 5.5. Mobility parameters of designed mixtures.

Mix-name	Mobility Parameters		w/c	w/p	Filler % (m.p.)
	IPS (µm)	MPT (µm)			
1H-311-0.68	1.06	0.52	0.68	0.68	0%
1M-319-0.60	0.92	0.47	0.60	0.60	0%
1L-328-0.52	0.79	0.42	0.52	0.52	0%
2H-250-0.68	0.63	0.42	0.68	0.54	21%
2M-250-0.60	0.53	0.37	0.60	0.47	22%
2L-250-0.52	0.44	0.33	0.52	0.40	24%
3H-200-0.83	0.60	0.41	0.83	0.54	35%
3M-200-0.74	0.51	0.37	0.74	0.47	36%
3L-200-0.64	0.42	0.32	0.64	0.40	38%
4H-150-1.09	0.57	0.39	1.09	0.54	50%
4M-150-0.97	0.49	0.35	0.97	0.47	51%
4L-150-0.84	0.40	0.31	0.84	0.40	52%

Note: filler percentage is related to the total mass of powders (m.p.).

5.4.4 Fabrication and testing methods

First coarse and fine aggregate was sieved based on sieves classification as per CSA A23.1 [58]. Twelve concrete mixtures with a proposed PPM-MP approach containing distinct ranges of cement content (e.g., 320, 250, 200, 150 kg/m^3) were manufactured using 40 litres pan mixer. Concrete constituents were mixtures for about 10 minutes and then the first slump test was performed (Slump – 0 min). At approximately 15 min, the rheology test was started (Rheology – 0 min). Another two readings of each test were performed after 15 and 30 minutes. Meanwhile, cylinders (length and diameter of which were 200 mm and 100 mm) were fabricated according to ASTM C 39 [60] for the hardened state test. The specimens were demoulded, ground, and moist cured for 28 days before performing a compressive strength test.

5.4.5 Fresh state assessment

Two main fresh state tests were performed: slump test (or concrete consistency) and rheological assessment over time (i.e., 0, 15, and 30 minutes). Concrete's consistency was measured using a conventional slump cone as per CSA A23.1 [58]. Then, slump loss, which is the rate of consistency loss over time, was calculated by Equation 5.6.

$$Slump\ Loss\ (\%) = \frac{(S_i - S_t)}{S_i} * 100 \qquad \text{Equation 5.6}$$

where S_i is the initial slump and S_t is the slump measured at a time (t).

A rheological test program was performed using a planetary rheometer (IBB rheometer - Figure 5.5) with an H-shape impeller (100 mm height and 130 mm length) and a bowl with a diameter of 360 mm and 250 mm height [61]. Previous study [62] states that IBB rheometer is recommended to evaluate concrete mixtures with conventional slump ranges (e.g., 40-300 mm). Therefore, mixtures

developed with low mobility parameters might present segregation on the rheological tests, hence, their results were not investigated due to rheometer limitations.

a) b)

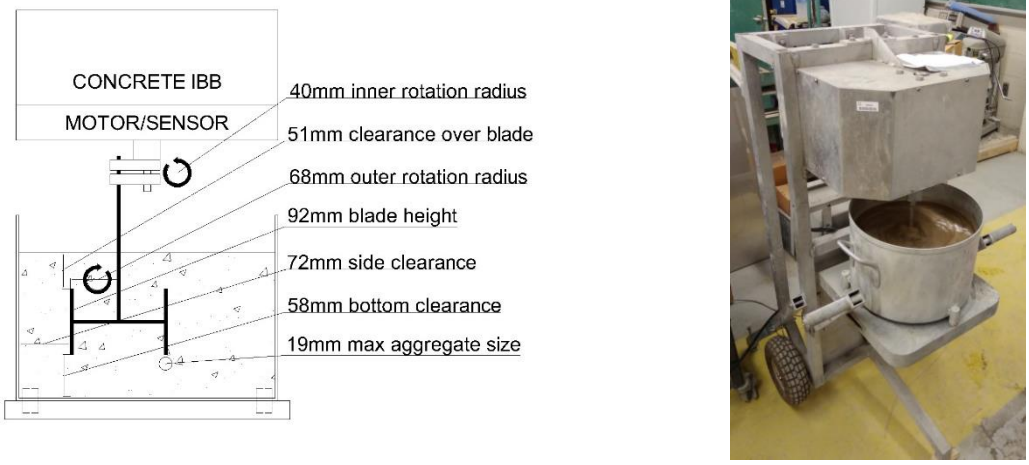

Figure 5.5. IBB rheometer a) measurements b) photo.

A pre-programmed cycle of 180 seconds was selected. Each cycle increases the shear rate up to 0.7 s^{-1} before decreasing it in the same stepwise manner while maintaining rotation for approximately 10 seconds at each step, as shown in Figure 5.6. First, a complete cycle was applied as a pre-shear regime. Another cycle was performed to appraise the rheological behaviour of each mixture. The IBB raw data were plotted for the rheological analysis. However, the IBB rheometer has two Bingham output parameters (i.e., G – yield stress in N.m, and H – plastic viscosity in N.m.s) that were not used in this study as the concrete mixtures evaluated do not present a Bingham behaviour. Moreover, the IBB rheometer results are not displayed in fundamental units (e.g., yield stress - Pa and plastic viscosity - Pa.s); hence, the results are used as a comparison amongst distinct mixtures investigated in this study. However, previous studies [61,62] concluded that the IBB outcomes yield a good correlation with other rheometers (e.g., BML, Btrheom, Cemagrefing, Two-Point apparatus)

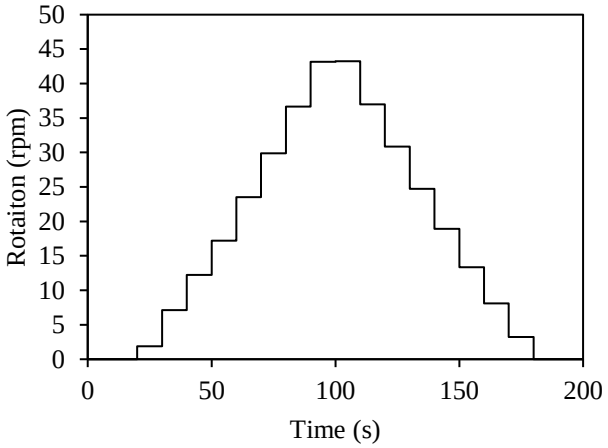

Figure 5.6. Test program used for analyzing the rheology cycle.

To further understand the rheological behaviour, modelling using the Herschel-Bulkley model was developed, and the rheological parameters were determined as per Equation 5.7.

$$\tau = \tau_0 + k_{HB}\dot{\gamma}^n \qquad \text{Equation 5.7}$$

where τ is the torque, τ_0 is the yield torque, k_{HB} is the viscosity constant of Herschel-Bulkley, $\dot{\gamma}$ is the rotation, and n is the flow index (dimensionless; n < 1 shear-thinning fluid and n >1 shear-thickening fluid).

Studies show that Herschel-Bulkley model usually provides a better fitting of the flow curves when analyzing non-Bingham models (i.e., fluids presenting shear-thinning or shear thickness behaviour) [28,63,64].

5.4.6 Hardened state assessment

The hardened state performance was assessed via compressive strength, bulk electrical resistivity (ER), and absorption measurements. The compressive strength test was conducted on three specimens of each of the twelve concrete mixtures tested according to ASTM C 39 [60].

A two point uniaxial electrical resistivity (ER) test, which is also known as bulk ER, was performed according to ASTM C1760 [65]. Three concrete cylinder specimens of each mixture were placed between two electrodes. It is worth noting that a wet sponge is placed between the interface concrete electrodes to ensure a proper electrical connection. The resistance (R) is displayed in the equipment and then electrical resistivity (ρ) can be calculated by multiplying the geometric factor and the resistance (Equation 5.8). The geometrical k-factor was calculated through Equation 5.9. In this work, the average k value of 4.15 cm was calculated based on the cylinders' dimensions.

$$\rho = k * R \qquad \text{Equation 5.8}$$

where k is concrete geometric factor, R is concrete resistance, and ρ is concrete electrical resistivity.

$$k = \frac{A}{\mathrm{L}} \qquad \text{Equation 5.9}$$

where k is concrete geometric factor, A is concrete sample cross sectional area, L is concrete sample length.

The water absorption test was performed based on Archimedes' immersion method [45]. At 28 days, one cylindrical sample of each mixture was cut into three sections of approximately 100 mm in diameter and 65 mm in height. The samples were placed in an oven at 60°C, avoiding the decomposition of concrete products caused by excessive temperature, for approximately 4 days, until the change in mass between two successive weights was less than 0.3%, at which point the specimens' dry mass (m_d) was measured. The samples were then immersed in water and subjected to vacuum ensuring water penetration. After 24 hours of immersion, the wet mass (m_w) was determined. The apparent water absorption (WA) was calculated by Equation 5.10.

$$\text{WA}\ (\%) = \frac{m_w - m_d}{m_d} * 100\% \qquad \text{Equation 5.10}$$

5.5 Results and discussion

5.5.1 Slump

Each concrete mixture group was developed with three proposed consistency values, which are equivalent to the mobility parameter classification (high, medium, and low). Regardless of the cement content and the mobility parameter selected, the concrete mixtures were able to achieve the target slump with an error within 20 mm (Figure 5.7). Yet, mixtures with higher cement content and no limestone fillers (G1) did not require admixtures for achieving the target slump. Analyzing the eco-friendly mixtures, which include limestone fillers, approximately the same total amount of admixture was required for the proposed slump due to their equivalent mobility parameters values (IPS and MPT - Table 5.5).

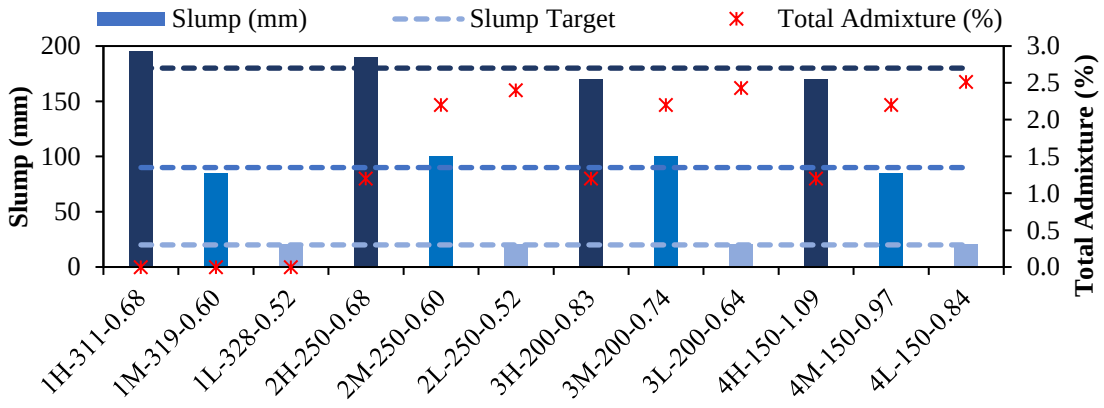

Figure 5.7. Slump of 12 mixtures developed

5.5.2 Slump loss over time

The slump was measured at 0, 15, and 30 minutes after mixing. Among the evaluated concrete mixtures, the ones containing higher IPS and MPT resulted in higher slump loss. Analyzing only

mixtures with higher mobility parameters (Figure 5.8a), 1H-311-0.68 yielded a lower slump loss over time, achieving 7.7% and 15.4% at 15 and 30 min highlighting the influence of LF on the slump loss. Mixture 2H-250-0.68 achieved only 21.1% of slump loss at 15 min, but at 30 min the slump decreased significantly similar to mixtures 3H-200-0.83 and 4H-150-1.09. However, at high mobility parameters, 4H-150-1.09, which contains 50% of LF, attained better overall performance than 3H-200-0.83 which contains 35% of LF. This behaviour was not observed on mixtures with medium and low mobility parameters (Figure 5.8b and c).

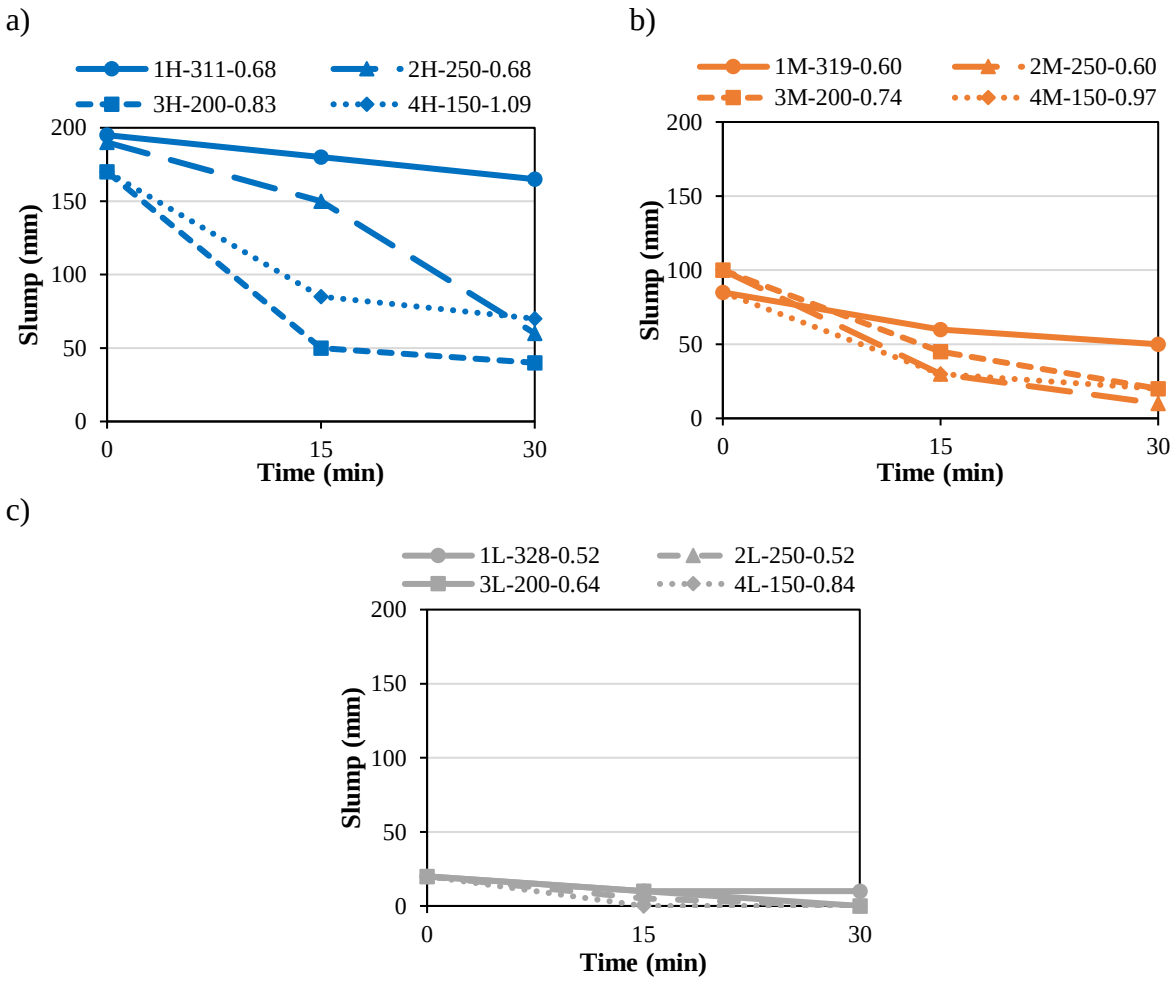

Figure 5.8. Slump over time for mixtures developed with a) high, b) medium, and c) low mobility parameters.

A previous study showed that the increase in LF can improve the flowability of self-consolidating mixtures when the powder volume is increased [33]. The change in powder volume also affected the mixtures' packing density which also influences the fresh state behaviour of the materials [8]. Contrary to the previous study [33], the current research maintained a constant volume of powder, mortar factor, and packing density within the twelve mixtures appraised. Therefore, the flowability behaviour of these mixtures is governed by the mobility parameters, that account for the water content, agreeing with the findings of [28]. Figure 5.9 confirms that the mobility parameters are one of the key factors affecting slump loss behaviour. Analyzing all mixtures investigated in this study, the slump loss at 30 min presents an accurate linear relationship with IPS and MPT with an R^2 of around 0.90. Moreover, IPS of control mixtures (G1) is considerably higher than the IPS of eco-friendly mixtures, whereas the MPT of G1 ranged from 0.42 to 0.52 µm which is similar or only 0.10 µm greater than other mixtures. Since control mixtures did not require any admixture to achieve the target slump, it may be concluded that the IPS is the key factor influencing the slump.

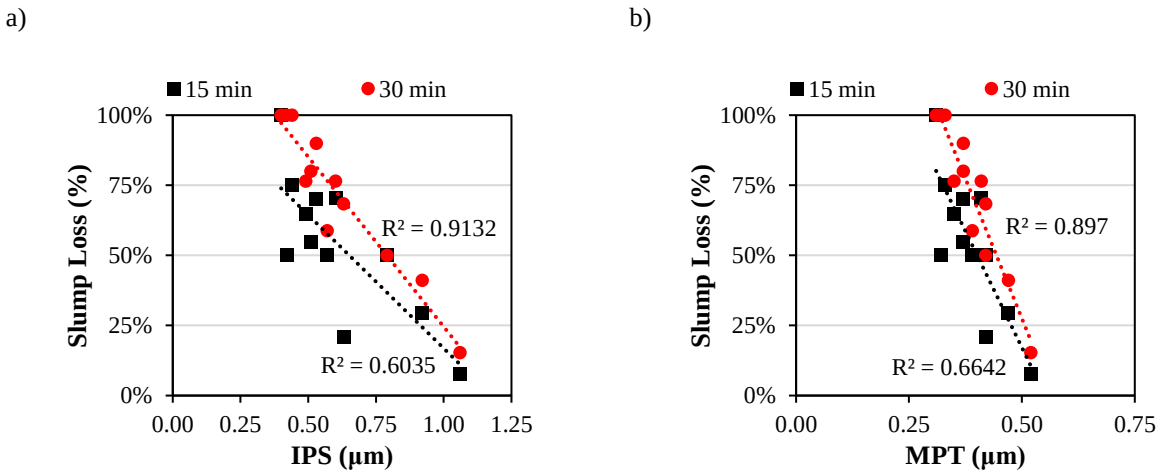

Figure 5.9. Influence of mobility parameters on the slump values.

Besides IPS (governed by water content), eco-efficient mixtures (G2, G3, and G4) contain limestone fillers, which change the system particle size distribution and roughness of particles compared to

control mixtures (G1) that only contain cement as a powder. The reduction of particle size distribution and particle roughness also affects materials' fresh state [8]. Since the percentage of limestone filler is constant within each group (i.e., G1, G2, G3, and G4 contain 0%, 22%, 36%, and 51% of LF, respectively), the PSD and roughness effect is steady when analyzing mixtures with similar cement content.

5.5.3 Rheological behaviour

The impact of the improvement of concrete sustainability on the rheology over time of the concrete mixtures was assessed in Figure 5.10. As previously mentioned, mixtures designed with low slump cannot be appraised in the IBB rheometer, hence, the rheological behaviour of only nine mixtures is discussed. First analyzing the 0min-rheological behaviour, the initial torque (0.04 s^{-1}) ranged from 3.7 to 10.6 N.m; whereas the maximum torque (0.7 s^{-1}) presented ranged from 6.8 to 24.31 N.m. Classifying the mixtures by the cement content, Group 1 (~320 kg/m^3) resulted in lower maximum torque than sustainable mixtures, while mixtures developed with 200 kg/m^3 required the highest maximum torque measured at 0.7 s^{-1}. Even though eco-friendly mixtures were developed with the same target slump (180 and 90 mm +/- 20 mm), mixtures developed with the lowest cement content (150 kg/m^3) resulted in the lowest torque, followed by mixtures with 250 kg/m^3 and then 200 kg/m^3. For instance, 2H-250-0.68, 3H-200-0.83, and 4H-150-1.09 were developed with the same slump and mobility parameters, but they achieved yield stress of 4.5, 7.5, and 4.2 N.m, respectively. Similar behaviour was seen on mixtures developed with medium mobility parameters, but the yield stress was on average 68% higher. Thus, the cement and filler content also affected the mixtures' rheological behaviour, besides the w/c, packing density, and mobility parameters. Analyzing the overall rheological aspect over time, all mixtures appraised presented shear-thinning behaviour, that is, the viscosity decreases with the increase of torque applied.

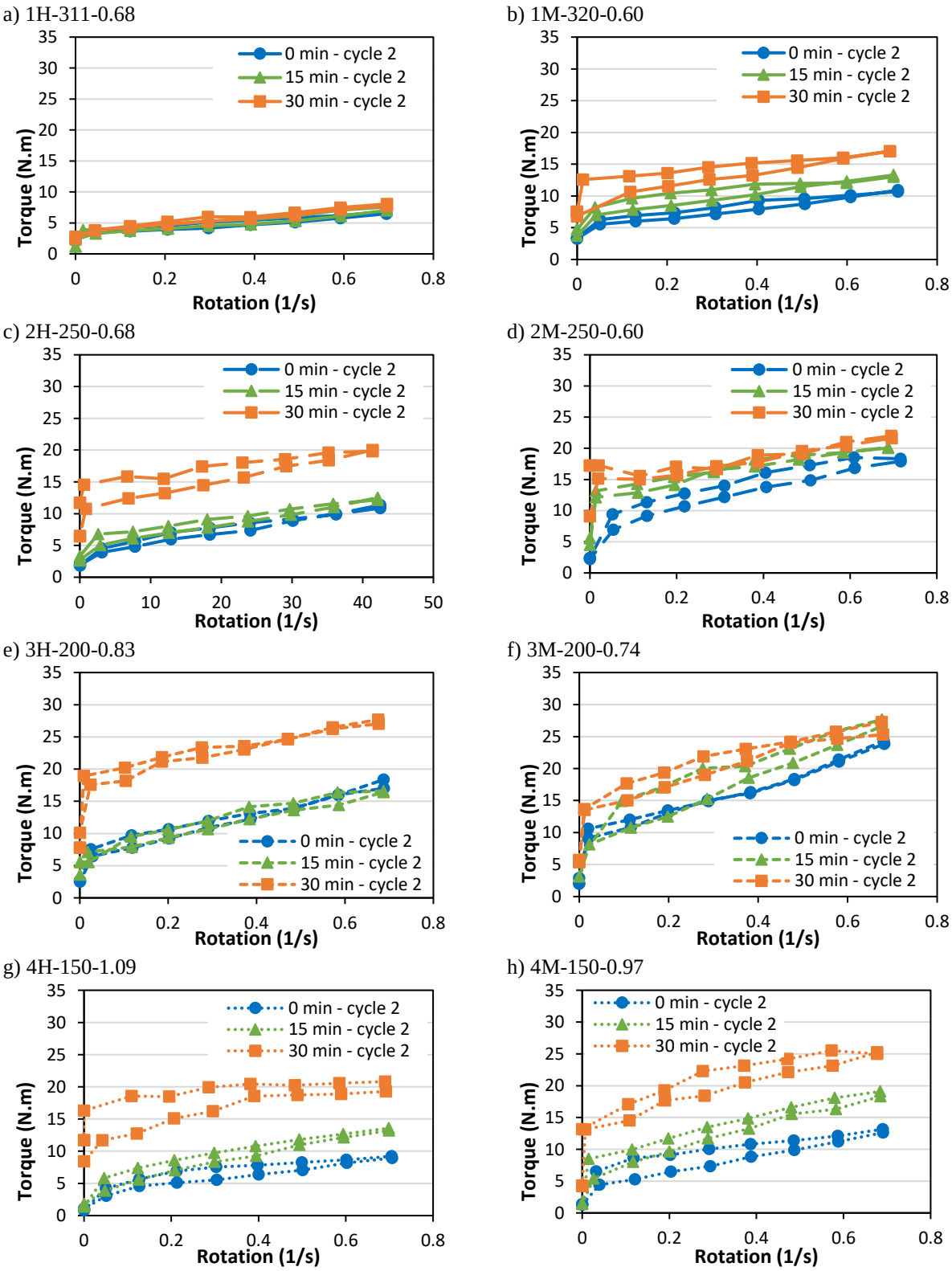

Figure 5.10.Rheological behaviour over time of mixture.

The rheological performance of control mixtures (G1) is less affected over time than mixtures developed with limestone fillers. Moreover, regarding eco-efficient mixtures (G2, G3, and G4), the torque was more affected on mixtures developed with higher w/c.

5.5.4 Modelling rheological behaviour

Herschel-Bulkley (HB) calculation was selected for modelling the rheological behaviour of concrete mixtures presenting shear-thinning characteristics. Figure 5.11 presents the experimental rheological profile compared to HB model. Analyzing Figure 5.11 and Table 5.6, it is clear that HB is a feasible tool that can be used to precisely investigate shear-thinning behaviour of concrete mixtures. Even though the rheology tests were performed after 0, 15, and 30 min, only mixture 3M-200-0.74 resulted in a slightly higher Sum Squared Error (SSE – 12.31, 6.89, and 13.63, respectively). All the other mixtures presented SSE lower than 10. Herschel-Bulkley model presents three main parameters, flow behaviour factor (n), initial torque (τ_0), and viscosity constant (k_{HB}). All mixtures analyzed presented a shear-thinning characteristic which is classified when $n < 1$, agreeing with results shown in Table 5.6. Another interesting parameter to analyze over time is the initial torque, which ranged from 1.18 to 4.83 N.m at 0 and 15- min tests but increased to up to 10.35 N.m at 30-min test. Regardless of the time of the testing, the initial torque has a slight increase with the decrease of cement content, except for mixtures developed with 150 kg/m^3 of cement that presented the lowest initial torque. The last HB parameter (viscosity constant - k_{HB}) denotes the slope of the rheological profile curve, where the higher k_{HB} values, the higher the system viscosity. Similarly to the initial torque, the lower the cement content, the higher the viscosity constant, except for mixtures developed with 150 kg/m^3 of cement that presented viscosity better than G2 mixtures (developed with 250 kg/m^3 of cement). Thus, there may be a *replacement filler* content threshold that up to a value it increases the viscosity and torque, whereas from that point on it starts to enhance

the fresh state behaviour of concrete mixtures.

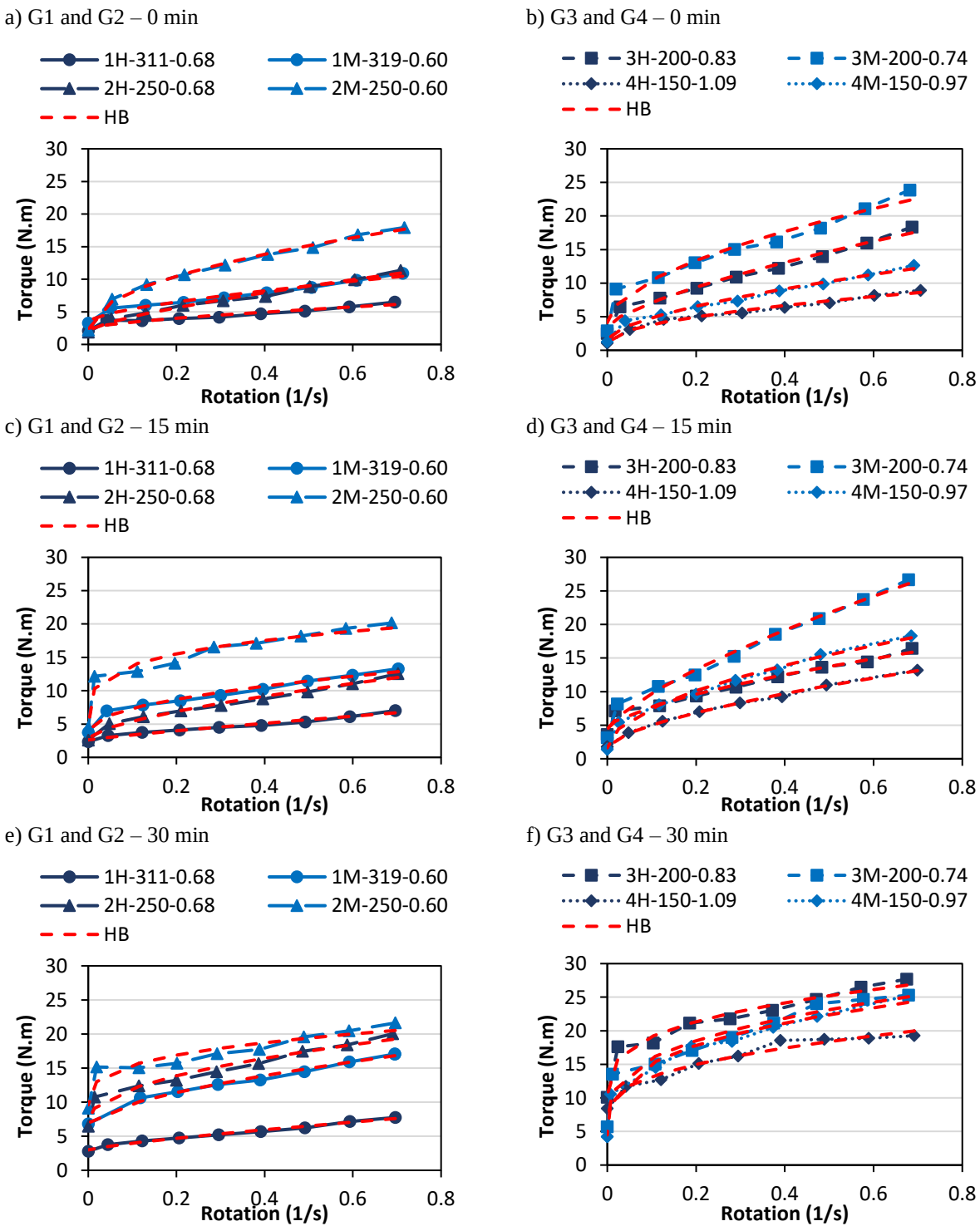

Figure 5.11. Precision of Herschel-Bulkley model to appraise the rheological performance of distinct groups and time of the test

Table 5.6. Herschel-Bulkley parameters and true viscosity equations.

0 min					
Mixture	**τ_0 (N.m)**	**k_{HB} (N.m-s^n)**	**n**	**SSE**	**True Viscosity (N.m/s^{-1})**
1H-311-0.68	2.48	4.69	0.70	1.04	$\gamma=3.28*\gamma^{-0.30}$
1M-319-0.60	3.68	8.54	0.69	1.37	$\gamma=5.86*\gamma^{-0.31}$
2H-250-0.68	2.18	11.30	0.74	0.91	$\gamma=8.34*\gamma^{-0.26}$
2M-250-0.60	2.34	18.08	0.50	0.65	$\gamma=8.96*\gamma^{-0.50}$
3H-200-0.83	3.41	18.24	0.69	4.66	$\gamma=12.61*\gamma^{-0.31}$
3M-200-0.74	4.14	22.52	0.55	12.31	$\gamma=12.48*\gamma^{-0.45}$
4H-150-1.09	1.18	8.94	0.54	0.64	$\gamma=4.79*\gamma^{-0.46}$
4M-150-0.97	1.68	13.16	0.62	1.63	$\gamma=8.12*\gamma^{-0.38}$
15 min					
Mixture	**τ_0 (N.m)**	**k_{HB} (N.m-s^n)**	**n**	**SSE**	**True Viscosity (N.m/s^{-1})**
1H-311-0.68	2.63	5.57	0.88	0.49	$\gamma=4.91*\gamma^{-0.12}$
1M-319-0.60	4.04	10.52	0.50	1.53	$\gamma=5.3*\gamma^{-0.50}$
2H-250-0.68	2.93	11.43	0.66	1.19	$\gamma=7.52*\gamma^{-0.34}$
2M-250-0.60	4.83	15.99	0.25	7.56	$\gamma=3.99*\gamma^{-0.75}$
3H-200-0.83	4.48	14.49	0.64	3.85	$\gamma=9.32*\gamma^{-0.36}$
3M-200-0.74	4.39	28.77	0.73	6.89	$\gamma=20.98*\gamma^{-0.27}$
4H-150-1.09	1.80	14.26	0.65	0.18	$\gamma=9.22*\gamma^{-0.35}$
4M-150-0.97	1.63	20.06	0.53	1.61	$\gamma=10.7*\gamma^{-0.47}$
30 min					
Mixture	**τ_0 (N.m)**	**k_{HB} (N.m-s^n)**	**n**	**SSE**	**True Viscosity (N.m/s^{-1})**
1H-311-0.68	3.00	6.14	0.80	0.30	$\gamma=4.94*\gamma^{-0.20}$
1M-319-0.60	6.95	12.44	0.64	0.85	$\gamma=7.94*\gamma^{-0.36}$
2H-250-0.68	7.25	14.29	0.48	5.40	$\gamma=6.85*\gamma^{-0.52}$
2M-250-0.60	9.60	12.28	0.32	9.57	$\gamma=3.98*\gamma^{-0.68}$
3H-200-0.83	10.45	18.61	0.33	6.84	$\gamma=6.18*\gamma^{-0.67}$
3M-200-0.74	6.49	21.31	0.35	13.63	$\gamma=7.56*\gamma^{-0.65}$
4H-150-1.09	8.33	13.74	0.45	3.19	$\gamma=6.2*\gamma^{-0.55}$
4M-150-0.97	4.49	22.37	0.32	5.40	$\gamma=7.2*\gamma^{-0.68}$

Through the Herschel-Bulkley equations calculated and displayed in Table 5.6, the true viscosity equation was calculated through the derivative of HB. To better visualize the viscosity change as a function of rotation, Figure 5.12 was created. It is clear that mixture 1H-311-0.68 yielded an almost contestant viscosity over time, which classifies as the only mixture with a Bingham behaviour (i.e., linear rheological profile). Moreover, mixtures developed with high mobility parameters yielded lower viscosity when comparing mixtures with the same cement content. The 3M-200-0.74 mix presented the highest viscosity result agreeing with the fact that it presents lower mobility

parameters and the threshold of *replacement fillers*. Due to the reduction of viscosity with the increase of rotation (shear-thinning behaviour), these mixtures are recommended for vibrated or pumped applications.

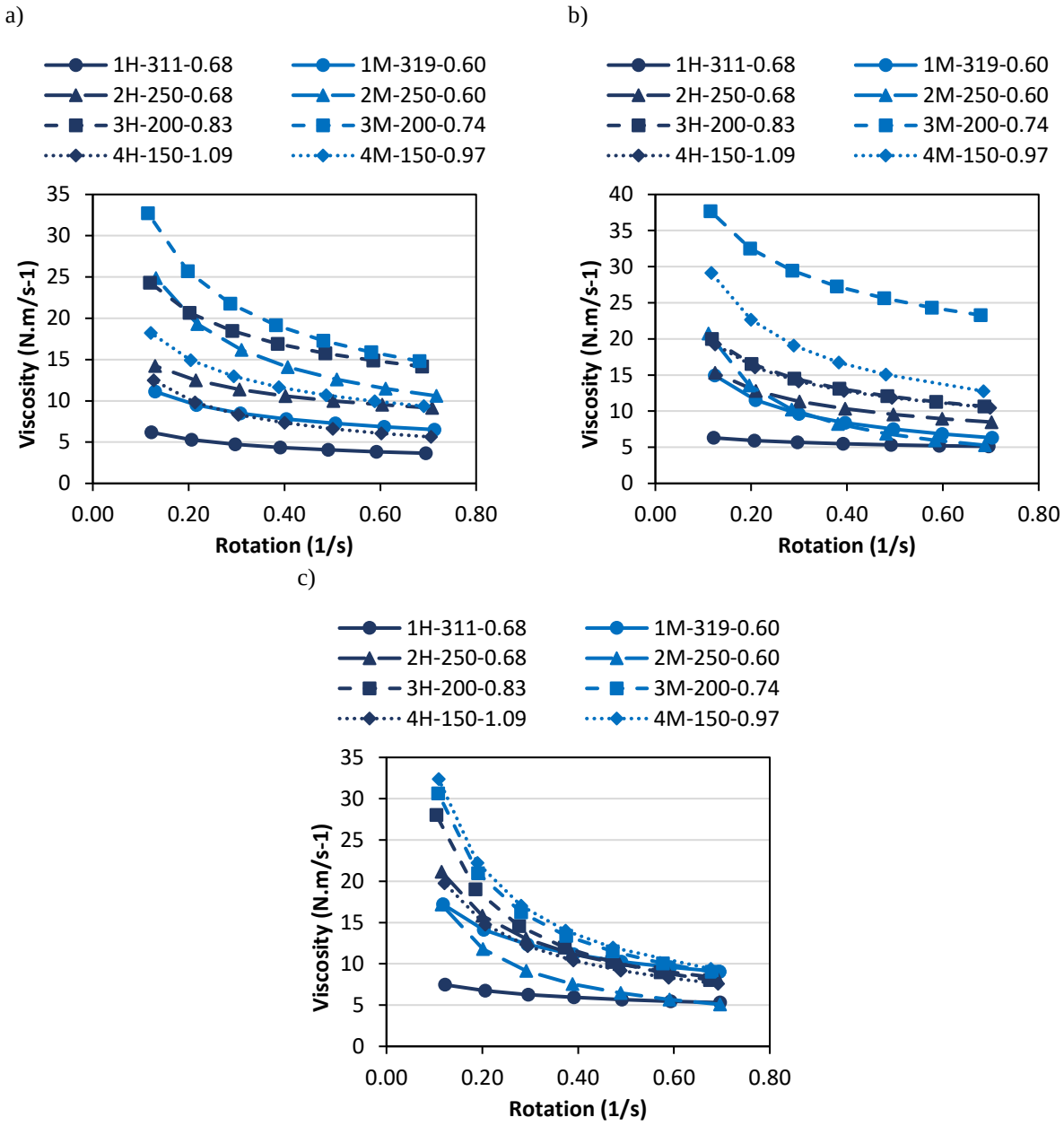

Figure 5.12. Viscosity behaviour calculated through Herschel-Bulkley model of the investigated mixtures at a) 0 min, b) 15 min, and c) 30 min.

5.5.5 Hardened state properties

The effect of cement content and w/c on the hardened state properties are analyzed in Figure 5.13. For this specific analysis, the mixtures were divided into control (G1) and eco-efficient (G2-G4) mixtures. As a first analysis of Figure 5.13a, compressive strength and bulk ER appear to be directly proportional to cement content, whereas absorption is inversely proportional to it. The compressive strength of G1 ranges from 27 to 38 MPa, whereas the G2 range is between 30 and 45 MPa. Although G1 and G2 were developed with the same w/c, G2 achieved on average a compressive strength 12% higher than G1, highlighting that even with lower cement content (250 kg/m^3) the usage of LF enhances the system's porosity and hydration. Analyzing mixtures with LF and cement contents between 150-250 kg/m^3 (G4, G3, and G2), up to 45, 31, and 26 MPa were achieved as 28-day compressive strengths, respectively. Moreover, it can be seen that mixtures with different cement content achieved similar compressive strength, including 2H-250-0.68 and 3M-200-0.74 (30.7 MPa) or 3H-200-0.83 and 4L-150-0.84 (26 MPa). The first case shows that even with a cement reduction of 50 kg/m^3 and a w/c increase of 0.06, these two concrete mixtures achieved the same compressive strength. While for the second example, the mixtures also provided a cement reduction of 50 kg/m^3, but in this case, the w/c is approximately the same. This result proves that the conventional w/c and compressive strength correlation cannot fully explain the behaviour of packed eco-efficient mixtures developed with LF. The Bulk ER performance was measured to further evaluate the microstructure of the sustainable mixtures developed (Figure 5.13b). The same trend as the compressive strength is seen in Bulk ER when compared to cement content and w/c. Yet, G1 and G2 reached approximately the same Bulk ER, ranging from 70 Ω.m to 36 Ω.m for mixtures with low to high w/c, respectively. Analyzing the eco-friendly mixtures (developed with 200 and 150 kg/m^3 of cement), the reduction in cement content and increase of w/c impact on the bulk ER were on average

20% and 40%, respectively, when compared to G2 (250 kg/m^3) mixtures. Moreover, eco-friendly mixtures developed with medium w/c have a greater reduction in Bulk ER.

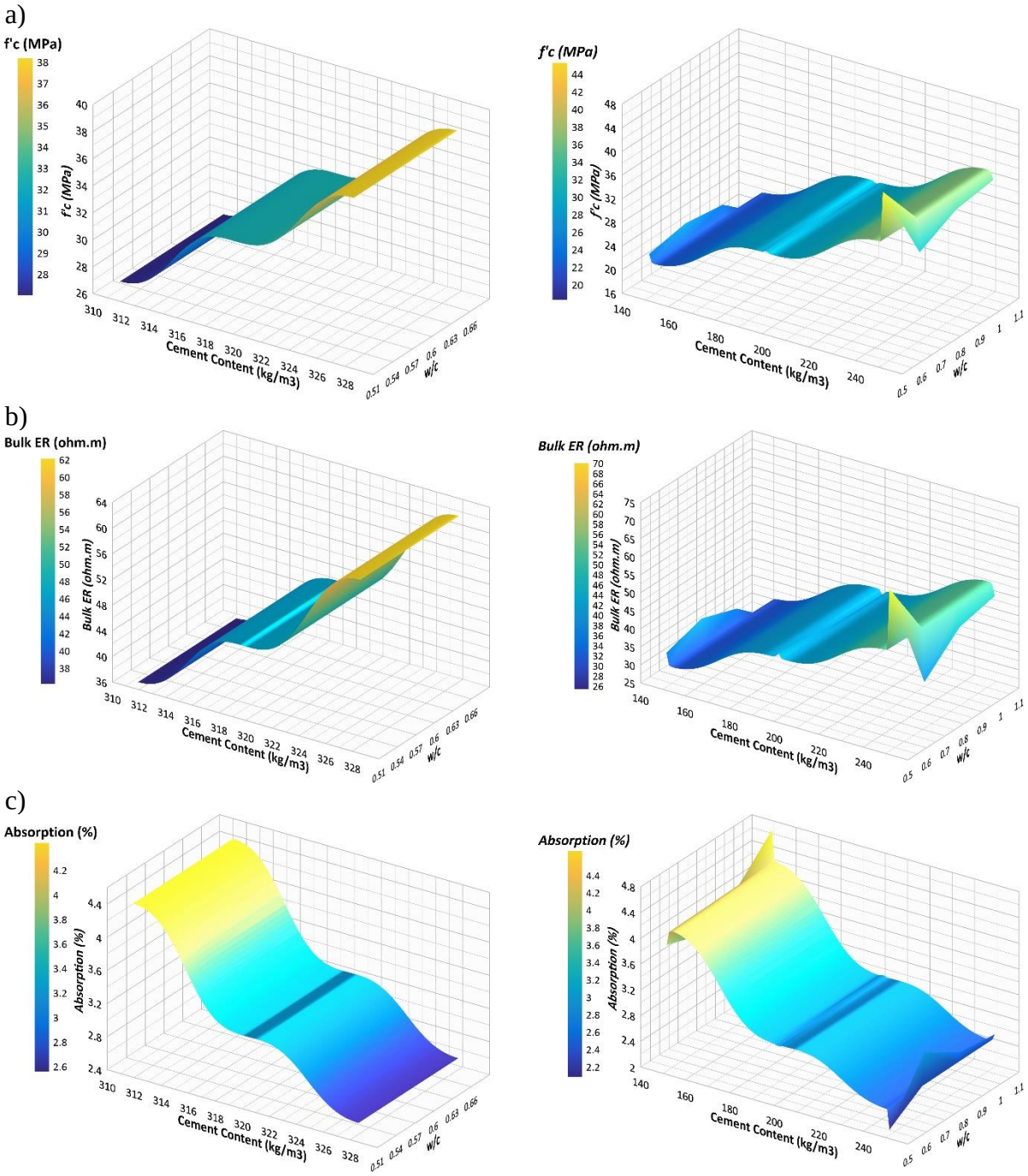

Figure 5.13. Influence of cement content and w/c on a) compressive strength, b) bulk electrical resistivity, and c) absorption.

Figure 5.13c displays the 28-day absorption characteristics of the developed mixtures. As expected, the absorption is highly affected by w/c. Nevertheless, comparing G1 and G2, which contain the same w/c and distinct cement content, G1 yielded an absorption on average 40% higher than G2, which may be explained due to the enhancement of the system matrix and nucleation points created by the limestone fillers. Moreover, the w/c of control mixtures (G1) has a higher impact on absorption than mixtures developed with limestone fillers and lower cement content. Moreover, G2 achieved a 28-day absorption of 2.0, 2.0, and 3.0% for low, medium, and high w/c, whereas G3 achieved 2.7, 2.9, and 3.0%. Although a higher w/c was required in G3 for fresh state proposes, the fillers aid the enhancement of the system matrix (i.e., reducing its absorption). Moreover, G4 mixtures, which have half of the cement content of the control mixtures, achieved similar absorption rates varying on average by 20%; for instance, 1H-311-0.68 and 4H-150-1.09 achieved absorptions of 4.4 and 4.7%, respectively.

5.5.6 Abrams, Lyse, and Molinari's Law

Several methods may be applied to optimize the concrete's mortar content that assists the improvement of materials' eco-efficient through the reduction of cement content. The mortar Content Optimization (MCO) method is one of the most well-known methods used to enhance concrete mix-design. Three main experimental steps must be applied to fully evaluate the mix-design developed: a) mechanical properties (Abram's law [66–70]); b) consistency requirements (Lyse's law [67–70]) and; c) eco-efficient aspects (Molinari's law [67–70]). These laws present the correlation between a) compressive strength and w/c; b) w/c and aggregate unit composition related to cement content (m); and c) m and cement content, respectively. Although four distinct families were developed in this study, they can be analyzed as one mix-design with distinct optimization levels (Figure 5.14). The first quadrant shows the correlation between compressive strength and w/c

has a downward trend, as per Abrams' law, in which 2H-250-0.52 presents the highest residual error of 6.1 MPa. Lyse's law (Quadrant IV) presents the required aggregate unit composition (m) for a selected w/c to achieve a target slump. One may note that the eco-efficient mixtures (G2, G3, and G4), developed with admixtures, would result in a straight line when correlating m and w/c. Therefore, the use of admixture affects Lyse's law trend. Lastly, Molinari's law (Quadrant III), indicates that the most eco-efficient mixtures require higher aggregate unit composition. Considering the class exposure class of CSA A23.1 [58], the requirements for concrete compressive strength range from 25-35 MPa. Mixtures from G1, G2, and G3 may be selected to develop concrete mixtures with CSA A23.1 exposure class (e.g., C-1, C-2, C-3, and F-1), which required compressive strengths of 35, 32, 30, and 30 MPa, respectively. While G3 and G4 mixtures are recommended for exposure class C4 and F2 require a minimum compressive strength of 25 MPa. To achieve concrete net-zero goal, mixtures must be designed not only due to their fresh and hardened state, and durability aspects but their sustainability must also be evaluated during the design. Figure 5.14 may assist in the optimization of the mixture's sustainability (Quadrant III) based on compressive strength (Quadrant I) and slump (Quadrant IV) requirements. The purpose of this chart is to aid users of PPM-MP design method in considering target parameters/performances such as sustainability (cement content – left x-axis), fresh state (slump – bottom right quadrant), and hardened state (compressive strength – top y-axis). Once these three main parameters are determined in accordance with the project requirements, the graph provides insights into the recommended w/c (right x-axis) and aggregate unit composition related to cement content (bottom y-axis) for the pre-selected performances.

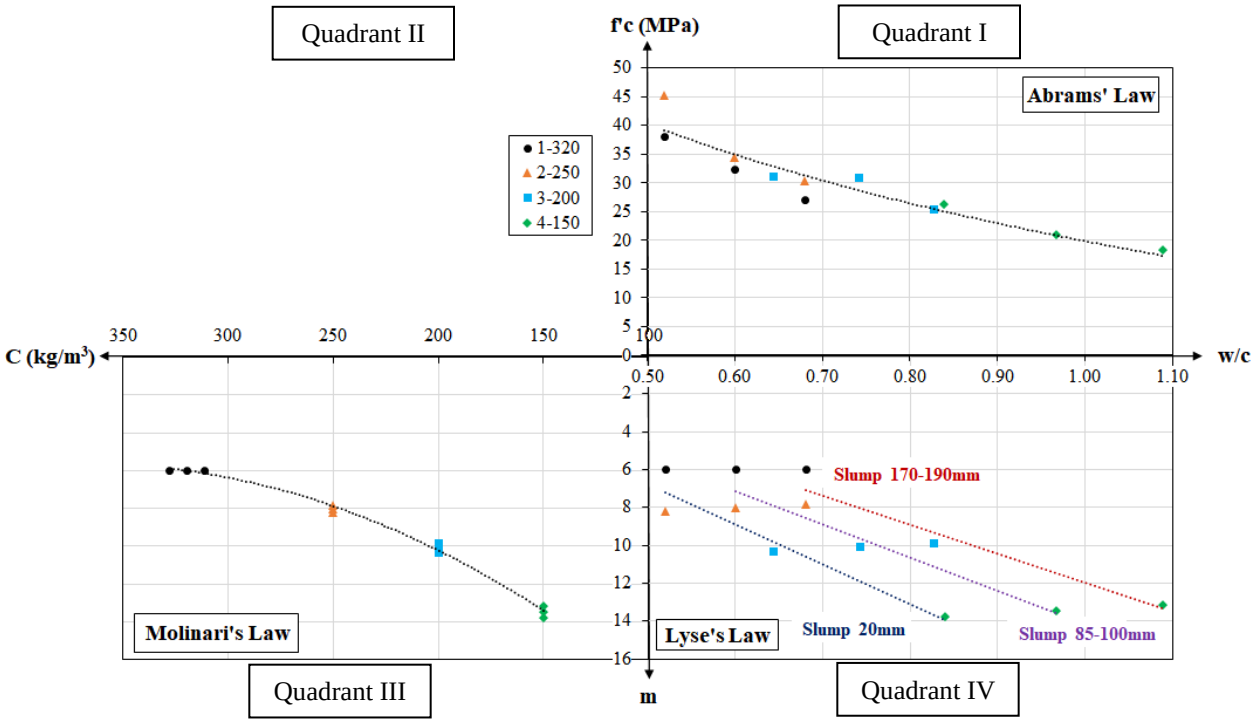

Figure 5.14. Mix-design three-quadrant diagram of mixtures appraised.

5.5.7 IPS$_{cement}$

Mobility parameters can be used to predict the fresh state behaviour of concrete mixtures; however, with a slight modification, this concept can also be applied to better understand the hardened state behaviour of highly packed mixtures. Similarly to the Abrams' Law relationship where the increase of w/c reduces the concrete compressive strength, IPS can be applied to understand materials' compressive strength. IPS measures the distance between the powder particles, which is also represented by the water film thickness between these particles. A modified version of the IPS called *IPS$_{cement}$* (Equation 5.11) can be used to calculate the distance between cement grains only instead of the distance of powder particles.

$$IPS_{cement} = \frac{2}{VSA_{cement}} * \left(\frac{1}{V_{S(cement)}} * \frac{1}{1 - P_{Of(cement)}} \right)$$ Equation 5.11

where IPS_{cement} is the distance among cement particles; VSA_{cement} is the volume surface area of the cement; $V_{S(cement)}$ is the volume solid fraction of the cement and $P_{Of(cement)}$ the dry porosity for pure cement. The volume unity accounts for the total volume of cement (cement + water).

When developing a highly-packed system with high limestone fillers concentrations, the use of additional parameters besides w/c is often suggested to predict compressive strength [25,29,71]. Equation 5.12 combines the IPS_{cement} theory with w/p, which accounts for the w/c and filler concentration, to predict the compressive strength of the mixtures developed in this study (Table 5.7).

$$f'c = {46.67}/{1.63^{\left(\frac{w}{p} * IPS_{cement}\right)}}$$ Equation 5.12

Table 5.7. Prediction of compressive strength through IPS_{cement}.

IPS_{cement}	w/p	$f'c = 46.68/ 1.63^{(w/p * IPScement)}$
1.08	0.68	$f'c=46.68*/1.63^{0.74}$
0.95	0.60	$f'c=46.68*/1.63^{0.57}$
0.81	0.52	$f'c=46.68*/1.63^{0.42}$
1.43	0.54	$f'c=46.68*/1.63^{0.77}$
1.28	0.47	$f'c=46.68*/1.63^{0.60}$
1.12	0.40	$f'c=46.68*/1.63^{0.44}$
2.21	0.54	$f'c=46.68*/1.63^{1.18}$
2.01	0.47	$f'c=46.68*/1.63^{0.95}$
1.76	0.40	$f'c=46.68*/1.63^{0.71}$
3.94	0.54	$f'c=46.68*/1.63^{2.14}$
3.55	0.47	$f'c=46.68*/1.63^{1.68}$
3.13	0.40	$f'c=46.68*/1.63^{1.26}$

Figure 5.15 exhibits the good correlations between the predicted and the experimental compressive strength based on the equations presented in Table 5.7. Considering all the mixtures, it achieved an

SSE of 112, when considering mixtures 1H-311-0.68 and 2L-250-0.52 are the only two dots outside the +/-10% range, whereas when these data is removed from the analysis, the SSE is equal to 22.

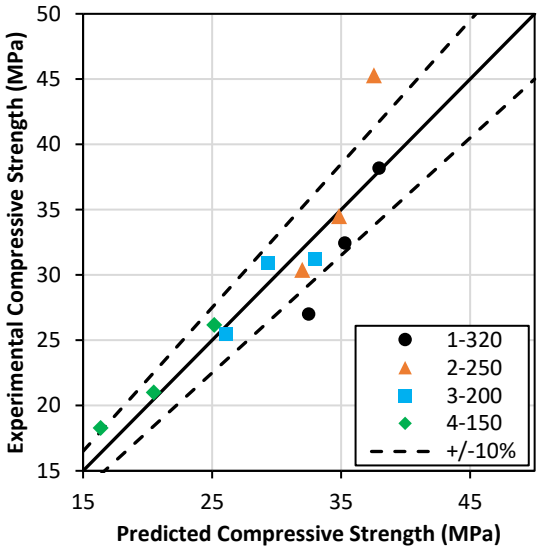

Figure 5.15. Mix-design monogram of mixtures appraised.

5.5.8 Global warming potential assessment

It is well known that the increase in greenhouse gases (GHG) in the past decades is affecting the current world temperature [55]. Cement, one of the main concrete components, is responsible for 3% of the global GHG produced annually [72]. Reducing mixtures' cement content will indeed increase their sustainability, as a ton of OPC produces approximately one ton of CO2 [51,73,74]. Yet, Global warming potential (GWP) was selected to accurately quantify the mixture's eco-efficiency. Figure 5.16a shows the GWP of the twelve mixtures optimized in this study calculated as per Table 5.2. Cement content is the major component of concrete's GWP, being responsible for 97%, 93%, 91%, and 88% of the total GWP of G1, G2, G3, and G4 mixtures, respectively. Control mixtures (G1), which contain 100% of OPC, yielded the highest CO_2 emission of 296 kg CO_{2eq}/m^3(on average) Although all mixtures were developed with the same packing density when they are optimized with limestone fillers the GWP can decrease up to 152.85 kg CO_{2eq}, which is

approximately 50% reduction when comparing G1 to G4.

a)

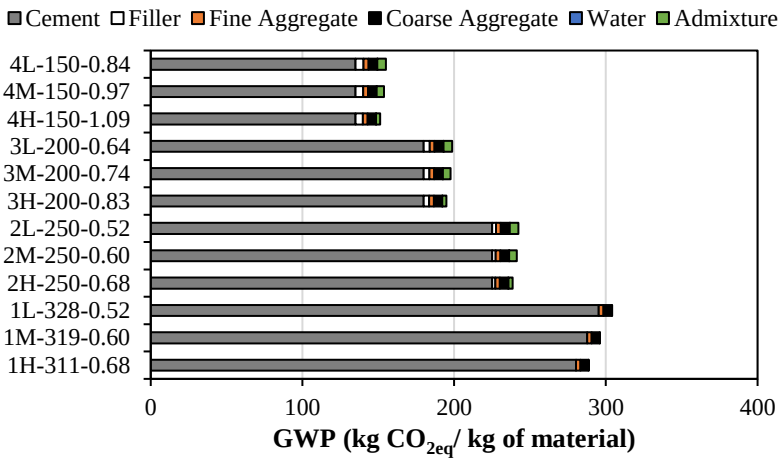

b)

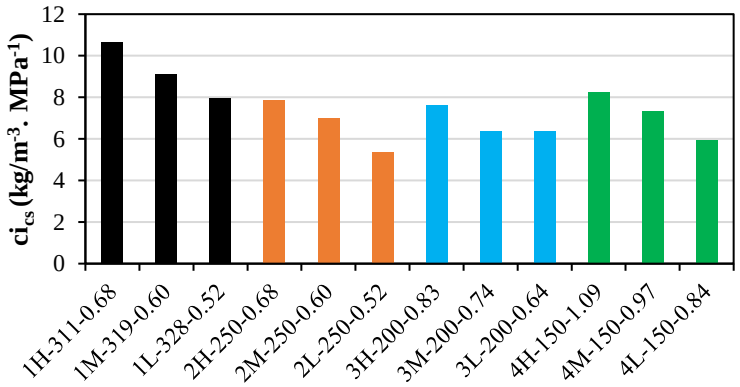

Figure 5.16. a) Global warming potential (in kg CO_{2eq}) for 1m^3 of concrete and b) CO_2 intensity index.

Based on Wallevik et al.'s [56] classification, G1, G2, G3, and G4 mixtures can be considered Semi-LCC, LCC_{250}, LCC_{200}, and LCC_{150}, respectively. Analyzing the CO_2 intensity index (Figure 5.16b), it is clear that G1 (mix proportioned without LF) is less optimized with ci_{cs} ranging from 10.7 to 8.0. While for mixtures of G2, G3, and G4, the CO_2 intensity index varied from 8.3 to 5.3. The concrete mixtures developed in this study can be considered eco-efficient when compared to conventional

concrete (20-40 MPa) produced worldwide that presents ci_{cs} around 10 kg/m^{-3}. MPa^{-1}.

5.6 Conclusions

- Besides the w/c, packing density, and mobility parameters, the cement and filler content also influences the rheological behaviour of mixtures.
- The mixture 3M-200-0.74 showed the highest viscosity due to its low mobility parameters and threshold of *replacement filler*.
- Eco-efficient mixtures developed present a shear-thinning behaviour due to the reduction of viscosity with the increase of rotation; hence, they are recommended for vibrated or pumped applications.
- This research concluded that the compressive strength of packed eco-efficient mixtures developed with LF cannot be fully explained by cement content, as mixtures with different cement content, achieved similar compressive strength, including 2H-250-0.68 and 3M-200-0.74 (30.7 MPa) or 3H-200-0.83 and 4L-150-0.84 (26 MPa).
- Mobility parameters can be used to aid the development of eco-efficient mixtures to achieve required fresh state properties, yet IPS_{cement} can be applied to predict the compressive strength.
- When using the proposed PPM-MP model, the mixtures developed in G1, G2, G3, and G4 can be considered as Semi-LCC, LCC_{250}, LCC_{200}, and LCC_{150}, respectively. However, when limestone fillers are applied to the system, GWP can decrease up to 152.85 kg CO_{2eq}, which is around 50% reduction when compared to control mixtures (G1).
- When compared to conventional concrete (20-40 MPa) produced worldwide that has ci_{cs} greater than 10 kg/m^{-3}. MPa^{-1}, the concrete mixtures developed in this study can be considered eco-efficient with ci_{cs} ranging from 10.7 to 5.3 kg/m^{-3}. MPa^{-1}.

- Concrete mixtures must be formulated to account for their sustainability aspects to meet the concrete net-zero goal. The proposed PPM-MP with the aid of the three-quadrant diagram (Figure 5.14) is a promising method that may be utilized to increase the sustainability of concrete mixtures for any required fresh and hardened state performance. However, only LF was applied as a second powder, and further improvements could be made with the use of SCMs.

5.7 Acknowledgments

The authors gratefully acknowledge the financial support that M. T. de Grazia benefits from the prestigious Vanier scholarship funded by NSERC (Natural Sciences and Engineering Research Council of Canada). The authors would also like to thank Dr. Gamal Elnabelsya and Dr. Muslim Majeed, technical officers in the Materials and Structures laboratory at the University of Ottawa's Department of Civil Engineering.

5.8 References

[1] M. Limbachiya, S.C. Bostanci, H. Kew, Suitability of BS EN 197-1 CEM II and CEM V cement for production of low carbon concrete, Constr. Build. Mater. 71 (2014) 397–405.

[2] J. Di Filippo, J. Karpman, J.R. Deshazo, J. Di Filippo, J. Karpman, J.R. Deshazo, The impacts of policies to reduce CO2 emissions within the concrete supply chain, Cem. Concr. Compos. 101 (2019) 67–82. https://doi.org/10.1016/j.cemconcomp.2018.08.003.

[3] W. Schakel, C.R. Hung, L.-A. Tokheim, A. Hammer Strømman, E. Worrell, A. Ramírez, Impact of fuel selection on the environmental performance of post-combustion calcium looping applied to a cement plant, Appl. Energy. 210 (2017) 75–87. https://doi.org/10.1016/j.apenergy.2017.10.123.

[4] H.F. Campos, N.S. Klein, J. Marques Filho, Proposed mix design method for sustainable high-strength concrete using particle packing optimization, J. Clean. Prod. 265 (2020) 1–15. https://doi.org/10.1016/j.jclepro.2020.121907.

[5] Joint statement: Canada's Cement Industry and the Government of Canada announce a partnership to establish Canada as a global leader in low-carbon cement and to achieve net-zero carbon concrete - Innovation, Science and Economic Development Canada, (n.d.). https://www.ic.gc.ca/eic/site/icgc.nsf/eng/07730.html (accessed March 17, 2022).

[6] Global Cement and Concrete Association, Our path to net zero, (2022). https://gccassociation.org/concretefuture/our-path-to-net-zero/ (accessed March 17, 2022).

[7] B.L. Damineli, F.M. Kemeid, P.S. Aguiar, V.M. John, Measuring the eco-efficiency of cement use, Cem. Concr. Compos. 32 (2010) 555–562.

[8] O. Ahmadah, H. Bessaies-Bey, A. Yahia, N. Roussel, A new mix design method for low-environmental-impact blended cementitious materials: Optimization of the physical characteristics of powders for better rheological and mechanical properties, Cem. Concr. Compos. 128 (2022). https://doi.org/10.1016/j.cemconcomp.2022.104437.

[9] S.A. Miller, V.M. John, S.A. Pacca, A. Horvath, Carbon dioxide reduction potential in the global cement industry by 2050, Cem. Concr. Res. 114 (2018) 115–124. https://doi.org/10.1016/j.cemconres.2017.08.026.

[10] B.L. Damineli, V.M. John, B. Lagerblad, R.G. Pileggi, Viscosity prediction of cement-filler suspensions using interference model: A route for binder efficiency enhancement, Cem. Concr. Res. 84 (2016) 8–19.

[11] K.L. Scrivener, V.M. John, E. Gartner, Eco-efficient cements : Potential economically viable solutions for a low-CO 2 cement-based materials industry, Cem. Concr. Res. 114 (2018) 2–26. https://doi.org/10.1016/j.cemconres.2018.03.015.

[12] Z.S. Ali, M. Hosseinpoor, A. Yahia, New aggregate grading models for low-binder self-consolidating and semi-self-consolidating concrete (Eco-SCC and Eco-semi-SCC), Constr. Build. Mater. 265 (2020) 120314. https://doi.org/10.1016/j.conbuildmat.2020.120314.

[13] J. Zachar, M. Asce, Sustainable and Economical Precast and Prestressed Concrete Using Fly Ash as a Cement Replacement, J. Mat. Civ. Eng. 23 (2011) 789–792.

[14] M.C.G. Juenger, R. Siddique, Recent advances in understanding the role of supplementary cementitious materials in concrete, Cem. Concr. Res. 78 (2015) 71–80.

[15] D. Youness, M. Hosseinpoor, A. Yahia, A. Tagnit-Hamou, Flowability characteristics of dry supplementary cementitious materials using Carr measurements and their effect on the rheology of suspensions, Powder Technol. 378 (2021) 124–144. https://doi.org/10.1016/j.powtec.2020.09.064.

[16] S.H. Kang, Y. Jeong, K.H. Tan, J. Moon, High-volume use of limestone in ultra-high performance fiber-reinforced concrete for reducing cement content and autogenous shrinkage, Constr. Build. Mater. 213 (2019) 292–305. https://doi.org/10.1016/j.conbuildmat.2019.04.091.

[17] U.N. Environment, K.L. Scrivener, V.M. John, E.M. Gartner, Eco-efficient cements: Potential economically viable solutions for a low-CO2 cement-based materials industry, Cem. Concr. Res. 114 (2018). https://doi.org/10.1016/j.cemconres.2018.03.015.

[18] Y. Knop, A. Peled, Packing density modeling of blended cement with limestone having different particle sizes, Constr. Build. Mater. 102 (2016) 44–50.

[19] J.L. Gallias, R. Kara-Ali, J.P. Bigas, The effect of fine mineral admixtures on water requirement of cement pastes, Cem. Concr. Res. . 30 (2000) 1543–1549. https://doi.org/10.1016/S0008-8846(00)00380-X.

[20] Y. Knop, A. Peled, Setting behavior of blended cement with limestone: influence of particle size and content, Mater. Struct. 49 (2016) 439–452.

[21] T. Oey, A. Kumar, J.W. Bullard, N. Neithalath, G. Sant, The filler effect: The influence of filler content and surface area on cementitious reaction rates, J. Am. Ceram. Soc. 96 (2013) 1978–1990. https://doi.org/10.1111/jace.12264.

[22] W. Grabowski, J. Wilanowicz, The structure of mineral fillers and their stiffening properties in filler-bitumen mastics, Mater. Struct. Constr. 41 (2008) 793–804. https://doi.org/10.1617/s11527-007-9283-4.

[23] R.C.O. Romano, H. Schreurs, V.M. John, R.G. Pileggi, Influence of the dispersion process in the silica fume properties, Cerâmica. 54 (2008) 456–461.

[24] A.K. Castro, V.C. Pandolfelli, Review: Concepts of particle dispersion and packing for special concretes production, 18 Cerâmica. 55 (2009) 18–32.

[25] V.M. John, B.L. Damineli, M. Quattrone, R.G. Pileggi, Fillers in cementitious materials — Experience, recent advances and future potential, Cem. Concr. Res. 114 (2018) 65–78. https://doi.org/10.1016/j.cemconres.2017.09.013.

[26] V. Bonavetti, H. Donza, G. Menéndez, O. Cabrera, E.F. Irassar, Limestone filler cement in low w/c concrete: A rational use of energy, Cem. Concr. Res. 33 (2003) 865–871. https://doi.org/10.1016/S0008-8846(02)01087-6.

[27] S.A.A.M. Fennis, J.C. Walraven, Using particle packing technology for sustainable concrete mixture design, Heron. 57 (2012) 73–101.

[28] M. Grazia, L.F.M. Sanchez, R. Romano, R.G. Pileggi, M.T. de Grazia, L.F.M. Sanchez, R. Romano, R.G. Pileggi, M. T. de Grazia, L. F. M. Sanchez, R. C. O. Romano, R. G. Pileggi, Evaluation of the Fresh and Hardened State Properties of Low-Cement Content (LCC) Systems, Mag. Concr. Res. 72 (2018) 1–14. https://doi.org/10.1680/jmacr.18.00271.

[29] M. T. de Grazia, L. F. M. Sanchez, R. C. O. Romano, R. G. Pileggi, M.T. de Grazia, L. Sanchez, R.C.O. Romano, R.G. Pileggi, M. T. de Grazia, L. F. M. Sanchez, R. C. O. Romano, R. G. Pileggi, Investigation of the use of continuous particle packing models (PPMs) on the fresh and hardened properties of low-cement concrete (LCC) systems, Constr. Build. Mater. 195 (2019) 524–536. https://doi.org/10.1016/j.conbuildmat.2018.11.051.

[30] M. Anson-Cartwright, Optimization of aggregate gradation combinations to improve concrete sustainability and durability, MASc Thesis, University of Toronto, 2011.

[31] P.R. de Matos, R.D. Sakata, L.R. Prudêncio, Eco-efficient low binder high-performance self-compacting concretes, Constr. Build. Mater. 225 (2019) 941–955. https://doi.org/10.1016/j.conbuildmat.2019.07.254.

[32] S. Kumar, M. Santhanam, S. Kunar, M. Santhanam, Particle packing theories and their application in concrete mixture proportioning : A review, Indian Concr. J. 77 (2003) 1324–1331.

[33] W. Zuo, J. Liu, Q. Tian, W. Xu, W. She, P. Feng, C. Miao, Optimum design of low-binder Self-Compacting Concrete based on particle packing theories, Constr. Build. Mater. 163 (2018) 938–948. https://doi.org/10.1016/j.conbuildmat.2017.12.167.

[34] B. Esmaeilkhanian, K.H. Khayat, O.H. Wallevik, Mix design approach for low-powder self-consolidating concrete: Eco-SCC-content optimization and performance, Mater. Struct. 50 (2017) 18. https://doi.org/10.1617/s11527-017-0993-y.

[35] S. Yousuf, S.A. Shammeh, D. Asirvatham, S. Dadsetan, L. Sanchez, N. Martin, M.T. De Grazia, R. Ziapourrazlighi, The use of low cement structural concrete as a sustainable alternative for civil industry, in: 10th ACI/RILEM Int. Conf. Cem. Mater. Altern. Bind. Sustain. Concr., 2017.

[36] S. Yousuf, L.F.M. Sanchez, S.A. Shammeh, The use of particle packing models (PPMs) to design structural low cement concrete as an alternative for construction industry, J. Build. Eng. 25 (2019) 100815. https://doi.org/10.1016/j.jobe.2019.100815.

[37] S.A.A.M. Fennis, J.C. Walraven, J.A. den Uijl, Compaction-interaction packing model: regarding the effect of fillers in concrete mixture design, Mater. Struct. 46 (2013) 463–478. https://doi.org/10.1617/s11527-012-9910-6.

[38] P. Goltermann, V. Johansen, L. Palbøl, Packing of Aggregates : An Alternative Tool to Determine the Optimal Aggregate Mix, ACI Mater. J. (1997) 435–442.

[39] M.N. Mangulkar, S.S. Jamkar, Review of particle packing theories used for concrete mix proportioning, Int. J. Sci. Eng. Res. 4 (2013) 143–148.

[40] J.E. Funk, D.R. Dinger, Predictive process control of crowded particulate suspensions, 1st ed., New York, 1994. https://doi.org/10.1007/978-1-4615-3118-0.

[41] I. Mehdipour, K.H. Khayat, Understanding the role of particle packing characteristics in rheo-physical properties of cementitious suspensions : A literature review, Constr. Build. Mater. 161 (2018) 340–353.

[42] R. Yu, P. Spiesz, H.J.H. Brouwers, Mix design and properties assessment of Ultra-High Performance Fibre Reinforced Concrete (UHPFRC), Cem. Concr. Res. 56 (2014) 29–39. https://doi.org/10.1016/j.cemconres.2013.11.002.

[43] F. De Larrard, A. Belloc, The influence of aggregate on the compressive strength of normal and high-strength concrete, ACI Mater. J. 94 (1997) 417–426.

[44] H.R. Shadkam, S. Dadsetan, M. Tadayon, L.F.M. Sanchez, A. Zakeri, An investigation of the effects of limestone powder and Viscosity Modifying Agent in durability related parameters of self-consolidating concrete (SCC), Constr. Build. Mater. 156 (2017) 152–160.

[45] R.C.D.O. Romano, D. Dos, R. Torres, R.G. Pileggi, Impact of aggregate grading and air-entrainment on the properties of fresh and hardened mortars, Constr. Build. Mater. 82 (2015) 219–226.

[46] I.R. Oliveira, A.R. Studart, R.G. Pileggi, V.C. Pandolfelli, Dispersão e Empacotamento de Partículas, Fazendo Arte Editorial, São Paulo, 2000.

[47] B. Lothenbach, G. Le Saout, E. Gallucci, K. Scrivener, Influence of limestone on the hydration of Portland cements, Cem. Concr. Res. 38 (2008) 848–860. https://doi.org/10.1016/j.cemconres.2008.01.002.

[48] T. Matschei, B. Lothenbach, F.P. Glasser, The role of calcium carbonate in cement hydration, Cem. Concr. Res. 37 (2007) 551–558. https://doi.org/10.1016/j.cemconres.2006.10.013.

[49] T.E. Oey, A. Kumar, J.W. Bullard, N. Neithalath, G. Sant, The Filler Effect: The Influence of Filler Content and Surface Area on Cementitious Reaction Rates, J. Am. Ceram. Soc. 96 (2013) 1978–1990. https://doi.org/10.1111/jace.12264.

[50] C. Varhen, I. Dilonardo, C. Romano, R.G. Pileggi, A. Figueiredo, Effect of the substitution of cement by limestone filler on the rheological behaviour and shrinkage of microconcretes, Constr. Build. Mater. 125 (2016) 375–386.

[51] A. Hasanbeigi, L. Price, E. Lin, Emerging Energy-Efficiency and CO2 Emission-Reduction Technologies for Cement and Concrete Production: A Technical Review, Renew. Sustain. Energy Rev. 16 (2012) 6220–6238.

[52] S. Licht, H. Wu, C. Hettige, B. Wang, J. Asercion, J. Lau, J. Stuart, STEP cement: Solar Thermal Electrochemical Production of CaO without CO2 emission, Chem. Commun. 48 (2012) 6019–6021. https://doi.org/10.1039/c2cc31341c.

[53] R. Kurad, J.D. Silvestre, J. de Brito, H. Ahmed, Effect of incorporation of high volume of recycled concrete aggregates and fly ash on the strength and global warming potential of concrete, J. Clean. Prod. 166 (2017) 485–502. https://doi.org/10.1016/j.jclepro.2017.07.236.

[54] W. Nguyen, D.M. Martinez, G. Jen, J.F. Duncan, C.P. Ostertag, Interaction between global warming potential, durability, and structural properties of fiber-reinforced concrete with high waste materials inclusion, Resour. Conserv. Recycl. 169 (2021) 105453. https://doi.org/10.1016/j.resconrec.2021.105453.

[55] A. Sahraei Moghadam, F. Omidinasab, S. Moazami Goodarzi, Characterization of concrete containing RCA and GGBFS: Mechanical, microstructural and environmental properties, Constr. Build. Mater. 289 (2021) 123134. https://doi.org/10.1016/j.conbuildmat.2021.123134.

[56] O.H. Wallevik, W.I. Mansour, F.H. Yazbeck, T.I. Kristjansson, EcoCrete-Xtreme: Extreme performance of a sustainable concrete, Proc. Int. Symp. Eco-Crete. (2014) 3–10.

[57] ACI Committee 211, Standard Practice for Selecting Proportions for Normal Heavyweight , and Mass Concrete (ACI 211 . 1-91) Reapproved 2002, 2004.

[58] CSA A23.1:19 / CSA A23.2:19, Concrete materials and methods of concrete construction / Test Methods and standard practices for concrete, Mississauga, ON, 2019.

[59] H.F.W. Taylor, Cement chemistry, Thomas Telford Publishing, 1997. https://doi.org/10.1680/cc.25929.

[60] ASTM C39, Standard Test Method for Compressive Strength of Cylindrical Concrete Specimens, 1999.

[61] P. Banfill, D. Beaupré, F. Chapdelaine, F. de Larrard, P. Domone, L. Nachbaur, T. Sedran, O. Wallevik, J.E. Wallevik, Comparison of concrete rheometers: international tests at LCPC (NISTIR 6819), Nantes, France, 2000.

[62] C. Ferraris, L. Brower, Comparison of Concrete Rheometers: International Tests at MB, (2003) 116.

[63] E. Güneyisi, M. Gesoglu, Z. Algin, H. Yazici, Rheological and fresh properties of self-compacting concretes containing coarse and fine recycled concrete aggregates, Constr. Build. Mater. 113 (2016) 622–630. https://doi.org/10.1016/j.conbuildmat.2016.03.073.

[64] D.J. De Souza, M. T. de Grazia, H.F. Macedo, L. F.M. Sanchez, G. P. de Andrade, O. Naboka, G. Fathifazl, P.C. Nkinamubanzi, Influence of the Mix Proportion and Aggregate Features on the Performance of Eco-Efficient Fine Recycled Concrete Aggregate Mixtures, Materials (Basel). 15 (2022) 1–27. https://doi.org/10.3390/ma15041355.

[65] ASTM C1760, Standard Test Method for Bulk Electrical Conductivity of Hardened Concrete, (2012) 1–5. https://doi.org/10.1520/C1760-12.2.

[66] A.M. Neville, Properties of Concrete, 5th ed., Pearson Education Limited, 2011.

[67] K. ßat, E. Alyamaç, R. Ince, A preliminary concrete mix design for SCC with marble powders, Constr. Build. Mater. 23 (2008) 1201–1210.

[68] P.J.M. Monteiro, P.R.L. Helene, S. Kang, Designing concrete mixtures for strength, elastic modulus and fracture energy, Mater. Struct. 26 (1993) 443–452.

[69] M.T. Marvila, A.R.G. Azevedo, S.N. Monteiro, Verification of the application potential of the mathematical models of lyse, abrams and molinari in mortars based on cement and lime, J. Mater. Res. Technol. 9 (2020) 7327–7334.

[70] F. Pelisser, A. Vieira, A.M. Bernardin, Efficient self-compacting concrete with low cement consumption, J. Clean. Prod. 175 (2018) 324–332. https://doi.org/10.1016/j.jclepro.2017.12.084.

[71] M.T. de Grazia, L.F.M. Sanchez, R.G. Pileggi, Evaluation of the fresh and hardened state properties of low cement content systems, Mag. Concr. Res. 72 (2018) 232–245.

[72] P. Van Den Heede, N. De Belie, Environmental impact and life cycle assessment (LCA) of traditional and “green” concretes: Literature review and theoretical calculations, Cem. Concr. Compos. 34 (2012) 431–442. https://doi.org/10.1016/j.cemconcomp.2012.01.004.

[73] M.C. Gonçalves, F. Margarido, Materials for Construction and Civil Engineering : Science, Processing, And Design, Springer International Publishing, 2015.

[74] T.R. Naik, M. Asce, S.S. Singb, M.M. Hossain, Permeability of high-strength concrete containing low cement factor, J. Energy Eng. 122 (1996) 21–39.

Chapter Six: Understanding and Predicting Hardened State Performance of Eco-efficient Concrete Mixtures

De Grazia, M. T.[a], Sanchez, L. F. M.[b], Yahia Ammar[c]

[a] Ph.D. Candidate – University of Ottawa, Department of Civil Engineering, ON, Canada.

[b] Associate Professor – University of Ottawa, Department of Civil Engineering, ON, Canada.
[c] Full Professor - Université de Sherbrooke, Department of Civil and Building Engineering, QC, Canada.

Abstract

Numerous research programs were conducted in the past to evaluate the fresh and hardened properties of PPM-proportioned concrete; yet, there is still a lack of fundamental understanding of key factors contributing to the evolution of engineering properties in packed systems, especially in eco-efficient mixtures. To answer this question, twelve eco-efficient (low cement content) mixtures containing distinct ranges of cement content (320, 250, 200, 150 kg/m^3) and slump values (180, 90, and 20 +/- 20 mm) were proportioned through a proposed PPM-MP approach. Samples were fabricated from each mixture and a comprehensive hardened state analysis (apparent porosity, surface electrical resistivity, compressive strength, and modulus of elasticity) was conducted over time. Results indicate that the proposed PPM-MP approach is a quite promising technique to proportion eco-efficient concrete targeting non-structural and structural applications (18-45 MPa). Finally, a modified Abrams law is proposed to facilitate the design of eco-efficient mixtures to meet distinct hardened state performance.

Keywords: *Eco-efficient concrete, low cement content, particle packing models, interparticle separation distance, maximum paste thickness.*

6.1 Introduction

The urgency to reduce the carbon footprint of the concrete construction industry has shifted the focus to its environmental impact while maintaining its performance and economic benefits. Concrete production is responsible for more than 7% of global carbon dioxide (CO_2) emissions, wherein over 92% is emitted during ordinary Portland cement (OPC) production [1–4]. Therefore, to reduce the adverse effects of OPC consumption, one of the most suitable strategies is the implementation of Particle Packing Model (PPMs) while mix proportioning concrete [4–11]. The study of packing of aggregate portions in concrete mixtures marked the beginning of PPM science in the late 19th century [12,13]. Although significant improvements in the hardened state aspects were discovered with the packing of aggregates, subsequent discrete and continuous PPMs were developed highlighting the importance of packing particles from the whole system (i.e., fine and coarse aggregates, and powders) [11–16]. Yet, it has been found that conventional and well-established hardened state laws, such as Abrams law, cannot fully capture the evolution of engineering properties of PPM proportioned mixtures, since they may develop quite distinct properties when compared to conventionally proportioned mixtures with the same w/c. Although studies concluded that the water-to-cement ratio (w/c) is still the main factor influencing the evolution of engineering properties of PPM-proportioned concrete, additional parameters were found necessary to be included so that better predictive models could be developed [7,17].

Regardless of the usage of PPMs, further improvements in concrete eco-efficiency can be achieved by partially replacing OPC with supplementary cementitious materials (SCMs) or inert fillers [5–7,11,18,19]; however, although the addition of SCMs contributes to concrete performance, durability, sustainability, and economic aspects [2,5,19–22], their availability does not increase at

the same rate as the cement demand [23–25]. Similar to SCMs, several types of inert fillers are used as a cement replacement, yet limestone fillers are the most commonly used due to their economy and availability worldwide, along with some interesting physical features, such as spherical shape, wide range of particle size distribution (PSD), and volumetric stability [26–29]. However, it is known that depending on its PSD and specific surface area (SSA), limestone fillers can positively or negatively impact the fresh and hardened performance of concrete mixtures [30–34]. The addition of fine PSD limestone fillers can increase the system's viscosity, negatively impacting its fresh behaviour due to the increase of the system's superficial surface. Conversely, fine PSD limestone fillers may further contribute to clinker hydration, which accelerates the concrete's compressive strength development at early ages [35]. Some fillers with similar PSD to OPC are used as direct replacements for OPC to improve concrete eco-efficiency. Normally, the use of limestone fillers is limited to 15% of cement content, when direct replacement is selected as the mix-design method to maintain concrete's hardened state properties [26]. However, to achieve eco-efficiency levels as per Net Zero targets [36,37], higher amounts of filler should be added to the system and thus a better understanding and prediction of engineering properties is required for mixtures incorporating higher amounts and types of limestone filler.

This project aims to thoroughly assess, understand, and predict the development of engineering properties of eco-efficient concrete mixtures designed through a combined particle packing models (PPMs) / mobility parameters (MP) approach so that sustainable mixtures bearing low cement content may be proportioned while meeting required hardened criteria.

6.2 Background

6.2.1 Proportioning concrete through particle packing models (PPMs)

Particle packing models (PPMs), which started in the late 19th century when Féret analyzed the influence of the aggregates packing on the hardened state of concrete [12], are currently applied in a wide range of materials, such as ceramics, concrete, and asphalt [38–41]. PPMs are implemented to optimize the system's gradation aiming to reduce its porosity [12,15]. Several PPMs are presented in the literature, and they may be divided into continuous and discrete models. The first continuous PPMs was created by Fuller in 1907 [12,15,41] whereas the first discrete model was created by Furnas between 1929 (i.e. binary) and 1931 (multimodal models) [12,13,15,41]; both pioneers of PPMs. Naturally, continuous and discrete models were enhanced over the years [11–13,15,16,41]; yet, researchers [7,42] suggest that real aggregate blends are better represented by continuous models as they consider that concrete contains particles of all sizes (i.e. no gaps throughout the whole particle size distribution) [12,15]. The most current continuous PPM is the so-called Alfred model or modified Andreasen model (Equation 6.1) [7].

$$CPFT = 100 * \left(\frac{{D_P}^q - {D_S}^q}{{D_L}^q - {D_S}^q}\right) \qquad \text{Equation 6.1}$$

where D_P is the particle size in question, CFPT is the cumulative percent finer than D_P, D_L and D_S are the largest and smallest particle size in the system, respectively, and q is a distribution factor (q-factor).

Based on computational analysis, it was determined that "optimum packing" is achieved when the distribution factor (q) is equal to 0.37 [12,41]. Conversely, it has been found that "optimum packing" reduces concrete flowability as the granular particles are close to one another and thus causing more

friction is presented in the system. Aiming to improve concrete flowability, q-factors of around 0.20-0.22 are often selected, since lower q-factors result in higher amounts of fines and a lower amount of coarse aggregates in the system, which generates suitable water-to-powder ratios, helping the coarse aggregate particles slippage.

Among the many benefits of using PPMs, densifying the material's microstructure remains the main objective [12,40]. Moreover, the higher the packing density, the lower the amount of voids between fine and coarse aggregates, which are filled by water and fine/ultrafine particles (≤ 125 μm i.e., binder and fillers); thus, packed systems require less binder which increases their eco-efficiency. Nevertheless, concrete mixtures designed through PPMs present challenges in the fresh state due to their highly packed and low porosity system. Mobility parameters may be introduced then, as a complementary approach to PPMs, for mix-proportioning eco-efficient mixtures while providing suitable performance in the fresh state. As such, two parameters have been proposed to clarify the mobility of granular systems: the interparticle spacing (IPS; Equation 6.2) and the maximum paste thickness (MPT; Equation 6.3) [7,43–45].

$$IPS = \frac{2}{VSA}\left[\frac{1}{V_s} - \frac{1}{(1 - P_{of})}\right] \quad \text{Equation 6.2}$$

where IPS is the interparticle spacing, VSA is the calculated volume surface area per cubic centimetre of powder, V_s is the volume fraction of fine solids (particles smaller than 125 μm), and P_{of} is the pore fraction assuming the densest packing of the fine particles.

$$MPT = \frac{2}{VSA_c}\left[\frac{1}{V_{sc}} - \frac{1}{(1 - P_{ofc})}\right] \quad \text{Equation 6.3}$$

where MPT is the distance between aggregates, VSA_c is the calculated volume surface area of aggregate (particles greater than 125 μm) fraction, V_{sc} is the volumetric aggregate solid fraction, and P_{ofc} is the pore of aggregate fraction assuming the densest packing.

The IPS is considered as the average distance between two adjacent particles smaller than 125 μm, which are normally separated by water [7,41,44–46]. Therefore, IPS can be understood as the thickness of the fluid (or water) amongst them. Likewise, MPT measures the maximum distance amongst particles greater than 125 μm; hence, MPT has a direct correlation to cement paste thickness around aggregate particles [7,43–45]. Consequently, it has been found that the lower the IPS and MPT, the lower the flowability of granular systems (i.e., the higher the viscosity and particles collisions for a given torque regime). Conversely, high IPS and MPT yield less viscous, more flowable mixtures [7,45,47].

6.2.2 Estimating the porosity of packed systems - Westman and Hungill

Since the modified Andreasen model is focused on the CPFT, a complementary algorithm published by Westman and Hugill in 1930 may be used to calculate the system maximum packing factor [41]. Equation 6.4 can therefore be used to calculate the packing factor (PF; ratio between tightly packed and loosely packed systems) of any granular system [41,45].

$$PF = 1 - \left(\frac{1}{CSR}\right)^{0.37} \qquad \text{Equation 6.4}$$

where CSR is the class size ratio between two consecutive particles diameter.

According to [41], the PF is inversely proportional to the maximum apparent volume (V_a; true volume of particles - Equation 6.5) since V_a is directly proportional to the system's porosity.

$$V_{a1} = a_1 x_1 \qquad \text{Equation 6.5}$$

$$V_{a2} = x_1 + a_2 x_2$$

$$V_{a3} = x_1 + x_2 + a_3 x_3$$

...

$$V_{ai} = \sum_{j=1}^{i-1} x_j \; {}_1 + a_i x_i$$

where a_i is the apparent volume of the i^{th} size particle in a monodispersed system, x_i is the mass fraction of i^{th} size particle, V_{ai} is the apparent volume of the mixture with n particle sizes, and n is the number of particle sizes.

It is well-established that filling a volumetric space with monodisperse spherical particles results in approximately one-fourth of empty spaces (i.e., packing density around 75%). However, the latter approach is mainly theoretical since granular systems are rarely made by completely spherical particles; hence, in practice, packing density lies between 60% and 64% [47]. As such, the porosity of real granular systems can be calculated with the modified Westman and Hugill algorithm - Equation 6.6 [41].

$$Porosity\ (\%) = \left(1 - \frac{1}{V_a}\right) * 40\% \qquad \text{Equation 6.6}$$

Although the Westman and Hugill model can be used to predict the granular porosity and packing factor of a system, it does not represent the hydrated system`s porosity, which is directly proportional

to the concrete mechanical properties. These characteristics are significantly influenced by the w/c, cement types and content, curing age, aggregate characteristics, and fillers [48]. Therefore, models that predict engineering properties, such as compressive strength, must be used while the mix-proportioning of PPM-designed concrete through optimizing the selection of parameters and meeting desired hardened state criteria.

6.2.3 Hardened state properties of PPM mixtures

PPMs allow the proportioning of eco-efficient concrete mixtures developed with low OPC content; for instance, OPC contents lower than 320 kg/m^3 are often observed in the literature [5–7,10,11,18,49]. However, their impact on the hardened state performance of concrete is still not entirely understood. Previous research [5,7,49] has shown that the compressive strength of these concrete mixtures can vary significantly within mixtures of similar w/c. For instance, Anson (2011) [10] developed three mixtures with w/b of 0.39 and four mixtures with w/b of 0.33. To increase the concrete's sustainability, this study used Modified Toufar as PPM in the aggregate portions and slag as a partial replacement for OPC. For mixtures developed with 0.39 w/b, the cement content ranged from 270 to 247.5 kg/m^3 and the slag content from 90 to 82.5 kg/m^3. Regardless of having the same w/b ratio, these mixtures yielded distinct compressive strengths ranging from 31.5 to 37.1 MPa after 28 days. For mixtures developed with 0.33 w/b, the cement content and slag varied from 292.5-349 and 97.5-116, respectively, while the 28-day compressive strength varied from 56.2 to 66.5 MPa. Matos et al. (2019) [5] also optimized the fine and coarse aggregates portion through experimental packing analysis to develop sustainable high-performance self-compacting concrete mixtures. Fly ash was used as a partial OPC replacement and concrete mixtures were proportioned with cement content ranging from 365 to 255 kg/m^3 and constant w/b of 0.48, achieving compressive strengths varying from 50.7 to 58.9 MPa at 28 days. Similarly, Ali et al., 2020 [49] investigated over 20

different mixtures proportioned with Fuller-Thompson distribution moduli (q) ranging from 0.4 to 0.5 and distinct volumetric sand-to-total aggregate ratios. Since the PPM has been used in the whole system (i.e., aggregates and powders), a better mix-optimization was reached, achieving a OPC content of 232 kg/m^3, combined with fly ash (62 kg/m^3) and silica fume (15 kg/m^3). Although the same binder content (total of 309 kg/m^3) and w/b (0.60) were selected on these mixtures, the compressive strength varied from 28 to 35 MPa. The same behaviour was observed by de Grazia et al. (2019) [7], where the 28-day compressive strength varied significantly for similar w/c ratio while the use of different q-factors on the Alfred model and adjusting the percentage of OPC replacement by limestone fillers. In this study, three ranges of cement content (150, 200, and 270 kg/m^3) and three water-to-cement- ratios (0.8, 0.6, 0.5, respectively) were investigated. The variation of q-factor between the two mixtures resulted in the following variations of compressive strength: 43-49 MPa, 54-56 MPa, and 66-70 MPa for mixtures designed with w/c of 0.8, 0.6, and 0.5, respectively. These investigations show that, for a given w/c, eco-efficient concrete mixtures designed via PPM present compressive strengths that are significantly higher than those of conventional concrete mixtures, highlighting the need of understanding and quantifying the impact of the above on the performance of eco-efficient PPM-proportioned concrete.

6.2.4 Impact of limestone fillers on concrete hardened state properties

Limestone filler is one of the few materials that exceeds OPC production, demonstrating its viability as a partial replacement for OPC in order to increase the sustainability of concrete mixtures [25]. Their average replacement ratio is usually around 20% to avoid losses in the concrete hardened state properties. However, European and South African standards allow an addition of limestone filler of up to 35% [25,27,50,51]. Previous research [35,52] has shown that up to 10% limestone filler can be added without affecting the hardened state properties of concrete because limestone filler partially

reacts with the available alumina to form carbo aluminate phases, which contribute to the strength and durability of concrete. The addition of limestone fillers can also have a positive impact on the hardened state properties by accelerating cement hydration (due to the formation of nucleation sites) and by reducing the system's overall porosity (phenomenon known as the filler effect) [35,44,45,53,54]. Moreover, the dilution effect, defined as an increase in water content per unit mass of cement particles (i.e., an increase in w/c), also have a positive impact on accelerating cement hydration at early ages. Besides this positive impact, the dilution effect can also have a negative impact on the concrete compressive strength due to the increase of w/c [25,35,50,53]. According to Lothenbach et al. (2018) [35], the main strength contributor is the enhancement of cement hydration rather than the influence of limestone fillers on the system's chemistry or physical packing. Yet, these studies were mainly performed on conventional concrete mixtures conventionally proportioned and with replacements up to 35%. However, when mixtures are proportioned with PPM, higher levels of OPC replacement by limestone fillers (up to 60%) were observed to still be possible while maintaining the required hardened state properties [45,55] and decreasing the carbon footprint of concrete.

6.2.5 Predicting hardened state properties of PPM-proportioned concrete

Back in the late 1990s, De Larrard and Belloc [43] proposed a different approach to better predict the mechanical performance (i.e., concrete compressive strength) of concrete mixtures proportioned with PPMs which evaluates the distance between the coarse aggregate particles. The *Maximum Paste Thickness* (MPT_{coarse}) concept accounts for the distance between the coarse aggregate particles that act as stiffer points surrounded by softer mortar in conventional concrete. As such, the mortar surrounding the aggregate particles experiences higher stresses. Results show that the lower the MPT_{coarse}, the higher the mechanical properties of PPM mix-designed mixtures [43,44,56]. Yet, De

Grazia et al. [7] found that when comparing mixtures with distinct OPC content and limestone filler, the MPT_{coarse} could not accurately predict their compressive strength because they were proportioned with similar PPM and q-factor, which resulted in a similar volume of aggregate, hence, similar MPT_{coarse}. The two mixtures proportioned through Alfred's model with distinct cement contents (from around 270 kg/m^3 to 155 kg/m^3) and limestone fillers presented compressive strength values ranging from 70 to 43 MPa, but MPT_{coarse} remained constant for mixtures with the same mix-design parameters regardless of OPC and filler content and w/c. Moreover, it was concluded that the sole use of the conventional Abrams law (i.e., strength as a function of the water-to-cement ratio) was not enough to explain the distinct behaviour found in the hardened state due to PPM and high amount of limestone fillers, as the constants A and B must be significantly modified in order to predict compressive strength of eco-efficient mixtures. John et al. [50] also verified that besides the w/c, additional parameters might be required for predicting the compressive strength of mixtures manufactured through PPMs and incorporating moderate to high amounts of inert fillers; thus, the water to fines (also known as water to powder - w/p) ratio was proposed. Although there were stronger correlations between compressive strength and w/p than with w/c, the use of w/p cannot replace the parameter w/c since fillers are an inert material that do not directly contribute to C-S-H formation (although it has been verified that limestone fillers may enhance the quality and amount of C-S-H formed in the system due to the increase of nucleation sites).

Kurda et al. [48] evaluated the reliability of several models (i.e., Abrams, Slates, ACI, Bolomey, and Féret model) when predicting the compressive strength of conventional concrete mixtures and it was concluded that Bolomey model is the most accurate when comparing the calculated compressive strength to experimental data. Yet, there is a lack of studies investigating the most

accurate model to predict compressive strength of highly packed concrete mixtures developed with low cement content.

6.2.6 Concrete eco-efficiency

Damineli et al. [57] proposed the use of the binder intensity (bi) index to appraise concrete eco-efficiency through the binder content with respect to a concrete property ratio (Equation 6.7). This equation quantifies the required amount of binder to produce one unit of any concrete property. Since 28-day compressive strength is the most commonly used property, it is the most applied in the bi-index.

$$bi = \frac{BC}{P} \qquad \text{Equation 6.7}$$

where bi is the binder intensity index, BC is the binder content (kg/m^3), and P is the performance requirement (e.g., compressive strength – MPa).

The majority of concrete produced worldwide has cement contents ranging from 250 to 500 kg/m³ and the vast majority of the bi-index found in conventional concrete (≤ 35Pa) are close to or higher than 10 kg.m^{-3}.MPa^{-1} [57]. Moreover, only roughly 2% of the concrete mixtures commonly used worldwide present cement contents lower than 250 kg/m³ of concrete [57]. Analyzing previous studies [5–7,10,11] that use distinct types of PPMs to produce eco-efficient concrete mixtures, 3 out of the 32 mixtures produced resulted in a bi-index greater than 10 kg.m^{-3}.MPa^{-1} thus, confirming the ability of PPMs to produce eco-efficient mixtures. Moreover, approximately 85% of the mixtures were produced with a cement content lower than 320 kg/m^3, wherein 80% of the mixtures were produced by packing only the aggregate portion. One may conclude that the optimization of the whole matrix is a key factor for concrete sustainability. Besides, it was proven that when more recent

PPMs are selected (i.e., modified Andreasen and Compressive Packing Model), the bi index is on average lower than the other methods.

6.3 Scope of the work

The main objective of this work is to comprehend the hardened state properties of highly packed eco-efficient concrete mixtures designed with limestone fillers. A total of 12 concrete mixtures were developed using a coupled PPM-MP approach, containing distinct ranges of cement content (e.g., 320, 250, 200, 150 kg/m^3) and incorporating two types of limestone fillers (i.e., performance filler to decrease the matrix porosity and replacement filler to target decrease in the cement content). Moreover, three ranges of fresh-state performance were investigated (i.e., slump of 180, 90, and 20 +/- 20 mm) which are the most common values associated with distinct applications as per ACI 211-1 [58] and CSA A23.1 [59]. Preliminary fresh state tests, including slump, air content, temperature, pH, and rheological profile were performed to fully appraise the mixtures developed. Then, their hardened state properties were investigated through compressive strength, modulus of elasticity, surface electrical resistivity, and apparent porosity. Meanwhile, the eco-efficiency of all mixtures was measured with the binder intensity (bi) index [57] to confirm their sustainability aspects. Two conventional methods (Abrams law and Eurocode 2) were selected to predict the compressive strength of those mixtures and different parameters are proposed to existing models to increase their suitability in predicting behaviour of eco-efficient mixtures. Finally, a new approach is proposed in this study aiming to facilitate the formulation of eco-efficient mixtures that meet compressive strength and cement content criteria.

6.4 Materials and methods

6.4.1 Raw materials characterization

The concrete mixtures investigated in this study were developed with natural sand and a granite coarse aggregate with a nominal maximum size of 19 mm. Two types of limestone fillers were used in the mixtures: 1) a performance filler (P) and 2) a replacement filler (R), having a PSD smaller than and similar to that of OPC, respectively. The PSD of the aggregates was determined through sieve analyses as per ASTM C136 [60], whereas for determining the PSD of the limestone fillers and OPC, a laser diffraction analysis was performed (Figure 6.1).

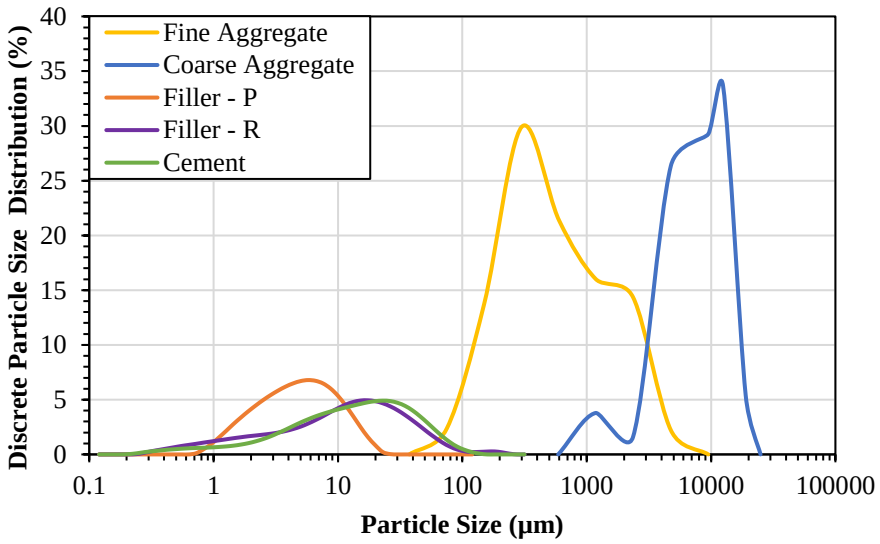

Figure 6.1. Particle size distribution of raw materials.

The materials' specific gravity and specific surface area analyses, through Brunauer-Emmett-Teller - BET method, is presented in Table 6.1. Moreover, the chemical composition of the general use (GU) Portland cement obtained by X-ray fluorescence (XRF) and the mineralogical phases calculated through Bogue [61] are presented in Table 6.2. A polycarboxylate-based high-range water

reducer and a lignosulfonate-based mid-range plasticizer were selected to improve the flowability of the concrete mixture when needed.

Table 6.1. Physical properties characterization.

Material	Specific gravity (g/cm^3)	Specific Surface Area - SSA (m^2/g)
GU cement	3.17	1.17
Filler - R	2.66	1.60
Filler - P	2.60	3.70
Fine Aggregate	2.74	0.92
Coarse Aggregate	2.81	0.11

Table 6.2. Chemical composition and mineralogical phases of GU cement.

GU cement	CaO	SiO_2	Al_2O_3	Fe_2O_3	SO_3	MgO	Na_2O	LOI
Composition (%)	61.5	19.4	4.9	3.7	3.9	2.4	0.95	1.9
Mineralogical phases	**C_3S**	**C_2S**	**C_3A**	**C_4AF**				
	53.5	15.5	6.7	11.2				

6.4.2 Mix-design procedure – PPM-MP approach

The eco-efficient concrete mixtures developed in this study (Table 6.3) were designed through a modified Alfred model combined with mobility parameters targeting three ranges of slump values (i.e., slump of 180, 90, and 20 ± 20mm); these values were associated to distinct applications as per ACI 211-1 [58] and CSA A23.1 [59]. As presented in the literature review section, a high distribution factor (i.e., q-factor) of 0.37 decreases the OPC usage in concrete, improving the eco-efficiency of the mixtures and decreasing the porosity of the system (2.8% for a q-factor of 0.37), as highlighted in Figure 6.2a and b, respectively.

De Grazia et al. [7] verified issues related to fresh state when selecting a q-factor of 0.37, including low flowability and slump. To enhance the fresh state behaviour of the highly packed mixtures, the

authors proposed to “break” Alfred’s PSD curve into two parts: powder (or fines) portion (with q-factor of 0.21) and aggregates portion (with q-factor of 0.37). Yet, results suggested that the slump only improved when the cement content of concrete was raised.

Table 6.3. Mix-design of 12 eco-efficient concrete mixtures.

Mixture	kg/m³													
	Powder			Fine Aggregate					Coarse Aggregate					
	OPC	Filler P	Filler R	150-300 mm	300-600 mm	600-1180 mm	1180-2360 mm	2360-4750 mm	4750-9500 mm	9500-12500 mm	12500-19000 mm	Water	SP	MR
1H-311-0.68	311	0	0	126	157	189	239	300	378	174	295	212	0.0	0.0
1M-319-0.60	320	0	0	130	161	194	246	307	388	178	303	192	0.0	0.0
1L-328-0.52	328	0	0	133	165	199	252	316	398	183	311	171	0.0	0.0
2H-250-0.68	250	39	25	133	165	199	252	316	398	183	311	170	1.9	1.9
2M-250-0.60	250	40	31	136	169	204	259	324	408	187	319	150	3.9	3.2
2L-250-0.52	250	41	37	140	173	209	265	332	418	192	326	130	3.9	3.9
3H-200-0.83	200	40	69	134	166	200	254	318	401	184	313	165	1.9	1.9
3M-200-0.74	200	41	74	137	169	204	259	324	409	188	319	148	3.8	3.1
3L-200-0.64	200	41	79	140	174	210	266	333	419	193	327	129	3.9	3.9
4H-150-1.09	150	40	111	138	170	204	256	319	399	182	309	163	2.4	1.2
4M-150-0.97	150	41	117	141	174	208	262	326	408	187	316	145	4.3	2.5
4L-150-0.84	150	42	122	144	178	213	268	333	417	191	323	126	3.9	3.9

Note: The labels depict the group per cement content, mobility parameter, cement content, w/c.

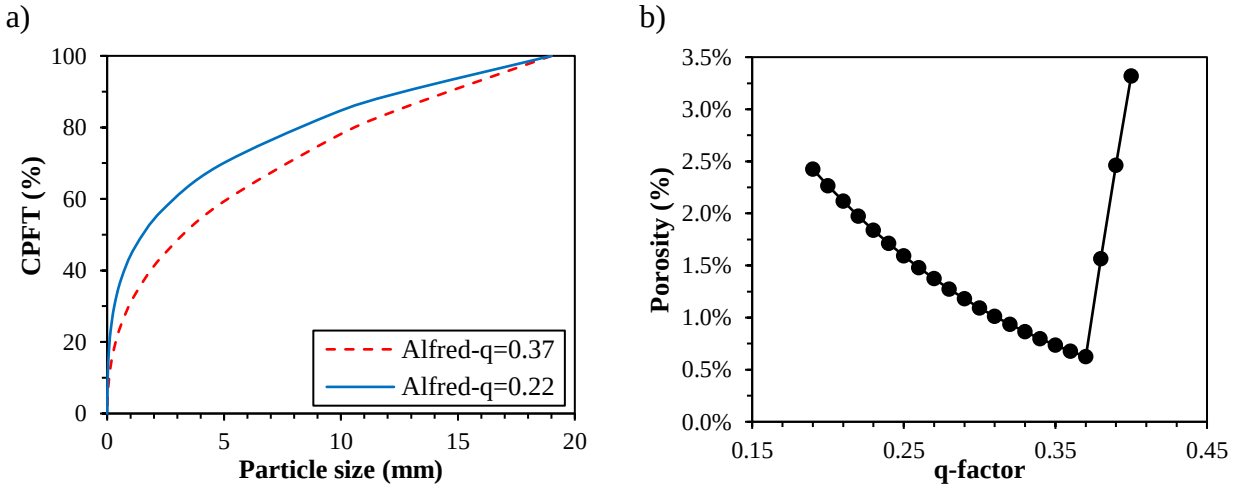

Figure 6.2. a) Difference between system PSD for mixtures developed with q-factors of 0.37 and 0.22 and b) Comparison of porosity with different q-factors.

Based on the study above, it has been verified that the selection of q-factors for both portions of Alfred’s model (i.e., powder and aggregates fractions) was a key factor to define the behaviour of concrete mixtures in the fresh state. Moreover, this parameter could be better understood whether

the distance amongst the granular particles was computed; the above discussion gave origin to the PPM-MP approach proposed in this work. First, Equation 6.1 was applied for the powder portion (from D_s to 80 μm) and aggregates portion (from 0.15 mm to D_L). It is worth noting that 80 μm represents the largest diameter available within the powders selected (i.e., Portland cement, replacement and performance fillers) and 0.15 mm represents the smallest diameter of fine aggregate. To achieve the lowest system's porosity through Alfred's model, q-factors of 0.34 and 0.31 ±0.1 in the powder and aggregate portion, respectively, were selected, yielding a final system with dry porosity of 3.0% ±0.1 (calculated through Equation 6.6).

Therefore, the 12 concrete mixtures were developed using Equation 6.8 for the powder portion and Equation 6.9 for the aggregate portion.

Powder portion (from D_s to 80 μm)	$$CPFT = 100 * \left(\frac{{D_P}^{0.34} - {D_S}^{0.34}}{0.8^{0.34} - {D_S}^{0.34}}\right)$$	Equation 6.8
Aggregates portion (from 0.15 mm to D_L)	$$CPFT = 100 * \left(\frac{{D_P}^{0.31} - 0.15^{0.31}}{{D_L}^{0.31} - 0.15^{0.31}}\right)$$	Equation 6.9

Three control mixtures were developed with 0% of limestone fillers, whereas nine mixtures were fabricated with the optimum amount of *performance filler* (~ 1.9% of total concrete dry volume) and three distinct amounts of *replacement filler* (~ 1.2, 3.2, and 5.1% of total concrete dry volume). The least square method was employed to calculate the optimum amount of *performance filler* (P) to be incorporated, based on the 0.34 q-factor curve of the powder portion. Due to the similar PSD between OPC and *replacement filler* (R), the amount of *replacement filler* was increased to achieve the target OPC contents (250, 200, and 150 kg/m^3, respectively).

To select the w/c, commonly used compressive strengths in the concrete industry (20, 25, 30 MPa) were considered; thus, three distinct water-to-cement ratios (w/c = 0.68, 0.60, 0.52) were selected for the control mixtures according to Abrams law to target the respective strengths. When comparing control mixtures (developed with 320 kg/m^3 of OPC) with mixtures containing 250 kg/m^3 of OPC, it was possible to use the same w/c pre-selected (i.e., 0.68, 0.60, 0.52). Yet, this w/c would result in a lack of free water for mixtures with 200 and 150 kg/m^3. In this case, to ensure similar flowability, the same mobility parameters (Table 6.4) were adopted for the nine eco-efficient mixtures manufactured with 250, 200, and 150 kg/m^3 of cement and different amounts of limestone fillers. It is worth highlighting that the fixed mobility parameters also resulted in a similar water-to-powder ratio (w/p; water / (cement + fillers)) for mixtures developed with limestone fillers. As such, w/p of 0.54, 0.47, and 0.40 yielded IPS of 0.60, 0.51, 0.42 ± 0.02 μm, and MPT of 0.41, 0.37, 0.32 ± 0.02 μm, respectively. Furthermore, all mixtures had the same mortar factor (Equation 6.10) of 61%.

$$\text{Mortar factor} = \frac{1+a}{1+m} = \frac{\frac{m_c + m_f + m_{F.A.}}{m_c}}{\frac{m_c + m_f + m_{F.A.} + m_{C.A.}}{m_c}} \qquad \text{Equation 6.10}$$

where m_c is mass of cement, m_f is mass of fillers, $m_{F.A.}$ is mass of fine aggregates and $m_{C.A.}$ is mass of coarse aggregates

To facilitate the recognition of the mixtures, they were divided into 4 groups based on their cement content; where group 1 (G1) represents the control mixtures (on average 320 kg/m^3 of cement), while group 4 represents the mixtures with the lowest cement content (150 kg/ m^3). Acronyms were given to mixtures based on their group number, mobility parameters (e.g., high - H, medium - M, low - L), cement content, and w/c. For example, mixture 2M-250-0.60 is from group 2 (G2), has

medium water content, 250 kg/m^3 of cement, and w/c of 0.60. The mobility parameters were then calculated and presented in Table 6.4.

Table 6.4. Mobility parameters of designed mixtures.

Mix-name	Mobility Parameters		w/c	w/p	Filler % (m.p.)
	IPS (µm)	MPT (µm)			
1H-311-0.68	1.06	0.52	0.68	0.68	0%
1M-319-0.60	0.92	0.47	0.60	0.60	0%
1L-328-0.52	0.79	0.42	0.52	0.52	0%
2H-250-0.68	0.63	0.42	0.68	0.54	21%
2M-250-0.60	0.53	0.37	0.60	0.47	22%
2L-250-0.52	0.44	0.33	0.52	0.40	24%
3H-200-0.83	0.60	0.41	0.83	0.54	35%
3M-200-0.74	0.51	0.37	0.74	0.47	36%
3L-200-0.64	0.42	0.32	0.64	0.40	38%
4H-150-1.09	0.57	0.39	1.09	0.54	50%
4M-150-0.97	0.49	0.35	0.97	0.47	51%
4L-150-0.84	0.40	0.31	0.84	0.40	52%

Note: filler percentage is related to the total mass of powders (m.p.).

6.4.3 Concrete and specimen fabrication

Thirty-five litres of concrete were manufactured for each of the twelve mixtures fabricated and distinct fresh state tests were performed (i.e., slump, air content, temperature, pH, and rheology). Then, sixteen cylinders (100 mm by 200 mm) were fabricated according to ASTM C 39 [62]. The specimens were left to moist-cure (i.e., 20°C and 100% RH) for 24 hours, demoulded, ground, and moist-cured under the same conditions for and additional 28 days before performing hardened state tests.

6.4.4 Fresh state assessment

After mixing each of the twelve mixtures appraised, the pH and temperature were measured using pH strips and a thermometer with a precision of 0.1°C. The slump, air content and rheological

characterization tests were then performed. The latter test used a planetary rheometer called IBB rheometer that contains an H-shape impeller (100 mm height and 130 mm length) and a bowl with a diameter of 360 mm and 250 mm height [63]. Moreover, this rheometer is recommended to appraise concrete mixtures with slumps ranging from 40 mm to 300 mm [64], suitable for 9 out of the 12 mixtures evaluated in this study. The IBB rheometer contains a pre-programmed cycle that increases the shear rate up to 0.7 s^{-1} and then decreases it in the same stepwise manner while maintaining the rotation for roughly 10 seconds at each step (180 seconds per cycle). A complete cycle was applied as a pre-shear regime followed by a second cycle to then plot the flow curves of each mixture appraised.

Although the IBB rheometer has two Bingham output parameters (i.e., G – yield stress in N.m, and H – plastic viscosity in N.m.s), it is known that not all concrete mixtures display a Bingham behaviour; therefore, to better investigate each mixture's rheological behaviour, the IBB dataset was retrieved and the flow curves were plotted [63,64]. It is worth highlighting that the IBB rheometer results are not presented in fundamental units (e.g., yield stress - Pa and plastic viscosity - Pa.s) [63,64], hence the results will be used for comparison amongst distinct mixtures rather than compared to data obtained in previous studies with the use of other rheometers. However, previous studies [63,64] concluded that the IBB outcomes yield good correlation with other rheometers (e.g., BML rheometer, Btrheom, Cemagrefing, Two-Point apparatus).

6.4.5 Hardened state assessment

The compressive strength, modulus of elasticity, surface electrical resistivity and apparent porosity were selected to evaluate the hardened state performance of the eco-efficient concrete mixtures. The compressive strength and electrical resistivity were determined at 7, 14, and 28 days. Meanwhile, to

complete the strength development curve, the compressive strength was also determined at 3 days and the modulus of elasticity at 28 days as per ASTM C469-17 [65]. The compressive strength test was carried out on three specimens of each of the twelve concrete mixtures as per ASTM C 39 [62]. Moreover, the surface electrical resistivity was performed using the four-probe (Wenner-array) technique using a commercially available device that automatically displays the surface electrical resistivity (i.e., measured through four equidistant probes).

The apparent porosity was determined at 28 days and is based on Archimedes immersion method [46] and used to compare the different concrete mixtures and evaluate their microstructure. and. After 7, 14, and 28 days of curing, one specimen of each mixture was cut axially into three forming slices of approximately 100 mm in diameter and 65 mm in height. The slices were placed in an oven at 60°C, avoiding the decomposition of cement hydration products caused by higher temperatures, until mass stabilization which occurred after 4 days of drying. Each specimens' dry mass (m_d) was determined when the difference between two successive weights measured within a 24 hour interval was less than 0.3%; previous trials were performed to conclude that 0.3% of mass change results in an apparent porosity difference smaller than 10%. The slices were then immersed in water and subjected to vacuum ensuring water penetration. After 24 hours of immersion, while maintaining vacuum, the immersed (m_i) and wet (m_w) mass values were determined. The apparent porosity (AP) was calculated using Equation 6.11.

$$\text{AP}\ (\%) = \frac{m_w - m_i}{m_w - m_d} * 100\% \qquad \text{Equation 6.11}$$

6.5 Results

6.5.1 Fresh state properties

Table 6.5 displays the pH, concrete temperature, fresh density and air content of all mixtures.

One can notice that the pH of the mixtures decreases with cement content, as expected, and ranged from 13 to 11.5. However, the concrete temperature and the fresh density were not affected by the decrease in cement content. It is worth noting that these mixtures were designed without air-entrained admixtures, hence their air content varied from 1.4 to 2.8% with an average of 2.0%, which is recommended for standard applications.

Table 6.5. Summary of fresh state properties of the 12 eco-efficient mixtures.

Mixture	pH	Concrete Temperature (°C)	Fresh Density (g/cm³)	Air Content (%)
1H-311-0.68	13.0	22.2	2551	1.5
1M-319-0.60	13.0	23.0	2575	2.3
1L-328-0.52	13.0	23.6	2617	2.1
2H-250-0.68	13.0	22.7	2595	2.2
2M-250-0.60	13.0	24.9	2588	2.8
2L-250-0.52	12.5	22.9	2625	2.1
3H-200-0.83	12.0	22.9	2591	2.1
3M-200-0.74	12.0	22.8	2625	2.1
3L-200-0.64	12.0	24.1	2596	1.8
4H-150-1.09	12.0	23.1	2614	2.0
4M-150-0.97	11.5	23.1	2635	2.0
4L-150-0.84	11.5	23.3	2626	1.4

For each mixture group with equal cement content, three target slumps (i.e., 180, 90, 20 +/- 20mm) were selected. Figure 6.3 shows the target slump per mixture group based on OPC content, the achieved slump values, and the mobility parameters (i.e., IPS and MPT). As observed, the reduction of cement content for eco-efficient mixtures resulted in a lower IPS due to the difference in volume specific area of the powders, whereas this decrease is less evident for the MPT, as it mainly accounts for the aggregates' physical characteristics and volume. Noticeably, only control mixtures (G1) have IPS values higher than 0.8, hence not requiring any admixture to achieve the target slumps. Meanwhile, eco-efficient mixtures that have IPS of 0.63, 0.53, and 0.44μm, required a total amount of admixture of 1.2, 2.2, and 2.45% (on average), respectively, to achieve the target slump.

Furthermore, control mixtures presented a slightly higher (0.10 µm) MPT than all other mixtures. This seems to indicate that the IPS, which is governed by water content, is the key factor influencing the slump.

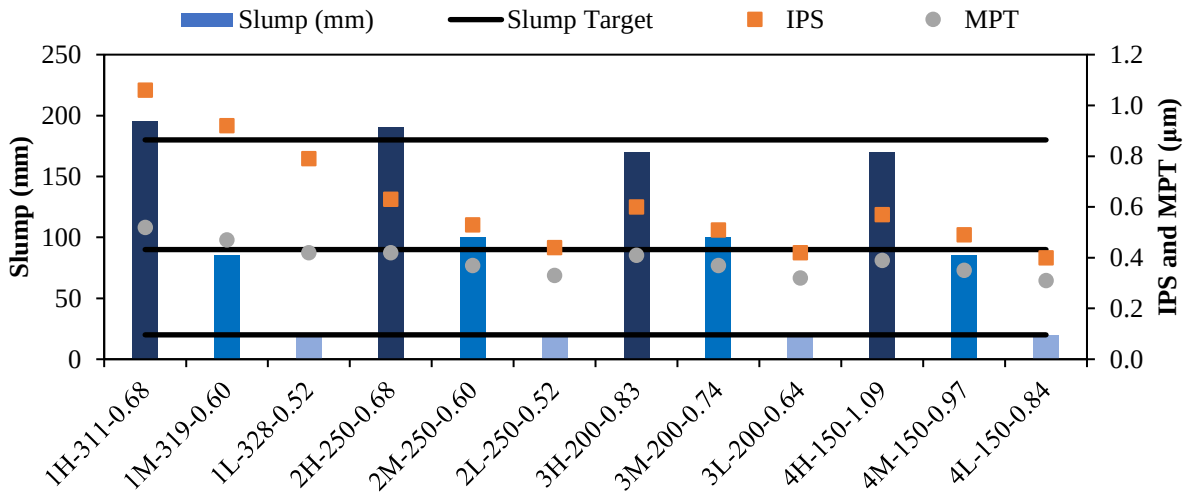

Figure 6.3. The influence of water content and total admixture on slump values.

To thoroughly appraise the fresh state behaviour of concrete mixtures, their rheological profiles were evaluated. It is worth noting that mixtures designed with a low slump (i.e., < 40 mm) could not be appraised in the IBB rheometer; hence, the rheological profile of nine mixtures (developed with high - H and medium - M mobility parameters) was evaluated and is presented in Figure 6.4. At a rotation of 0.04 s^{-1}, mixtures with high (Figure 6.4a) and medium (Figure 6.4b) mobility parameters achieved average torques of 5 N.m and 8 N.m, respectively. Figure 6.4a and b show maximum torque ranging from 6.8 to 17.03 N.m and 10.66 to 24.31 N.m, respectively. Regardless of the mobility parameters, mixtures with high cement content (1H-311-0.68 and 1M-319-0.60) yielded lower maximum torque than the more sustainable mixtures, whereas mixtures developed with 200 kg/m^3 required the highest maximum torque measured at 0.7 s^{-1}. Analyzing the more sustainable mixtures, one may notice that mixtures developed with the lowest cement content (150 kg/m^3)

resulted in the lowest torque, followed by mixtures with 250 kg/m^3 and then 200 kg/m^3. Although mixtures 2H-250-0.68, 3H-200-0.83, and 4H-150-1.09 had the same slump and mobility parameters, their rheological behaviours were not consistent. Likewise, the same trend could be observed for mixtures 2M-250-0.60, 3M-200-0.74, and 4H-150-0.97. These results indicate that both the cement and filler contents affect the rheological behaviour of eco-efficient concrete mixtures. Furthermore, all mixtures presented shear-thinning behaviour, that is, the viscosity decreases with the increase of applied torque.

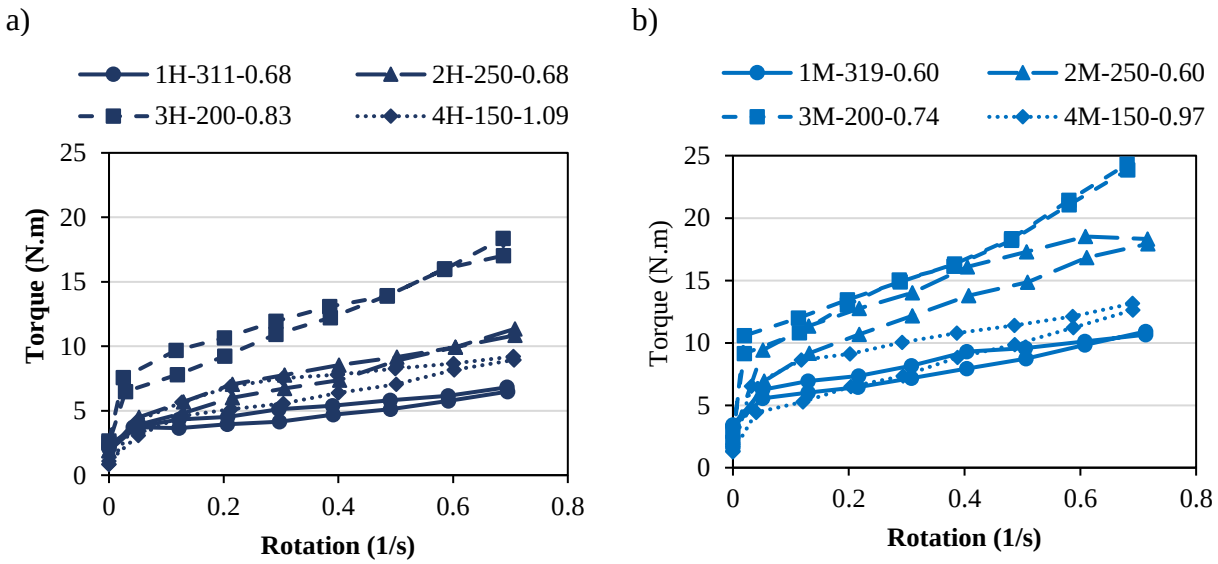

Figure 6.4. Rheological behaviour over time of mixture a) mixtures with high (H) mobility parameters and b) mixtures with medium (M) mobility parameters.

6.5.2 Compressive strength

To better understand the impact of OPC content on compressive strength, Figure 6.5a compares results between G1 (average cement content of 320 kg/m^3) and G2 (cement content of 250 kg/m^3) that contain similar w/c. Interestingly, concrete mixtures incorporating 250 kg/m^3 achieved on average a compressive strength 12% higher than G1; the greatest difference (around 7 MPa) was found on mixtures with low w/c (2L-250-0.52 and 1L-328-0.52). This result, which compares

mixtures with the same mix-design and w/c, highlights that limestone fillers enhance the system's inner quality (i.e., hydration and inner porosity). Regarding strength development, one may notice that the filler effect (i.e., enhancement of the cement hydration) occurs especially after 7 days, in which all mixtures containing limestone fillers yielded higher compressive strength than mixtures developed with pure OPC.

a)

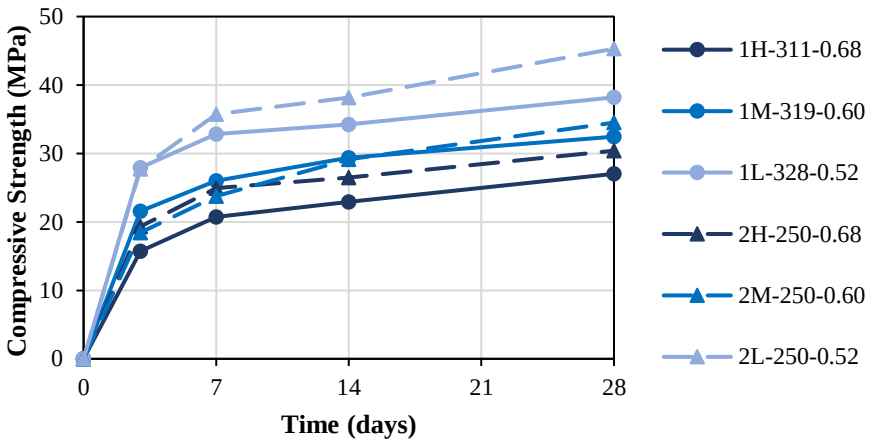

b)

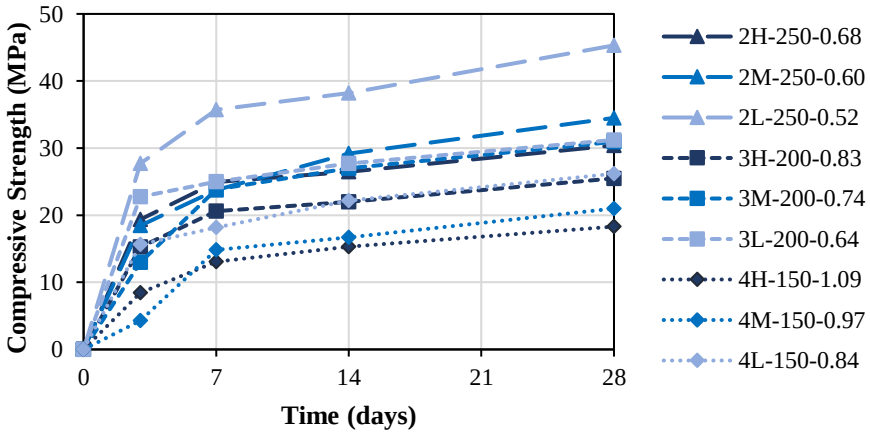

Figure 6.5. Compressive Strength a) G1 and G2, b) G2, G3, G4 (mixtures with filler).

Evaluating the eco-efficient mixtures, Figure 6.5b presents those containing limestone filler (G2, G3, and G4) with distinct w/c and similar w/p. Evidently, the higher the cement content, the lower the w/c; hence the better the hardened performance. However, mixtures manufactured with 250,

200, and 150 kg/m^3 yielded 28-days compressive strength of 45, 31, and 26 MPa, respectively, when a low w/c was used. Moreover, mixtures 2H-250-0.68 and 3M-200-0.74 yielded 30.7 MPa at 28-days, showing that because of the lower OPC content, the 3M-200-0.74 mixture required a higher w/c without having any impact on its compressive strength. Similarly, this behaviour was observed for the mixtures 3H-200-0.83 and 4L-150-0.84, which achieved 26 MPa at 28-days. Analyzing the strength gain over time, one verifies that mixtures 4M-150-0.97 and 4H-150-1.09 yielded extremely low 3-day compressive strength (i.e., 4.3 MPa and 8.4 MPa), which might be justified by the low amount of cement content and high w/c. The 28-day compressive strength of the mixtures tested ranged from 18.3 to 45.3 MPa, confirming the viability of using eco-efficient mixtures in various structural and non-structural applications.

6.5.3 Modulus of elasticity

The modulus of elasticity for each mixture is presented in Figure 6.6 where one may observe that the higher the cement content, the higher the difference of the 28-day modulus of elasticity within the same group. The modulus of elasticity, therefore, ranged from 32 GPa to 24 GPa for G1, whereas the range gradually decreased with the decrease in cement content and from 24 to 21 GPa for G4. Thus, the influence of the w/c on the modulus of elasticity is less significant for eco-efficient developed with lower cement content and containing limestone filler. This may once again be attributed to the enhancement of the system matrix through the usage of limestone fillers. Yet, as expected, the higher the w/c, the lower the modulus of elasticity regardless of the cement content. On the other hand, for mixtures with similar w/c and distinct cement content (i.e., G1 and G2), a better performance was achieved for mixtures containing less cement (i.e., G2 with a modulus of elasticity from 27.5 to 31.5 GPa) and a sharper increase was observed per w/c.

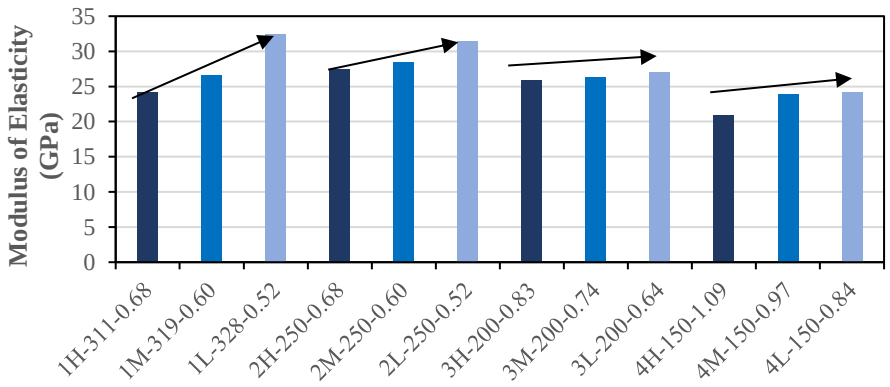

Figure 6.6. Modulus of elasticity of eco-efficient mixtures.

6.5.4 Surface electrical resistivity

To further assess the microstructure of the sustainable mixtures, the surface electrical resistivity of the twelve mixtures was measured (Figure 6.7). One may notice that surface electrical resistivity follows similar trends as observed for the compressive strength. Although from Figure 6.5, mixtures developed with 250 kg/m^3 (G2) yielded better performance (i.e., compressive strength) than G1 companion mixtures with equal w/c, the surface electrical resistivity of G1 and G2 are approximately the same (Figure 6.7a) ranging from 11.5 kΩ.cm (1L-328-0.52 and 2L-250-0.52) to 6.5 kΩ.cm (1H-311-0.68 and 2H-250-0.68). Figure 6.7b shows that mixtures 4H-150-1.09 and 4M-150-0.97 achieved the lowest overall 28-day surface electrical resistivity of 4.2 kΩ.cm. Moreover, mixtures with w/c between 0.68 and 0.84 (2H-250-0.68, 3H-200-0.83, 3M-200-0.74, and 4L-150-0.84) yielded 28-day surface electrical resistivity of approximately 6.2 kΩ.cm regardless of the cement content. Meanwhile, mixtures with a w/c below 0.64 (2m-250-0.60, 2l-250-0.52, 3l-200-0.64) achieved 28-day surface electrical resistivity higher than 9.7 kΩ.cm.

a)

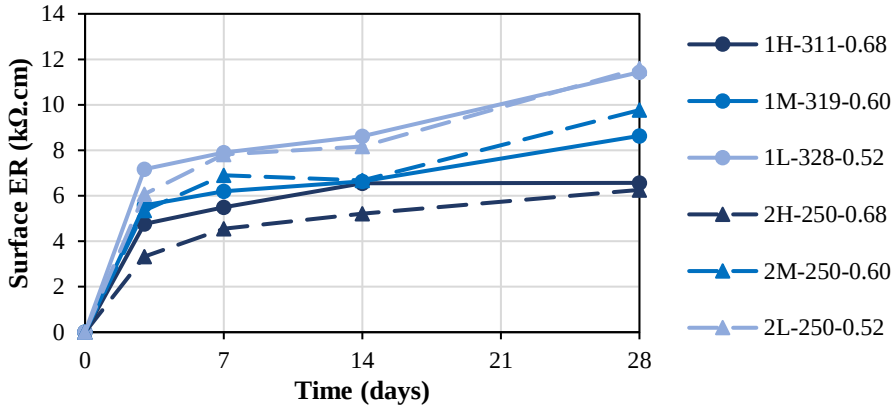

b)

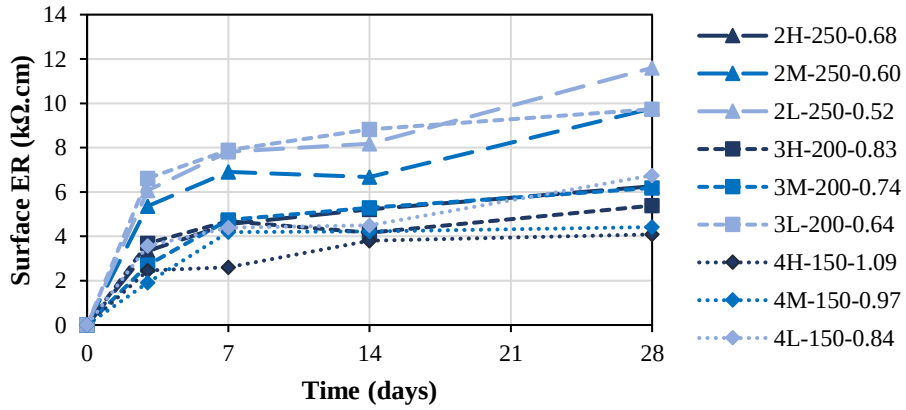

Figure 6.7. Surface electrical resistivity a) G1 and G2, b) G2, G3, G4 (mixtures with filler).

6.5.5 Apparent porosity

The apparent porosity of all mixtures at 28 days is displayed in Figure 6.8 which shows that the higher the w/c, the higher the porosity of the mixtures containing the same cement content. Nevertheless, comparing G1 and G2, which contain the same w/c and distinct OPC contents (i.e., 320 and 250 kg/m^3), the apparent porosity of G1 ranged from 10.4 to 6.2% whereas values of 7.3 to 5.0% were obtained for G2; the latter presenting the lowest overall porosity. This may be explained due to the enhancement of the system matrix and nucleation points created by limestone fillers. Moreover, the apparent porosity of the control mixtures (G1) is more affected by the w/c than for

mixtures containing limestone fillers and lower cement contents (G2, G3, and G4). Compared to G2, G3 contains 50 kg/m^3 less cement and on average a 22% higher w/c. Moreover, G3 and G2 presented similar apparent porosity at 28-days yet, G2 achieved a 28-day compressive strength of 45, 35, and 30 MPa for low, medium, and high w/c, whereas G3 achieved 31, 30, and 25 MPa.

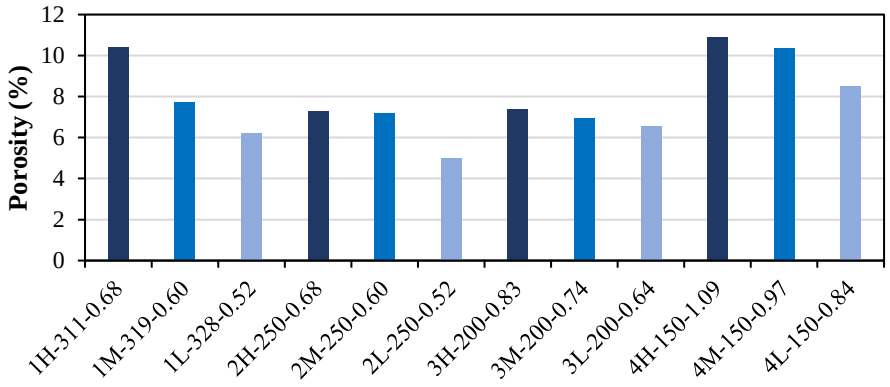

Figure 6.8. Apparent porosity of eco-efficient mixtures.

6.6 Discussion

6.6.1 Analysis of hardened state properties

To better comprehend the hardened state results gathered throughout this study, Figure 6.9 presents the relationship between the compressive strength (which is directly proportional to the other hardened state properties – modulus of elasticity and surface electrical resistivity) and parameters correlated to material microstructure (i.e., porosity, w/c, Volume of aggregates (Vaggregates), and percentage of fillers). It is worth emphasizing that all mixtures were proportioned with the same dry packing density of 96.8% and mortar factor of 61%.

Analyzing Figure 6.9, it is clear that the w/c is the governing factor of all hardened state properties and microstructure characteristics for all mixtures. Yet, the slight increase of aggregate volume of mixtures within the same group seems to influence their increased hardened state properties. The

apparent porosity, which is one of the main characteristics of concrete microstructure, is therefore not mainly governed by the w/c for mixtures containing limestone filler. Mixtures 2H-250-0.68 and 2M-250-0.60 yield approximately the same porosity even though they were mix-proportioned with a w/c difference of 12%.

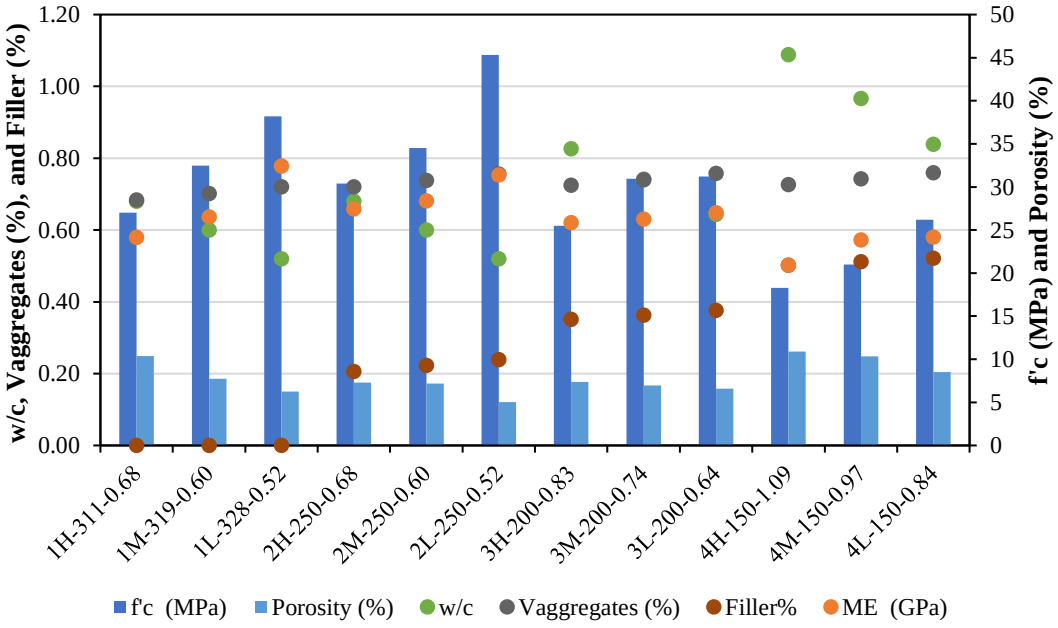

Figure 6.9. Comparison between hardened state properties and mix-design characteristics.

The same trend is seen for mixtures 3H-200-0.83 and 2M-250-0.60. Since mixtures using 250 and 200 kg/m^3 of cement content were mix-proportioned with 22 and 36% of filler (on average), respectively, the results show that the limestone fillers may have lessened the overall apparent porosity of the mixtures. These results indicate that although a higher amount of filler is used in G3 (200 kg/m^3 of cement content), the fillers contributed to the enhancement of the system's microstructure (i.e., reducing its porosity). However, G3 mixtures did not achieve higher compressive strengths due to their higher w/c. This phenomenon is more pronounced for G4 mixtures, where the apparent porosity is on average 10%, which is higher than G1. Furthermore,

regardless of cement content or w/c, the mixtures 2H-250-0.68 and 3M-200-0.74 achieved comparable apparent porosity, compressive strength, and ME, suggesting a 36% limestone filler threshold when a PPM is used to proportion eco-efficient concrete without compromising short-term performance.

6.6.2 Demonstration of the eco-efficiency of concrete mixtures

The binder intensity (bi) index is a useful metric used to evaluate the eco-efficiency of concrete mixtures. Figure 6.10 compares the results of the current research with the international records correlating binder intensity with compressive strength.

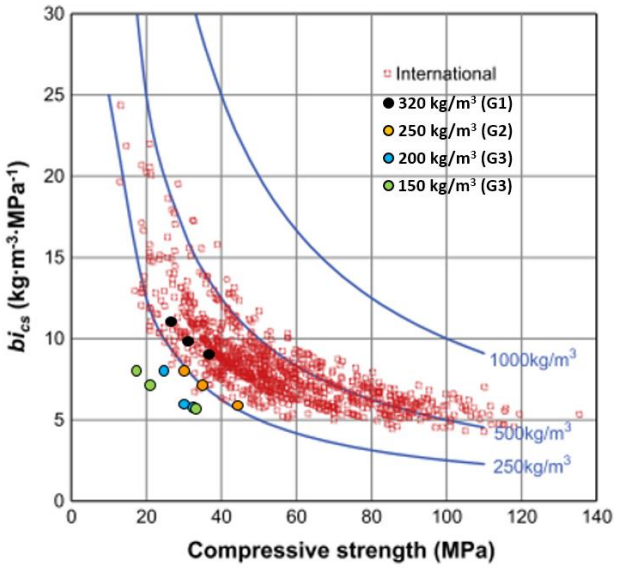

Figure 6.10. Relationship between binder intensity and compressive strength of the twelve eco-efficient mixtures compared with international records [57].

One may notice that roughly 2% of the concrete mixtures commonly used worldwide have cement contents lower than 250 kg/m³ and the majority of the concrete mixtures produced worldwide contain cement content around 375 kg/m^3 as per standards and guidelines [57,66]. Moreover, analyzing mixtures with a compressive strength between 20 and 40 MPa, the bi-index was on

average 10 kg/m^3. MPa^{-1} [67]. When PPMs are used only in the aggregate fraction, the bi-index can be improved with the use of slag and fly ash. Studies [5,10] show that binder indices range from 6.1 to 11.4 kg/m^3.MPa^{-1} for mixtures having strengths from 63.9 to 31.5 MPa, respectively. Agreeing with previous studies [57,66], mixtures with a compressive strength higher than 40 MPa are considered more sustainable than conventional mixtures (<40MPa). Similar to this study, [11] selected Alfred model (also known as Modified Andreasen) to develop three eco-efficient mixtures using fly ash as a partial replacement of cement which achieved a bi-index of 13.2 kg/m^3.MPa^{-1} for mixtures with a 41 MPa compressive strength. Indeed, more sustainable mixtures were achieved by using distinct PPM methods combined with fillers thus, obtaining a bi-index ranging from 6.3 to 10.3 kg/m^3.MPa^{-1} for mixtures of 30 to 49 MPa strengths [6]. Yet, two conventional mixtures (i.e., compressive strength of 36 and 37 MPa) reached a bi-index of 8.5 kg/m^3.MPa^{-1}, highlighting the importance of combining the use of PPM with fillers as a partial replacement of cement.

Nonetheless, the twelve concrete mixtures investigated in this work were plotted based on their group, G1 (black), G2 (orange), G3 (blue), and G4 (green). The first group, G1, which is the only group with the Modified-Alfred Model without limestone fillers, achieved the highest bi-index (on average 10 kg/m^3. MPa^{-1}). One may notice that these values are below most of the concrete produced around the world, thus confirming their sustainability. However, mixtures from G2, G3, and G4 reached a higher level of eco-efficiency. As such, they contain a high limestone filler percentage, that is, on average, 22%, 36%, and 51%, respectively, highlighting the positive contributions of this inert filler not only in the hardened state but also in terms of sustainability. Within these groups, mixtures with high, medium, and low w/c achieved bi-indices of around 8.1, 7.0, and 5.9 kg/m^3. MPa^{-1} regardless of the cement content. These results emphasize the importance of using the proposed method (Modified-Alfred Model) combined with the usage of limestone fillers to develop

eco-efficient concrete mixtures, agreeing with previous results [6]. Moreover, this study is focusing on using only GU-cement and limestone filler, hence, the bi-index might have been even lower when this approach is combined with SCMs.

6.6.3 Compressive strength prediction through conventional models

Based on the Eurocode 2 (EN1992-1-1:2004) calculation (Equation 6.12), concrete compressive strength at a given age (t) depends on the cement type coefficient represented (s). Three cement coefficients are recommended, s=0.20 for cement of strength Classes CEM 42.5R, CEM 52.5N, and CEM 52.5R; s=0.25 for cement of strength Classes CEM 32.5R, CEM 42.5N; and s=0.38 for cement of strength Classes CEM 32.5N.

$$f_{cm}(t) = e^{\left\{s\left[1-\left(\frac{28}{t}\right)^{\frac{1}{2}}\right]\right\}} \qquad \text{Equation 6.12}$$

where $f_{cm}(t)$ is the mean concrete compressive strength at a given age t, t is the age of concrete in days, and s is the coefficient of cement type.

Considering the concrete mixtures investigated in this work and plotting them against their compressive strength development using EN1992-1 (Table 6.6 and Figure 6.11), one can see that the prediction of compressive strength is very precise, especially at ages greater than 7 days.

Figure 6.11c and d show the misprediction of 3-day compressive strength of mixtures 3L-200-0.64 and 4M-150-0.97. Moreover, analyzing Table 6.6, the s-parameter required to achieve the minimum square error (MSE) aligns with the EN1992-1 recommendation which ranges from 0.20 to 0.38, except for 1L-328-0.52 and 4M-150-0.97 that achieved s-parameters of 0.16 and 0.39, respectively. However, since only one type of cement was used, only one cement coefficient ought to be selected.

Despite this anomaly, one can notice that for mixtures with 320 kg/ m^3 of cement (G1) – where no fillers are used, the higher the w/c the lower the cement coefficient, whereas sustainable mixtures incorporating limestone fillers presented an inverse relationship between the coefficient parameter.

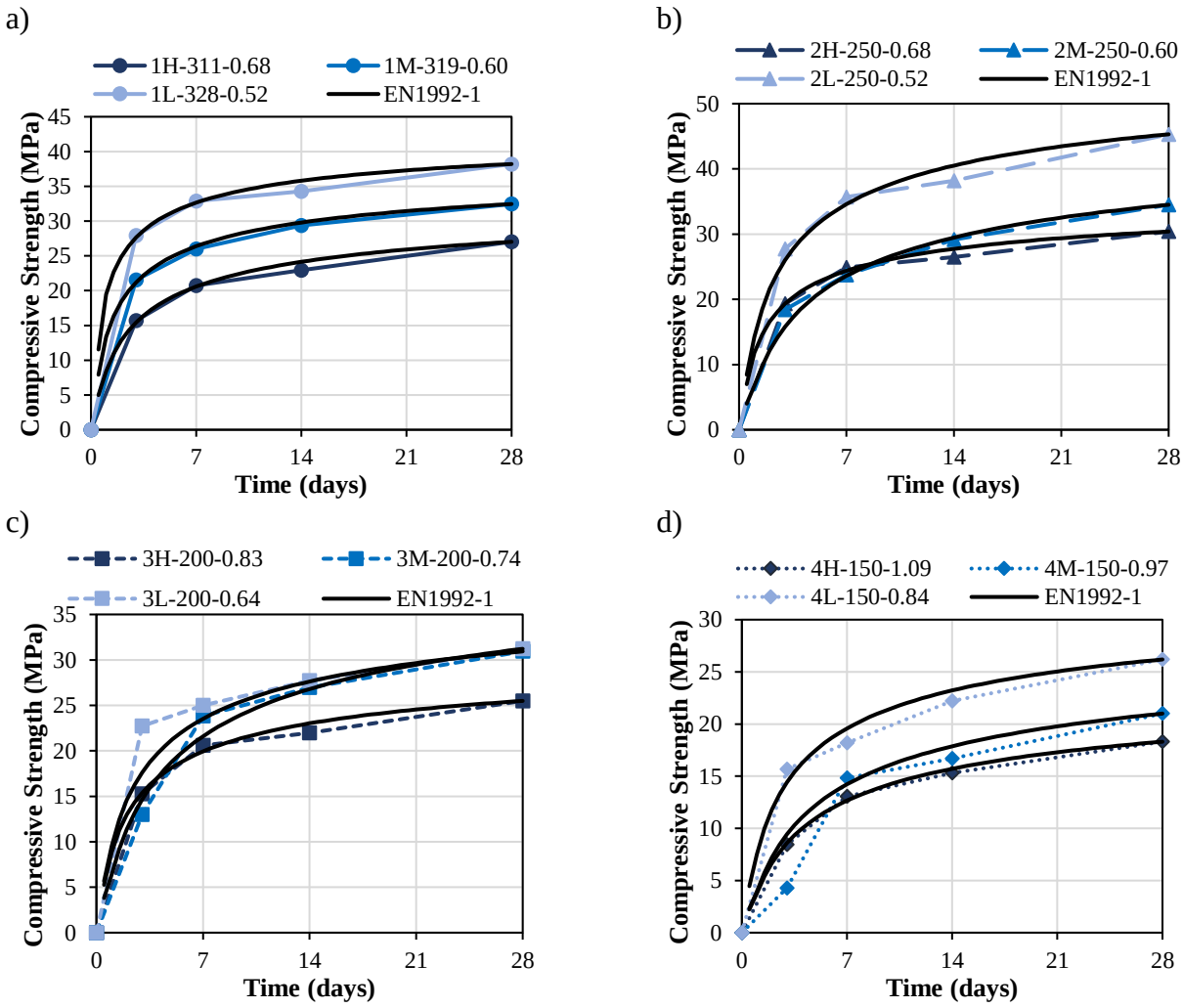

Figure 6.11. 28-day Compressive Strength development using EN1992-1 for a) 1-320 kg/m^3, b) 2-250 kg/m^3, 3-200 kg/m^3, 4-150 kg/m^3

Another conventional method used to predict compressive strength of concrete is Abrams law (Figure 6.12), created in 1918, which states that the mechanical performance of concrete is inversely proportional to its porosity, which is in turn set by the w/c [68,69]. Additionally, two empirical constants (A and B) are conventionally selected based on raw material features (cement and

aggregate type and amounts). Although A and B are adopted and only valid for the mix-design being appraised, conventional values of A ranging from 96 to 100 N/mm^2 and B ranging from 7 to 10 can be selected for predicting the 28-day compressive strength of concrete [48].

$$f'_c = \frac{A}{B^{w/c}} \qquad \text{Equation 6.13}$$

where f'_c is the concrete compressive strength at 28-days, w/c is the water to cement ratio, and A and B are empirical constants.

Table 6.6. EN1992-1 parameters of highly packed concrete mixtures.

Mixtures	s	MSE
1H-311-0.68	0.27	1.53
1M-319-0.60	0.21	0.47
1L-328-0.52	0.16	2.48
2H-250-0.68	0.22	1.91
2M-250-0.60	0.38	0.12
2L-250-0.52	0.27	6.69
3H-200-0.83	0.25	1.56
3M-200-0.74	0.27	0.51
3L-200-0.64	0.37	7.82
4H-150-1.09	0.37	0.35
4M-150-0.97	0.39	1.73
4L-150-0.84	0.29	4.54

To appraise the impact of PPMs on Abrams law, Figure 6.12 was developed comparing the studied mixtures based on their cement content and different w/c. Mixtures with 320 kg/m^3 of cement content (G1) showed a compressive strength trend similar to the Abrams law, whereas PPM mixtures without limestone fillers achieved on average 28% higher compressive strength than conventional mixtures. However, PPM mixtures developed with limestone fillers presented a higher trend than

G1 mixtures. One may notice that G2, G3, and G4 may be considered to have a single relationship to w/c regardless of its cement content. However, their percentage increase when compared to conventional mixtures are distinct, being 44%, 60%, and 100% for G2, G3, and G4, respectively. Therefore, one verifies that whenever PPM is used to improve the system packing density, the w/c is not the only parameter affecting the compressive strength and thus, new parameters are needed to fully explain the hardened properties of these systems, which is in agreement with previous studies [7,40,50].

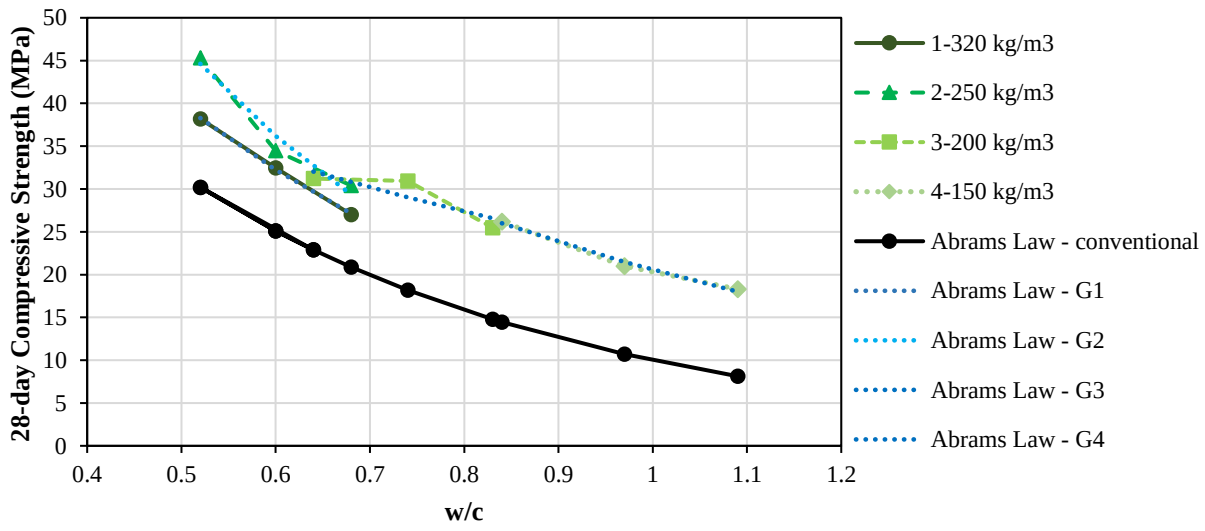

Figure 6.12. 28-day Compressive Strength Correlation with w/c and Conventional Abrams law.

When the Abrams law's parameters (A and B) are adjusted for the analyzed group, a good prediction of the compressive strength can be made through the w/c. Table 6.7, therefore, presents the suggested Abrams law's parameters used for each group using the minimum square error (MSE) method. One can see that A and B parameters are directly affected by the mixture's cement content. Hence, one of the main disadvantages of this method is that previous experimental work of three mixtures with the same mix-design but varying the w/c must be performed to determine Abrams

law's parameters. Furthermore, the same analysis was performed with w/p rather than w/c, as previously proposed by [50]; Table 6.7 are also presented the Abrams law's parameters for this analysis. Although compressive strength can be predicted through w/p with MSE of 0.07, 4.98, 5.46, and 0.51 for G1, G2, G3, and G4, respectively, no direct trend between Abrams law's parameters and cement content is observed.

Table 6.7. Suggested Abrams law parameters of highly packed concrete mixtures.

w/c				
Group	**1-320 kg/m^3**	**2-250 kg/m^3**	**3-200 kg/m^3**	**4-150 kg/m^3**
A=	117.1	173.9	60.0	89.3
B=	8.6	13.7	2.7	4.3
w/p				
Group	**1-320 kg/m^3**	**2-250 kg/m^3**	**3-200 kg/m^3**	**4-150 kg/m^3**
A=	117.1	140.8	55.8	73.9
B=	8.6	18.3	4.0	13.6

Figure 6.13 presents a summary of the predicted compressive strength based on the three abovementioned methods. Notwithstanding the flaws presented in these methods to predict eco-friendly concrete mixtures, one may notice that Eurocode 2 is the best method to predict these mixtures' compressive strength above 7-days. The second-best method is the Abrams law mixtures using w/p, followed by Abrams law mixtures using w/c.

6.6.4 A proposed method to predict compressive strength of eco-efficient concrete mixtures

The discussion in section 8.6.2 highlights the importance of creating a new prediction method to evaluate highly packed systems developed with inert fillers. As the section above illustrated, the sole use of the conventional Abrams law (incorporating the w/c parameter) is not enough to fully understand the behaviour of mixtures proportioned with inert fillers that, although do not hydrate, the filler contribute to compressive strength for two main reasons: 1) more space for hydration

products of cement and 2) more specific surface area for enhancing nucleation sites the filler effect [70]. On the other hand, this study shows that mixtures with the same w/p can achieve distinct compressive strengths, agreeing with previous results [7]. Therefore, to account for both factors (i.e., w/c and w/p), a modified version of Abrams law is proposed in Equation 6.14. One may notice that a k-factor, which is directly proportional to w/p (Equation 6.15) is incorporated into the proposed method to account for the amount of powder in the granular system.

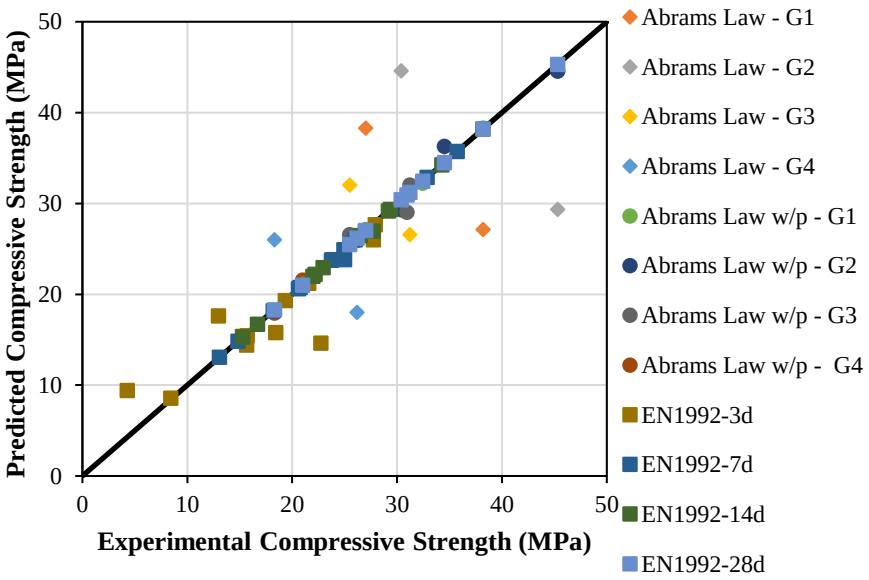

Figure 6.13. Summary compressive strength prediction based on distinct methods.

$$f'c = \frac{78.2}{3.8^{\left(\frac{w}{c}*k\right)}} * \alpha \qquad \text{Equation 6.14}$$

where w/c is the water-to-cement ratio, k is w/p coefficient, α is hydration coefficient (1 = 100% hydrated – 28 days results).

$$k = \left(2.1 * \frac{w}{p}\right)^{0.5} \qquad \text{Equation 6.15}$$

where w/p is the water-to-powder ratio, k is w/p coefficient

Figure 6.14 presented the good correlations between the predicted and the experimental compressive strength. Considering all the mixtures, a total sum of squares error of 152.7, 70.5, 35.7, and 46.9 was obtained for 3, 7, 14, and 28-day results. Based on the cement type used (GU), the hydration coefficient (α) was calculated as 0.60, 0.78, 0.87, and 1 for results at 3, 7, 14, and 28 days, respectively. This model (Equation 6.14) can be applied for distinct cement types by adjusting the α-parameter to account for the cement kinetics.

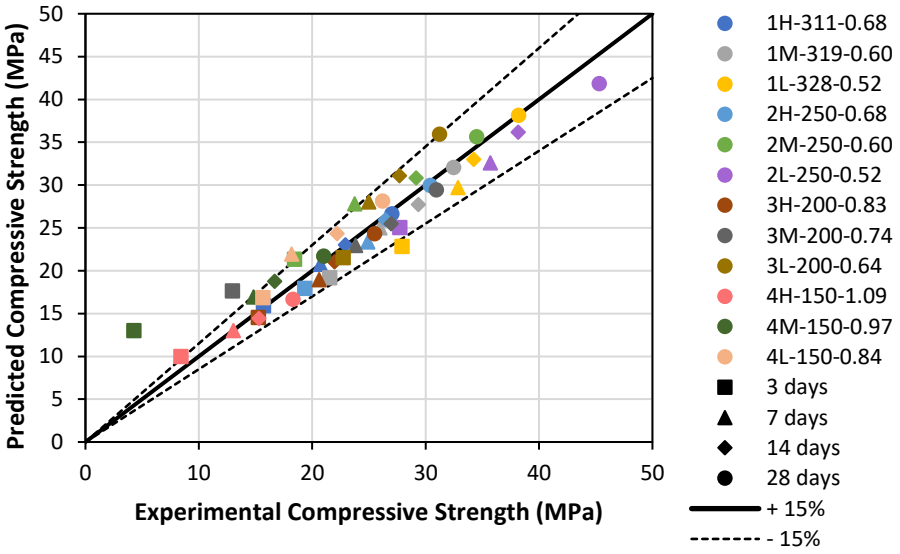

Figure 6.14. Summary of compressive strength prediction based on the proposed method.

From Figure 6.14, one can notice that the model is slightly less precise for 3-day results, which are represented by a squared marker. Nonetheless, mixtures 1L-328-0.52, 3M-200-0.74, and 4M-150-0.97 account for 80% of total sum of squares error, with the latter having the worst correlation between predicted and experimental compressive strength. The model accuracy increases with cement hydration, with most 7-day results presenting a predicted compressive strength that is less than 15% different from the experimental one, except for mixtures 4L-150-0.84 and 2M-250-0.60, which achieved a percentage difference of 21% and 17%, respectively. Moreover, at higher degree

of hydration (14 and 28-day results), all correlations are within the 15% margin. This, therefore, confirms the improvement achieved by the proposed model, while proving the mixtures with low w/c may be near their threshold. Figure 14 results indicate that w/c remains the main factor influencing the compressive strength gain of highly packed, eco-efficient mixtures; however, the use of the proposed method may significantly improve the prediction of the compressive strength at any given age of those sustainable mixtures.

6.7 Conclusions

The current work appraised the feasibility of producing eco-efficient concrete mixtures for distinct fresh state applications (i.e., slumps of 180, 90, and 20 +/- 20 mm) and hardened state requirements (ranging from 18 to 38 MPa) through the proposed Modified-Alfred Model. Based on the results presented in this paper, the main conclusions are:

- The proposed PPM-MP approach is a promising technique to be used to improve the sustainability of concrete mixtures for any required project. Yet, only limestone fillers were used, and further improvements may be achieved with the use of other industry by-products such as SCMs.

- The apparent porosity was a useful tool to evaluate the microstructure of the eco-efficient mixtures. Mixtures 2H-250-0.68, 2M-250-0.60, 3H-200-0.83 and 2M-250-0.60 achieved similar apparent porosity regardless of the cement content and percentage of limestone fillers, hence, it might suggest a threshold value of limestone fillers of 36% when PPM is used.

- The strength predictions for the eco-efficient mixtures achieved better results when adjusting the EN1992-1 and Abrams' law parameters; the former was able to better predict the compressive strength of the eco-friendly mixtures analyzed.

- A new method to predict compressive strength of eco-efficient mixtures is proposed. In general, the w/c direct affects mixtures' microstructure and hardened state properties. Yet, when analyzing highly packed mixtures with high limestone filler content, w/p must be also accounted to better predict compressive strength to improve precision.

- The binder intensity (bi) index was used to evaluate the eco-efficiency of the proposed concrete mixtures used in this study. The use of limestone fillers significantly contributed to the concrete's eco-efficiency, as mixtures with high, medium, and low w/c achieved bi-indices of less than 10 kg/m^3. MPa^{-1}, with the lowest achieved bi-index of 5.9 kg/m^3. MPa^{-1}.

6.8 References

[1] M. Limbachiya, S.C. Bostanci, H. Kew, Suitability of BS EN 197-1 CEM II and CEM V cement for production of low carbon concrete, Constr. Build. Mater. 71 (2014) 397–405.

[2] J. Di Filippo, J. Karpman, J.R. Deshazo, J. Di Filippo, J. Karpman, J.R. Deshazo, The impacts of policies to reduce CO2 emissions within the concrete supply chain, Cem. Concr. Compos. 101 (2019) 67–82. https://doi.org/10.1016/j.cemconcomp.2018.08.003.

[3] W. Schakel, C.R. Hung, L.-A. Tokheim, A. Hammer Strømman, E. Worrell, A. Ramírez, Impact of fuel selection on the environmental performance of post-combustion calcium looping applied to a cement plant, Appl. Energy. 210 (2017) 75–87. https://doi.org/10.1016/j.apenergy.2017.10.123.

[4] H.F. Campos, N.S. Klein, J. Marques Filho, Proposed mix design method for sustainable high-strength concrete using particle packing optimization, J. Clean. Prod. 265 (2020) 1–15. https://doi.org/10.1016/j.jclepro.2020.121907.

[5] P.R. de Matos, R.D. Sakata, L.R. Prudêncio, Eco-efficient low binder high-performance self-compacting concretes, Constr. Build. Mater. 225 (2019) 941–955. https://doi.org/10.1016/j.conbuildmat.2019.07.254.

[6] W. Zuo, J. Liu, Q. Tian, W. Xu, W. She, P. Feng, C. Miao, Optimum design of low-binder Self-Compacting Concrete based on particle packing theories, Constr. Build. Mater. 163 (2018) 938–948. https://doi.org/10.1016/j.conbuildmat.2017.12.167.

[7] M. T. de Grazia, L. F. M. Sanchez, R. C. O. Romano, R. G. Pileggi, M.T. de Grazia, L. Sanchez, R.C.O. Romano, R.G. Pileggi, M. T. de Grazia, L. F. M. Sanchez, R. C. O. Romano, R. G. Pileggi, Investigation of the use of continuous particle packing models (PPMs) on the fresh and hardened properties of low-cement concrete (LCC) systems, Constr. Build. Mater. 195 (2019) 524–536. https://doi.org/10.1016/j.conbuildmat.2018.11.051.

[8] H.F. Campos, N.S. Klein, J. Marques Filho, M. Bianchini, Low-cement high-strength concrete with partial replacement of Portland cement with stone powder and silica fume designed by particle packing optimization, J. Clean. Prod. 261 (2020). https://doi.org/10.1016/j.jclepro.2020.121228.

[9] G. Andrade, G. Puente, D. Andrade, G. De Castro, M. Pepe, R. Dias, T. Filho, Design of structural concrete mixtures containing fine recycled concrete aggregate using packing model, Constr. Build. Mater. 252 (2020) 119091. https://doi.org/10.1016/j.conbuildmat.2020.119091.

[10] M. Anson-Cartwright, Optimization of aggregate gradation combinations to improve concrete sustainability and durability, MASc Thesis, University of Toronto, 2011.

[11] S. Kumar, M. Santhanam, S. Kunar, M. Santhanam, Particle packing theories and their application in concrete mixture proportioning : A review, Indian Concr. J. 77 (2003) 1324–1331.

[12] S.A.A.M. Fennis, J.C. Walraven, Using particle packing technology for sustainable concrete mixture design, Heron. 57 (2012) 73–101.

[13] P. Goltermann, V. Johansen, L. Palbøl, Packing of Aggregates : An Alternative Tool to Determine the Optimal Aggregate Mix, ACI Mater. J. (1997) 435–442.

[14] D. Dinger, J. Funk, Predictive process control of crowded particulate suspensions, 1st ed., New York, 1994.

[15] M.N. Mangulkar, S.S. Jamkar, Review of particle packing theories used for concrete mix proportioning, Int. J. Sci. Eng. Res. 4 (2013) 143–148.

[16] I. Mehdipour, K.H. Khayat, Understanding the role of particle packing characteristics in rheo-physical properties of cementitious suspensions : A literature review, Constr. Build. Mater. 161 (2018) 340–353.

[17] M.T. de Grazia, L.F.M. Sanchez, R.G. Pileggi, Evaluation of the fresh and hardened state properties of low cement content systems, Mag. Concr. Res. 72 (2018) 232–245.

[18] B. Esmaeilkhanian, K.H. Khayat, O.H. Wallevik, Mix design approach for low-powder self-consolidating concrete: Eco-SCC-content optimization and performance, Mater. Struct. 50 (2017) 18. https://doi.org/10.1617/s11527-017-0993-y.

[19] K. Scrivener, F. Martirena, S. Bishnoi, S. Maity, Calcined clay limestone cements (LC3), Cem. Concr. Res. 114 (2018) 49–56. https://doi.org/10.1016/j.cemconres.2017.08.017.

[20] S. Ruan, C. Unluer, Influence of supplementary cementitious materials on the performance and environmental impacts of reactive magnesia cement concrete, J. Clean. Prod. 159 (2017) 62–73. https://doi.org/10.1016/j.jclepro.2017.05.044.

[21] M. C. G. Juenger, R. Siddique, Recent advances in understanding the role of supplementary cementitious materials in concrete, Cem. Concr. Res. 78 (2015) 71–80. https://doi.org/10.1016/j.cemconres.2015.03.018.

[22] F. Pacheco Torgal, S. Miraldo, J.A. Labrincha, J. De Brito, An overview on concrete carbonation in the context of eco-efficient construction: Evaluation, use of SCMs and/or RAC, Constr. Build. Mater. 36 (2012) 141–150. https://doi.org/10.1016/j.conbuildmat.2012.04.066.

[23] J. Zachar, M. Asce, Sustainable and Economical Precast and Prestressed Concrete Using Fly Ash as a Cement Replacement, J. Mat. Civ. Eng. 23 (2011) 789–792.

[24] M.C.G. Juenger, R. Siddique, Recent advances in understanding the role of supplementary cementitious materials in concrete, Cem. Concr. Res. 78 (2015) 71–80.

[25] U.N. Environment, K.L. Scrivener, V.M. John, E.M. Gartner, Eco-efficient cements: Potential economically viable solutions for a low-CO2 cement-based materials industry, Cem. Concr. Res. 114 (2018). https://doi.org/10.1016/j.cemconres.2018.03.015.

[26] K.L. Scrivener, V.M. John, E. Gartner, Eco-efficient cements : Potential economically viable solutions for a low-CO 2 cement-based materials industry, Cem. Concr. Res. 114 (2018) 2–26. https://doi.org/10.1016/j.cemconres.2018.03.015.

[27] S.H. Kang, Y. Jeong, K.H. Tan, J. Moon, High-volume use of limestone in ultra-high performance fiber-reinforced concrete for reducing cement content and autogenous shrinkage, Constr. Build. Mater. 213 (2019) 292–305. https://doi.org/10.1016/j.conbuildmat.2019.04.091.

[28] J.L. Gallias, R. Kara-Ali, J.P. Bigas, The effect of fine mineral admixtures on water requirement of cement pastes, Cem. Concr. Res. . 30 (2000) 1543–1549. https://doi.org/10.1016/S0008-8846(00)00380-X.

[29] E. Berodier, K. Scrivener, Understanding the filler effect on the nucleation and growth of C-S-H, J. Am. Ceram. Soc. 97 (2014) 3764–3773. https://doi.org/10.1111/jace.13177.

[30] A.M. Rashad, S.R. Zeedan, A preliminary study of blended pastes of cement and quartz powder under the effect of elevated temperature, Constr. Build. Mater. 29 (2012) 672–681. https://doi.org/10.1016/j.conbuildmat.2011.10.006.

[31] B. Lagerblad, E. Forssberg, The function of fillers in concrete, Mater. Struct. 37 (2004) 74–81.

[32] M. Cyr, P. Lawrence, E. Ringot, Efficiency of mineral admixtures in mortars: Quantification of the physical and chemical effects of fine admixtures in relation with compressive strength, Cem. Concr. Res. 36 (2006) 264–277. https://doi.org/10.1016/j.cemconres.2005.07.001.

[33] M. Cyr, P. Lawrence, E. Ringot, Mineral admixtures in mortars: Quantification of the physical effects of inert materials on short-term hydration, Cem. Concr. Res. 35 (2005) 719–730. https://doi.org/10.1016/j.cemconres.2004.05.030.

[34] I. Mehdipour, K.H. Khayat, Understanding the role of particle packing characteristics in rheo-physical properties of cementitious suspensions: A literature review, Constr. Build. Mater. 161 (2018) 340–353. https://doi.org/10.1016/j.conbuildmat.2017.11.147.

[35] B. Lothenbach, G. Le Saout, E. Gallucci, K. Scrivener, Influence of limestone on the hydration of Portland cements, Cem. Concr. Res. 38 (2008) 848–860. https://doi.org/10.1016/j.cemconres.2008.01.002.

[36] Joint statement: Canada's Cement Industry and the Government of Canada announce a partnership to establish Canada as a global leader in low-carbon cement and to achieve net-zero carbon concrete - Innovation, Science and Economic Development Canada, (n.d.). https://www.ic.gc.ca/eic/site/icgc.nsf/eng/07730.html (accessed March 17, 2022).

[37] Global Cement and Concrete Association, Our path to net zero, (2022). https://gccassociation.org/concretefuture/our-path-to-net-zero/ (accessed March 17, 2022).

[38] A.K.H. Kwan, K.W. Chan, V. Wong, A 3-parameter particle packing model incorporating the wedging effect, Powder Technol. 237 (2013) 172–179. https://journals-scholarsportal-info.proxy.bib.uottawa.ca/pdf/00325910/v237icomplete/172_a3ppmitwe.xml (accessed September 26, 2019).

[39] T. Baghaee Moghaddam, H. Baaj, Application of compressible packing model for optimization of asphalt concrete mix design, Constr. Build. Mater. 159 (2018) 530–539.

[40] S.A.A.M. Fennis, J.C. Walraven, J.A. den Uijl, Compaction-interaction packing model: regarding the effect of fillers in concrete mixture design, Mater. Struct. 46 (2013) 463–478. https://doi.org/10.1617/s11527-012-9910-6.

[41] J.E. Funk, D.R. Dinger, Predictive process control of crowded particulate suspensions, 1st ed., New York, 1994. https://doi.org/10.1007/978-1-4615-3118-0.

[42] R. Yu, P. Spiesz, H.J.H. Brouwers, Mix design and properties assessment of Ultra-High Performance Fibre Reinforced Concrete (UHPFRC), Cem. Concr. Res. 56 (2014) 29–39. https://doi.org/10.1016/j.cemconres.2013.11.002.

[43] F. De Larrard, A. Belloc, The influence of aggregate on the compressive strength of normal and high-strength concrete, ACI Mater. J. 94 (1997) 417–426.

[44] H.R. Shadkam, S. Dadsetan, M. Tadayon, L.F.M. Sanchez, A. Zakeri, An investigation of the effects of limestone powder and Viscosity Modifying Agent in durability related parameters of self-consolidating concrete (SCC), Constr. Build. Mater. 156 (2017) 152–160.

[45] M. Grazia, L.F.M. Sanchez, R. Romano, R.G. Pileggi, M.T. de Grazia, L.F.M. Sanchez, R. Romano, R.G. Pileggi, M. T. de Grazia, L. F. M. Sanchez, R. C. O. Romano, R. G. Pileggi, Evaluation of the Fresh and Hardened State Properties of Low-Cement Content (LCC) Systems, Mag. Concr. Res. 72 (2018) 1–14. https://doi.org/10.1680/jmacr.18.00271.

[46] R.C.D.O. Romano, D. Dos, R. Torres, R.G. Pileggi, Impact of aggregate grading and air-entrainment on the properties of fresh and hardened mortars, Constr. Build. Mater. 82 (2015) 219–226.

[47] I.R. Oliveira, A.R. Studart, R.G. Pileggi, V.C. Pandolfelli, Dispersão e Empacotamento de Partículas, Fazendo Arte Editorial, São Paulo, 2000.

[48] R. Kurda, A. Salih, P. Shakor, P. Saleh, R. Alyousef, H. Ahmed, F. Aslanif, Mix design of concrete: Advanced particle packing model by developing and combining multiple frameworks, Constr. Build. Mater. 320 (2022). https://doi.org/10.1016/j.conbuildmat.2021.126218.

[49] Z.S. Ali, M. Hosseinpoor, A. Yahia, New aggregate grading models for low-binder self-consolidating and semi-self-consolidating concrete (Eco-SCC and Eco-semi-SCC), Constr. Build. Mater. 265 (2020) 120314. https://doi.org/10.1016/j.conbuildmat.2020.120314.

[50] V.M. John, B.L. Damineli, M. Quattrone, R.G. Pileggi, Fillers in cementitious materials — Experience, recent advances and future potential, Cem. Concr. Res. 114 (2018) 65–78. https://doi.org/10.1016/j.cemconres.2017.09.013.

[51] V. Bonavetti, H. Donza, G. Menéndez, O. Cabrera, E.F. Irassar, Limestone filler cement in low w/c concrete: A rational use of energy, Cem. Concr. Res. 33 (2003) 865–871. https://doi.org/10.1016/S0008-8846(02)01087-6.

[52] T. Matschei, B. Lothenbach, F.P. Glasser, The role of calcium carbonate in cement hydration, Cem. Concr. Res. 37 (2007) 551–558. https://doi.org/10.1016/j.cemconres.2006.10.013.

[53] T.E. Oey, A. Kumar, J.W. Bullard, N. Neithalath, G. Sant, The Filler Effect: The Influence of Filler Content and Surface Area on Cementitious Reaction Rates, J. Am. Ceram. Soc. 96 (2013) 1978–1990. https://doi.org/10.1111/jace.12264.

[54] C. Varhen, I. Dilonardo, C. Romano, R.G. Pileggi, A. Figueiredo, Effect of the substitution of cement by limestone filler on the rheological behaviour and shrinkage of microconcretes, Constr. Build. Mater. 125 (2016) 375–386.

[55] M.T. De Grazia, L. Sanchez, R.C.O. Romano, R.G. Pileggi, Investigation of Alfred Model Effect on the Fresh and Hardened State Properties of Low-Cement Content (LCC) Systems, Constr. Build. Mater. Accepted (2017) 1–26.

[56] Y.-Y. Chen, B. Le, A. Tuan, C.-L. Hwang, Effect of paste amount on the properties of self-consolidating concrete containing fly ash and slag, Constr. Build. Mater. 47 (2013) 340–346.

[57] B.L. Damineli, F.M. Kemeid, P.S. Aguiar, V.M. John, Measuring the eco-efficiency of cement use, Cem. Concr. Compos. 32 (2010) 555–562.

[58] ACI Committee 211, Standard Practice for Selecting Proportions for Normal Heavyweight , and Mass Concrete (ACI 211 . 1-91) Reapproved 2002, 2004.

[59] CSA A23.1-14/A23.2-14, Concrete Materials and Methods of Concrete Construction/Methods of Test and Standard Practices for Concrete, 2014.

[60] ASTM C136, Standard test method for sieve analysis of fine and coarse aggregates., (2016) 8.

[61] H.F.W. Taylor, Cement chemistry, Thomas Telford Publishing, 1997. https://doi.org/10.1680/cc.25929.

[62] ASTM C39, Standard Test Method for Compressive Strength of Cylindrical Concrete Specimens, 1999.

[63] P. Banfill, D. Beaupré, F. Chapdelaine, F. de Larrard, P. Domone, L. Nachbaur, T. Sedran, O. Wallevik, J.E. Wallevik, Comparison of concrete rheometers: international tests at LCPC (NISTIR 6819), Nantes, France, 2000.

[64] C. Ferraris, L. Brower, Comparison of Concrete Rheometers: International Tests at MB, (2003) 116.

[65] ASTM C469, Standard Test Method for Static Modulus of Elasticity and Poisson’s Ratio of Concrete in Compression, 2017.

[66] B.L. Damineli, V.M. John, Developing Low CO2 Concretes: Is Clinker Replacement Sufficient? The Need of Cement Use Efficiency Improvement, in: Key Eng. Mater. Trans Tech Publ., 2012: pp. 342–351.

[67] F. Pelisser, A. Vieira, A.M. Bernardin, Efficient self-compacting concrete with low cement consumption, J. Clean. Prod. 175 (2018) 324–332. https://doi.org/10.1016/j.jclepro.2017.12.084.

[68] A.M. Neville, Properties of Concrete, 5th ed., Pearson Education Limited, 2011.

[69] P.J.M. Monteiro, P.R.L. Helene, S. Kang, Designing concrete mixtures for strength, elastic modulus and fracture energy, Mater. Struct. 26 (1993) 443–452.

[70] B. Lothenbach, K. Scrivener, R.D. Hooton, Cement and Concrete Research Supplementary cementitious materials, Cem. Concr. Res. 41 (2011) 1244–1256. https://doi.org/10.1016/j.cemconres.2010.12.001.

Chapter Seven: Performance appraisal of eco-efficient low-alkali concrete to develop alkali-aggregate reaction (AAR) in the laboratory

De Grazia, M. T.[a], Trottier, C.[a], Sanchez, L. F. M.[b]

[a] Ph.D. Candidate – University of Ottawa, Department of Civil Engineering, ON, Canada.

[b] Associate Professor – University of Ottawa, Department of Civil Engineering, ON, Canada.

Abstract

Although eco-efficient mixtures proportioned through a coupled particle packing models (PPMs) – mobility parameters (MP) approach demonstrated suitable performance in the fresh and short-term hardened state, further studies are still required to assess their durability and long-term aspects. This work evaluates the performance of four eco-efficient mixtures proportioned with varying cement contents (325, 250, 200, and 150 kg/m^3) against one of the leading causes of premature deterioration of concrete infrastructure worldwide: alkali-silica reaction (ASR). Specimens from the above mixtures along with a control mixture containing 420 kg/m^3 were manufactured incorporating two distinct types of highly reactive aggregates (Springhill coarse aggregate and Texas sand) and stored in conditions enabling ASR-induced development (38°C and 100% R.H.); the specimens were monitored over time and microscopic analysis was performed to better understand ASR-induced deterioration in these mixtures. Results show the potential to reduce ASR-expansion with the use of PPM-MP approach.

Keywords: *Eco-efficient concrete, low cement content, particle packing models, alkali-aggregate reaction (ASR), microscopic characterization, crack propagation, damage rating index (DRI).*

7.1 INTRODUCTION

The global cement and concrete industries' goal to achieve Concrete Net Zero by 2050 has prompted sustainability commitments to aim for a minimum reduction of 15MTs in greenhouse gases (GHG) by 2030 [1,2]. Thus, the construction industry has shifted its main emphasis to reducing CO_2 emissions during concrete production while maintaining its fresh and hardened state performance. Considering that cement is responsible for 92% of the total CO_2 emitted during concrete production, it is evident that efforts to reduce its overall use in concrete will reduce GHG [3–6]. As such, past investigations confirmed that eco-efficient mixtures may be produced through the use of Portland cement replacements, such as supplementary cementitious materials (SCMs) or inert fillers [4,7–12]; likewise, other researchers demonstrated the possibility of decreasing cement content by using advanced mix-design techniques, such as particle packing models (PPMs) [6,9,13–18]. Besides the sustainability benefits of reducing cement and using industry by-products (i.e., SCMs and inert fillers) through PPMs, optimizing concrete's mix-design may also improve its durability and long-term performance, which in turn reduces the potential of a shortened service life. Such improvements correspond to the enhancement of the system's granular skeleton by reducing concrete's porosity [19,20]. Although such improvement may enhance concrete performance against distinct deterioration mechanisms (i.e., carbonation, corrosion, freezing and thawing, etc.), the durability behavior of eco-efficient concrete is not yet fully investigated. Reducing the cement content of concrete to improve its sustainability decreases the system's pH, which may diminish its ability to control corrosion of steel reinforcement with the protective layer formed at high pH levels. On the other hand, the low porosity levels of eco-efficient mixtures developed with PPM may actually improve concrete's resistance to carbonation. Decreasing cement (and thus alkalis) content can also be advantageous when the concrete bears reactive aggregates against the development of

alkali-silica reaction (ASR). ASR, one of the most harmful deterioration mechanisms affecting concrete structures around the globe, is a chemical reaction between the alkalis from the concrete's pore solution (Na^+, K^+ and OH^-) and some unstable mineral phases found within the aggregates; this reaction generates a secondary product (i.e., alkali silica gel) which swells upon moisture uptake, leading to induced expansion and cracking of the affected concrete. ASR-induced cracks are primarily formed within the reactive aggregates particles and then run to the cement paste, linking to one another, and negatively impacting the mechanical properties and physical integrity of affected concrete [21–26]. Despite the fact that several studies show that ASR can be prevented or at least partially mitigated with the use of SCMs [23,27–29], only a few studies focus on the mitigation of ASR-induced development through the alkali control in the system [30–33]. This work aims to evaluate the performance of eco-efficient low-alkali concrete, proportioned through PPMs and incorporating inert fillers, against alkali-aggregate reaction (AAR) induced development in laboratory conditions.

7.2 BACKGROUND

7.2.1 Eco-efficient concrete

The concrete industry's shift towards lowering GHG has added sustainability as a target criteria which can be measured by *Global Warming Potential* [34–38], *Binder Intensity Index* [39], and *Low Carbon Concrete Classes* [40]; the first being the most commonly used in the industry. As such, conventional concrete mixtures, designed for 25-40 MPa compressive strength, are usually produced with cement contents ranging from 250 kg/m^3 to 500 kg/m^3 [39,41], resulting in a GWP higher than 300 kg CO_{2eq} per cubic metric of concrete produced [36] (i.e., cement content of 300 kg/m^3) thus, considered unsustainable. Yet, less than 5% of the regularly used concrete mixtures globally have cement contents lower than 250 kg/m^3 [39]. Previous studies, therefore, support the

effectiveness of employing a Particle Packing Model (PPM) to create more sustainable concrete [9,14,15,18,42]. However, conventional mix-design methods still rely on empirical models despite the fact that particle packing science and the corresponding development of such mathematical models began in the late 1800s. Naturally, PPM has advanced over time [19,20,42–45], with the most recent models being the modified Andreasen (also known as Alfred model) and the Compressive Packing Model which have been observed to perform better in terms of system durability and sustainability [34,35] compared to conventional concrete and previous PPMs. The modified Andreasen or Alfred model is a continuous PPM where all particle sizes are considered without any gaps throughout the particle size distribution and can be calculated using Equation 7.1.

$$CPFT = 100 * \left(\frac{{D_P}^q - {D_S}^q}{{D_L}^q - {D_S}^q} \right) \quad \text{Equation 7.1}$$

where D_P is the particle size in question, CFPT is the cumulative percent finer than D_P, D_L and D_S is the largest and smallest particle size in the system, respectively, and q is a distribution factor (q-factor).

Alternatively, the Compressive Packing Model is a discrete PPM that considers distinct particle size classes and can be applied using software such as Betonlabpro and RENE LCPC [46].

The primary objectives of PPMs, regardless of the type selected, are to enhance the system's packing density thus, decrease its porosity by reducing the voids between the fine and coarse aggregate which are filled with water and powders (i.e., fillers and binders). Along with the eco-efficient characteristic of concrete mixtures proportioned through PPMs, the porosity reduction leads to increase in the material's durability [19,47]. Indeed, further improvements in the material's eco-

efficiency and porosity can be achieved by partially replacing Portland cement with other powders, such as supplementary cementitious materials (SCMs) or limestone fillers [4,7–12,48].

7.2.2 Assessing AAR-induced expansion and deterioration in the laboratory

A number of test procedures have been developed, studied, and standardized over the last decades to appraise the potential reactivity performance of aggregates in the laboratory; amongst those, one may say that the accelerated mortar bar test - AMBT (ASTM C1260) and the concrete prism test - CPT (ASTM C1293) are currently the most used worldwide. Both have advantages and disadvantages; the AMBT test appraises the potential reactivity of aggregates and the efficiency of preventive measures against ASR-induced development in the laboratory. It is a fast test procedure, taking only 16 days for analysis. However, it has been found that false negatives and or positives may be encountered in this test due to its extremely aggressive environment (1M NaOH at 80 ºC) and or process (aggregates crushing to sand fractions) [49]. Otherwise, the CPT is the most reliable test procedure currently used to appraise the reactivity of aggregates and assess the efficiency of preventive measures against ASR. It is considered a reliable procedure since concrete specimens are manufactured and stored under conditions closer to the field (100% RH and 38ºC) [50]. However, it is a time-consuming procedure taking 1 year for assessing the reactivity of aggregates and 2 years to appraise the efficiency of preventive measures. Moreover, it has been found that induced expansion results obtained through this the CPT in the laboratory are often lower to similar concrete mixtures exposed to field conditions due to the important amount of leaching happening over the test [31,33,50]. To minimize leaching, concrete mixtures fabricated and tested in the CPT must be boosted to 40% of the cement alkalis, which is often the amount of leaching observed during a 1-year test [33,51–54]. For instance, when a cement with Na_2O_{eq} of 0.90% is selected, the concrete mixtures must be boosted to 1.25% Na_2O_{eq} to meet the additional 40% of alkalis. Although this

action can overcome leaching issues on conventional concrete, this measure poses problems to assess the performance of eco-efficient low-alkali systems in the laboratory [33,54].

7.2.3 Preventing alkali-silica reaction (ASR)

One alternative to preventing ASR-development is through the reduction of concrete alkali loading by decreasing the cement content or using SCMs that reduce the system's total alkali content. Reactive aggregates may be used in conjunction with this strategy, according to standards such as CSA A23.2-27A, where a minimum percentage of SCMs (by mass of total cementitious materials) is recommended, based on the total alkali content (Na_2O_{eq}) of the system (PC + SCMs) and the required prevention level [28–31,50,51]. According to CSA A23.2-27A recommendations (Table 7.1), deleterious ASR can be mitigated when the system's total alkali content contributed by the Portland cement is less than 3.0 kg/m^3, 2.4 kg/m^3, 1.8 kg/m^3, and 1.2 kg/m^3 for the prevention levels of W (mild), X (moderate), Y (strong), and Z (very strong), respectively.

Fournier et al. [55] evaluated ASR-induced development of concrete mixtures incorporating a variety of reactive fine and coarse aggregates and two alkali loadings (boosted - total alkali content of 5.25 kg/m^3 and unboosted - total alkali content of 3.78 kg/m^3). Regardless of the aggregate reactivity, the boosted mixtures resulted in greater expansions over time due to the higher alkali content of the system. Yet, the aggregate type and nature presented a significant impact on the expansion development of concrete containing various amounts of alkalis. When incorporating ultra high/very high, high, and moderate/marginal reactive aggregates, mixtures developed with an alkali content of 3.78 kg/m^3 (unboosted) achieved on average 18%, 27%, and 43% lower expansion than conventional CPT mixtures (boosted mixtures) [55].

Table 7.1. ASR-expansion levels classification [26]**.**

Degree of damage [26]	**Range of expansion level (% at one year)** [26]	**Prevention level (CSA A23.2-27A)**	**System's total alkali content (kg/m^3) contributed by the Portland cement (CSA A23.2-27A)**
Negligible	0.00 to 0.03	-	-
Marginal	0.05 to 0.10	Mild – W	3.0
Moderate	0.11 to 0.19	Moderate – X	2.4
High	0.20 to 0.29	Strong – Y	1.8
Very high	0.30 to 0.50	Very Strong -Z	1.2
Ultra high	≥ 0.50		

Einarsdottir and Hooton [33] also tested low-alkali concrete mixtures under conventional and modified CPT conditions to reduce leaching. After two years of testing, mixtures developed with 100% Portland cement (alkali content ranging from 3.35 to 6.06 kg/m^3) leached 25-50% of alkalis, whereas low-, medium- and high-alkali mixtures made with 15% to 50% SCMs leached between 18% and 32%. Thus, it was recommended to keep adding 40% of alkalis to CPT mixtures, particularly for low-alkali systems, to counteract leaching effects and thus low induction expansion in the laboratory.

7.2.4 Microscopic tools used to assess damage in damaged concrete

ASR-damage is frequently associated with the presence of cracks in concrete [21,25]. The Damage Rating Index (DRI) is a semi-quantitative (and qualitative by nature) microscopic tool developed to assess the type of damage and its extent in conventional concrete using a stereomicroscope (approximately 15-16x magnification) [25,26]. Petrographic distress features, such as cracks in the aggregate and cement paste, are counted in 1 cm^2 squares at the surface of a polished concrete section. Weighting factors, further modified by Villeneuve and Fournier [56] (shown in Table 7.2), are applied to the crack counts to balance the importance of each type of crack based on the observed distress mechanism. Closed cracks in aggregate (CCA) are given the lowest weighting factor (i.e.,

0.25) since such cracks may be a result of rock formation/weathering and/or aggregate processing. While less likely to be associated with ASR, CCA may become opened due to ASR as they can serve as 'fast-track channels' to the reactive minerals. As such, open cracks in the aggregate without and with gel (OCA and OCAG, respectively) present a higher degree of damage and have a weighing factor of 2. At higher ASR expansion/damage levels, the cracks extend from the aggregates to the cement paste, hence, these petrographic distress features are classified with a higher weighting factor of 3, representing the severity of such cracks which are not limited to ASR [57–59]. For comparison purposes, the final DRI number is the sum of the weighted counts normalized to 100 cm^2. In summary, the higher the expansion, the greater the DRI number following an almost linear correlation. Moreover, studies [21,60] have proposed using an extended version of the DRI (i.e., without applying weighting factors) to evaluate crack propagation and distribution within an affected concrete.

Table 7.2. DRI weighing factors for ASR-affected concrete [56]**.**

Petrographic Features	Weighing Factor
Closed Cracks in Aggregate (CCA)	0.25
Opened Cracks in Aggregates (OCA)	2
Crack With Reaction Product in Coarse Aggregate (OCAG)	2
Coarse Aggregate Debonded (CAD)	3
Disaggregate/Corroded Aggregate Particle (DAP)	2
Cracks in Cement Paste (CCP)	3
Cracks with Reaction Product in Cement Paste (CCPG)	3

The level of concrete expansion is an important parameter to consider when analyzing ASR-affected specimens as it is frequently associated with concrete degree of damage. Sanchez et al. [25] proposed a general qualitative model of crack propagation for conventional ASR-affected concrete based on distinct expansion levels. The cracks can be classified based on two patterns either sharp type cracks

(A) and/or onion skin type cracks (B) as illustrated in Figure 7.1. The increase in concrete expansion may indicate the stage of ASR-development, where at higher stages, the crack within the aggregates begins to propagate and reach the cement paste, thus lowering of mechanical properties of the concrete [48,58,61].

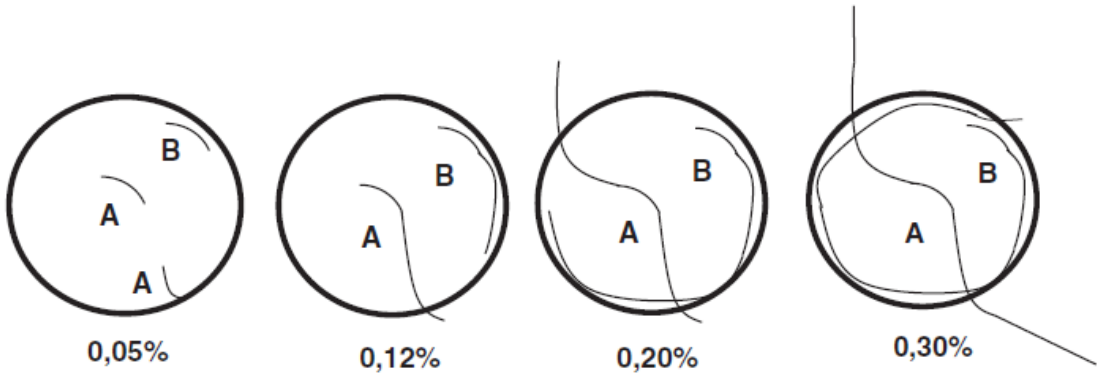

Figure 7.1. Qualitative model of ASR crack propagation over distinct expansions level [25]**.**

Although Sanchez et al. [58] have extensively evaluated a wide range of aggregate types through the DRI, all mixtures exhibit the same alkali loadings (boosted with alkalis) as per ASTM C1293 [50], where the amount of equivalent alkalis in the cement (Na_2O_{eq}) was increased to 1.25 kg/m^3 (i.e. 5.25 kg/m^3 of alkalis in the concrete mix) by adding NaOH to the mixing water. Therefore, the development of the ASR-induced cracks in more sustainable low alkali systems was neither investigated nor correlated with expansion over previous works.

7.3 SCOPE OF THE WORK

Some authors investigated the effect of ASR-induced expansion and damage on low cement (and alkali) mixtures [23,27–29]; however, there are very few results (if any) in the literature on mixtures proportioned with PPMs incorporating inert fillers and highly reactive coarse and or fine aggregates. Moreover, very few studies can be found in the literature that evaluate low alkali systems without

the use of SCMs [30–33]. Therefore, this study aims to appraise the performance of eco-efficient low alkali concrete proportioned through PPMs and incorporating inert fillers against ASR-induced development in the laboratory. Two highly reactive aggregates, a coarse (i.e., Springhill – greywacke) and fine (i.e., Texas – natural sand) were selected for the study. Four distinct types of eco-efficient mixtures were developed using the reactive Springhill coarse aggregate containing distinct cement content ranges (i.e., 325, 250, 200, 150 kg/m^3), while two sustainable mixtures (i.e., 325 and 250 kg/m^3) incorporating the reactive Texas sand, both of which were proportioned using the proposed modified-Alfred-model. Moreover, two types of limestone fillers (performance filler, with a lower PSD than OPC, used to reduce the paste porosity and replacement filler, with a similar PSD than OPC, to reduce cement content) were incorporated into the mixtures to further enhance their eco-efficiency. Specimens were fabricated from all the above mixtures and were then subjected to conditions enabling ASR (i.e., 38°C and 100% R.H. as per ASTM C1293 [50]) and compared to control mixtures developed with 420 kg/m^3, as per ASTM C1293 [50]. Evaluation of induced expansion and mass change over time was performed, along with a thorough assessment of crack generation and propagation through the Damage Rating Index (DRI) conducted on samples from all mixtures. Finally, analysis of the surface electrical resistivity and porosity are also performed and used to further evaluate the microstructure of the mixtures and damage induced by ASR.

7.4 MATERIALS AND METHODS

7.4.1 Raw materials characterization

The concrete mixtures investigated in this study were developed with two distinct types of reactive aggregates: 1) a highly reactive coarse aggregate – Springhill and 2) a highly reactive fine aggregate – Texas, combined with non-reactive natural sand and a granite coarse aggregate with a maximum nominal size of 19 mm, respectively. To improve the mixtures sustainability, two types of limestone

fillers were also used in the mixtures: 1) a performance (P) filler and 2) a replacement filler (R) having a particle size distribution smaller than and similar to that of the Portland cement used in this study, respectively. The particle size distribution of the aggregates was determined through sieve analyses as per ASTM C136 [62], whereas for the limestone filler and Portland cement, a laser diffraction analysis was performed (Figure 7.2). The materials' specific gravity and absorptions are presented in Table 7.3.

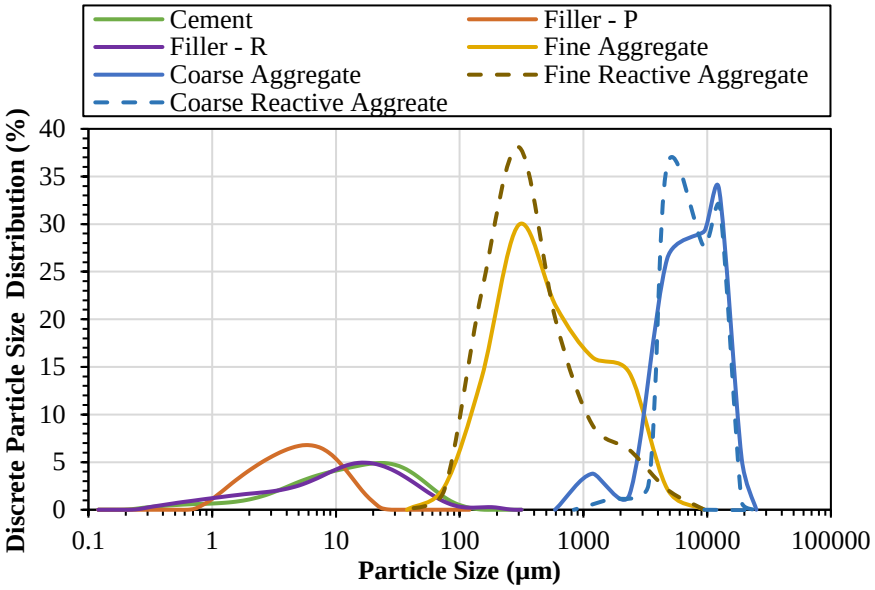

Figure 7.2. Particle size distribution of raw materials.

To improve the flowability of the sustainable concrete mixtures, a polycarboxylate-based high-range water reducer and a lignosulfonate-based mid-range plasticizer were used when necessary. Inductively Coupled Plasma (ICP) analysis was performed and the Na_2O_{eq} of the admixtures were found to be 0.19% and 0.88%, respectively, which can be considered a low alkali content contributing to 2 and 11 g, respectively, per cubic meter of concrete and thus causing not much impact to ASR development, as previously investigated by Leemann et al. [63] on concrete mixtures incorporating polycarboxylate-based superplasticizer that contributes to 17 g/m^3 of concrete.

Table 7.3. Physical properties characterization.

Material	Location	Rock type	Specific gravity (g/cm^3)	Absorption (%)	CPT- 365 days, expansion (%)
General Use (GU) cement	Saint-Basile, Quebec (Canada)	-	3.17	-	
Filler - R	Ottawa, Ontario (Canada)	Limestone	2.66	-	
Filler - P	Ottawa, Ontario (Canada)	Limestone	2.60	-	
Non-reactive Fine Aggregate	Bracebridge, Ontario (Canada)	Orthoclase, Quartz, Cristoballite, Albite, Bytowmite, Cordierite, Illite, Muscovite, Larnite	2.74	0.37	0.0177
Fine Reactive Aggregate (Texas -T)	El Paso, Texas (USA)	Polymictic sand (granites, mixed volcanic, quartzite, chert, quartz) [25]	2.59	0.78	
Non-Reactive Coarse Aggregate	Bracebridge, Ontario (Canada)	Granite	2.81	0.71	0.0189
Coarse Reactive Aggregate (Springhill - S)	Fredericton, New Brunswick (Canada)	Greywacke	2.68	0.89	

7.4.2 Mix-design procedure – modified-Alfred model

The eco-efficient concrete mixtures developed in this study were designed through a proposed modified Alfred model selected as per previous studies [64,65]. A high distribution factor (i.e., q-factor) of 0.37 was selected since it provides eco-efficient mixtures with the lowest dry-porosity (2.8% for a q-factor of 0.37). Yet, to overcome issues in the fresh state when selecting such q-factor, the Alfred model particle size distribution range was divided (or broken) into two parts: powder portion (from D_s to 80 μm) and aggregate portion (from 80 μm to D_l) as per [15]. It is worth noting that 80 μm represents the largest diameter available within the powders selected (i.e., Portland cement, replacement and performance limestone fillers). Moreover, to achieve the lowest system porosity with a broken Alfred model, q-factors of 0.34 and 0.31 ±0.1 in the powder and aggregate portion, respectively, were selected, yielding a system with a dry porosity of 3.0% ±0.1 (calculated

through Westman and Hugill algorithm). The least square method was then applied to calculate the optimum amount of performance filler (P) based on the 0.34 q-factor curve of the powder.

Table 7.4 presents the four sustainable mixtures developed with the PPM-method (i.e., 2C-325P, 3C-250P, 4C-200P, and 5C-150P). Additionally, a control mixture was developed with a cement content of 420 kg/m^3, as per ASTM C1293 [50]). All mixtures used a Portland cement (CSA Type GU, ASTM Type 1) with a high alkali content (i.e., 0.86% $Na_2O_{eq.}$) and the total alkali content was boosted by 40% raising the system's $Na_2O_{eq.}$using reagent grade sodium hydroxide pellets to accelerate ASR development. The superplasticizer and mid-range admixture alkali contents were considered negligible, due to their average $Na_2O_{eq.}$contribution of 0.002 kg/m^3 and 0.011 kg/m^3, respectively, when compared to the total alkali content contribution from the cement and added sodium hydroxide. It is also worth noting that 2C-325P is the only PPM mixture without limestone fillers, whereas the other three mixtures were developed with the optimum amount of performance fillers (~ 1.9% of total concrete dry volume) and three distinct amounts of replacement filler (~ 1.2, 3.2, and 5.1% of total concrete dry volume) to achieve cement contents of 250, 200, and 150 kg/m^3, respectively.

Furthermore, all mixtures had the same mortar factor of 61%. The concrete mixtures were named based on the amount of cement and mix-design (i.e., A: ACI method and P: PPM method), with the label 1C containing more cement and the label 5C containing less cement (e.g., 1C-420-A and 5C-150-P)To represent the Springhill and Texas reactive aggregate incorporated into the mixtures, letters S or T, respectively, are added to the mixture's name in the results and discussion sections. A summary of the CPT mixtures' alkali contents are shown in Table 7.5

Table 7.4. Mix-design of eco-efficient concrete mixtures selected to be evaluated for long-term performance.

Mix-name	kg/m³													
		Powder		Fine Aggregate					Coarse Aggregate					
	OPC	Filler P	Filler R	150-300 mm	300-600 mm	600-1180 mm	1180-2360 mm	2360-4750 mm	4750-9500 mm	9500-12500 mm	12500-19000 mm	Water	SP	MR
1C-420A	420	0	0	860	0	0	0	0	311	302	302	189	0	0
2C-325P	325	0	0	132	163	197	250	313	376	173	293	179	1.9	1.9
3C-250P	250	41	33	137	170	205	260	326	392	180	306	145	3.9	3.2
4C-200P	200	42	81	141	174	210	267	334	402	184	313	124	0	0
5C-150P	150	42	122	144	177	213	268	333	397	182	308	126	0	0

Note: labels #C represents the cement content of the mixture, A represents the ACI mix-design method, P represents the PPM mix-design method, OPC stands for ordinary Portland cement, SP stands for Superplasticizer and MR stands for mid-range admixture.

Table 7.5. Total, initial and added alkalis of CPT-mixtures with 40% boosting of alkalis.

Mixture	Concrete total alkali content (kg/m³)	Cement alkali content (kg/m³)	Amount of alkali added for boosting (kg/m³)
1X-420A-Y-Z	5.06	3.61	1.44
2X-325P-Y-Z	3.91	2.79	1.12
3X-250P-Y-Z	3.01	2.15	0.86
4X-200P-Y-Z	2.41	1.72	0.69
5X-150P-Y-Z	1.81	1.29	0.52

7.4.3 Fabrication of concrete specimens

A total of 120 cylinders (100 mm diameter x 200 mm length) were fabricated in the laboratory to test concrete made with a reactive coarse aggregate, whereas 72 cylinders were manufactured to assess the ASR development of a reactive fine aggregate. The specimens were then left to moist-cure (i.e., 20°C and 100% RH) for 24 hours, demoulded and moist-cured under the same conditions for an additional 24 hours after which small holes of 8.5 mm in diameter and 19 mm in length were drilled into both ends of the cylinders in preparation for stainless steel stud installation used for longitudinal expansion measurements. The studs were glued to each end of the cylinder with a fast-setting cement paste slurry, and left to moist-cure under the same aforementioned conditions for 24 hours. Initial measurements (i.e., “0” readings) were performed between 24 and 48 hours after the studs were installed. Then, the specimens were stored in conditions to accelerate ASR induced

expansion (i.e., 38°C and 100% RH) as per ASTM C1293 [50] and monitored over time (i.e., mass change and longitudinal expansion measurements).

7.4.4 Experimental procedures

7.4.4.1 Surface electrical resistivity and apparent porosity

In addition to the mass change and longitudinal expansion measurements, the surface electrical resistivity was used to evaluate the inner quality [66] and durability performance [67] of eco-efficient concrete mixtures subjected to ASR over the course of a year. The electrical resistivity was therefore performed using the four-probe (Wenner-array) technique with a commercially available device that automatically displays the surface electrical resistivity (i.e., measured through four equipment probes).

The apparent porosity was performed based on Archimedes immersion method [68] to initially evaluate the inner quality of the concrete mixtures followed by the influence of ASR over time. The initial apparent porosity was determined at 28 days (i.e., stored in conditions without enabling ASR as per [58] while all other apparent porosity measurements were performed every four months until one year was reached. One specimen of each mixture was cut axially into three, forming slices of approximately 100 mm in diameter and 65 mm in height. The slices were placed in an oven at 60°C, avoiding the decomposition of cement hydration products caused by excessive temperature, until mass stabilization which occurred after 4 days of drying. The specimens' dry mass (m_d) was determined when the difference between two successive weights was less than 0.3; previous trials were performed to conclude that 0.3% of mass change results in an apparent porosity difference smaller than 10%. The slices were then immersed in water and subjected to vacuum ensuring water

penetration. After 24 hours of immersion, while maintaining vacuum, the immersed (m_i) and wet (m_w) mass values were determined. The apparent porosity (AP) was calculated using Equation 7.2.

$$\text{AP}\ (\%) = \frac{m_w - m_i}{m_w - m_d} * 100\% \qquad \text{Equation 7.2}$$

7.4.4.2 The damage rating index (DRI)

The Damage Rating Index (DRI) is a semi-quantitative, and qualitative in nature, a microscopic tool developed to assess the cause and extent of ASR damage in conventional concrete [25,26]. Concrete cylinders were cut axially in half using a masonry saw equipped with a notched diamond blade followed by successive grinding and polishing using a mechanical rotating steel wheel upon which magnetic grinding and polishing disks are attached whose grits are 30, 60, 140, 280 (80-100 µm), 600 (20-40 µm), 1200 (10-20 µm) and 3000 (4-8 µm). Once a flat and reflective surface was achieved, the DRI was performed using a stereomicroscope at 16x magnification and distress features (i.e., cracks) associated with ASR damage were counted in a grid of 1 cm^2 squares placed on the surface of the polished concrete section. Weighting factors are then applied to the observed distress features to balance their importance based on the distress mechanism appraised [56]. The final DRI number is thus the sum of the weighted values normalized to 100 cm^2 for comparative purposes. Moreover, the extended version of the DRI as per Sanchez et al. was used to further investigate the crack distribution and characteristics for each mixture affected by ASR through the microscopic features as counts per 100 cm^2 and their proportions (%) as well as the crack density (i.e., the sum of open cracks in the aggregate and cement paste without and with gel per 1 cm^2).

7.5 RESULTS

7.5.1 ASR kinetics in eco-efficient concrete mixtures

The average mass gain over the course of one year (i.e., average mass gain at a given age) of all concrete mixtures incorporating coarse reactive aggregate (Springhill – S) and fine reactive aggregate (Texas – T) are illustrated in Figure 7.3a and b, respectively, including the data range bars. The standard deviation in order of decreasing cement content (i.e., from 420 to 150 kg/m^3) for each mixture incorporating the coarse reactive aggregate is as follows: 0.04 – 0.07%, 0.08 – 0.13%, 0.14 – 0.23%, 0.05 – 0.10%, and 0.14 – 0.22%. Likewise, the standard deviation for the mixtures incorporating the fine reactive aggregate in order of decreasing cement content is: 0.06 – 0.11%, 0.04 – 0.10%, and 0.05 – 0.09%. Overall, the mass gain over time seems more gradual for the Springhill mixtures when compared to the Texas mixtures, regardless of the cement content, capturing the influence of the reactive aggregate type (i.e., coarse vs fine). The mixture made with Springhill and 420 kg/m^3 of cement content presents a higher mass gain after 366 days at 1.34% followed by a total mass gain of 1.13% for both mixtures with 325 kg/m^3 and 250 kg/m^3 and 0.21% and 0.46% for mixtures with 200 kg/m^3 and 150 kg/m^3 of cement content, respectively.

Interestingly, the Springhill mixture with a cement content of 250 kg/m^3 shows a higher mass gain when compared to that of 325 kg/m^3 until 273 days (i.e., 1.01%) after which their mass gains are very similar; the former following a similar mass gain as the mixture with a cement content of 420 kg/m^3 until 95 days (i.e., 0.81%). The Texas mixtures, on the other hand, reached a mass gain plateau after 276 days, following the trend of decreasing cement content (i.e., 1.57% for 420 kg/m^3, 1.35% for 325 kg/m^3, and 1.16% for 250 kg/m^3). Similarly to Springhill mixtures, 2C-325P-T and 3C-250P-T show comparable mass gain over time, yet after 155 days, the former one spiked reaching a mass gain 16% higher until the end of the test.

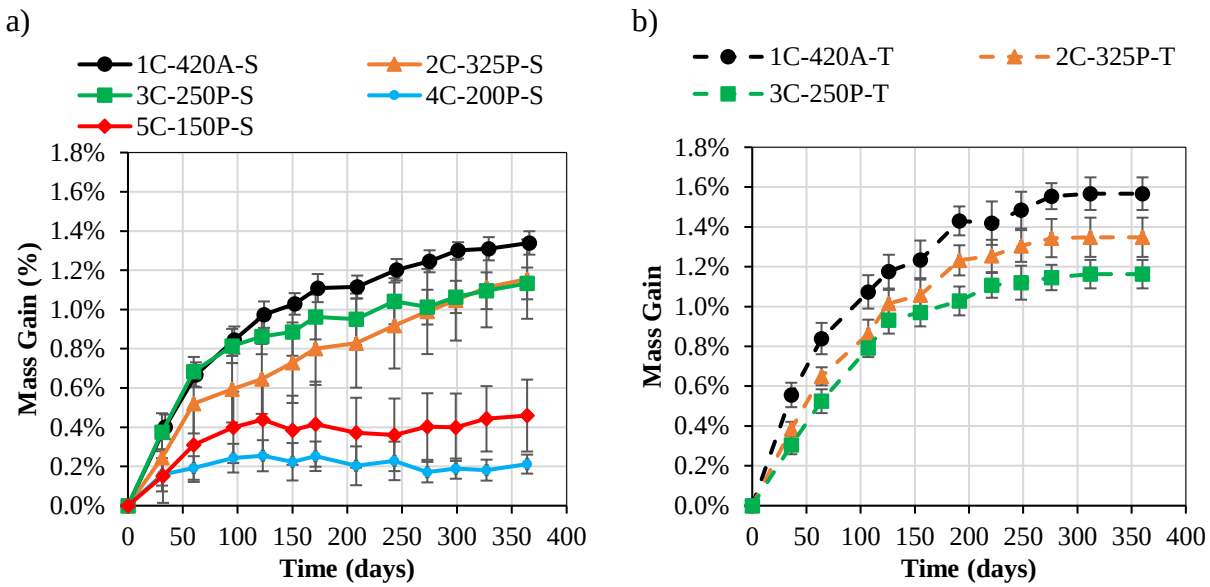

Figure 7.3. Mass as a function of time for a) Springhill and b) Texas mixtures.

The average expansion as a function of time (i.e., average measured expansion at a given age) for Springhill and Texas mixtures are presented in Figure 7.4a and b, respectively, including the data range bars. The standard deviation in order of decreasing cement content (i.e., from 420 to 150 kg/m^3) for each mixture incorporating the coarse reactive aggregate is as follows: 0.01 – 0.07%, 0.02 – 0.13%, 0.01 – 0.03%, 0.01 – 0.03%, and 0.00 – 0.03%. Similarly, the standard deviation for the mixtures incorporating the fine reactive aggregate in order of decreasing cement content is: 0.03 – 0.07%, 0.02 – 0.06%, and 0.01 – 0.05%. Analyzing Figure 7.4 one may observe that the expansion over time is significantly affected by the aggregate type where the Texas mixtures achieve higher expansion levels at any given time, presenting a sharper increase.

The overall expansion levels achieved after one year by both mixtures follow the same trend per cement content where the highest expansion is achieved by the 420 kg/m^3 (i.e., 0.56% and 0.78% for the Springhill and Texas mixtures, respectively) and the lowest overall expansion corresponds to the lowest cement content per reactive aggregate type. The expansion after one year for the eco-

efficient Springhill mixtures with a cement content of 325 kg/m^3 is 0.47% while a significant decrease in the overall expansion is observed for mixtures incorporating limestone fillers. Although the mixture with 250 kg/m^3 of cement had a significant mass gain compared to the other eco-efficient mixtures, its expansion after one year of 0.18% is more comparable to mixtures developed with low cement (i.e., 200 and 150 kg/m^3) at 0.09% for the 200 and 150 kg/m^3 of cement mixtures. Meanwhile, all mixtures made with Texas sand achieve expansion levels above those observed for the Springhill mixtures after one year at 0.65% and 0.61% for the sustainable mixtures with cement contents of 325 and 250 kg/m^3.

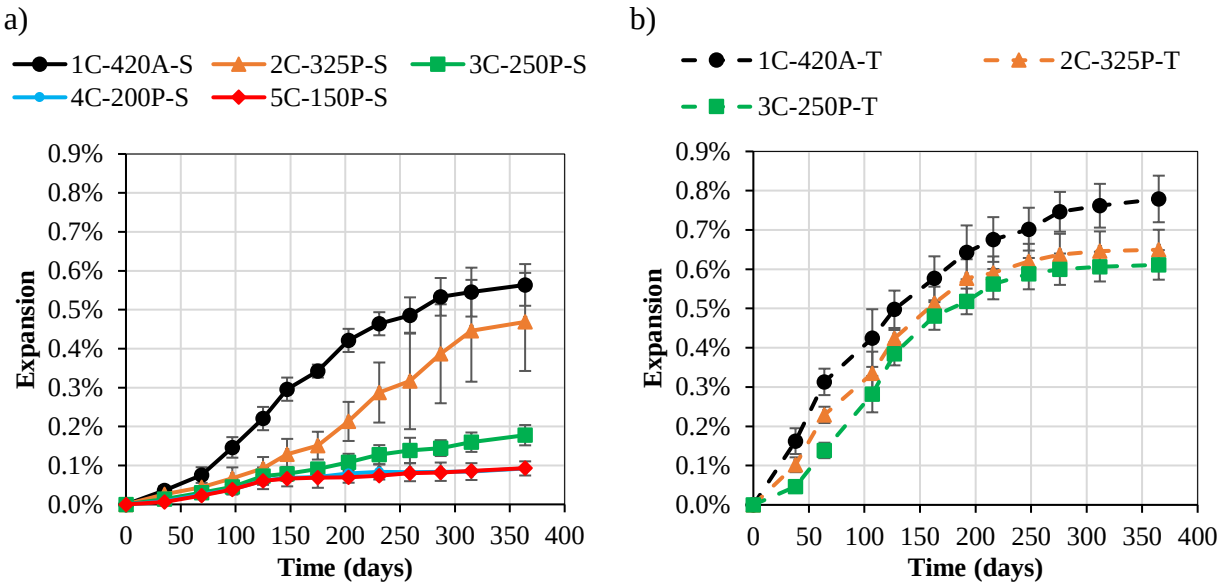

Figure 7.4. Expansion as a function of time for a) Springhill and b) Texas mixtures.

7.5.2 Surface electrical resistivity

Periodical surface electrical resistivity tests were performed to assess the inner quality of the concrete as ASR progressed and the average values at a given age are present in Figure 7.5, including data range bars. The overall standard deviation is between 0.3 and 1.7 kΩ.cm for Springhill mixtures, and from 0.31 to 1.81 kΩ.cm for Texas mixtures.

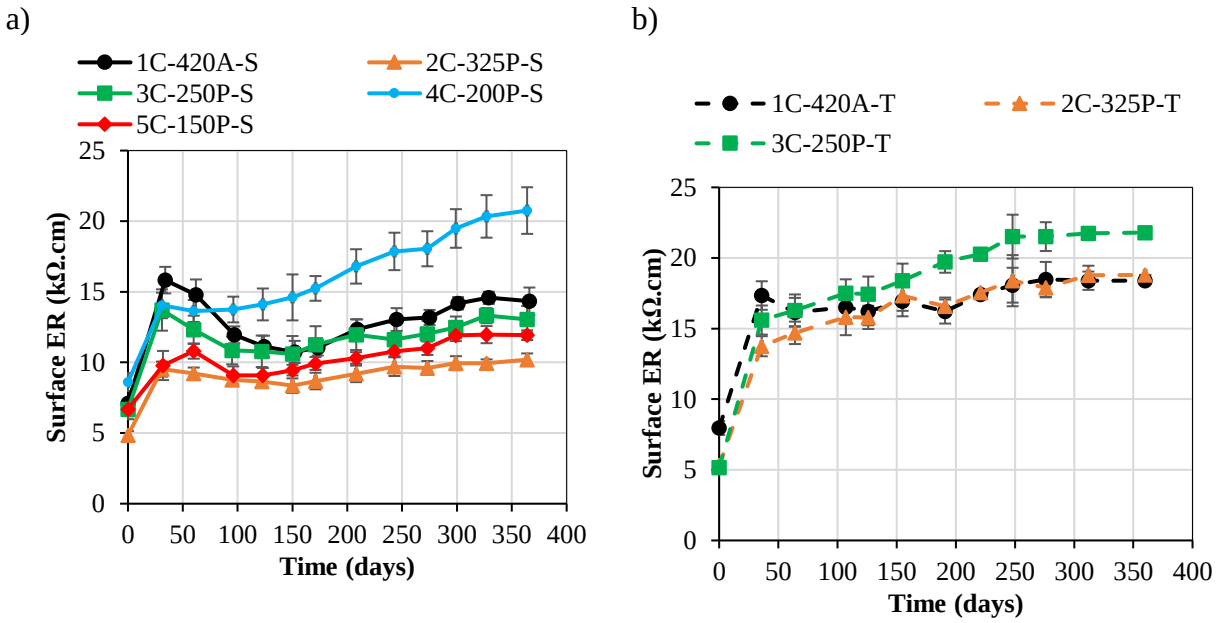

Figure 7.5. Surface electrical resistivity development for a) Springhill and b) Texas mixtures.

Regardless of the reactive aggregate selected, mixtures presented similar trends when comparing the surface electrical resistivity over time, where values sharply increase up to a peak at approximately 30 days, followed by a slightly descending period up to 95-150 days, and presenting an almost steady output until reaching the one-year testing period with the exception of the 200 kg/m^3 of cement Springhill mixture where the surface electrical resistivity seems to be in continuous increase. No apparent trend is observed among all of the mixtures. Electrical resistivities ranging from 10 to 15 kΩ.cm were obtained after one year for all Springhill mixtures except for the 200 kg/m^3 mixture producing higher electrical resistivities (20.8 kΩ.cm). Likewise, after one-year testing, Texas mixtures showed electrical resistivity values ranging from 18.4 to 21.8 kΩ.cm

7.5.3 Apparent porosity

The apparent porosity can also be used as a parameter to evaluate concrete's microstructure. Evaluating the sound concrete before being subjected to ASR, Figure 7.6a shows that all Springhill mixtures presented apparent porosities ranging from 8.1 to 10.1%, with the two most sustainable

mixtures (i.e., 5C-150-P-S and 4C-200P-S) having the lowest and highest porosity, respectively, and in a similar trend, the apparent porosity ranged from 8.6 to 9.8% for the Texas mixtures (Figure 7.6b).

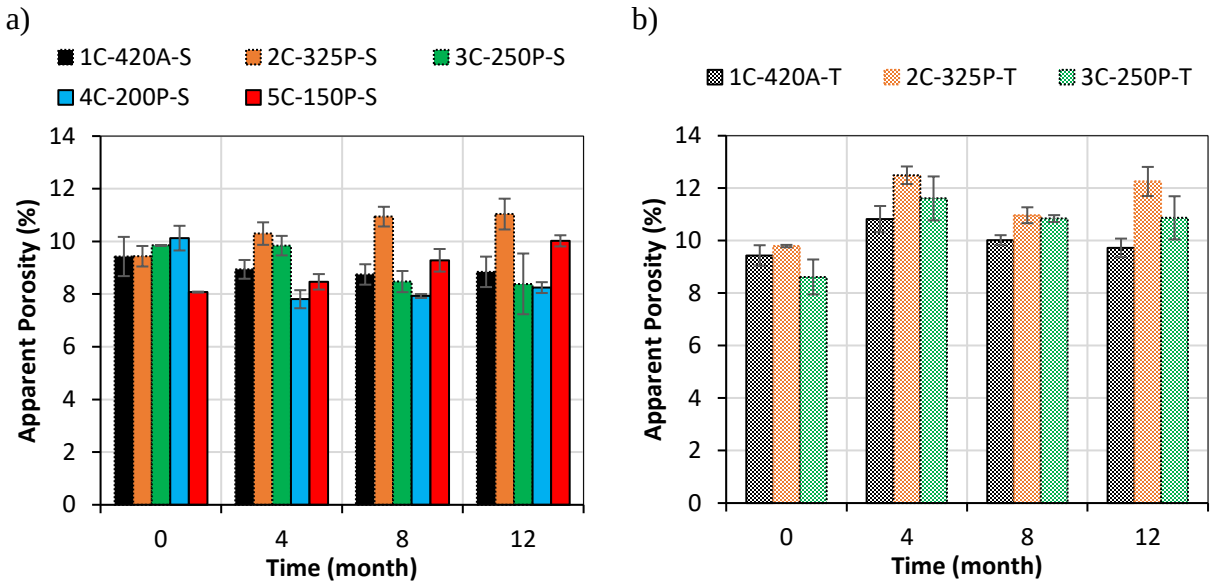

Figure 7.6. Apparent porosity variation for a) Springhill and b) Texas mixtures.

Evidently, the sound concrete with 420, 325 and 250 kg/m^3 of cement, developed for both Springhill and Texas mixtures, have very similar apparent porosities; however, when the porosity is evaluated against ASR development (i.e., 4, 8, and 12 months), the apparent porosity captures the distinct effect of the aggregate (or ASR source). Texas mixtures, therefore, showed a greater increase after 4 months in apparent porosity, reaching values between 10.8 and 12.5%, compared to the Springhill mixtures (i.e., between 7.8 and 10.3%) yet, was followed by a decrease in apparent porosity after 8 months with values of 10-11%. This same trend was observed for Springhill mixtures, except 325kg/m^3 and 150 kg/m^3 followed a distinct trend. Mixture 1C-420A-S, having the highest cement content, resulted in an almost constant apparent porosity over time of 9.4 to 8.8%, while mixtures developed with PPM presented distinct behaviours. The apparent porosity of mixtures 2C-325P-S

and 5C-150P-S increased until 12 months (i.e., from 9.4% and 8.1% to 11.0% and 10.0%, respectively) whereas the porosity of mixture 4C-200P-S decreased from 10.1 to 8.2%.

7.5.4 Damage rating index (DRI)

The DRI number was used to evaluate the progression of ASR damage over one year. Figure 7.7a, therefore, shows the increase in DRI number as a function of the concrete's expansion level for all mixtures. Regardless of the reactive aggregate type, at 0% of expansion, all concrete mixtures present a DRI number lower than 150, followed by an upward parallel trend up to 0.20% expansion, where the DRI number ranged between 550 and 700. It should be noted that Springhill mixtures developed a with cement content of 250 kg/m^3 or lower achieved a maximum expansion level of only 0.18% after one year of testing and therefore present the lowest overall DRI numbers (i.e., 426, 357, 334 for the 250, 200 and 150 kg/m^3 of cement, respectively).

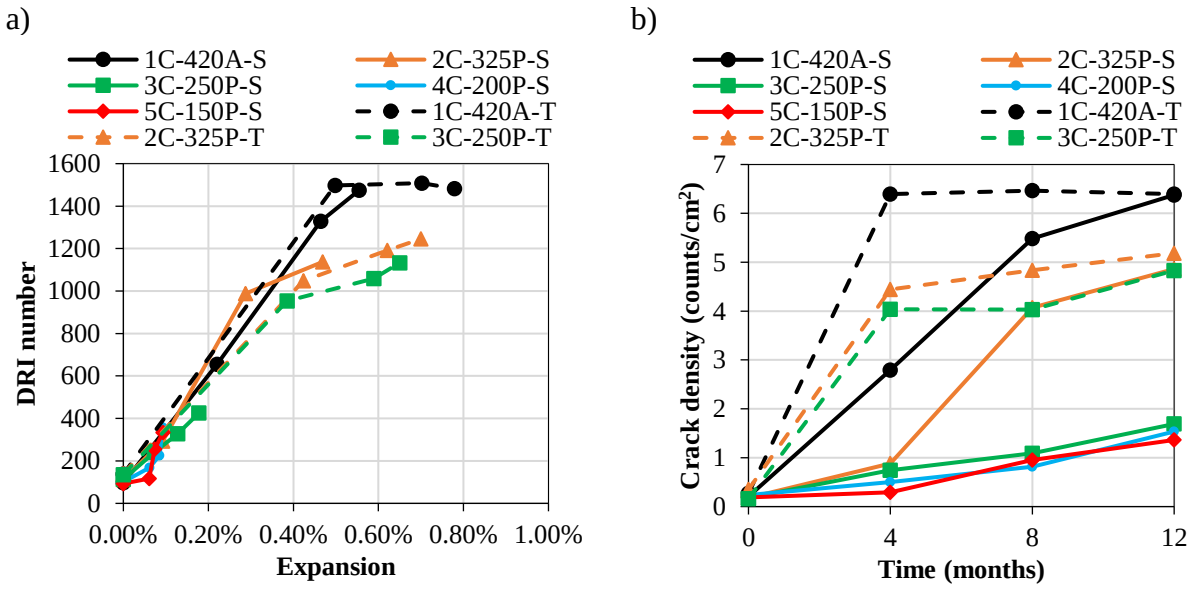

Figure 7.7. a) DRI number and b) crack density as a function of expansion.

Mixtures with 420 kg/m^3 of cement followed a parallel trend up to 0.50% expansion level with an average DRI number of 1450 yet, the Texas mixture presented a slightly higher DRI number

followed by levelling off trend with a DRI number of 1508 at 0.70% of expansion. Regarding PPM mixtures, the slope of the curve begins to flatten for the 2C-325P-S mixture after 0.29% (with a DRI number of 988) expansion, whereas Texas-PPM mixtures exhibit the same trend only after 0.40% of expansion (with DRI of 1049 and 953 in order of decreasing cement content). Overall, control mixtures achieved similar ultimate DRI numbers of 1475 and 1482, for Springhill and Texas mixtures, respectively, while PPM mixtures developed without limestone fillers (i.e., 2C-325P-S and 2C-325P-T) achieved DRI numbers of 1137 and 1246 after one year, respectively. In addition, the mixtures developed with cement contents of 250 kg/m^{3}or less produced less damage as captured by the DRI number yet, 3C-250P-T obtained a DRI number of 1133 illustrating the distinct behaviour of the highly reactive Texas sand.

To further assess the effect of ASR damage through its ASR features and ASR crack propagation, the crack density was plotted as a function of time for all mixtures (Figure 7.7b). The crack density sums the total amount of open cracks in the aggregate and cement paste (i.e., with and without gel) and normalizes those counts per square centimetre. The sound concrete mixtures (shown as 0-month results) achieved a crack density lower than 0.35 counts/cm^2. Control mixture developed with Springhill reactive aggregate (1C-420A-S) had a linear increase in crack density until 8 months of exposure, whereas mixtures 2C-325P-S had a sudden increase in crack density after 4 months. Between 8 and 12 months of testing, these two mixtures presented similar behaviour, with the crack density of 2C-325P-S being approximately 25% lower than that of 1C-420A-S. In general, Springhill mixtures developed with low cement (250, 200, and 150 kg/m^3) resulted in a significantly lower crack density, highlighting the efficacy of the mix-design proposed. One may note that Springhill mixtures did not reach a plateau, after a 12-month test indicating that the amount of reaction has not stabilized and that further cracks may form if the test is continued. Conversely, mixtures developed

with Texas sand had a crack density increase until reaching a plateau, regardless of the reactive aggregate type, cement content, and mix-design selected. These mixtures presented similar crack densities at 4 and 8 months, indicating that no further considerable distress occurred due to the ASR-reaction. Considering the ASR-expansion levels classification as per [26], at low expansion (0.05%) levels, CD ranged between 0.3 and about 1.2 cracks/cm^2, whereas at higher expansion levels (0.2%), CD ranged between 2.2 and about 2.8 cracks/cm^2, aggreging with previous findings [21,25]. Furthermore, at very high expansion levels (> 0.40%), CD reached 6.4 cracks /cm^2.

7.5.5 Microscopic analysis of ASR distress

To better understand the generation and propagation of ASR-damage within sustainable concrete mixtures, the extended version of the DRI presented by [25], in which the deterioration features (cracks in counts/100 cm^2 and proportions, as Figure 7.8a and b illustrates, respectively) are appraised without the weighing factors are normalized for 100 cm^2 surface area, was performed. The distinction of gel in the distress feature is omitted thus, the counts are combined (i.e., OCA+OCAG and CCP+CCPG). Overall, the number of distress features is directly proportional to the increase of expansion over time. However, at high deterioration levels (> 0.35%), the cracks start to connect with one another, resulting in a reduction in counts or even a slight reduction in total cracks. Moreover, the ultra-high reactive (Texas) mixtures resulted in a greater number of cracks than the highly reactive (Springhill) mixtures. Regardless of the reactive aggregate type used, mixtures developed with more cement content (420 kg/m^3) show the highest counts (approximately 1000 counts/100cm^2 max. count) followed by mixtures with 325 kg/m^3 of cement at max. 850 counts / 100cm^2 on average. When fillers are added to PPM mixtures (≤ 250 kg/m^3), the reactive aggregate type starts to influence the number of cracks; as such, 3C-250P-T has the greatest max. count (820 counts/100 cm^2) compared to 3C-250P-S (467 counts/100 cm^2). Interestingly, the 4C-200P-S and

5C-150P-S both have similar max. counts at less than 400 counts/100 cm^2 after 12 months. In terms of features over time, 1C-420A-S shows a significant increase in open cracks in aggregate (OCA+OCAG) at 4 months (i.e., 235 counts/100 cm^2), whereas 2C-325P-S only presents this behaviour from 4 to 8 months (i.e., from 85 to 346 counts/100 cm^2). Cracks in the cement paste on the other hand are less abundant for both mixtures reaching maximum values of 119 and 81 counts/100 cm^2 for the Springhill CC and PPM mixture without filler, respectively.

PPM mixtures with filler have a significantly lower number of open cracks in the aggregate throughout reaching between 134 and 156 counts/100 cm^2 while presenting a negligible number of cracks in the cement paste (CCP+CCPG) after 12 months. Yet, all Texas mixtures have had a significant amount of open cracks in aggregate (OCA+OCAG) and cracks in cement paste (CCP+CCPG) since the 4-month mark, regardless of the mix-design type and cement content used. Although PPM-Texas mixtures presented a 20% lower amount of features than the control one (1C-420A-T), the effectiveness of PPM is more pronounced on Springhill mixtures, with up to 57% fewer distress features.

Figure 7.8 highlights the percentage of microscopic features of each mixture investigated. Initially, all mixtures presented more than 90% of close cracks in aggregates (CCA), while over time, the amount of open cracks in aggregate (OCA+OCAG) and cracks in cement paste (CCP+CCPG) both increase. Similarly to Figure 7.8a, after the 4-month analysis, the level of CCA dramatically decreased (50%) for mixtures 1C-420A-S and all Texas mixtures, capturing the effect of such cracks becoming opened due to ASR. Yet, during the course of 8-month experiments, PPM-Springhill mixtures continue to show CCA as the most predominant feature (> 50%), followed by OCA+OCAG (< 35%) and CCP+CCPG (< 10%). Moreover, total cracks in the aggregate and cracks

in the cement paste seem to stabilize in both mixtures with a high cement content (420 kg/m^3), with CCA ranging from 35% to 50%, OCA+OCAG ranging from 55% to 40%, and CCP+CCPG ranging from 10% to 15% while this is not apparent in both PPM mixtures without filler nor the most sustainable Texas mixture with 250 kg/m^3 of cement.

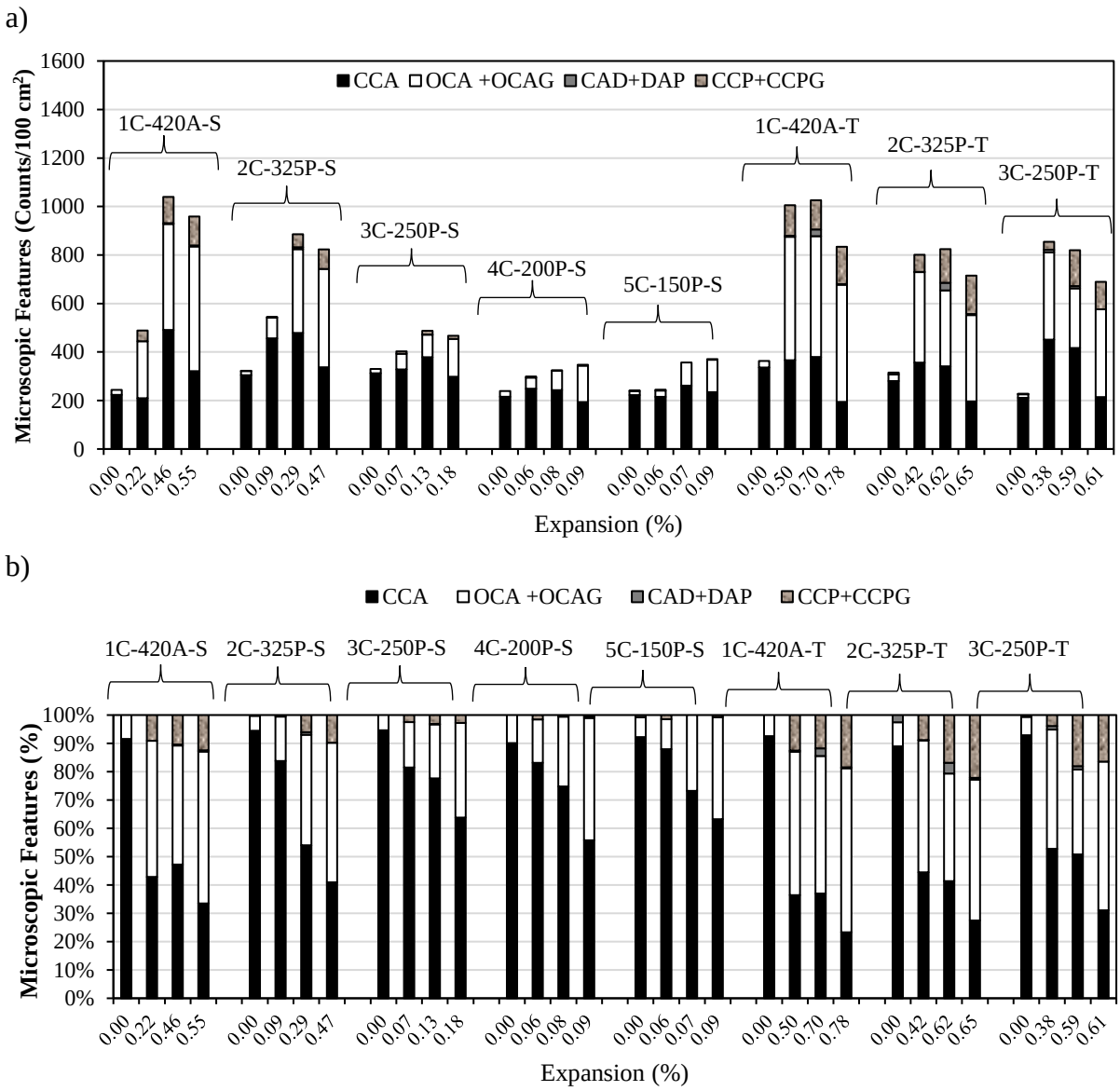

Figure 7.8. Distress features a) absolute value and b) relative value after 0, 4, 8, and 12 months.

7.6 DISCUSSION

7.6.1 Qualitative and quantitative analysis of eco-efficient mixtures

For a better understanding of the influence of the mix-design selection, Figure 7.9a and b present the mass percentage and volumetric fraction of each component selected for the mix-design developed in this study, while Figure 7.9c and d presents a sample for a visual (qualitative) comparison between mixtures developed with 420 and 150 kg/m^3 of cement.

In terms of mass (Figure 7.9a), cement content accounts for 18% of the total components selected on 1C-420A. Yet, when the selected PPM model is applied, the cement content mass can decrease to 14%, or up to 6% when limestone fillers (≤ 7%) are added. This is indeed feasible due to the increase of fine aggregates from 36% in the control mixture (1C-420A) to roughly 45% in the PPM-mixtures.

The mass of coarse aggregate is maintained constant at approximately 36%, regardless of the mix-design method Analyzing the volume occupied by each component (Figure 7.9b), cement content occupies 13% and 5% of the total volume of 1C-420A and 5C-150P, respectively. The cement paste colour of concrete specimens is affected by differences in cement content, as shown in Figure 7.9c and 9d, where a darker colour represents more cement. Moreover, the fine aggregates ranged from 31% to 41%, hence accounting for 10% more volume in PPM-mixtures, which can be visually presented in Figure 7.9c and d. Conversely, regardless of mix-design procedure, coarse aggregate volume is approximately 33% therefore, the reactive component of the mixtures using the reactive coarse aggregate (i.e., Springhill – S) is also kept constant. Considering this information, to avoid an increase in reactive fine aggregate on the PPM-Texas mixtures, approximately 10% of the total

volume is composed of non-reactive fine aggregate; thus, the volume of fine reactive aggregate on all Texas mixtures was kept constant at 31%.

a)

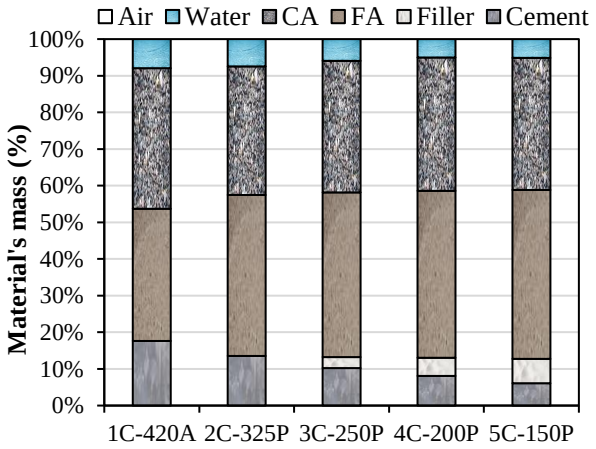

b)

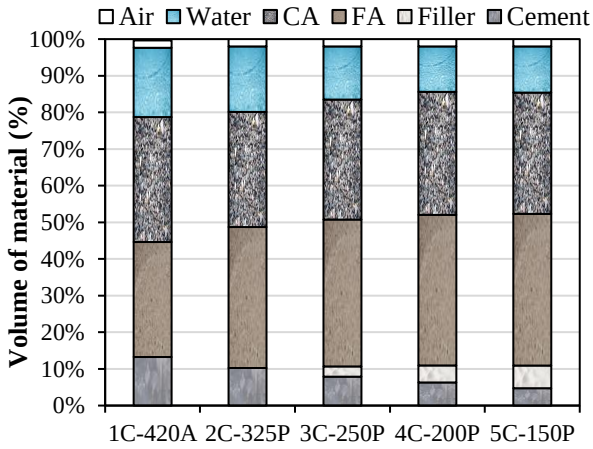

c)

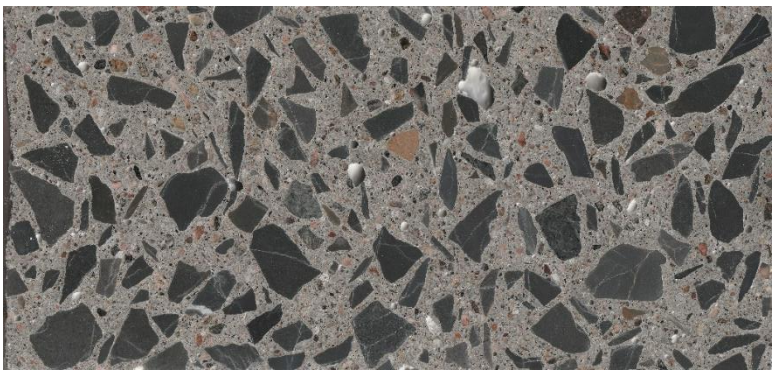

d)

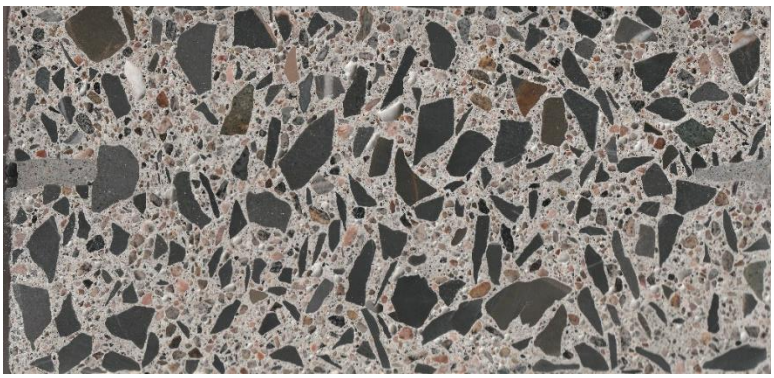

Figure 7.9. a) Mass percentage and b) volumetric fraction of each component incorporated in the mix-design; c) representation of 1C-420A and d) representation of 5C-150P.

Furthermore, lowering the cement paste through the use of PPM can be beneficial for a variety of distress mechanisms, such as freezing and thawing exposure conditions [69]. Although further studies are required to confirm the durability aspects of PPM mixtures, the concrete's electrical resistivity is an important parameter that can evaluate the likelihood of corrosion. As per studies published [67,70], these mixtures would be considered to have a moderate risk of corrosion of steel reinforcement. However, the electrical resistivity of the concrete increased after 12 months despite having suffered from ASR damage. No apparent trend is observed between the cement content, electrical resistivity, and porosity over time. In addition, the mixture made with 200 kg/m3 of cement presented the highest initial and final electrical resistivity values, the highest initial porosity yet, the lowest final porosity values. This mixture also presented the lowest mass gain overall and one of the two lowest recorded expansion levels throughout and damage captured by the DRI number. This could be an indication of the concrete inner quality improving over time, even being subjected to ASR deterioration.

7.6.2 The effect of alkali Content on ASR-induced expansion

The influence of the cement content changes significantly based on the reactive aggregate type. Analyzing Figure 7.10, one may notice that mixtures developed with limestone filler and lower cement content ($\leq$ 250 kg/m^3) resulted in considerably lower expansion levels when the highly reactive coarse aggregate (i.e., Springhill – S) is selected, whereas the influence of cement content is not as significant for the ultra-high reactive fine aggregate (Texas -T) mixtures. PPM mixtures incorporating fillers show the potential to further mitigate ASR yet, even though additional measures or materials such as SCMs may be used, their amounts correspond to a fraction of the cement content, which will result in more sustainable use of such materials while being able to use aggregates otherwise deemed unusable in concrete. Comparing the Springhill PPM mixtures with

control mixtures (Figure 7.10c), one may see that all PPM mixtures delivered an outstanding performance at 4 months, presenting an expansion 67.5% lower than the mixture with 420 kg/m^3 of cement.

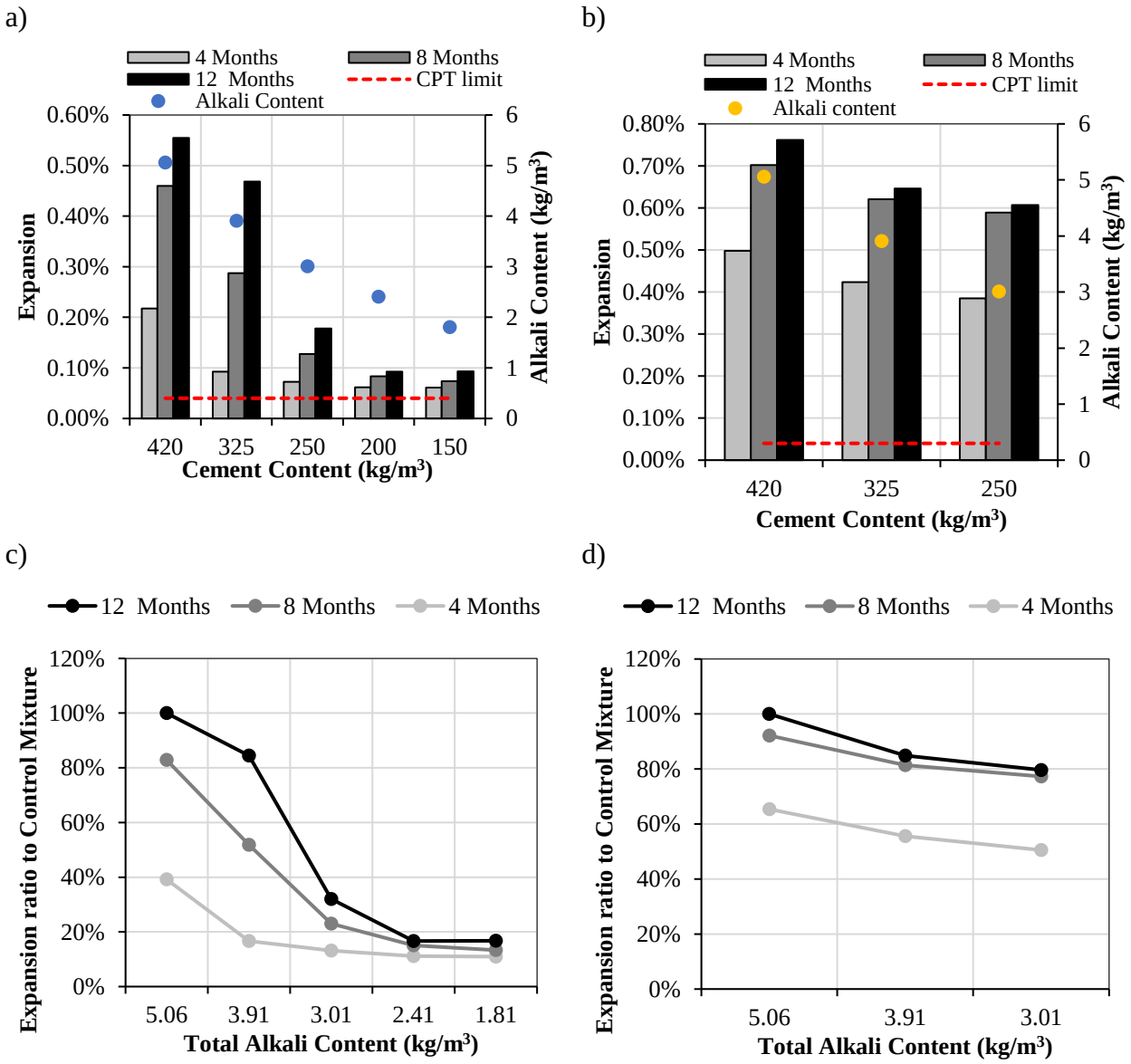

Figure 7.10. The effect of alkali content on expansion over time and expansion ratio to control mixture for a) and c) Springhill mixtures (highly reactive); b) and d) Texas mixtures (ultra-high reactive).

Yet after 8 months, the expansion of the mixture developed with 325 kg/m^3 increased, resulting in 83% of the expansion of the control mixture after 12 months. Meanwhile, the final expansions of mixtures 3C-250P-S, 4C-200P-S, and 5C-150P-S represent 32%, 16%, and 16%, respectively, of the 1C-420A-S final expansion. The same trend is observed in Figure 7.10d, in which the Texas PPM mixtures presented better performance at 4 months. However, 2C-325P-T and 3C-250P-T yielded a final expansion of only 15% and 20%, respectively, lower than mixture 1C-420P-T hence, capturing the distinct effect of the aggregate type on ASR.

7.6.3 Distress development of ASR damage in sustainable concrete mixtures

The DRI is an extremely useful tool, due to both its quantitative and qualitative nature, to evaluate the progression of features indicating the development of ASR damage in concrete specimens. Figure 7.11 highlights the key differences between the highly reactive coarse aggregate (Springhill - S) and ultra-high reactive fine aggregate (Texas - T). After being stored in conditions enabling ASR (i.e., 38°C and 100% RH) for 12 months, the sustainable concrete mixtures (i.e., those produced through PPM) incorporating Springhill yielded a final DRI of up to 1137. Yet, PPM-Springhill mixtures incorporating limestone filler (≤ 250 kg/m^3), reached maximum DRI numbers of 426 after the 12-month testing period, highlighting the effectiveness of the proposed mix-design to suppress the expansion and damage caused by ASR. Conversely, the control mixture using 420 kg/m^3 of cement and the ultra-high reactive fine aggregate (Texas - T) achieved a 12-month DRI number of 1482, which is higher than PPM-Texas mixtures, that is, mixtures improved through the optimized mix-design method. The ultimate expansion of an ultra-high reactive fine aggregate (0.75%) differs significantly from that of a high-reactive coarse aggregate (0.55%). Hence, the ability of PPM-Texas mixtures to develop lower distress features than the control mixture using 420 kg/m^3 of cement and the highly reactive coarse aggregate (Springhill - S), even at higher expansion

levels, demonstrates the feasibility of using PPM to reduce expansion in concrete subjected to ASR damage. In terms of Texas mixtures, the control mixture had a 12-month DRI of 1600, while those with 325 and 250 kg/m^3 of cement had 21% and 30% lower distress features, respectively.

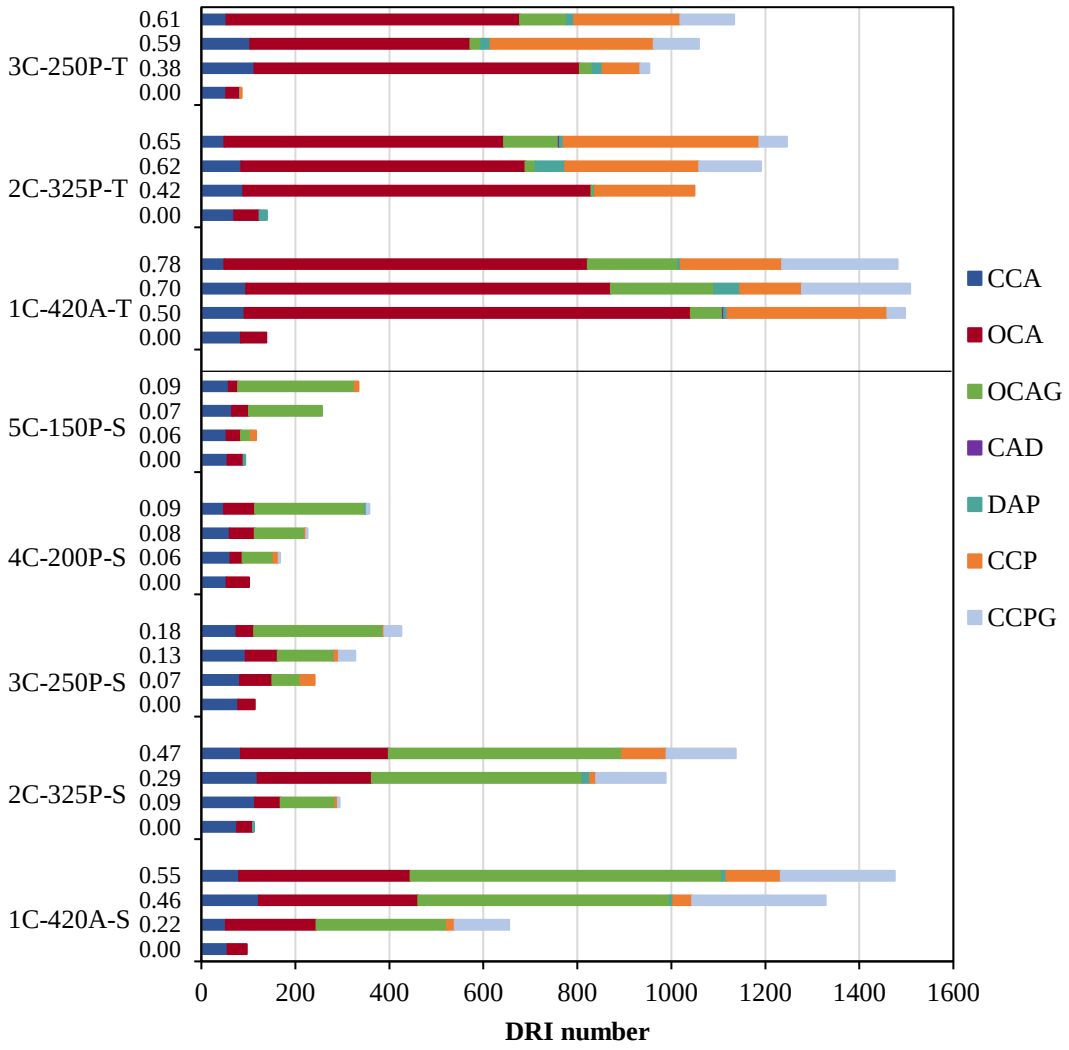

Figure 7.11. Relationship between Damage Rating Index and expansion for concrete developed with different cement content and reactive aggregate.

Moreover, when PPM mixtures are used, the amount of cracks in the cement paste is lower, indicating that the ASR-developed is at an earlier age, concentrating the cracks within the aggregates. The amount of gel produced is only slightly lower on PPM-mixtures, yet it is

significantly affected by the aggregate type, with Springhill mixtures producing more reaction products visible at a magnification of 16x. Images captured through the stereomicroscope for mixtures incorporating Texas (8 months test) and Springhill (12 months test) are illustrated in Figure 7.12. Distinct exposure durations were selected to demonstrate and visually compare the difference in distress features due to reactive aggregate type (Texas vs Springhill) when similar cement content (e.g., 420 or 325 kg/m^3) were selected, which resulted in similar DRI number (around 1500 and 1150, respectively).

a) 1C-420A-S
(12 months; 0.55%; DRI:1475)

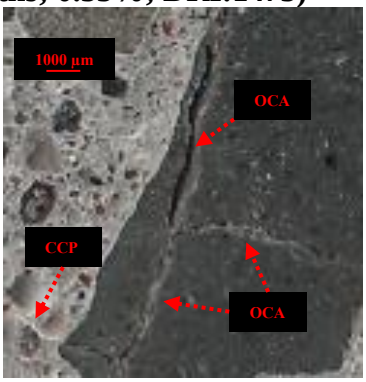

b) 2C-325P-S
(12 months; 0.47%; DRI: 1137)

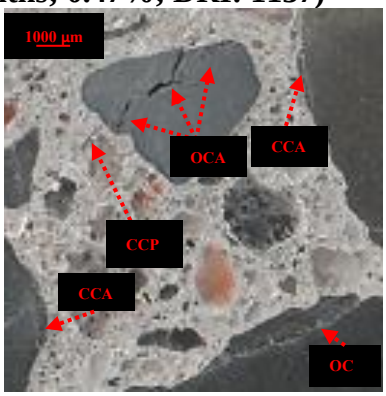

f) 1C-420A-T
(8 months; 0.70%; DRI: 1508)

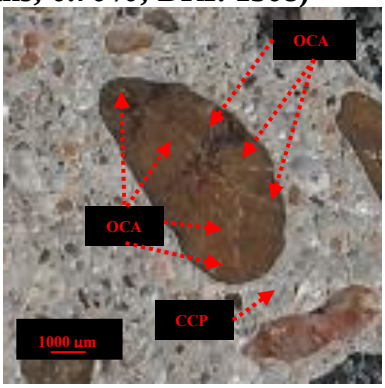

g) 2C-325P-T
(8 months; 0.62%; DRI: 1191)

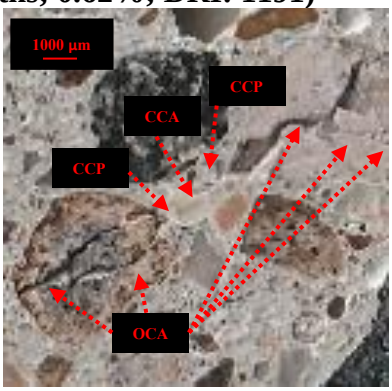

c) 3C-250P-S
(12 months; 0.18%; DRI: 426)

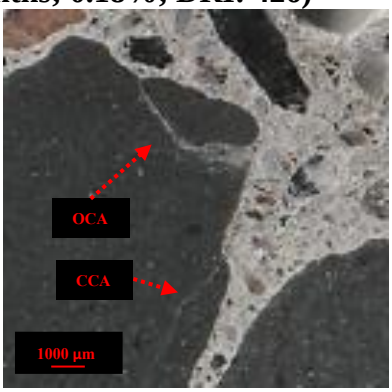

h) 3C-250P-T
(8 months; 0.59%; DRI: 1059)

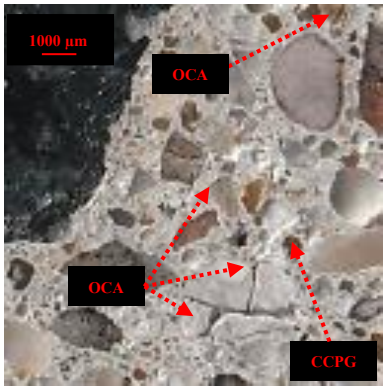

d) 4C-200P-S
(12 months; 0.09%; DRI: 354)

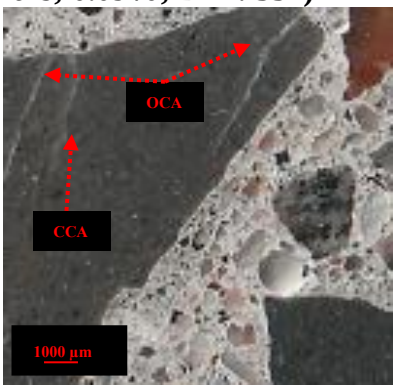

e) 5C-150P-S
(12 months; 0.09%; DRI: 334)

Figure 7.12. Distress features in mixtures incorporating Springhill (a-e) and Texas (f-h) in order of decreasing cement content.

Generally, the DRI numbers obtained with respect to the expansion level correspond to that proposed by Sanchez et al. [58]. However, a difference is observed between the DRI numbers achieved at different times although the expansion level is very similar and within the same category of damage degree. This is most apparent for the 200 and 150 kg/m^3 of cement mixtures where an expansion level difference of only 0.01% (from 0.08% at 8 to 0.09% at 12-month testing) resulted in an increase of up to 56% in DRI numbers. This may therefore highlight the fact that the expansion level may not necessarily indicate the level of actual damage, especially in sustainable mixtures which were also observed in mixtures using recycled concrete affected by ASR [21].

7.6.4 Behaviour prediction of eco-efficient concrete affected by ASR

de Grazia et al. [71] have proposed a model (Equation 7.3) based on Larive's equation to better describe ASR-induced expansion in the laboratory, accounting for five parameters studied, including aggregate type and nature/reactivity, temperature, alkali content, and relative humidity.

$$\varepsilon(t,\theta) = \xi(t)\varepsilon^{\infty} = \frac{1 - e^{-\frac{t}{\tau_c\, k_{c,T}\, k_{c,RH}\, k_{c,\%A} k_{c,E}}}}{1 + e^{-\frac{\left(t - \tau_l\, k_{L,T}\, k_{L,RH}\, k_{L,\%A} k_{L,E}\right)}{\tau_c\, k_{c,T}\, k_{c,RH}\, k_{c,\%A} k_{c,E}}}} \times \left(k_{Inf,T}\, k_{Inf,RH}\, k_{Inf,E}\, k_{Inf,\%A}\right)\varepsilon^{\infty} \quad \text{Equation 7.3}$$

where t is elapsed time; $\varepsilon\ (t)$ is the expansion at a given elapsed time; ε^{∞} is the maximum expansion at infinity (or ultimate expansion); τ_c is the characteristic time (as a function of the aggregate type and nature/reactivity); τ_l is the latency time (as a function of the aggregate type and nature/reactivity); $k_{C,T}, k_{C,RH}, k_{C,E}, k_{C,,\%A}$ are the temperature, humidity, exposure and alkali content coefficients impacting the characteristic time; $k_{L,T}, k_{L,RH}, k_{L,E}, k_{L,,\%A}$ is the temperature, humidity, exposure and alkali content coefficients impacting the latency time; $k_{inf,T}, k_{inf,RH}, k_{inf,E}, k_{inf,\%A}$ is the temperature, humidity, exposure and alkali content coefficients influencing the maximum expansion.

These coefficients were proposed based on previous research demonstrating the effects of the aforementioned parameters on ASR-kinetics (i.e., latency (τ_l) and characteristic (τ_c) times) and final expansion (i.e., ε^{∞}, or expansion at infinity). Equation 7.3 can be used in the laboratory to better predict ASR-kinetics and unrestrained induced expansion based on the aggregate features and test conditions to avoid the need for additional laboratory tests. Using the alkali content coefficients as

per [71], and interpolating when required, Equation 7.3 was applied against the current laboratory experimental work to validate the modified Larive model.

In this study, the Springhill mixtures developed with 100% cement content, that is, without using limestone fillers (1C-420A-S and 2C-325P-S) displayed an *S-shaped* curve, characteristic of laboratory-made specimens [71] based on Larive model [25]. This curve may therefore be divided into four distinct phases: 1) The formation of ASR-secondary products, also known as ASR-gel, and their likely accommodation within reactive aggregates and adjacent cement paste with little to no expansion; 2) The initial convex shape of the curve represents the expected expansion due to moisture uptake from the reaction product, which causes cracking as indicated by the ascending part of the expansion curve; 3) After the inflection point of the S-shape curve, deteriorative cracks occur within the aggregate particles and adjacent cement paste changing the curve shape changes from "convex" to "concave"; hence, decreasing ASR-expansion rate; 4) The consumption of reactants (alkalis and/or silica) from the system causing the reaction/expansion development to level off. However, ultra-high reactive mixtures made with the Texas sand did not exhibit *S-shape* curve, hence, their performance can be classified through phases 3 and 4 only. It is worth noting that the latency (τ_l) and characteristic (τ_c) times were retrieved from the aggregate type and nature reactivity coefficient table [71]. Yet, the expansions at infinity for the Springhill and Texas mixtures were chosen to be 0.40% and 0.87%, respectively. Figure 7.13 shows the comparison between the modified Larive model and the current laboratory results. One can see that control mixtures (1C-420A) presented a good correlation with the model proposed by [71], in which they were able to accurately predict the expansion of both reactive aggregates (i.e. Springhill and Texas). Yet, the alkali coefficient proposed based on boosted and non-boosted mixtures investigated by Fournier et al. [55], did not mimic the ASR-kinetics and final expansion of PPM-mixtures.

Based on the gap of the previous study investigating low-cement concrete mixtures developed with PPM, new calibration curves were performed. The final results are presented in Figure 7.14, whereas the alkali content coefficients are presented in Table 7.6.

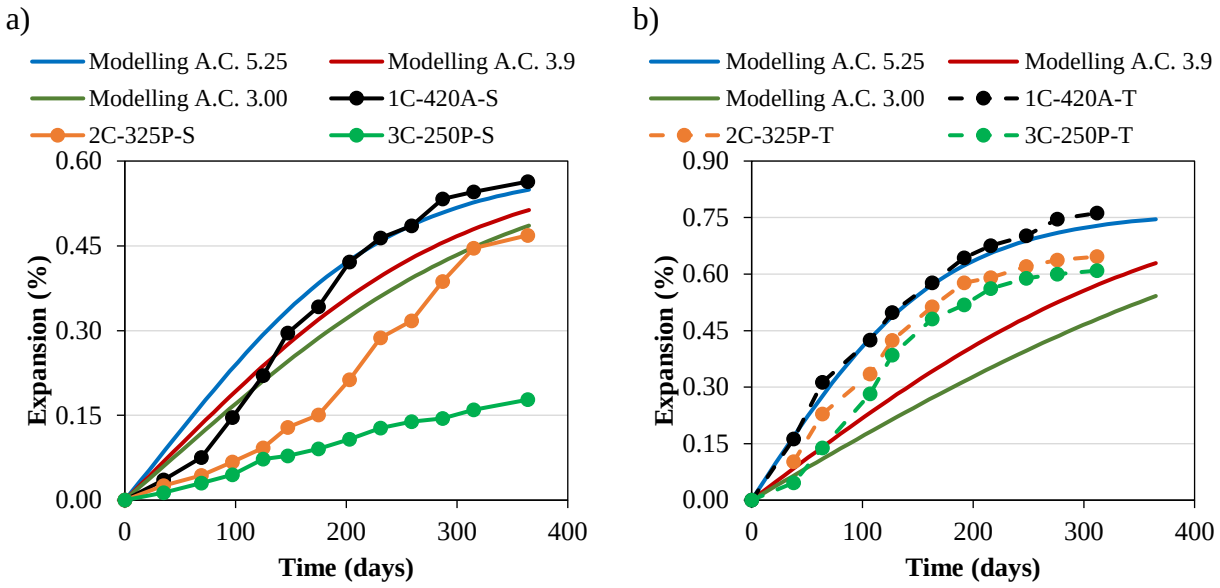

Figure 7.13. Comparison of the present laboratory findings and the modified Larive's model a) Springhill Mixtures and b) Texas Mixtures.

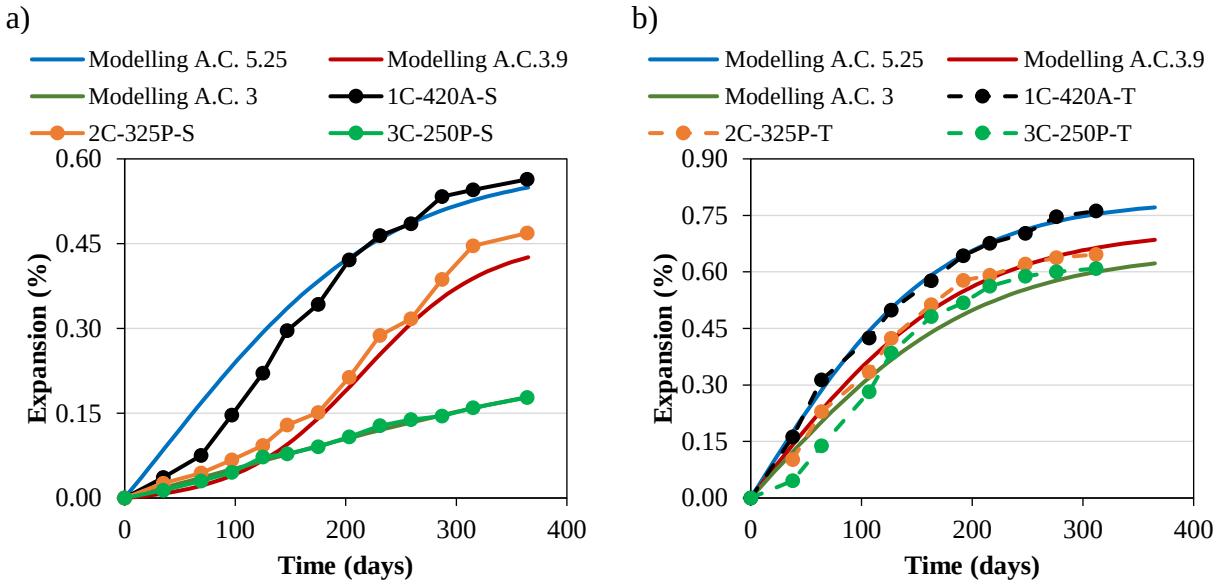

Figure 7.14. Calibration of the present laboratory findings and the modified Larive model for PPM- a) Springhill Mixtures and b) Texas Mixtures.

Based on the results of the experiments, alkali coefficients were proposed for ultra-high reactive fine aggregate and high reactive coarse aggregate. Further studies are needed to validate the use of these coefficients for different PPM-models and greater variability in aggregate type and nature. For concrete mixtures developed with an alkali concentration of 3.90 kg/m^3, the ultimate alkali expansion coefficients ranged from 0.79 to 1.13, whereas mixtures developed with alkali content of 3.0 kg/m^3 has a constant ultimate alkali expansion coefficients of 0.73. Moreover, for mixtures manufactured with alkali contents of 3.9 and 3.0 kg/m^3, the latency time alkali coefficient ranged from 1.00 to 4.92 and from 1.00 to 2.32, respectively. Both of these coefficients are higher for coarse reactive aggregate than fine reactive aggregate. Yet, this trend is not seen for characteristic time alkali coefficient for mixtures with alkali content of 3.9 kg/m^3, where the coefficient is 1.12 (coarse reactive aggregate) compared to 1.33 (fine reactive aggregate). Furthermore, mixtures with an alkali content of 3.0 kg/m^3 show a significant increase (from 4.47 to 1.42) in the characteristic time alkali coefficient modifying ASR development.

Table 7.6. Alkali content coefficients proposed for sustainable mixtures developed with PPM-models [71].

		PPM mixtures: Alkali Content of 3.9			PPM mixtures: Alkali Content of 3.0		
		K%a-ъc	K%a- ъl	K%a-exp	K%a-ъc	K%a- ъl	K%a-exp
ASR Fine	Ultra High	1.33	1.00	0.79	1.42	1.00	0.73
ASR Coarse	High	1.12	4.92	1.14	4.47	2.32	0.73

7.7 CONCLUSIONS

The purpose of this study was to investigate the effect of low cement content mixtures proportioned through PPM on ASR damage evolution. Six PPM-mixtures were made with two types of reactive aggregate (Springhill – coarse aggregate and Texas – fine aggregate) and distinct cement content

(325, 250, 200, and 150 kg/m^3). Moreover, PPM-mixtures were compared to control mixtures containing 420 kg/m^3 of cement. The main findings of the current research are presented hereafter:

- The overall ASR-kinetics is greatly affected by cement content. The addition of limestone filler, which allowed the reduction of cement content to be equal to or lower than 250 kg/m^3 completely modified ASR-expansion development.
- Mixtures incorporating Springhill reactive aggregate show the potential to mitigate ASR with the sole use of PPM and cement reduction, further improvement can be made using additional measures or materials such as SCMs.
- After the 12-month testing period, control mixtures (420 kg/m^3) containing Springhill achieved a DRI of 1475, whereas sustainable concrete mixtures (PPM-mixtures) yielded a final DRI of up to 1137. Moreover, PPM-Springhill mixtures incorporating limestone filler ($\leq$ 250 kg/m^3) achieved maximum DRI numbers of 426, demonstrating the effectiveness of the proposed mix-design in mitigating ASR expansion and damage. This positive effect is also seen on Texas-mixtures (i.e., containing ultra- high reactive fine aggregate), where the control mixture (420 kg/m^3 of cement) achieved a 12-month DRI number of 1482, whereas PPM-Texas mixtures reached DRI lower than 1246.
- Generally, the DRI numbers obtained can be directly correlated with a level of expansion, yet a difference is observed between the DRI numbers achieved for sustainable mixtures. Moreover, mixtures made with 200 and 150 kg/m^3 of cement mixtures showed similar expansion of 0.075% and 0.09% after 8 to 12-month testing, respectively, but the DRI number increased from 241 to 346 on average.
- New alkali coefficients for the Modified Larive model were proposed, allowing it to be applied to eco-efficient mixtures made with ultra-high reactive fine aggregate and high

reactive coarse aggregate. Further research is needed to validate the use of these coefficients for different PPM-models, as well as greater variation in aggregate type and nature.

7.8 ACKNOWLEDGMENTS

The authors gratefully acknowledge the financial support that M. T. de Grazia and C. Trottier benefit from the prestigious Vanier scholarship funded by NSERC (Natural Sciences and Engineering Research Council of Canada). The authors would also like to thank Dr. Gamal Elnabelsya and Dr. Muslim Majeed, technical officers in the Materials and Structures laboratory at the University of Ottawa's Department of Civil Engineering.

7.9 AUTHORS' CONTRIBUTIONS

Conceptualization, M.T.d.G. and L.F.M.S.; methodology, M.T.d.G., C.T. and L.F.M.S.; formal analysis, M.T.d.G.; data curation, M.T.d.G; writing-original draft preparation, M.T.d.G.; writing – review and editing, C.T. and L.F.M.S; supervision L.F.M.S.

7.10 COMPETING INTERESTS

The authors declare that they have no competing financial interests or personal relationships that could have an impact on the work reported in this paper.

7.11 REFERENCES

[1] Joint statement: Canada's Cement Industry and the Government of Canada announce a partnership to establish Canada as a global leader in low-carbon cement and to achieve net-zero carbon concrete - Innovation, Science and Economic Development Canada, (n.d.). https://www.ic.gc.ca/eic/site/icgc.nsf/eng/07730.html (accessed March 17, 2022).

[2] Global Cement and Concrete Association, Our path to net zero, (2022). https://gccassociation.org/concretefuture/our-path-to-net-zero/ (accessed March 17, 2022).

[3] M. Limbachiya, S.C. Bostanci, H. Kew, Suitability of BS EN 197-1 CEM II and CEM V cement for production of low carbon concrete, Constr. Build. Mater. 71 (2014) 397–405.

[4] J. Di Filippo, J. Karpman, J.R. Deshazo, J. Di Filippo, J. Karpman, J.R. Deshazo, The impacts of policies to reduce CO2 emissions within the concrete supply chain, Cem. Concr. Compos. 101 (2019) 67–82. https://doi.org/10.1016/j.cemconcomp.2018.08.003.

[5] W. Schakel, C.R. Hung, L.-A. Tokheim, A. Hammer Strømman, E. Worrell, A. Ramírez, Impact of fuel selection on the environmental performance of post-combustion calcium looping applied to a cement plant, Appl. Energy. 210 (2017) 75–87. https://doi.org/10.1016/j.apenergy.2017.10.123.

[6] H.F. Campos, N.S. Klein, J. Marques Filho, Proposed mix design method for sustainable high-strength concrete using particle packing optimization, J. Clean. Prod. 265 (2020) 1–15. https://doi.org/10.1016/j.jclepro.2020.121907.

[7] K. Scrivener, F. Martirena, S. Bishnoi, S. Maity, Calcined clay limestone cements (LC3), Cem. Concr. Res. 114 (2018) 49–56. https://doi.org/10.1016/j.cemconres.2017.08.017.

[8] S. Ruan, C. Unluer, Influence of supplementary cementitious materials on the performance and environmental impacts of reactive magnesia cement concrete, J. Clean. Prod. 159 (2017) 62–73. https://doi.org/10.1016/j.jclepro.2017.05.044.

[9] P.R. de Matos, R.D. Sakata, L.R. Prudêncio, Eco-efficient low binder high-performance self-compacting concretes, Constr. Build. Mater. 225 (2019) 941–955. https://doi.org/10.1016/j.conbuildmat.2019.07.254.

[10] M. C. G. Juenger, R. Siddique, Recent advances in understanding the role of supplementary cementitious materials in concrete, Cem. Concr. Res. 78 (2015) 71–80. https://doi.org/10.1016/j.cemconres.2015.03.018.

[11] F. Pacheco Torgal, S. Miraldo, J.A. Labrincha, J. De Brito, An overview on concrete carbonation in the context of eco-efficient construction: Evaluation, use of SCMs and/or RAC, Constr. Build. Mater. 36 (2012) 141–150. https://doi.org/10.1016/j.conbuildmat.2012.04.066.

[12] V.M. John, B.L. Damineli, M. Quattrone, R.G. Pileggi, Fillers in cementitious materials — Experience, recent advances and future potential, Cem. Concr. Res. 114 (2018) 65–78. https://doi.org/10.1016/j.cemconres.2017.09.013.

[13] S.A.A.M. Fennis, Design of Ecological Concrete by Particle Packing Optimization, Delft University of Technology, 2011.

[14] W. Zuo, J. Liu, Q. Tian, W. Xu, W. She, P. Feng, C. Miao, Optimum design of low-binder Self-Compacting Concrete based on particle packing theories, Constr. Build. Mater. 163 (2018) 938–948. https://doi.org/10.1016/j.conbuildmat.2017.12.167.

[15] M. T. de Grazia, L. F. M. Sanchez, R. C. O. Romano, R. G. Pileggi, M.T. de Grazia, L. Sanchez, R.C.O. Romano, R.G. Pileggi, M. T. de Grazia, L. F. M. Sanchez, R. C. O. Romano, R. G. Pileggi, Investigation of the use of continuous particle packing models (PPMs) on the fresh and hardened properties of low-cement concrete (LCC) systems, Constr. Build. Mater. 195 (2019) 524–536. https://doi.org/10.1016/j.conbuildmat.2018.11.051.

[16] H.F. Campos, N.S. Klein, J. Marques Filho, M. Bianchini, Low-cement high-strength concrete with partial replacement of Portland cement with stone powder and silica fume designed by particle packing optimization, J. Clean. Prod. 261 (2020). https://doi.org/10.1016/j.jclepro.2020.121228.

[17] G. Andrade, G. Puente, D. Andrade, G. De Castro, M. Pepe, R. Dias, T. Filho, Design of structural concrete mixtures containing fine recycled concrete aggregate using packing model, Constr. Build. Mater. 252 (2020) 119091. https://doi.org/10.1016/j.conbuildmat.2020.119091.

[18] M. Anson-Cartwright, Optimization of aggregate gradation combinations to improve concrete sustainability and durability, MASc Thesis, University of Toronto, 2011.

[19] S.A.A.M. Fennis, J.C. Walraven, Using particle packing technology for sustainable concrete mixture design, Heron. 57 (2012) 73–101.

[20] M.N. Mangulkar, S.S. Jamkar, Review of particle packing theories used for concrete mix proportioning, Int. J. Sci. Eng. Res. 4 (2013) 143–148.

[21] C. Trottier, R. Ziapour, A. Zahedi, L. Sanchez, F. Locati, Microscopic characterization of alkali-silica reaction (ASR) affected recycled concrete mixtures induced by reactive coarse and fine aggregates, Cem. Concr. Res. 144 (2021) 106426. https://doi.org/10.1016/j.cemconres.2021.106426.

[22] M. Rashidi, M.C.L. Knapp, A. Hashemi, J.Y. Kim, K.M. Donnell, R. Zoughi, L.J. Jacobs, K.E. Kurtis, Detecting alkali-silica reaction: A multi-physics approach, Cem. Concr. Compos. 73 (2016) 123–135. https://doi.org/10.1016/j.cemconcomp.2016.07.001.

[23] B. Fournier, M.-A. Bérubé, Alkali–aggregate reaction in concrete: a review of basic concepts and engineering implications, Can. J. Civ. Eng. 27 (2000) 167–191.

[24] J. Lindgård, Ö. Andiç-Çakir, I. Fernandes, T.F. Rønning, M.D.A. Thomas, Alkali-silica reactions (ASR): Literature review on parameters influencing laboratory performance testing, Cem. Concr. Res. 42 (2012) 223–243. https://doi.org/10.1016/j.cemconres.2011.10.004.

[25] L.F.M.L.. Sanchez, B.. Fournier, M.. Jolin, J. Duchesne, Reliable quantification of AAR damage through assessment of the Damage Rating Index (DRI), Cem. Concr. Res. 67 (2015) 74–92. https://doi.org/10.1016/j.cemconres.2014.08.002.

[26] L. Sanchez, B. Fournier, M. Jolin, D. Mitchell, J. Bastien, Overall assessment of Alkali-Aggregate Reaction (AAR) in concretes presenting different strengths and incorporating a wide range of reactive aggregate types and natures, Cem. Concr. Res. 93 (2017) 17–31. https://doi.org/10.1016/j.cemconres.2016.12.001.

[27] B. Fournier, R. Chevrier, A. Bilodeau, P.-C. Nkinamubanzi, N. Bouzoubaa, Comparative Field and Laboratory Investigations on the Use of Supplementary Cementing Materials (SCMs) to Control Alkali-Silica Reaction (ASR) In Concrete, 15th Int. Conf. Alkali-Aggregate React. (ICAAR. (2016).

[28] M.H. Shehata, M.D.A. Thomas, Use of ternary blends containing silica fume and f ly ash to suppress expansion due to alkali-silica reaction in concrete, Cem. Concr. Reserach. 32 (2002) 341–349. https://doi.org/10.1016/S0008-8846(01)00680-9.

[29] CSA A23.2-27A, Standard pratice to identify degree of alkali-reactivity of aggregates and to indentify measures to avoid deleterious expasion in concrete, CSA International, Mississauga, Ontario (Canada), 2009.

[30] W. Yujiang, A.E. Deng, M. Ae, T. Mingshu, Alkali release from aggregate and the effect on AAR expansion, Mater. Struct. 41 (2008) 159–171. https://doi.org/10.1617/s11527-007-9227-z.

[31] M.-A. Berube, J. Frenette, Testing Concrete for AAR in NaOH and NaCl solutions at 38°C and 80°C, Cem. Concr. Compos. 16 (1994) 189–198.

[32] S.U. Einarsdóttir, Modifications to Laboratory Test Methods to Evaluate the Beneficial Effects of Low-Alkali Binders on the Alkali-Silica Reaction Modifications to Laboratory Test Methods to Evaluate the Beneficial Effects of Low-Alkali Binders on the Alkali-Silica Reaction, University of Toronto, 2017.

[33] S.U. Einarsdottir, R. Douglas Hooton, Modifications to ASTM C1293 that allow testing of low-Alkali binder systems, ACI Mater. J. 115 (2018) 739–747. https://doi.org/10.14359/51702350.

[34] Z.S. Ali, M. Hosseinpoor, A. Yahia, New aggregate grading models for low-binder self-consolidating and semi-self-consolidating concrete (Eco-SCC and Eco-semi-SCC), Constr. Build. Mater. 265 (2020) 120314. https://doi.org/10.1016/j.conbuildmat.2020.120314.

[35] B. Esmaeilkhanian, K.H. Khayat, O.H. Wallevik, Mix design approach for low-powder self-consolidating concrete: Eco-SCC-content optimization and performance, Mater. Struct. 50 (2017) 18. https://doi.org/10.1617/s11527-017-0993-y.

[36] R. Kurad, J.D. Silvestre, J. de Brito, H. Ahmed, Effect of incorporation of high volume of recycled concrete aggregates and fly ash on the strength and global warming potential of concrete, J. Clean. Prod. 166 (2017) 485–502. https://doi.org/10.1016/j.jclepro.2017.07.236.

[37] W. Nguyen, D.M. Martinez, G. Jen, J.F. Duncan, C.P. Ostertag, Interaction between global warming potential, durability, and structural properties of fiber-reinforced concrete with high waste materials inclusion, Resour. Conserv. Recycl. 169 (2021) 105453. https://doi.org/10.1016/j.resconrec.2021.105453.

[38] A. Sahraei Moghadam, F. Omidinasab, S. Moazami Goodarzi, Characterization of concrete containing RCA and GGBFS: Mechanical, microstructural and environmental properties, Constr. Build. Mater. 289 (2021) 123134. https://doi.org/10.1016/j.conbuildmat.2021.123134.

[39] B.L. Damineli, F.M. Kemeid, P.S. Aguiar, V.M. John, Measuring the eco-efficiency of cement use, Cem. Concr. Compos. 32 (2010) 555–562.

[40] O.H. Wallevik, W.I. Mansour, F.H. Yazbeck, T.I. Kristjansson, EcoCrete-Xtreme: Extreme performance of a sustainable concrete, Proc. Int. Symp. Eco-Crete. (2014) 3–10.

[41] B.L. Damineli, V.M. John, Developing Low CO2 Concretes: Is Clinker Replacement Sufficient? The Need of Cement Use Efficiency Improvement, in: Key Eng. Mater. Trans Tech Publ., 2012: pp. 342–351.

[42] S. Kumar, M. Santhanam, S. Kunar, M. Santhanam, Particle packing theories and their application in concrete mixture proportioning : A review, Indian Concr. J. 77 (2003) 1324–1331.

[43] J.E. Funk, D.R. Dinger, Predictive process control of crowded particulate suspensions, 1st ed., New York, 1994. https://doi.org/10.1007/978-1-4615-3118-0.

[44] P. Goltermann, V. Johansen, L. Palbøl, Packing of Aggregates : An Alternative Tool to Determine the Optimal Aggregate Mix, ACI Mater. J. (1997) 435–442.

[45] I. Mehdipour, K.H. Khayat, Understanding the role of particle packing characteristics in rheo-physical properties of cementitious suspensions : A literature review, Constr. Build. Mater. 161 (2018) 340–353.

[46] S.A.A.M. Fennis, J.C. Walraven, Using particle packing technology for sustainable concrete mixture design, Heron. 57 (2012) 73–101.

[47] S.A.A.M. Fennis, J.C. Walraven, J.A. den Uijl, Compaction-interaction packing model: regarding the effect of fillers in concrete mixture design, Mater. Struct. 46 (2013) 463–478. https://doi.org/10.1617/s11527-012-9910-6.

[48] D.J. De Souza, L.F.M. Sanchez, M.T. De Grazia, Evaluation of a direct shear test setup to quantify AAR-induced expansion and damage in concrete, Constr. Build. Mater. 229 (2019). https://doi.org/10.1016/j.conbuildmat.2019.116806.

[49] C.S. Shon, S.L. Sarkar, Evaluation of modified ASTM C 1260 accelerated mortar bar test for alkali-silica reactivity, Cem. Concr. Res. 32 (2002) 1981–1987. https://doi.org/10.1016/S0008-8846(02)00903-1.

[50] ASTM C1293, Standard Test Method for Determination of Length Change of Concrete Due to Alkali-Silica Reaction, West Conshohocken, 2018. https://doi.org/10.1520/C1293-18.

[51] Y. Kawabata, K. Yamada, Y. Sagawa, S. Ogawa, Alkali-Wrapped Concrete Prism Test (AW-CPT) - New testing protocol toward a performance test against alkali-silica reaction, J. Adv. Concr. Technol. 16 (2018) 441–460. https://doi.org/10.3151/jact.16.441.

[52] J. Lindgård, E.J. Sellevold, M.D.A. Thomas, B. Pedersen, H. Justnes, F. Rønning, Alkali-silica reaction (ASR)-performance testing: Influence of specimen pre-treatment, exposure conditions and prism size on concrete porosity, moisture state and transport properties, Cem. Concr. Res. 53 (2013) 145–167. https://doi.org/10.1016/j.cemconres.2013.05.020.

[53] M.-A. Bérubé, J. Duchesne, J.F. Dorion, M. Rivest, Laboratory assessment of alkali contribution by aggregates to concrete and application to concrete structures affected by alkali-silica reactivity, Cem. Concr. Res. 32 (2002) 1215–1227.

[54] P. Rivard, M.A. Bérubé, J.P. Ollivier, G. Ballivy, Decrease of pore solution alkalinity in concrete tested for alkali-silica reaction, Mater. Struct. Constr. 40 (2007) 909–921. https://doi.org/10.1617/s11527-006-9191-z.

[55] B. Fournier, J.H. Ideker, K.J. Folliard, M.D.A. Thomas, P.C. Nkinamubanzi, R. Chevrier, Effect of environmental conditions on expansion in concrete due to alkali-silica reaction (ASR), Mater. Charact. 60 (2009) 669–679. https://doi.org/10.1016/j.matchar.2008.12.018.

[56] V. Villeneuve, B. Fournier, Determination of the damage in concrete affected by ASR–the damage rating index (DRI), in: 14th Int. Conf. Alkali-Aggregate React. Concr., Austin (Texas), 2012: p. electronic.

[57] R.-P. Martin, L. Sanchez, B. Fournier, F. Toutlemonde, Evaluation of different techniques for the diagnosis & prognosis of Internal Swelling Reaction (ISR) mechanisms in concrete, Constr. Build. Mater. 156 (2017) 956–964.

[58] L.F.M. Sanchez, T. Drimalas, B. Fournier, D. Mitchell, J. Bastien, Comprehensive damage assessment in concrete affected by different internal swelling reaction (ISR) mechanisms, Cem. Concr. Res. 107 (2018) 284–303.

[59] A. Zahedi, L. Saliba, L. Sanchez, A.J. Boyd, Reliability of the Damage Rating Index to Assess Condition of Concrete Affected by External Sulfate Attack, Mag. Concr. Res. (2022) 1–14. https://doi.org/10.1680/jmacr.22.00061.

[60] C. Trottier, A. Zahedi, R. Ziapour, L. Sanchez, F. Locati, Microscopic assessment of recycled concrete aggregate (RCA) mixtures affected by alkali-silica reaction (ASR), Constr. Build. Mater. 269 (2021). https://doi.org/10.1016/j.conbuildmat.2020.121250.

[61] N. Smaoui, B. Bissonnette, B. Fournier, B. Durand, Mechanical Properties of ASR-Affected Concrete Containing Fine or Coarse Reactive Aggregates, ASTM Int. 3 (2006) 1–16. https://doi.org/10.1520/JAI12010.

[62] ASTM C136, Standard test method for sieve analysis of fine and coarse aggregates., (2016) 8.

[63] A. Leemann, B. Lothenbach, C. Thalmann, Influence of superplasticizers on pore solution composition and on expansion of concrete due to alkali-silica reaction, Constr. Build. Mater. 25 (2011) 344–350. https://doi.org/10.1016/j.conbuildmat.2010.06.019.

[64] M.T. De Grazia, L. Sanchez, R.C.O. Romano, R.G. Pileggi, Investigation of Alfred Model Effect on the Fresh and Hardened State Properties of Low-Cement Content (LCC) Systems, Constr. Build. Mater. Accepted (2017) 1–26.

[65] D.J. De Souza, M. T. de Grazia, H.F. Macedo, L. F.M. Sanchez, G. P. de Andrade, O. Naboka, G. Fathifazl, P.C. Nkinamubanzi, Influence of the Mix Proportion and Aggregate Features on the Performance of Eco-Efficient Fine Recycled Concrete Aggregate Mixtures, Materials (Basel). 15 (2022) 1–27. https://doi.org/10.3390/ma15041355.

[66] M. T. de Grazia, H. Deda, L. F.M. Sanchez, The influence of the binder type & aggregate nature on the electrical resistivity of conventional concrete, J. Build. Eng. 43 (2021) 102540. https://doi.org/10.1016/j.jobe.2021.102540.

[67] P. Azarsa, R. Gupta, Electrical Resistivity of Concrete for Durability Evaluation: A Review, Adv. Mater. Sci. Eng. 2017 (2017). https://doi.org/10.1155/2017/8453095.

[68] R.C.D.O. Romano, D. Dos, R. Torres, R.G. Pileggi, Impact of aggregate grading and air-entrainment on the properties of fresh and hardened mortars, Constr. Build. Mater. 82 (2015) 219–226.

[69] C. Trottier, M.T. de Grazia, H.F. Macedo, L.F.M. Sanchez, G.P. de Andrade, D.J. de Souza, O. Naboka, G. Fathifazl, P.C. Nkinamubanzi, A. Demers, Freezing and Thawing Resistance of Fine Recycled Concrete Aggregate (FRCA) Mixtures Designed with Distinct Techniques, Materials (Basel). 15 (2022) 1–23. https://doi.org/10.3390/ma15041342.

[70] Giatec Scientific, Surf ^{TM} User Manual, Version 2.1, n.d.

[71] M. T. de Grazia, N. Goshayeshi, R. Gorga, L. F.M. Sanchez, A.C. Santos, D.J. Souza, Comprehensive semi-empirical approach to describe alkali aggregate reaction (AAR) induced expansion in the laboratory, J. Build. Eng. 40 (2021). https://doi.org/10.1016/j.jobe.2021.102298.

Chapter Eight: Assessment of Laboratory Test Procedures to Evaluate ASR-Induced Expansion and Deterioration of Eco-Efficient Concrete

De Grazia, M. T.[a], Trottier, C.[a], Sanchez, L. F. M.[b]

[a] Ph.D. Candidate – University of Ottawa, Department of Civil Engineering, ON, Canada.

[b] Associate Professor – University of Ottawa, Department of Civil Engineering, ON, Canada.

Abstract

The concrete prism test (CPT) is considered the most reliable laboratory test procedure for determining aggregate reactivity. However, the CPT has some important drawbacks: the amount of leaching occurring over the test period, which may jeopardize the test outcomes. To avoid leaching, the amount of alkalis in the CPT specimens is boosted by the addition of NaOH into the mixing water; this action disables the evaluation of the reactivity of aggregates in low alkali mixtures. This work aims to assess the efficiency of three proposed test setups (wrapped, soaked, and encapsulated) to appraise ASR-induced expansion and damage development of non-boosted mixtures with low amount of alkalis (3.61, 2.79, and 2.15 kg/m^3) in the laboratory. Results indicate that, regardless of the testing protocol selected, mixtures achieved similar final expansions when the total system alkali content is over 3.01 kg/m^3; below that, cement alkali content governs the distress features.

Keywords: *alkali-aggregate reaction (ASR), low alkali system, laboratory test methods, particle packing models, microscopic characterization, crack propagation, damage rating index (DRI).*

8.1 Introduction

The concrete construction industry has been a target for emitting an important amount of greenhouse gases globally thus, reducing the overall adverse effects of concrete production has remained the focus of several researchers worldwide. As the production of cement emits 7.5% of the global CO_2, approaches to reduce its content in concrete have been proposed from using alternatives such as supplementary cementitious materials (SCM) to optimizing its usage through particle packing models (PPM) [1–3]. Although concrete materials with a low cement content present advantages in terms of sustainability and have been shown to provide targeted mechanical properties [4–7], concrete used in the field will be exposed to numerous environmental conditions and durability-related issues which may compromise its service life and counteract the sustainability aspect of the material. Moreover, lowering the cement content in concrete corresponds to a reduction in the total alkalis in the system which leads to a decrease in concrete pH. As a result, the concrete's natural ability to control some durability-related issues such as corrosion of steel reinforcement bars due to carbonation may be negatively affected; conversely, this reduction may be extremely beneficial when the concrete bears aggregates prone to develop alkali-silica reaction (ASR). ASR is a chemical reaction between the alkali hydroxides (Na^+, K^+ and OH^-) from the concrete pore solution and some unstable phases from the aggregates used to make concrete. ASR generates a secondary product (i.e., silica gel) that swells upon water uptake, leading to induced expansion and cracking.

Over the last decades, a number of test procedures and recommendations were developed to appraise the potential reactivity of aggregates and the efficiency of preventive measures against ASR-induced development. Amongst those, the accelerated mortar bar test – AMBT (ASTM C1260 and CSA A23.2-25A and the concrete prism test – CPT (ASTM C1293 and CSA A23.2-14A) are by far the

most used and accepted worldwide. Both the AMBT and CPT are test procedures conducted to evaluate the potential reactivity of aggregates in the laboratory prior to their use. One of the primary benefits of the AMBT, which has led to its widespread use around the world, is its short time period (16 days) and low cost. Yet, after a number of research programs, it has been found that the AMBT presents important drawbacks when assessing the aggregates' reactivity and preventive measures in the laboratory, such as crushing of the aggregates (which may alter the composition and texture of the aggregate) and harsh conditions of the test, leading to false positive and false negative results [8,9]). Conversely, the CPT was found to be a much more reliable test procedure, simulating with more accuracy the expansive behaviour of aggregates and the efficiency of preventive measures in concrete. Nevertheless, it is quite long time period (12 months or 24 months, either for aggregates or preventive measures appraisal, respectively) along with the excessive leaching of the alkalis [9–11] observed over the test. To avoid high discrepancies between induced expansion results obtained through the CPT in the laboratory and those of concrete exposed to field conditions, concrete mixtures fabricated and tested in the CPT must be boosted by 40% of the cement alkalis, which is frequently the amount of leaching observed during a 1-year test [31,49-52]. Although this action can overcome leaching issues in conventional concrete (CC), CPT might present problems for evaluating the performance of low alkali systems developed with or without supplementary cementitious materials (SCM) [11,12]. In this context, Einarsdottir and Hooton [11] investigated distinct modifications to CPT setup to reduce leaching issues and improve the performance of this protocol when evaluating low-alkali binder concrete mixtures. Besides the CPT, different non-standard laboratory test methods (e.g., alkali-wrapped concrete prism test (AW-CPT), concrete cylinder test (CCT), and soaked/immersed) have been suggested in the literature [13–19] as advanced techniques to evaluate ASR expansion in concrete without leading to leaching issues. Although these protocols

present many advantages over CPT [10,11,16,19–21], further studies are required to confirm the best approach to evaluating ASR-developed in low-alkali systems. Therefore, the purpose of this work is to compare the development of ASR-expansion in low-alkali mixtures using various test setups in comparison to the standard method and to assess the influence of the alkali boost in low-alkali systems.

8.2 Background

8.2.1 Alkali-silica reaction (ASR) in conventional concrete (CC)

Alkali-Silica Reaction (ASR) continues to be one of the most prominent distress mechanisms in concrete leading to pre-mature deterioration. ASR is a chemical reaction that occurs between the unstable silica found within the aggregates and the alkalis present in concrete's pore solution (Na^+, K^+ and OH^-). This reaction forms a secondary product (i.e., silica gel) that is hygroscopic and swells upon water uptake. The pressure exerted by this swelling causes tensile stresses larger than those that the aggregate can resist; hence, cracking the reactive aggregates. With the development of ASR, the cracks propagate from the reactive aggregates into the cement paste, in which significant losses in mechanical properties have been reported in previous studies [22–27]. Generally, ASR-induced deterioration (crack pattern: crack generation and propagation) in CC begins with the generation of cracks inside the aggregate particles; those cracks increase in length and width and eventually propagate to the cement paste with the increase in expansion, as shown in Figure 8.1, regardless of the aggregate nature and crack type (i.e., sharp type cracks -A and onion skin type cracks B).

The loss in mechanical properties consequently corresponds to the location of the crack and the extent of the crack propagation where cracks within the aggregate will influence the modulus of elasticity as this property is governed by the aggregate and its bond to the cement paste whereas the

compressive strength will be significantly compromised when cracks have extended into the cement paste [27–29]. Moreover, the aggregate interlock affecting the shear strength of the concrete is diminished at early stages of ASR damage [30,31].

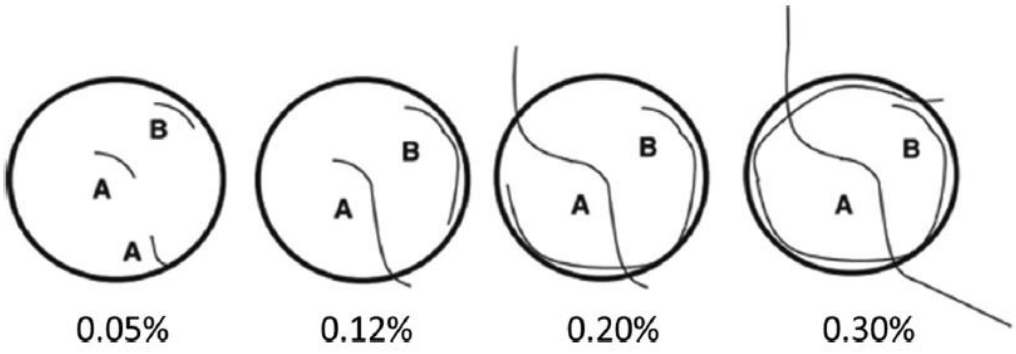

Figure 8.1. Qualitative model of crack propagation in ASR-affected CC as proposed by Sanchez et al. [26].

Previous studies have reported that such damage can be further understood by combining mechanical tests (i.e., modulus of elasticity, compressive strength, Stiffness Damage Test (SDT) [29]) with microscopic tests (i.e., damage rating index – DRI [26,32]). The primary advantage of incorporating the DRI, a semi-quantitative and qualitative microscopic tool, is its ability to understand the cause and extent of damage in concrete while correlating it with the expansion level. [26,32]. The DRI is therefore conducted on sawn, ground, and polished concrete sections (200 mm x 100 mm) using a stereomicroscope at 15-16x magnification. The distress features (i.e., cracks) are then counted in a grid composed of squares of 1 cm^2 on the polished reflective surface after which weighting factors are applied to the distinct distress features based on their importance towards a certain distress mechanism and the weighted sums are normalized to 100 cm^2 for comparative purposes. The weighting factors were selected based on the severity of the feature [33], where: the lowest factor of 0.25 is attributed to closed cracks in the aggregate (CCA) most likely caused by weathering or processing as opposed to being associated to ASR damage; a factor of 2 denotes the

progression of ASR within the aggregate results in open cracks in the aggregate without or with gel (OCA and OCAG, respectively) and; the extension of cracks in the cement paste without or with gel (CCP and CCPG, respectively) are captured by a weighting factor of 3. In 2015, Sanchez et al. [26] proposed the extended version of the DRI that evaluates the distress features without the weighting factors as counts/100 cm^2 and percentages along with the crack density which is the sum of the OCA+OCAG and CCP+CCPG as counts/cm^2, providing additional insight into understanding the propagation of ASR-induced cracks.

8.2.2 Low alkali concrete affected by Alkali-Silica Reaction (ASR)

Fournier et al. [34] evaluated the influence of ASR-induced development of concrete mixtures incorporating a variety of reactive fine and coarse aggregates and two alkali loadings (boosted and non-boosted). Mixtures with boosted alkalis have their equivalent alkalis in the cement (Na_2O_e) raised to 1.25 kg/m^3 (i.e., total alkali content of 5.25 kg/m^3) as per the CPT standard (ASTM C 1293), while non-boosted mixtures contain 0.90% of Na_2O_e (i.e., total alkali content of 3.78 kg/m^3). Regardless of the aggregate reactivity, the boosted mixtures resulted in greater expansions over time due to the higher alkali content of the system. Yet, the aggregate type and nature have a significant impact on the expansion development of concrete containing varying amounts of alkalis. When incorporating reactive aggregates with varying reactive potentials (i.e., ultra-high/very high, high, and moderate/marginal), mixtures developed with an alkali content of 3.78 kg/m^3 (non-boosted) achieved on average 18%, 27%, and 43% lower expansions, respectively, than conventional CPT mixtures (boosted mixtures) [34]. To complement this study, de Grazia et al. [35] proposed a modified version of Larive's model to evaluate ASR-evolution under laboratory test conditions. It was concluded that, in addition to the aggregate type and nature, three other factors, such as

temperature, total alkali content, and relative humidity, are major contributors to ASR-development and must be considered to describe ASR-induced expansion more precisely in the laboratory.

Likewise, Einarsdottir and Hooton [11] also evaluated low-alkali binder concrete mixtures and proposed different methods to modify the CPT method and reduce leaching issues. After two years of testing, mixtures developed with 100% Portland cement (alkali content ranging from 3.35 to 6.06 kg/m^3) leached 25-50% of their alkalis, whereas low-, medium- and high-alkali mixtures (where Portland cement was replaced with 15% to 50% SCMs) leached between 18% and 32%. Thus, boosting the concrete mixtures is recommended, particularly for low-alkali mixtures, which can exhibit a "false" acceptable expansion in laboratory tests due to leaching while deleterious expansion in the field could be observed when conditions are favourable to limit leaching. In addition to alkali boosting, it is suggested to store each specimen in a plastic bag covering two-thirds of its height (from top to bottom) to improve CPT method and minimize leaching on low alkali systems.

8.2.3 Laboratory test techniques to assess low alkali concrete affected by Alkali-Silica Reaction

The CPT protocol has been and still remains the most popular method used to evaluate the potential reactivity of aggregates in concrete (CSA A23.2-14A or ASTM C 1293). In this test, specimens must be stored at 100% relativity humidity (R.H.) and 38^{o}C while their expansion is monitored over 52 weeks [9]. If the specimens achieve a maximum expansion lower than 0.04% at 52 weeks, the aggregate investigated can be considered non-reactive. However, controversy exists regarding this method due to excessive leaching of the alkalis [9–11]. To minimize the impact of leaching on expansion values, concrete mixtures assessed under CPT conditions must be boosted (i.e., addition of alkalis to the concrete mixture) to 40% of the cement alkalis, which is equivalent to the total alkali

leaching that will occur during a 1-year test [9,11]. As such, if a cement with Na_2O_{eq} of 0.90% is selected, the concrete mixtures must be boosted to 1.25% Na_2O_{eq} to meet the 40% boost requirement.

Despite the fact that the CPT is currently used worldwide, different non-standard laboratory test methods [14–16] have been suggested in the literature as an advanced method to evaluate ASR expansion in concrete without leading to leaching issues.

Lindgård et al. [14,15] evaluated four concrete mixtures using modified versions of the draft RILEM aggregate concrete prism tests; AAR-3, 2000 (38 °C, wrapped prisms) [13] tested at 38 °C and 60 °C then compared to the standard CPT. Basically, the wrapped method consists in wrapping the concrete specimens in a cotton cloth saturated in a basic solution of 1.5M OH^- or 0.15M OH^- solution, which is equivalent to pH of 14.2 and 13.2, respectively. Since the pH of the cloth is higher than that of the concrete, specimens show greater expansion at 38°C when compared to the CPT, yet, almost no expansion (on average 0.06%) was observed on wrapped specimens when the temperature was increased to 60°C. Similarly, Kawabata et al. [16] proposed the Alkali-Wrapped Concrete Prism Test (AW-CPT) where concrete specimens are wrapped with a saturated cloth, but in this case, the alkali concentration of the solution is calculated using Equation 8.1, mimicking the concrete's pore solution hydroxide ion concentration. Although the alkali leaching was significantly reduced when compared to the CPT method, the alkali content of concrete mixtures was increased by 20% due to the transfer of alkalis from the saturated cloth to the concrete pores, likely due to uptake during the cement hydration [16]. Moreover, it was concluded that at 60°C along with high alkali boosting, the ASR gel was extruded out without significantly expanding the specimen. Temperatures below 40°C were therefore recommended for ASR gel to exert the required tensile pressure within the concrete matrix to cause cracking.

$$[OH^-] = \frac{0386\ x\ Na_2O_{eq}}{w/c}$$ Equation 8.1

Another method proposed by several authors is the soaked method, where concrete specimens are submerged into a NaOH solution at 38ºC and 80 ºC. Yet, concerns were raised about the amount of alkali released by the aggregates when specimens are soaked in different types of solutions (e.g. immersed in 1M NaOH, 1M NaCl or water) [36]. During the first 6 months, specimens soaked in a NaOH solution produced higher expansions compared to those soaked in a NaCl solution, even though the solutions presented the same amounts of alkalis, which might be attributed to the replacement of the OH^- ions released by portlandite and Cl^- ions entering in the pore solution. Then, after one year at 38ºC, mixtures soaked in NaOH expanded less (0.30%) than specimens soaked in NaCl (0.44%). Both soaked conditions, however, resulted in greater expansion than mixtures exposed to standard CPT test conditions (0.20%) [36]. Likewise, Gao et al. [17] studied the soaked method with three different storage concentrations (i.e., 0.77, 1.00, and 1.25 mol/l). It is worth noting that the mixtures' alkali contents were also boosted with NaOH to match the pore solution of the storage solution concentration. It was concluded that when specimens are stored with an abundance of alkalis, the alkali concentration does not affect the expansion. Moreover, it was recommended to use smaller specimens to accelerate the test procedure and achieve the final expansion in a shorter time. [36].

Furthermore, the concrete cylinder test (CCT) was proposed by Naranjo in 2012 [18] and further evaluated [16,19], where a cylindrical mould is used to insulate the concrete specimen from alkali leaching. The specimens are cast shorter than the height of the moulds which are lined with filter paper to transfer water that is ponded on the surface to the concrete's lateral surface. It was therefore

concluded that the CCT provided higher overall expansions after two years. Nonetheless, these three test setups presented promising performance yet, further developments are required to validate their applicability regardless of the system's alkali content and the solution's concentration as well as their ability to be compared to field concrete.

8.3 Scope of the work

Many authors investigated the efficiency of different laboratory tests to appraise ASR-induced expansion and damage in conventional concrete [10,11,16,19–21]; however, concerns remain when using those laboratory tests for low-alkali systems especially due to the addition of alkalis to the concrete mixture to compensate for alkali leaching for one year. Therefore, this study assesses the effectiveness of three different laboratory test setups (i.e., wrapped – W, soaked – S, and encapsulated – E) without the addition of alkalis into the concrete mixtures to evaluate ASR-development of low-alkali systems in comparison to the standardized CPT procedure (i.e., with the addition of alkalis to the concrete mixture). Three mixtures proportioned through an advanced mix-design technique (i.e., particle packing model – PPM and limestone fillers as the primary Portland cement replacement) were developed with systems' alkali contents of 3.61, 2.79, and 2.15 kg/m^3 and one type of highly reactive coarse aggregate (Springhill – Greywacke). Conclusions are then drawn based on results obtained throughout this study: surface electrical resistivity and porosity were measured to assess the impact of the test setup on ASR development in low-alkali and sustainable mixtures. Finally, the damage rating index (DRI) along with its extended version was used to evaluate the overall damage and its extent with respect to expansion achieved per test setup at intervals of 4 months (i.e., 0, 4, 8, 12 months).

8.4 Materials and methods

8.4.1 Materials and mixture proportions

All concrete mixtures used Portland cement (CSA Type GU, ASTM Type 1) with a high alkali content (i.e., 0.86% $Na_2O_{eq.}$). Three initial concrete mixtures were selected to vary the alkali content (i.e., 3.61, 2.79, and 2.15 kg/m^3) by adjusting the cement content (i.e., 420, 325, 250 kg/m^3, respectively) while incorporating a highly reactive coarse aggregate (Springhill – Greywacke) or a highly reactive fine aggregate (Texas – Polymictic sand) to induce ASR expansion and damage in the concrete. Moreover, to further reduce the alkali content of mixtures made with Springhill, cement contents of 200 and 150 kg/m^3 were designed to provide alkali contents of 1.72 and 1.29 kg/m^3. The total alkali content was boosted (when required as per ASTM C1293 and CSA A23.2-14A) by 40%, raising the system's $Na_2O_{eq.,}$ using reagent-grade sodium hydroxide pellets added in mix water to accelerate ASR development. A superplasticizer and mid-range water reducer admixture were required and used for mixtures containing 325 and 250 kg/m^3 and the alkali content was measured through the Inductively Coupled Plasma (ICP) analysis, which was considered negligible, due to their average $Na_2O_{eq.}$contribution of 0.002 kg/m^3 and 0.011 kg/m^3, respectively, when compared to the total alkali content contribution from the cement and added sodium hydroxide [37]. Inert limestone fillers (i.e., a performance (P) filler and a replacement filler (R) having a particle size distribution smaller than and similar to that of the Portland cement used in this study, respectively) were used to reduce the cement content in mixtures containing 250, 200, and 150 kg/m^3 of cement. The particle size distribution of the aggregates was determined through sieve analyses as per ASTM C136/CSA A23.2-2A [38,39], whereas for the limestone filler and Portland cement, a laser diffraction analysis was performed (Figure 8.2). Additional physical properties of the raw material,

including specific gravity, absorptions, and 365 days-expansion measured through CPT test, are presented in Table 8.1.

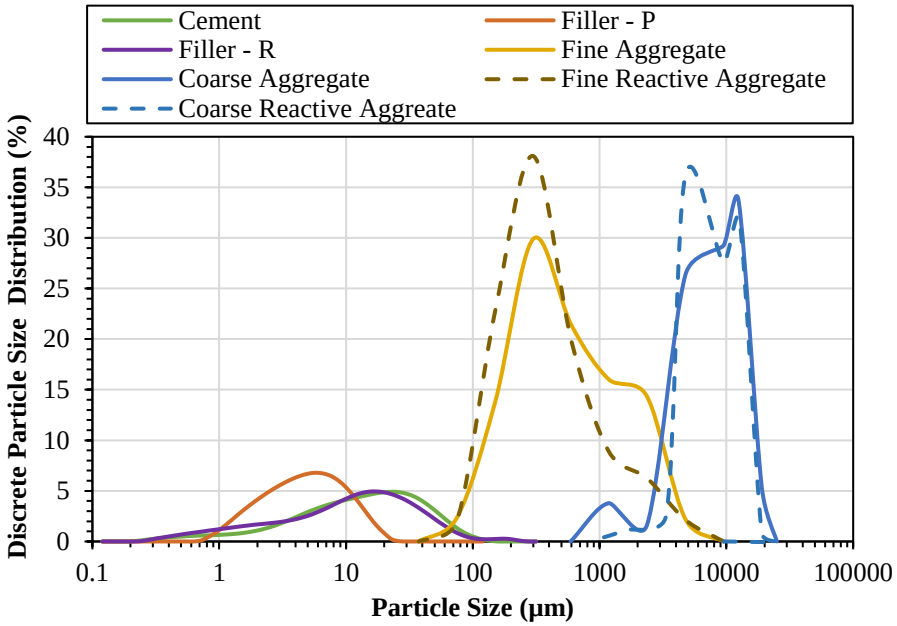

Figure 8.2. Particle size distribution of raw materials.

This study selected four eco-efficient mixtures developed with 325, 250, 200, and 150 kg/m^3 of cement content based on a previous study conducted by the author, in which twelve eco-efficient concrete mixtures were developed through a modified Alfred model combined with mobility parameters (i.e., PPM-MP approach). The modified Andreasen (also known as Alfred model) is one of the most recent continuous PPM [40–45] that takes into account all particle sizes without gaps throughout the particle size distribution, whereas mobility parameters were applied to achieve desirable flowability.

Table 8.1. Physical properties characterization.

Material	Location	Rock type	Specific gravity (g/cm^3)	Absorption (%)	CPT- 365 days, expansion (%)
General Use (GU) cement	Saint-Basile, Quebec (Canada)	-	3.17	-	
Filler - R	Ottawa, Ontario (Canada)	Limestone	2.66	-	
Filler - P	Ottawa, Ontario (Canada)	Limestone	2.60	-	
Non-reactive Fine Aggregate	Bracebridge, Ontario (Canada)	Orthoclase, Quartz, Cristoballite, Albite, Bytowmite, Cordierite, Illite, Muscovite, Larnite	2.74	0.37	0.0177
Fine Reactive Aggregate (Texas -T)	El Paso, Texas (USA)	Polymictic sand (granites, mixed volcanic, quartzite, chert, quartz) [26]	2.59	0.78	
Non-Reactive Coarse Aggregate	Bracebridge, Ontario (Canada)	Granite	2.81	0.71	0.0189
Coarse Reactive Aggregate (Springhill - S)	Fredericton, New Brunswick (Canada)	Greywacke	2.68	0.89	

The mixtures were proportioned to achieve the lowest system's porosity through the Alfred model, where q-factors of 0.34 and 0.31 ±0.1 in the powder (Equation 8.2) and aggregate (Equation 8.3) portion, respectively, were selected, yielding a final system with dry porosity of 3.0% ±0.1 (calculated with the modified Westman and Hugill algorithm [43].)

Powder portion (from D_s to 80 μm)

$$CPFT = 100 * \left(\frac{{D_P}^{0.34} - {D_S}^{0.34}}{0.8^{0.34} - {D_S}^{0.34}} \right) \quad \text{Equation 8.2}$$

Aggregates portion (from 0.15 mm to D_L)

$$CPFT = 100 * \left(\frac{{D_P}^{0.31} - 0.15^{0.31}}{{D_L}^{0.31} - 0.15^{0.31}} \right) \quad \text{Equation 8.3}$$

where D_P is the particle size in question, CFPT is the cumulative percent finer than D_P, D_L and D_S is the largest and smallest particle size in the system, respectively, and q is a distribution factor (q-factor).

Furthermore, all mixtures present the same mortar factor of 61%, which maintains the same amount of aggregate consistent within the low alkali mixtures. Additionally, a control mixture was developed with a cement content of 420 kg/m^3, as per ASTM C1293/CSA A23.2-14A [9]). The summary of the five mixtures selected in this study is presented in Figure 8.3 and Table 8.2.

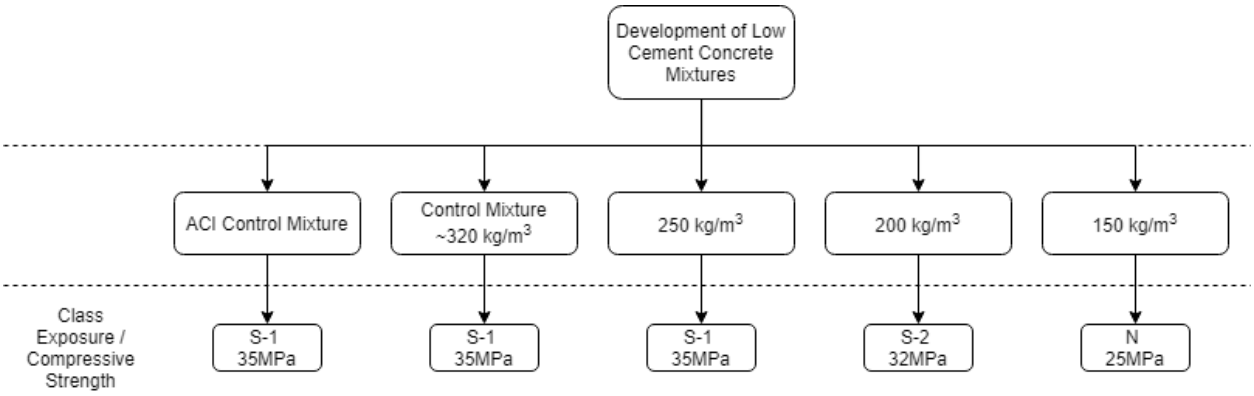

Figure 8.3. Summary characteristics of the mixtures evaluated.

The concrete mixtures were named based on their level of cement content (Number 1 means the concrete with the most cement, while number 5 means that with less cement.), test protocol (C–T - C, Wrapped - W, Soaked - S, and Encapsulated – E), cement content, mix-design selected (i.e., A: ACI method and P: PPM method), reactive aggregate incorporated (Springhill - S and Texas -T), and boosting conditions (BST – boosted mixtures and NBST – non boosted mixtures). For example, mixture 1C-420A-S: (1) has the highest amount of cement content; (C) is tested using the CPT test setup; (420) contains 420 kg/m^3 of cement content, (A) is developed with ACI mix-design method, and (S) contains Springhill as reactive aggregate. It is worth noting that Table 8.2 replaces the test protocol letters (C, W, S, or E) with X reactive aggregate letters (S or T) with Y, and boosting

conditions (concrete mixture boosted with alkalis - BST or non-boosted - NBST) with Z, as these parameters have no effect on the mix-proportions.

Table 8.2. Mix-design of eco-efficient concrete mixtures selected to be evaluated for long-term performance.

Mix-name	kg/m³													
		Powder		Fine Aggregate				Coarse Aggregate						
	OPC	Filler P	Filler R	150-300	300-600	600-1180	1180-2360	2360-4750	4750-9500	9500-12500	12500-19000	Water	SP	MR
1X-420A-Y-Z	420	0	0	860	0	0	0	0	311	302	302	189	0	0
2X-325P-Y-Z	325	0	0	132	163	197	250	313	376	173	293	179	1.9	1.9
3X-250P-Y-Z	250	41	33	137	170	205	260	326	392	180	306	145	3.9	3.2
4X-200P-Y-Z	200	42	81	141	174	210	267	334	402	184	313	124	0	0
5X-150P-Y-Z	150	42	122	144	177	213	268	333	397	182	308	126	0	0

Note: labels #X replace test protocol letters (C, W, S, or E), A represents the ACI mix-design method, P represents the PPM mix-design method, #Y replaces reactive aggregate letters (S or T), #Z replaces BST (boosted) or NBST (non-boosted), OPC stands for ordinary Portland Cement, SP stands for Superplasticizer and MR stands for mid-range admixture.

8.4.2 Fabrication of concrete specimens

A total of 384 cylinders (100 mm diameter x 200 mm length) were fabricated in the laboratory to appraise concrete made with a reactive coarse aggregate, whereas 144 cylinders were manufactured to assess the ASR development of a reactive fine aggregate.

Forty litres of concrete were manufactured for each of the twenty-two mixtures. The specimens were left to moist-cure (i.e., 23°C and 100% RH) for 24 hours, demoulded and moist-cured under the same conditions for an additional 24 hours after which small holes of 8.5 mm in diameter and 19 mm in length were drilled into both ends of the cylinders in preparation for stainless steel stud installation used for longitudinal expansion measurements. The studs were glued to each end of the cylinder with a fast-setting cement paste slurry, and left to moist-cure under the same aforementioned conditions for 24 hours. Initial measurements (i.e., “0” readings) were performed between 24 and 48 hours after the studs were installed. Then, the specimens were stored based on conditions to accelerate ASR-induced expansion through one of the four test protocols and

monitored over time. The mass change and longitudinal expansion measurements were performed monthly on all cylinders.

8.4.3 Test setups to evaluate ASR-induced expansion in the laboratory

Four test protocols (CPT - C, wrapped - W, soaked - S, and encapsulated – E) were selected (Figure 8.4). It is worth noting that mixtures developed to be tested under CPT conditions have a 40% alkali boost, whereas the others are non-boosted mixtures in contact or soaked in a 0.4M solution of NaOH which mimics the concrete pore solution molarity [37,46,47] to minimize the leaching effects as presented in previous studies [37,46,47]. A summary of the CPT mixtures' alkali contents is therefore shown in Table 10.3 and each protocol is further described in the following sections.

Table 8.3. Total, initial and added alkalis of CPT-mixtures with 40% boosting of alkalis.

Mixture	Concrete total alkali content (kg/m^3)	Cement alkali content (kg/m^3)	Amount of alkali added for boosting (kg/m^3)
1X-420A-Y-Z	5.06	3.61	1.44
2X-325P-Y-Z	3.91	2.79	1.12
3X-250P-Y-Z	3.01	2.15	0.86
4X-200P-Y-Z	2.41	1.72	0.69
5X-150P-Y-Z	1.81	1.29	0.52

8.4.4 Concrete prism test

The first test setup is the concrete prism test (CPT) which is a standardized method where specimens must be stored at 100% relativity humidity (R.H.) and 38^{o}C [9,48]. Specimens were then stored over water using a plastic rack into sealed 22-litre plastic buckets lined with a piece of moisture-wicking fabric to ensure 100% R.H. throughout the pail, as shown in Figure 8.5a. However, this method is known to be subjected to excessive leaching of the alkalis, thus leading to lower expansion [9–11]. To minimize the impact on the expansion values, concrete mixtures fabricated to be tested under CPT conditions must be boosted to 40% of the cement alkalis, by adding alkalis to the concrete's

mixing water, which is equivalent to the total alkali leaching that will occur during a 1-year test [9,11].

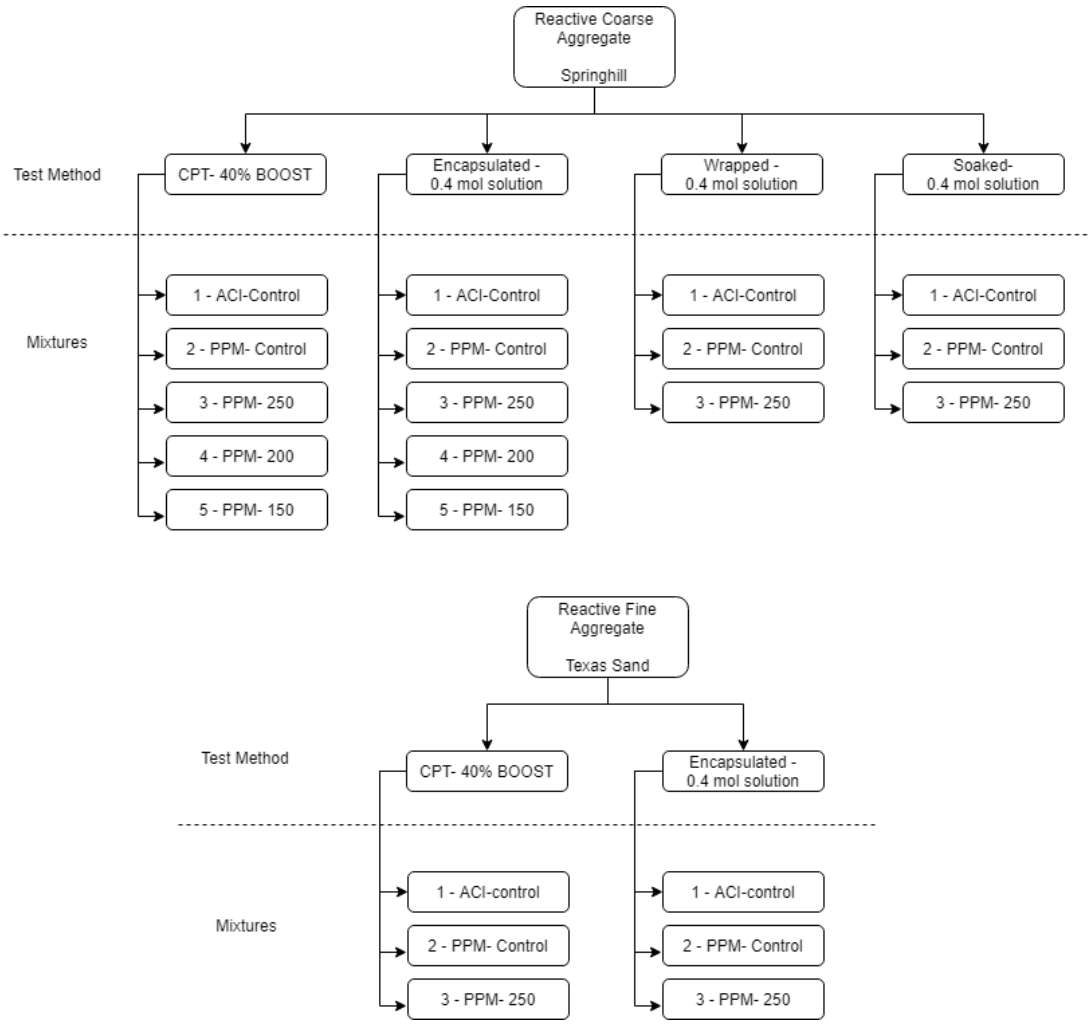

Figure 8.4. Summary AAR test setup methods and mixtures appraised.

8.4.4.1 Encapsulated method

Based on the Concrete Cylinder Test (CCT) method [16,18,19], concrete specimens were then placed inside polyethylene-low density plastic bags with 50 ml in 0.4 M NaOH solution and stored at 38ºC. Air was expelled from the plastic bags, and they were tied with elastic bands to ensure the solution was in contact with the specimen as shown in Figure 8.5b.

8.4.4.2 Wrapped method

Similar to the method developed by [14,15], concrete specimens were wrapped in a wet non-woven cloth soaked in the 0.4 M NaOH solution and covered with polyethylene-film and exposed to a temperature of 38^{o}C (Figure 8.5c).

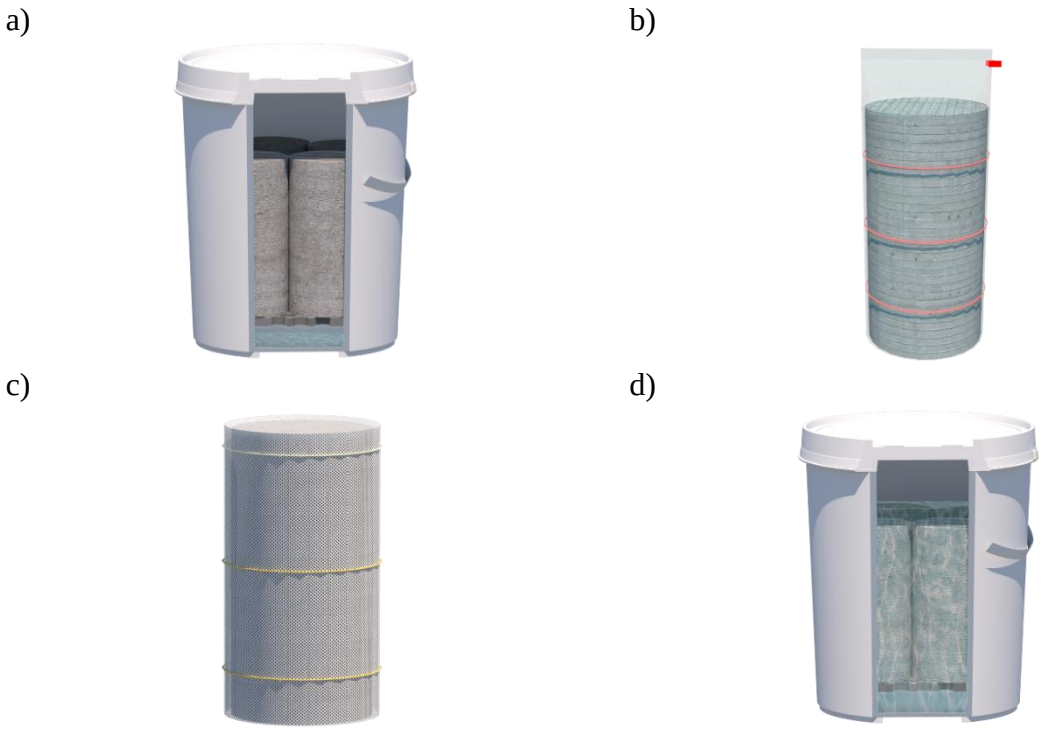

Figure 8.5. Testing setups a) CPT, b) Encapsulated, c) Wrapped, and d) Soaked

8.4.4.3 Soaked method

Similar to previous studies [17,36], specimens were fully submerged in a 0.4 M NaOH solution in sealed 22-litre plastic pails and stored at 38^{o}C. To ensure that all surfaces of the specimens were in contact with the solution, plastic racks were placed at the bottom of the buckets (Figure 8.5d).

8.4.5 Test procedure to appraise ASR-induced deterioration

8.4.5.1 Surface electrical resistivity and apparent porosity

The surface electrical resistivity and apparent porosity were performed at 0-, 4-, 8-, and 12-month to evaluate the microstructure and the durability performance of concrete mixtures subjected to ASR over one year. The surface electrical resistivity was performed using the four-probe (Wenner-array) technique with a commercially available device that automatically displays the surface electrical resistivity (i.e., measured between four equipment probes). The apparent porosity was performed based on Archimedes immersion method [49]. First, the initial apparent porosity was determined at 28 days (i.e., stored in conditions without enabling ASR as per [29]) and all subsequent apparent porosity measurements were performed every four months of ASR exposure conditions. On the day of testing, one specimen of each mixture was divided into three equal slices, each measuring roughly 100 mm in diameter and 65 mm in height. The slices were placed in an oven at 60°C to avoid cement hydration product decomposition caused by elevated temperatures until mass stabilization which occurred after 5 days of drying. The specimens' dry mass (m_d) was determined when the difference between two successive weights was less than 0.3%; previous trials were performed to conclude that 0.3% of mass changed resulting in an apparent porosity difference smaller than 10%. The slices were then immersed in water and vacuumed for 24 hours to ensure water penetration. After that, the immersed (m_i) and wet (m_w) mass values were measured and the apparent porosity (AP) was calculated using Equation 8.4.

$$\text{AP}\ (\%) = \frac{m_w - m_i}{m_w - m_d} * 100\% \qquad \text{Equation 8.4}$$

8.4.5.2 The damage rating index (DRI)

The Damage Rating Index (DRI) is a semi-quantitative microscopic tool developed to assess the cause and extent of ASR damage in conventional concrete using a stereomicroscope at 15-16x

magnification [26,27]. Concrete cylinders, which were cut longitudinally in half, were subjected to microscopic examinations at 0-, 4-, 8-, and 12-month following ASR exposure conditions. After cutting the cylinders using a masonry saw equipped with a notched diamond blade, the specimens were prepared using a mechanical rotating steel wheel to which magnetic grinding and polishing disks are attached whose grits are 30, 60, 140, 280 (80-100 µm), 600 (20-40 µm), 1200 (10-20 µm) and 3000 (4-8 µm). Once a flat and reflective surface was achieved, the DRI and microscopic examinations were performed and distress features (i.e., cracks) associated with ASR damage were counted in a grid of one cm^2 squares placed on the surface of the polished concrete section. Then, weighting factors, based on ASR distress mechanisms, are given to the observed distress features to balance their value and the final DRI number is computed as per the total of the weighted values normalized to 100 cm^2 for comparative purposes [33]. Further investigation of the crack distribution and characteristics for each mixture affected by ASR was conducted using the extended version of the DRI described by Sanchez et al. [33]., which includes microscopic features as counts per 100 cm^2, microscopic features as proportions (%), and crack density (i.e., the sum of open cracks in the aggregate and cement paste with and without gel per 1 cm^2).

8.5 Results

8.5.1 ASR kinetics and development in low alkali concrete mixtures

The mass gain and expansion over time were measured for a period of one year for each concrete mixture exposed to the various testing conditions used in this study (Figure 8.6). The following figures are displayed per concrete mixture type (i.e., cement content) while the alkali content within the mixture varies with the type of setup used. Therefore, the alkali contents displayed in Figure 8.6a, which presents concrete made with a cement content of 420 kg/m^3, are 5.06 kg/m^3 for the mixture made using the CPT procedure (i.e., boosted – BST) and 3.61 kg/m^3 for the three other

procedures (i.e., non-boosted – NBST). Similarly, Figure 8.6b presents mixtures developed with 325 kg/m^3 of cement content and alkali content is 3.91 and 2.79 kg/m^3 for BST and NBST mixtures, respectively; whereas Figure 8.6c shows mixtures manufactured with 250 kg/m^3 of cement in which the alkali content is 3.01 (BST) and 2.15 kg/m^3 (NBST). Regarding the mass variation results, the minimum and maximum standard deviation of the NBST test setups (encapsulated - E, soaked - S, and wrapped - W) are as follows: 0.05 – 0.37%, 0.10 – 0.32%, and 0.05 – 0.26%, respectively, while for the BST test method (CPT) the standard deviation ranged from 0.04 to 0.23%. Overall, regardless of the cement content, mixtures tested under the soaked conditions presented the highest mass variations while the CPT presented the smallest mass variation and no clear trend regarding the other test setups is observed. After one year of testing, a wider range of values is obtained for the mixtures made with 325 kg/m^3 (i.e., 1.15% to 2.30%) while the mixtures made with the highest and lowest cement contents presented mass variations ranging from 1.34% to 2.04% and 1.11% to 1.78%, respectively.

Up to 200 days, mixtures made with 420 kg/m^3 of cement content (Figure 8.6a) and tested under soaked conditions presented lower mass gain than mixtures made with 325 and 250 kg/m^3 (Figure 8.6b and c), yet, after one year, the final mass variation, for the mixtures in order of decreasing cement content, was 2.04%, 2.3% and 1.78%. However, the other two NBST test setups (encapsulated and wrapped) exhibit different behaviour, with a more gradual mass gain over time. The mass gain after one year of testing for encapsulated mixtures with 420, 325, and 250 kg/m^3 was 1.70%, 1.67%, and 1.52%, respectively, whereas for wrapped mixtures, 1.63%, 1.73%, and 1.11% mass gain was observed.

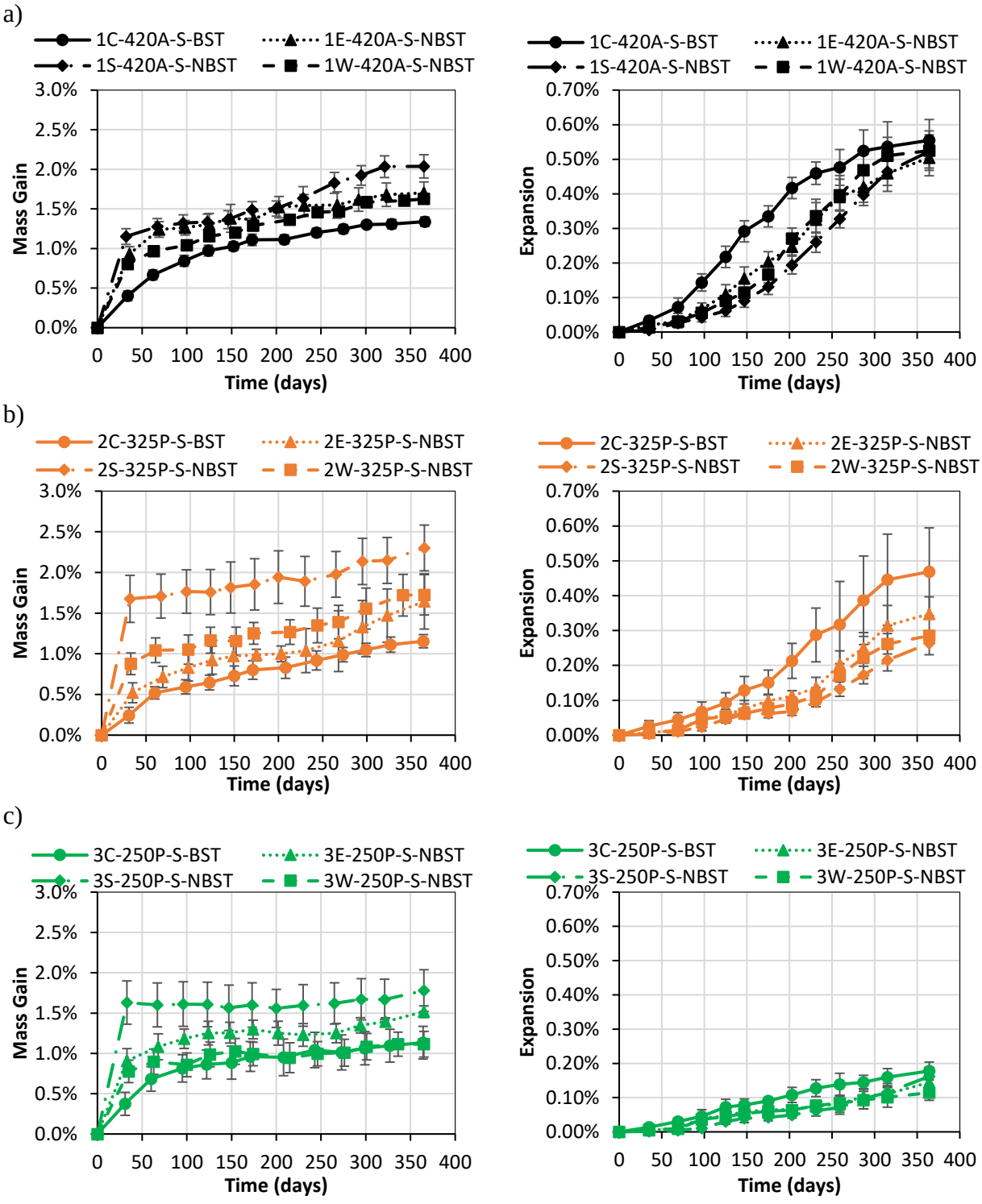

Figure 8.6. Mass and expansion as a function of time for boosted and non-boosted mixtures with cement alkali content a) 3.61 kg/m^3, b) 2.79 kg/m^3, and c) 2.15 kg/m^3.

Interestingly, for CPT-boosted mixtures, the final mass gain was slightly higher for mixtures developed with a higher cement content (1.34%) than for mixtures developed with lower cement contents (1.15% and 1.13%). Although the CPT-boosted mixtures showed an overall lower mass gain than other test procedures, 250 kg/m^3 mixture tested in the wrapped condition presented a similar mass gain trend after 200 days. Furthermore, after 300 days of testing, mixtures with a higher cement content (420 kg/m^3) show similar mass gain in encapsulated and wrapped test conditions.

The average measured expansion for a year, along with the data range bars, are presented in Figure 8.6a, b and c for mixtures developed with 420, 325, and 250 kg/m^3, respectively. The standard deviation intervals for all expansion results ranged from 0.002% to 0.07%. The overall expansion over time is significantly affected by the mixture cement content, regardless of the test setup where it is highest for the mixture with the most cement (between 0.52% and 0.55%) followed by mixtures with 325 kg/m^3 of cement content (i.e., from 0.26% to 0.47%, presenting the widest range, especially for 2C-325P-S-BST) while the lowest overall expansion was achieved by the mixtures with the lowest cement content (i.e., between 0.11% and 0.16%). Although boosted and non-boosted mixtures developed with 420 kg/m^3 of cement content achieved comparable final expansion, the boosted mixtures achieved the highest values when analyzing mixtures with lower cement content. Moreover, mixtures developed with 420 kg/m^3 of cement content (Figure 8.6a) exhibit a sharper increase in expansion, especially after 70 days. Figure 8.6b (325 kg/m^3 of cement content) shows a smoother increase of expansion, with the sharpest increase occurring after 200 days. However, for this cement content, boosted mixtures (tested under CPT conditions) expanded significantly more (0.47%) than the NBST test setups (0.35%, 0.28%, and 0.26% for encapsulated, wrapped, and soaked, respectively). Furthermore, Figure 3c (250 kg/m^3 cement content) shows no sharp increase in expansion, that is, it presents a gradual increase over a one-year test. Boosted mixtures (tested

under CPT conditions) achieved slightly higher expansion (0.18%) than NBST mixtures, which reached 0.14%, 0.11%, and 0.16% for encapsulated, wrapped, and soaked conditions, respectively.

Although the mixtures under soaked conditions had a significant mass gain compared to the other tests procedure, their expansions after one year were comparable to or marginally lower than other NBST results. Meanwhile, all mixtures tested under CPT test conditions had the lowest mass gain and the highest expansion development after one year of test.

8.5.2 Surface electrical resistivity

The surface electrical resistivity was recorded monthly to evaluate the inner quality of the ASR-affected concrete mixtures tested under different test conditions. The average surface electrical resistivity is shown in Figure 8.7 along with data range bars. In general, mixtures developed with a higher cement content reached higher surface electrical resistivity over time.

Regardless of the cement content, CPT-boosted mixtures presented higher electrical resistivity values; yet no specific trend is observed when NBST test procedures are used. The overall standard deviation ranges from 0.28 to 1.46 kΩ.cm for the boosted mixtures while for the non-boosted mixtures, the overall standard deviation is between 0.25-1.49 kΩ.cm, 0.28-1.00 kΩ.cm, and 0.17-1.04 kΩ.cm for encapsulated, wrapped, and soaked conditions, respectively.

Maximum values are generally observed at approximately 30 days, with the boosted mixtures showing the highest values without presenting a trend with cement content (i.e., 15.8 kΩ.cm for 420 kg/m^3, 9.5 kΩ.cm for 325 kg/m^3 and 13.7 kΩ.cm kg/m^3). Figure 8.7a (420 kg/m^3 cement content mixtures) shows that regardless of test setup, the maximum surface electrical resistivity was achieved initially at approximately 30 days after which a slightly descending period up to 150 days

and presenting an almost steady output until reaching the one-year testing period with the exception of the 1C-420A-S-BST, which followed a slight increase in the electrical resistivity.

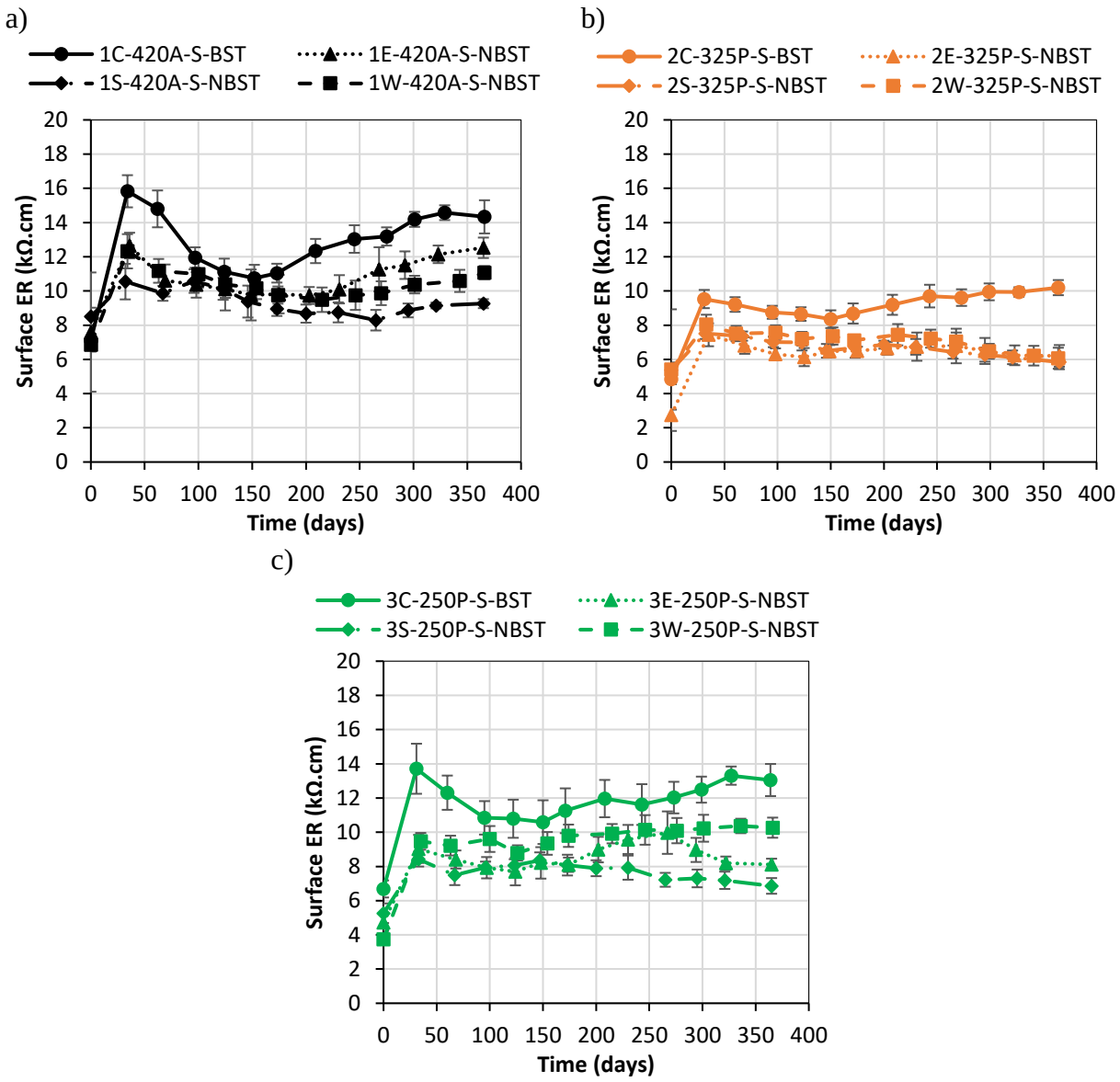

Figure 8.7. Surface electrical resistivity development for boosted and non-boosted mixtures with cement alkali content a) 3.61 kg/m^3, b) 2.79 kg/m^3, and c) 2.15 kg/m^3.

A similar trend is seen in Figure 8.7b and c, yet it is less pronounced in mixtures developed with 325 kg/m^3 cement content (Figure 8.7b). Electrical resistivities ranging from 10.2 to 14.3 kΩ.cm were obtained after one year for CPT-boosted mixtures, whereas this interval ranged from 6.2 to

12.5 kΩ.cm, from 6.1 to 11.1 kΩ.cm, and from 5.8 to 9.3 kΩ.cm, for mixtures tested under encapsulated, wrapped, and soaked conditions, respectively. Interestingly, all NBST mixtures with 325 kg/m^3 cement content had roughly the same surface electrical resistivity values after 250 days of testing while presenting the lowest overall values.

8.5.3 Apparent porosity

The apparent porosity is another technique to evaluate the internal quality of concrete affected by ASR (Figure 8.8). For concrete mixtures at 28 days, without being subjected to ASR, one can see that all mixtures had similar apparent porosity (ranging from 9.2 to 10.1%). The overall standard deviation for CPT-boosted mixes varied from 0.36 to 1.15%, whereas for NBST tests setups are between 0.06 and 1.18% cm, 0.11 to 0.66 cm, and 0.08 to 0.98 cm, for Encapsulated, Wrapped, and Soaked, respectively. However, when the porosity is compared based on ASR development (i.e., 4, 8, and 12 months), the apparent porosity highlights significantly different porosity evolution due to cement content and ASR development.

From Figure 8.8a (mixtures with 420 kg/m^3 of cement), one may see that CPT-boosted mixtures presented an almost constant apparent porosity over time of 9.2 to 8.8%, while NBST mixtures had a decrease of porosity at 4 months, reaching their peak at 12 months, except for 1W-420A-S-NBST which maintained constant porosity (around 8.10%) after 4 months testing. A similar trend for NBST mixtures is seen in Figure 8.8b (mixtures with 325 kg/m^3 of cement), but in this case, the apparent porosity of 2C-325P-S-BST increased gradually over one year of testing. Conversely, mixtures made with 250 kg/m^3 of cement (Figure 8.8c) had an overall decrease in porosity with ASR development on all testing methods.

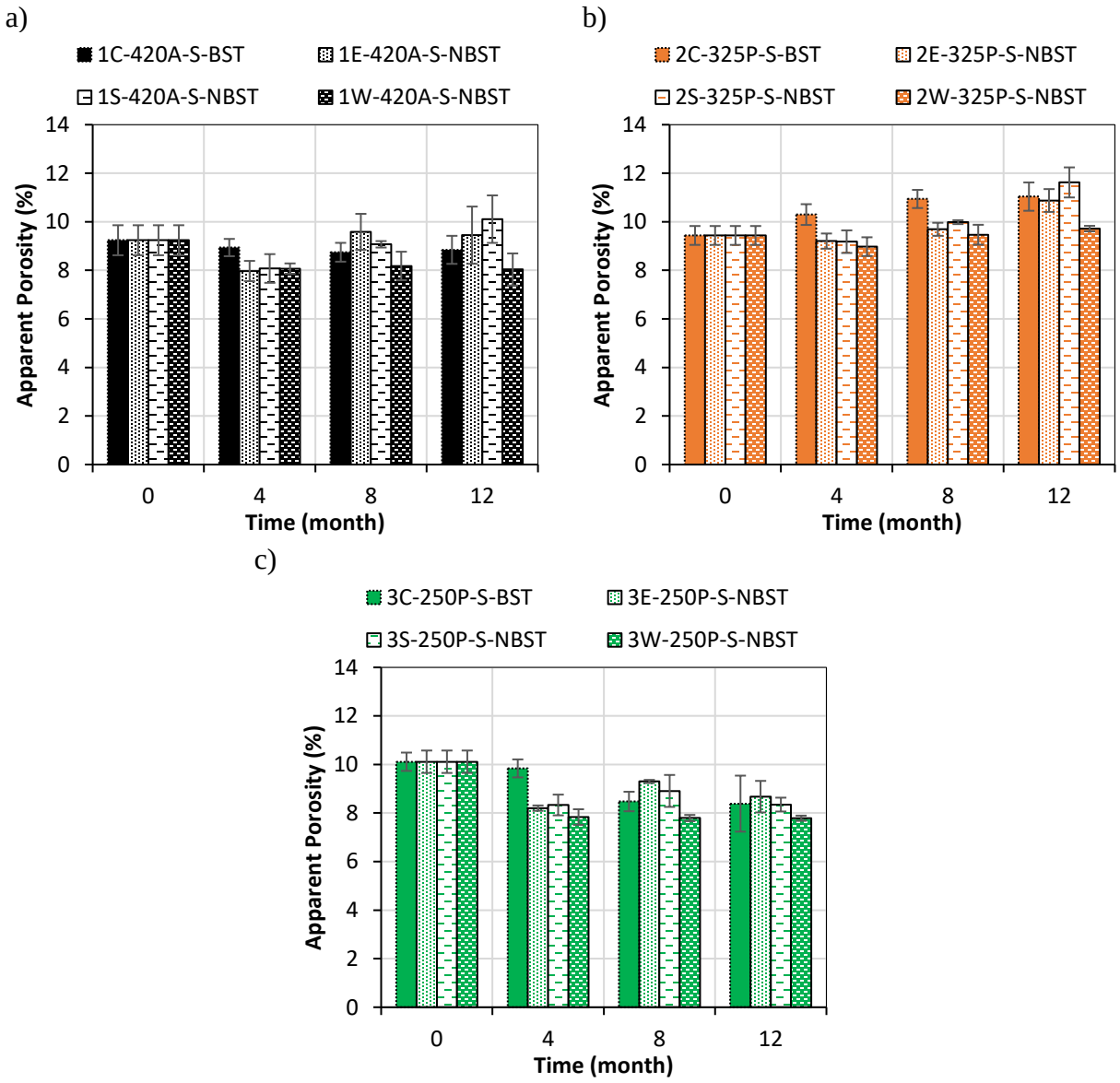

Figure 8.8. Apparent porosity variation for boosted and non-boosted mixtures with cement alkali content a) 3.61 kg/m^3, b) 2.79 kg/m^3, and c) 2.15 kg/m^3.

8.5.4 Damage rating index (DRI)

The DRI numbers as a function of ASR-expansion level are shown in Figure 8.9a. As expected, the DRI number increases as a function of expansion, regardless of the test protocol and cement content.

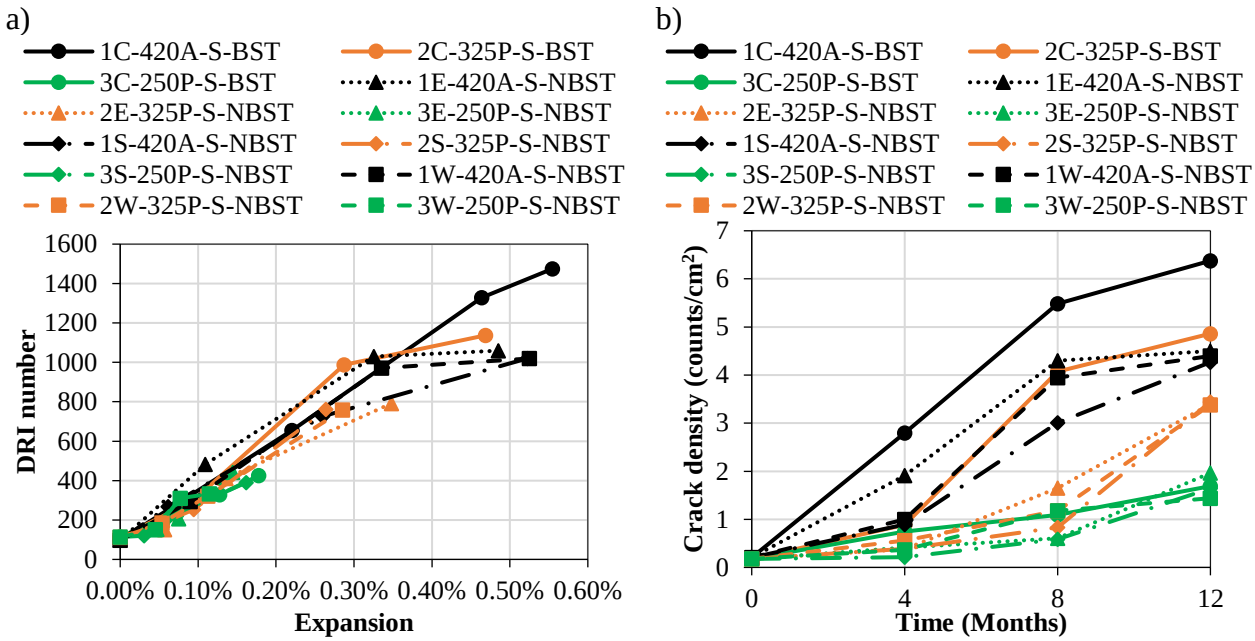

Figure 8.9. a) DRI number and b) crack density as a function of expansion.

At 0% expansion, all concrete mixtures present a DRI number lower than 115, followed by an upward parallel trend up to 0.10% expansion, where the DRI number ranged from around 250 to 470. It is to be noted that the last point for each mixture/setup represents the DRI number and expansion after 365 days. Mixtures developed with 250 kg/m^3 of cement content reached maximum expansion levels of 0.18% and a DRI number of 426 using the CPT-boosted test protocol, whereas NBST ones achieved on average 0.14% expansion at 365 days and an average DRI number of 388. At 0.20% expansion, the DRI number continued to increase for all mixtures and setups varying from 520 to 710. However, at higher expansion levels (> 0.20%), the DRI number presented a higher variation based on the cement content and test procedure. For instance, mixtures with 420 kg/m^3 followed a parallel trend up to a 0.30% expansion level with an average DRI number of 900 after which 1C-420A-S-BST continued to increase up to 0.55% expansion reaching a DRI number of 1475. However, NBST mixtures reached a lower DRI number (on average 1033) after 365 days with similar expansion (roughly 0.52%). Regarding mixtures with 325 kg/m^3 of cement content, the DRI

number of 2C-325P-S-BST continued to increase up to 0.30% of expansion reaching 988, after which a less pronounced increase is observed up until the final expansion of 0.47% is reached representing a DRI number of 1137. Conversely, NBST mixtures made with 325 kg/m^3 of cement content, reached maximum expansion levels and DRI numbers of 0.35% and 792, 0.29% and 758, and 0.26% and 762 for encapsulated, wrapped, and soaked, respectively.

The crack density (i.e., the unweighted sum of open cracks in the aggregate and cracks in the cement paste as counts/cm^2) was plotted as a function of time for the three mixtures and the four tests protocol investigated in this study to further assess the effect of ASR damage (Figure 8.9b). The average crack density was 0.19 counts/cm^2 for sound concrete followed by a distinct crack density development based on the alkali content (i.e., mixture cement content) and test protocols (i.e., boosted vs non-boosted). The control mixture developed with higher cement content (1C-420A-S-BST) had a linear increase in crack density reaching 5.49 counts/cm^2 at 8 months of exposure while presenting the highest overall crack density. Although 1E-420A-S-NBST exhibited similar behaviour during the same period, the slope of the curve was less steep resulting in a crack density of 4.30 counts/cm^2 after 8 months. Conversely, the other two non-boosted test setups (wrapped and soaked) showed a significantly lower crack density number at 4 months (0.95 counts/cm^2 on average) than 1E-420A-S-NBST (1.91 counts/cm^2). Yet, at 8-month test, 1W-420A-S-NBST reached a similar crack density to 1E-420A-S-NBST. Meanwhile, after 12 months all non-boosted mixtures developed with 420 kg/m^3 of cement reached a similar crack density of 4.4 counts/cm^2, which is significantly lower than the boosted mixture of 6.38 counts/cm^2. Analyzing mixtures developed with 325 kg/m^3 of cement, one may notice that at 4 months, the boosted mixture (2C-325P-S-BST) had a similar crack density (0.88 counts/cm^2) to NBST mixtures (0.38, 0.56, and 0.38 for encapsulated, wrapped, and soaked, respectively). However, at 8 months of exposure, non-

boosted mixtures maintained a low crack density ranging from 1.65 to 0.83 counts/cm^2, while boosted mixtures peaked achieving crack density of 4.07 counts/cm^2. At 12 months, this difference decreased as the crack density was 4.86, 3.39, 3.38, and 3.44 for 2C-325P-S-BST, 2E-325P-S-NBST, 2W-325P-S-NBST, and 2S-325P-S-NBST, respectively. An opposite behaviour is observed for mixtures developed with a lower alkali content (i.e., 250 kg/m^3 of cement), where the final crack density ranged from 1.96 to 1.44 counts/cm^2, indicating that the testing protocol had no effect on the crack density.

8.6 Discussion

8.6.1 The effect of alkali content on asr-induced expansion

For a better understanding of the influence of the concrete alkali content, Figure 8.10a correlates concrete alkali content with the expansion of the mixtures evaluated at 4, 8, and 12 months. It is well known that the higher the alkali content, the more susceptible concrete is to ASR-expansion. Nonetheless, after four months of testing, the difference in expansion between concrete with lower alkali content and concrete with higher alkali content is less than 0.15%.

This discrepancy is most pronounced at 8 and 12 months, where it is roughly 0.40% for both ages. However, this increase in the expansion is partially attributed to the alkali added to the system (i.e., the boosted mixtures), which resulted in a concrete total alkali content of 5.06, 3.91, and 3.01 kg/m^3 for mixtures developed incorporating 420, 325, and 250 kg/m^3 of cement, respectively. In this context, Figure 8.10b clarifies the effect of the alkali boost on the one-year expansion test. For mixtures developed with higher cement content (420 kg/m^3), boosted mixtures yielded an expansion 150% and 50% higher than non-boosted mixtures at 4 and 8 months, but they achieved roughly the same final expansion at 12 months. These findings raise the possibility that the alkali boosting added

to the mixtures has a significant impact on the expansion development and crack pattern of ASR-affected mixtures, raising the question of whether laboratory results can accurately represent real structures.

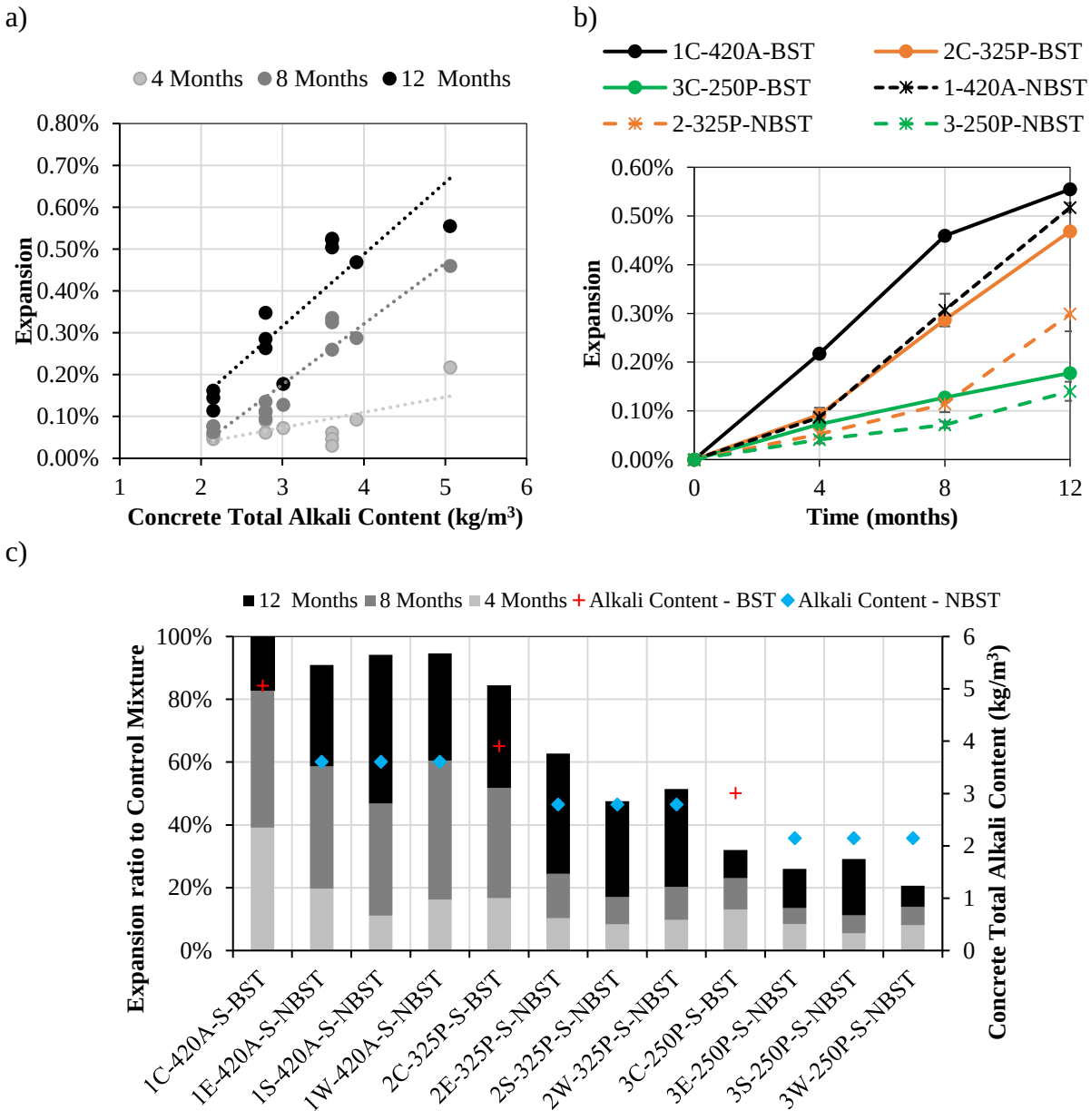

Figure 8.10. Correlation between a) concrete alkali content and expansion, b) boosted and non-boosted test protocols and expansion, and c) 12-month expansion ratio compared to the 420 kg/m³ control mixture.

Yet, another concern can be raised for mixtures developed with low cement content (325 and 250 kg/m^3), in which boosted mixture yielded expansions 177%, 252%, and 157% higher than non-boosted mixtures at 4, 8, and 12 months for mixtures developed with a cement content of 325 kg/m^3, whereas these percentages are 178%, 179%, and 127% for mixtures developed with a cement content of 250 kg/m^3 at the same period. In this case, one may question the feasibility of the standard CPT-boosted test in evaluating low cement mixtures, as the noticeably higher expansion of the boosted mixtures at the end of the testing period appears to be governed by the additional alkali rather than the cement alkali. Figure 8.10c further investigates the effect of cement content and testing setup of all mixtures compared to the final expansion of the control mixture (420 kg/m^3 of cement content) tested under CPT testing conditions. Non-boosted mixtures (encapsulated, soaked, and wrapped) developed with 420 kg/m^3 of cement content achieved 91%, 94%, and 95% of the final expansion of 1C-420A-S-BST. Analyzing mixtures developed with 325 kg/m^3 of cement testing under CPT, encapsulated, soaked, and wrapped testing conditions, their final expansion is 84%, 63%, 48%, and 51%, respectively, compared to the control mixture (1C-420A-S-BST). Finally, this difference is even higher for mixtures developed with lower cement content, in which the final expansion is on average 27% of 1C-420A-S-BST.

8.6.2 Qualitative analysis of the influence of testing protocol on crack development

Images were captured using a 16-megapixel digital camera connected to a stereomicroscope to assess differences in the type, size, and length of distress features produced by concrete mixtures subjected to ASR damage under different testing conditions. Figure 8.11a, b, and c show the crack characteristics of mixtures developed with a cement content of 420, 325, and 250 kg/m^3, respectively, and tested under CPT exposure conditions, whereas Figure 8.11d-f, Figure 8.11g-i, and Figure 8.11j-l show the distress features of non-boosted mixtures tested under encapsulated, soaked,

and wrapped exposure conditions in order of decreasing cement content. Analyzing the boosted mixtures (Figure 8.11a-c), one can notice that the lower the cement content the smaller the crack width. Although all non-boosted test setups exhibit the same behaviour (Figure 8.11d-l), the difference in crack width is less pronounced.

a) 1C-420A-S-BST; expansion: 0.55%; alkali content: 5.06 kg/m^3

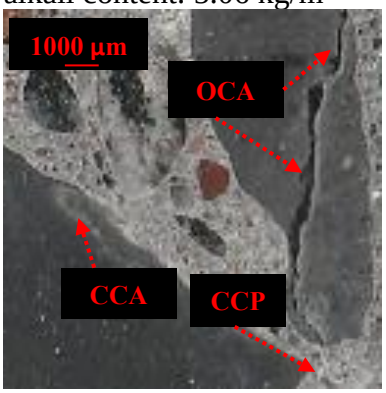

b) 2C-325P-S-BST; expansion: 0.47%; alkali content: 3.91 kg/m^3

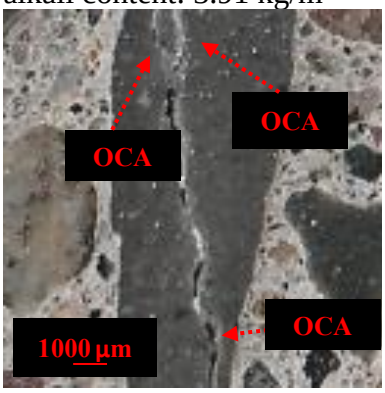

c) 3C-250P-S-BST; expansion: 0.18%; alkali content: 3.01 kg/m^3

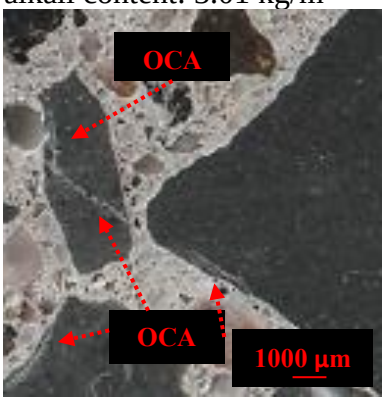

d) 1E-420A-S-NBST; expansion:0.49%; alkali content: 3.61 kg/m^3

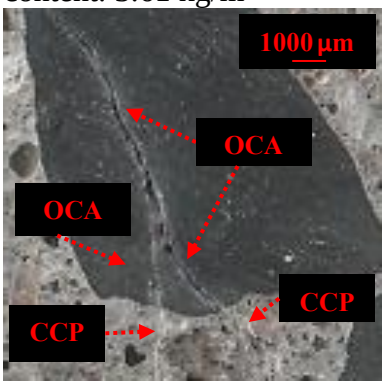

e) 2E-325P-S-NBST; expansion: 0.35%; alkali content: 2.79 kg/m^3

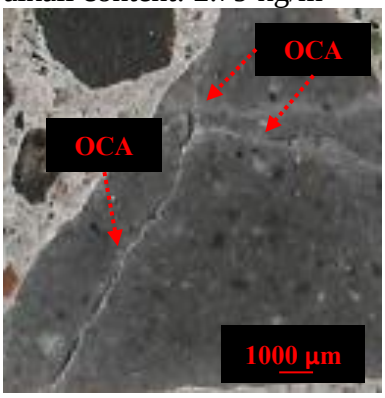

f) 3E-250P-S-NBST; expansion: 0.14%; alkali content: 2.15 kg/m^3

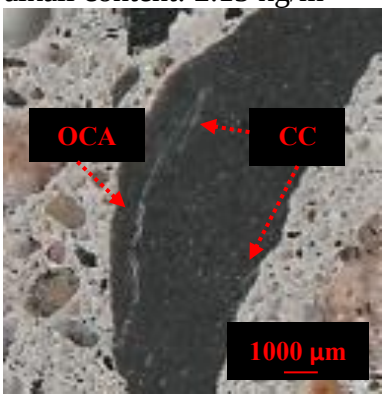

g) 1S-420A-S-NBST; expansion:0.52%; alkali content: 3.61 kg/m^3

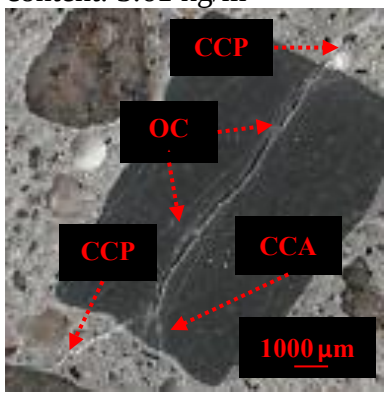

h) 2S-325P-S-NBST; expansion: 0.26%; alkali content: 2.79 kg/m^3

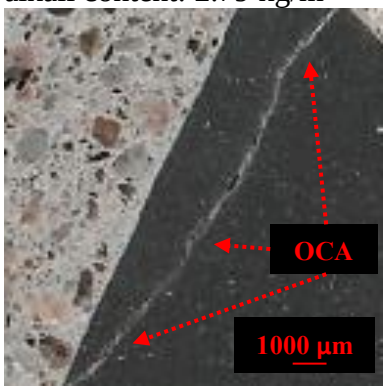

i) 3S-250P-S-NBST; expansion: 0.16%; alkali content: 2.15 kg/m^3

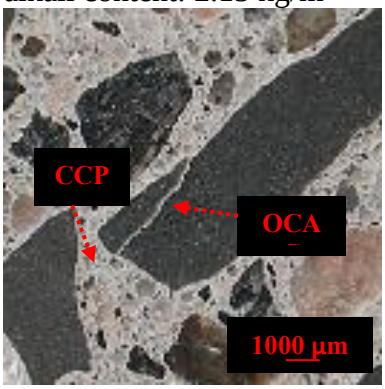

j) 1W-420A-S-NBST; expansion:0.52%; alkali content: 3.61 kg/m^3

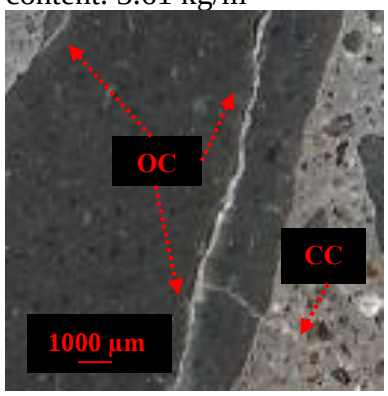

k) 2W-325P-S-NBST; expansion: 0.29%; alkali content: 2.79 kg/m^3

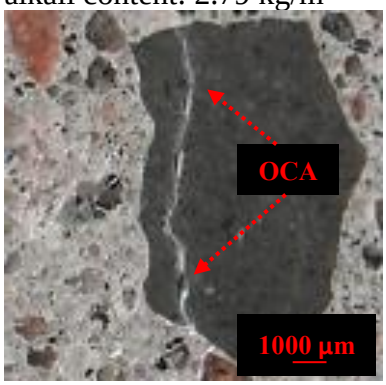

l) 3W-250P-S-NBST; expansion: 0.11%; alkali content: 2.15 kg/m^3

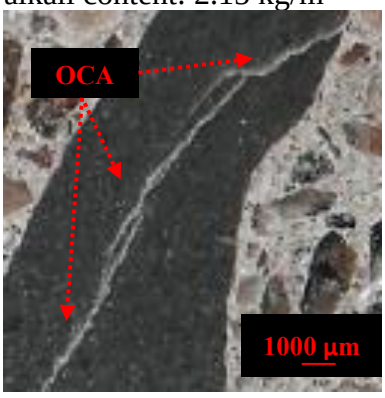

Figure 8.11. Distress features of mixtures tested at 12 months: CPT (a-c), Encapsulated (d-f), Soaked (g-i), and Wrapped (j-l) in order of decreasing cement content.

When comparing mixtures with the same cement content, boosted mixtures also had larger cracks due to the high alkali content. When comparing a mixture with similar alkali content (3.76 kg/m^3 +/- 0.15), the crack width of 2C-325P-S-BST (3.91 kg/m^3 of alkali content) is slightly wider than non-boosted mixtures developed with 420 kg/m^3 of cement content (3.61 kg/m^3 of alkali content). This demonstrates that adding sodium hydroxide widens cracks in mixtures with cement equal to or higher than 325 kg/m^3. As a result, it may be questioned whether mixtures evaluated under CPT can accurately simulate the type, width, and propagation of cracks found in concrete mixtures exposed

to field conditions. Yet, the opposite behaviour is observed for the crack width of 3C-250P-S-BST (3.01 kg/m^3 of alkali content) which is slightly thinner than that of non-boosted mixtures developed with 325 kg/m^3 cement content (2.79 kg/m^3 alkali content). In this case, the crack width may be governed by the cement content, even though the total system alkali content is lower. Quantitative analysis of the influence of testing protocol on crack development

To quantitatively understand the impact of the test protocol on the generation and propagation of ASR-damage within the mixtures investigated, Figure 8.12a and b illustrate the extended version of the DRI presented by [26] as cracks in counts/100 cm^2 and proportions, respectively. In this study, the distinction of gel in the distress feature is omitted, thus, the counts are combined (i.e., OCA+OCAG and CCP+CCPG) and the deterioration features are appraised without the weighing factors. The number of distress features is directly proportional to the increase in expansion over time, as shown in Figure 8.12. However, at high levels of deterioration (> 0.26%), the cracks begin to connect with one another, resulting in a decrease in counts or even a slight decrease in total cracks. Boosted mixtures tested under CPT exposure conditions show higher counts after one year, with 959, 823, and 467 counts/100 cm^2 in decreasing order of cement content. The same decreasing trend in crack counts is observed in the non-boosted mixtures when compared to mixtures with lower cement content.

Mixtures with a higher cement content (420 kg/m^3) have the highest counts, with 959, 580, 611, and 629 counts/100 cm^2 for mixtures tested using the CPT, encapsulated, soaked, and wrapped testing protocols, respectively, whereas mixtures with a lower cement content (325 kg/m^3) also have the lower counts, with 823, 552, 512, and 525 counts/100 cm^2 when using the same testing protocols, respectively. Interestingly, regardless of the testing protocol, mixtures developed with the lowest

cement content (250 kg/m^3) achieved an average of 373 counts/100 cm^2. Yet, 3C-250P-S-BST has 35% more microscopic features than non-boosted mixtures with the same cement content.

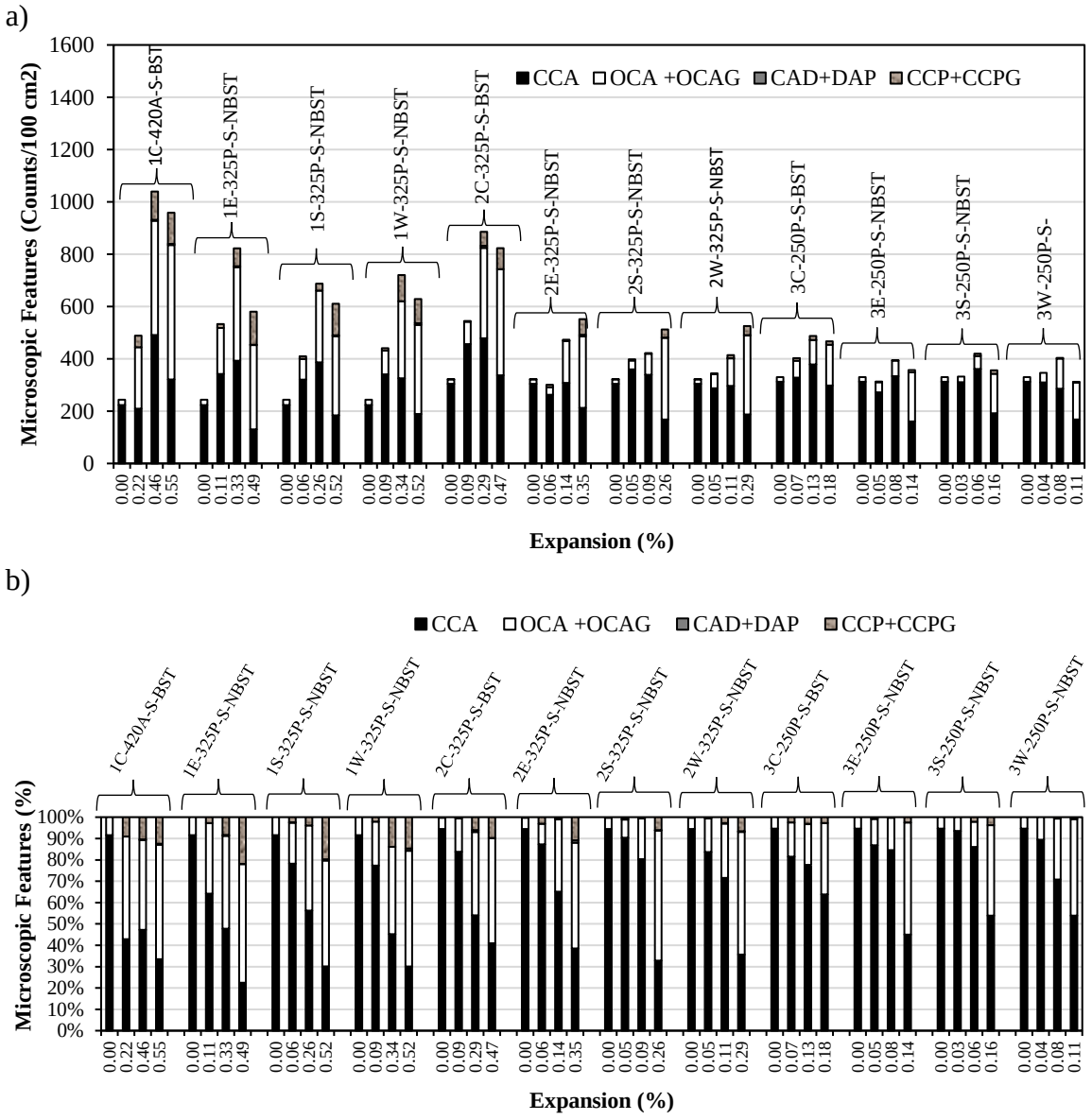

Figure 8.12. Distress features a) absolute value and b) relative value after 0, 4, 8, and 12 months.

The percentage of microscopic features of each mixture appraised is shown in Figure 8.12b. At 0% expansion, all mixtures have more than 90% of close aggregate cracks (CCA), but with ASR-

development, the number of features in the aggregate (OCA+OCAG) and the cement paste (CCP+CCPG) increases. In the case of mixtures with a higher cement content (420 kg/m3), the level of CCA dropped to less than 50% after 4 months on boosted mixtures and 12 months on non-boosted mixtures, due to the increase in OCA+OCAG as CCA become opened. As such, CCA, generally caused through weathering and processing and not typically associated with ASR development but rather potential reaction sites, are still the main feature of non-boosted mixtures when no additional alkali content is added. A similar trend is observed for mixtures developed with 325 kg/m^3, where after 12 months, CCA is no longer predominant regardless of the testing protocol. Conversely, mixtures developed with lower cement content (250 kg/m^3) had CCA ranging from 45% to 65%, OCA+OCAG ranging from 50% to 30%, and CCP+CCPG around 5% after one-year testing.

8.6.3 ASR-induced distress development in low alkali concrete mixtures

The DRI semi-quantitatively represents the damage of concrete affected by ASR and its bar charts capture the distinct distress features. Figure 8.13 highlights the key differences between concrete mixtures with the same cement content that were tested under different exposure conditions and mixtures with different cement content that were tested under similar exposure conditions.

After being stored in CPT conditions (i.e., 38°C and 100% RH) for 12 months, concrete mixtures yielded a final DRI of 1475, 1137, and 426 in order of decreasing cement content (420-250 kg/m^3). Although the system's total alkali content decreased in a step of 1.0 +/- 0.15 kg/m^3, concrete developed with a total alkali content of 3.01 kg/m^3 (3C-250P-S-BST) has a significantly lower amount of distress features than the other two mixtures (containing 5.06 and 3.91 kg/m^3 of total alkali content, respectively). Interestingly, for non-boosted mixtures, in which the total alkali contents were 3.61, 2.79, and 2.15 kg/m^3 for mixtures developed with cement content of 420, 325,

and 250 kg/m^3, the DRI number decreases more steadily, reaching an average DRI number of 1033, 770, and 388 in decreasing order of total alkali content. It might exhibit one of the two patterns: 1) an increase in distress features due to the additional alkali content added for boosting and/or 2) a possible threshold of the total alkali content of 3.01 kg/m^3, in which the alkali from the cement governs the distress features regardless of whether the mixture is boosted or not. The latter behaviour is also explained when analyzing the expansion of mixtures 3C-250P-S-BST and non-boosted mixtures developed with cement content of 250 kg/m^3, which have similar total alkali content (3.01-2.79 kg/m^3), in this case, non-boosted mixtures with higher cement content reached significantly higher DRI number (on average 770) than 2C-325P-S-BST (426).

Regarding the type of distress features, the higher the system's alkali content, the greater the final expansion and amount of cracks in the cement paste, indicating that the ASR-developed is at an advanced stage, in which the crack within the aggregates begins to propagate and reach the cement paste. On the other hand, mixtures developed with a total alkali content of 3.01 kg/m^3 or lower, the cement content governs the final expansion and the amount of distress features; as such, 2E-325P-S-NBST, 2S-325P-S-NBST, and 2W-325P-S-NBST reached a final expansion and DRI number of 0.35% and 792, 0.26% and 762, and 0.29% and 758, respectively, whereas 3C-250P-BST reached a significantly lower final expansion (0.18%) and DRI number (426), resulting in a lower amount of cracks in the cement paste, comparable with the other non-boosted mixtures developed with same cement content. These findings agree with the qualitative model of ASR crack propagation over distinct expansion levels proposed by Sanchez et al. [26].

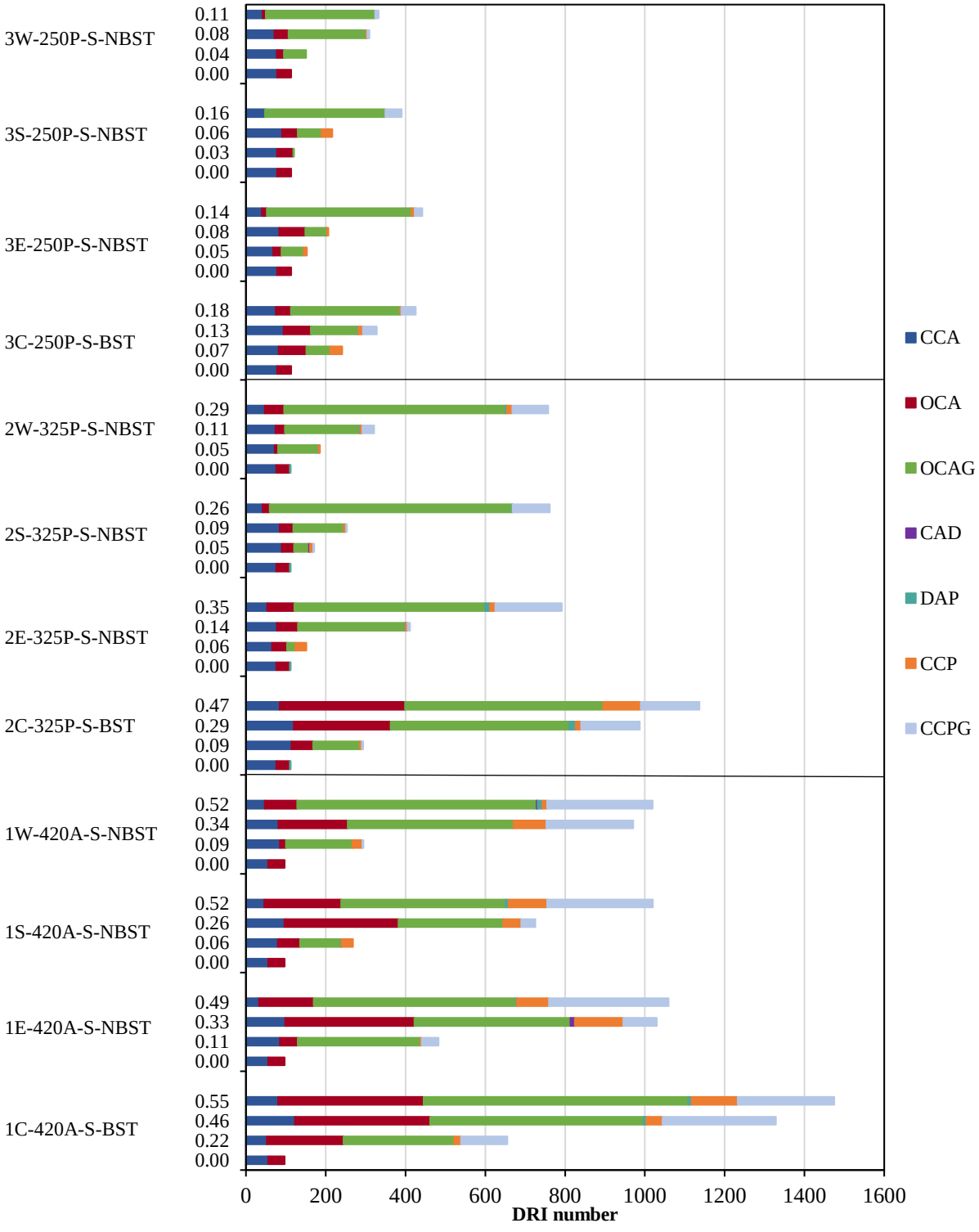

Figure 8.13. Relationship between expansion and Damage Rating Index for the twelve concrete appraised.

8.6.4 Lower alkali content mixtures (Boosted vs. Non-boosted)

To further investigate the influence of cement alkali content and boosted alkali content, four additional concrete mixtures with cement alkali contents of 200 and 150 kg/m^3 were manufactured and tested under CPT (boosted) and encapsulated (non-boosted) exposure conditions. The total alkali contents of the boosted mixtures were 2.41 and 1.81 kg/m^3, respectively, whereas the cement alkali contents of the non-boosted mixtures were 1.72 and 1.29 kg/m^3. As per CSA A23.2-27A, reactive aggregates may be used in conjunction with the strategy of reducing the system's total alkali content contributed by the Portland cement, in this context, non-boosted mixtures, without the addition of SCMs, are in accordance with prevention level Y (strong), with the total alkali content being less than 1.8 kg/m^3.

Figure 8.14a shows that regardless of cement content, encapsulated mixtures presented higher mass gain than CPT mixtures, exhibiting similar behaviour as previously observed in Figure 8.6a, b, and c with different cement content. Yet, in terms of expansion (Figure 8.14b), no difference is seen between boosted and non-boosted mixtures, as such the final expansion was 0.09% and 0.09% for 4C-200P-S-BST and 5C-150P-S-BST, respectively, while 4E-200P-S-NBST and 5E-150P-S-NBST reached 0.08% and 0.07%, respectively. Interestingly, despite having similar total alkali loadings, 4C-200P-S-BST (the total alkali loadings of 2.41 kg/m^3) produced lower final expansion than 3E-250P-S-NBST (the total alkali content of 2.15 kg/m^3). It agrees with the findings presented in section 6.4, which show that when the total alkali content of the system is less than 3.01 kg/m^3, the cement content governs the expansion and distress features, regardless of whether the mixture is boosted or not. In this case, 3E-250P-S-NBST contains more cement than 4C-200P-S-BST, resulting in greater expansion (0.14% vs. 0.08%).

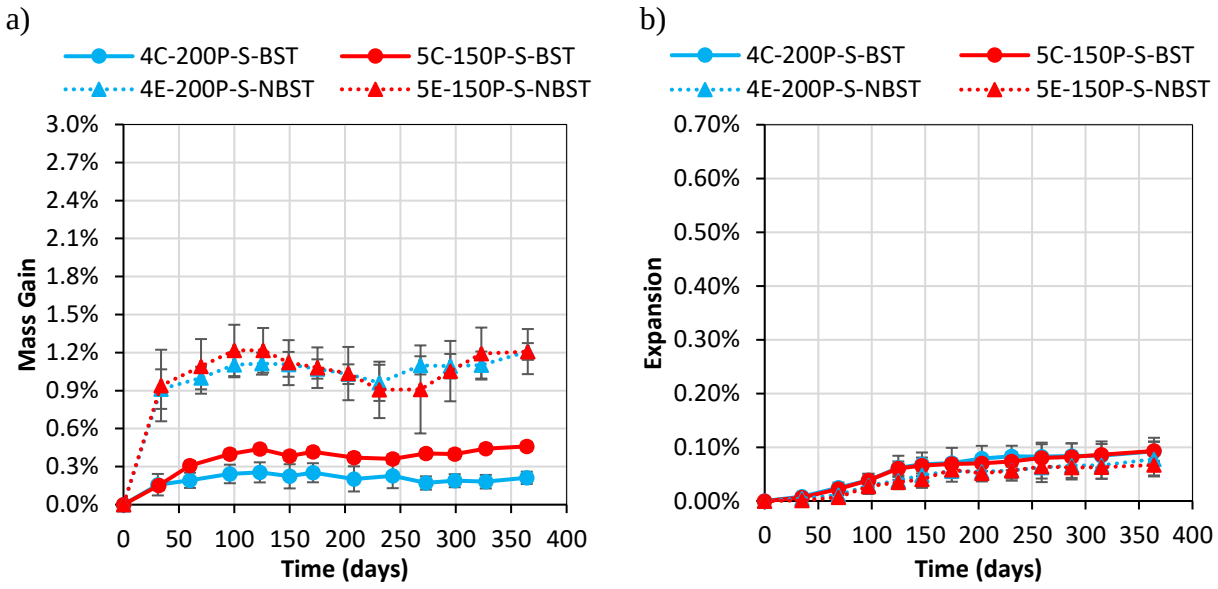

Figure 8.14. Mass (a) and expansion (b) as a function of time for boosted and non-boosted mixtures with cement content of 200 kg/m^3 and 150 kg/m^3.

The DRI numbers for the lowest cement contents evaluated in this study, regardless of the test conditions, remain the lowest overall values throughout the study. Similar results are observed from the microscopic features (Figure 8.15a and b), where 3E-250P-S-NBST achieved higher values (DRI number of 442 and crack density of 1.96) when compared to 4C-200P-S-BST (DRI number of 357 and crack density of 1.54). Yet, Figure 16a shows that the DRI numbers follow the same trend over time as other mixtures investigated with higher cement content. Meanwhile, the crack density remains significantly lower (below 2 counts/cm^2 after one year) for all mixtures with 250 kg/m^3 of cement or less when compared to those with higher contents. Nevertheless, the distinction between setups is less apparent for lower cement contents, highlighting that at low alkali systems (< 3.01 kg/m^3), the alkali added has no effect on ASR development.

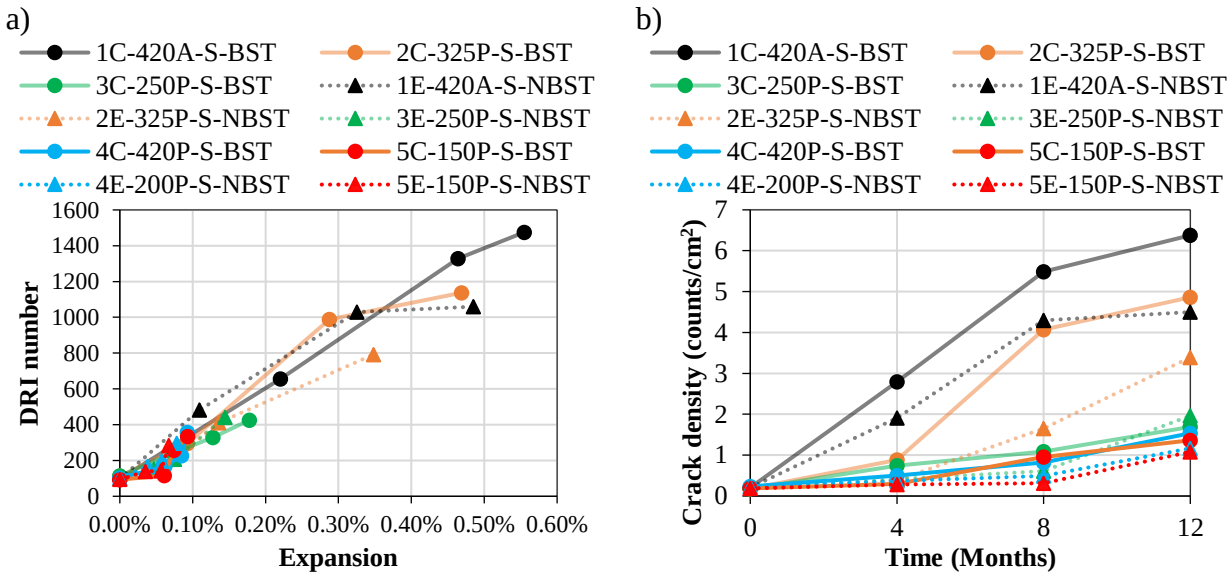

Figure 8.15. Comparison of a) DRI number and b) Crack density of boosted and non-boosted mixtures with cement content ranging from 420 to 150 kg/m^3.

8.6.5 Fine reactive aggregate type (Boosted vs. Non-boosted)

As ASR is affected not only by the alkali content of the pore solution in concrete but also by the amount of unstable silica found within the aggregates, the influence of the type of reactive aggregate on the boosted and non-boosted test setup was further investigated. Six additional concrete mixtures were developed with a fine ultra-high reactive aggregate – Texas sand. Figure 8.16a, in contrast to previous findings (Figure 8.15a, and Figure 8.6a, b, and c) on mixtures incorporating coarse reactive aggregate (Springhill), shows that regardless of cement content, encapsulated mixtures presented lower mass gain and final expansion when compared to mixtures exposed to CPT conditions. Although mixtures containing 420 kg/m^3 cement content and Springhill reactive aggregate achieved similar final expansions for boosted and non-boosted mixtures, the difference in the final expansion for Texas mixtures is larger for boosted and non-boosted mixtures (Figure 8.16b). In decreasing order of cement content, CPT-Texas mixtures achieved 12-month expansion of 0.78%, 0.65%, and

0.61%, while encapsulated-Texas mixtures reached 12-month expansion of 0.60%, 0.55%, and 0.48%.

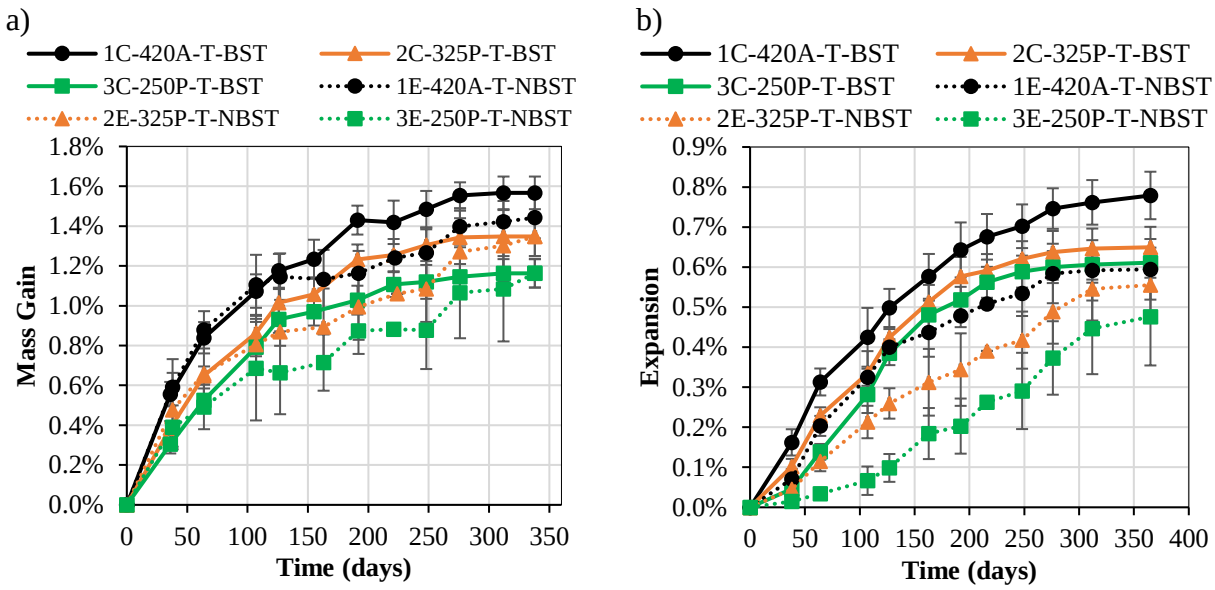

Figure 8.16. Mass (a) and expansion (b) as a function of time for boosted and non-boosted mixtures developed with fine reactive aggregate.

Figure 8.17, on the other hand, shows that the DRI number versus expansion relationship continues to follow the same trend over time for mixtures containing Texas and Springhill reactive aggregates. All boosted mixtures made with the Texas sand present a less sharp increase in DRI numbers after reaching values of (in increasing cement content) 931, 1049 and 1497 at 0.38%, 0.42% and 0.50% of expansion, respectively, even though expansion continues to increase until 0.65%, 0.70% and 0.80% with DRI numbers of 1133, 1246 and 1482, respectively. This trend was only observed for the boosted mixture at 325 kg/m^3 of cement content using Springhill reactive coarse aggregate and the non-boosted Texas sand mixture with 420 kg/m^3 of cement while encapsulated. Cracks may have therefore reached their maximum lengths while widening to induce the measured expansions.

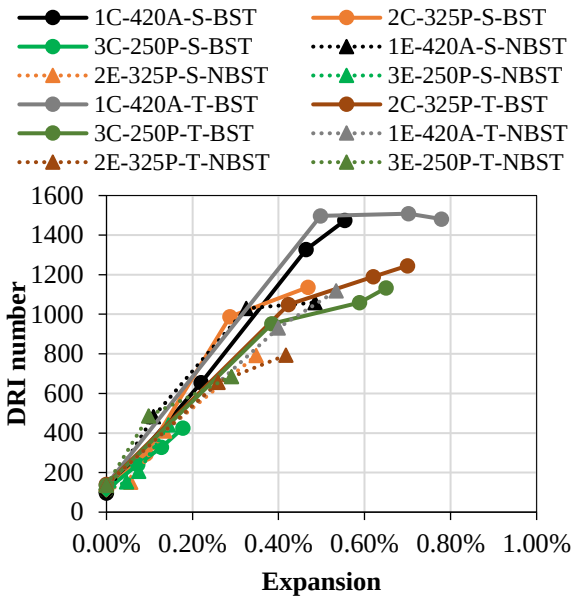

Figure 8.17. Comparison of DRI number of boosted and non-boosted mixtures incorporating coarse (Springhill) or fine (Texas) reactive aggregate.

8.7 Conclusions

The purpose of this study was to investigate the effectiveness of four different laboratory test setups (i.e., CPT, wrapped – W, soaked – S, and encapsulated – E) with and without the addition of alkalis into the concrete mixtures to evaluate the ASR-development of low alkali systems. Boosted mixtures had a total alkali content ranging from 5.06 to 1.81 kg/m^3, whereas non-boosted mixtures had levels of alkali content ranging from 3.61 to 1.29 kg/m^3. The main findings of the current research are as follows:

- After one year of testing, all mixtures tested under CPT test conditions had the lowest mass gain and the highest expansion development (except for 1C-420A-S-BST at 12 months). Although the soaked mixtures gained significantly more mass than the other test procedures, their expansion after one year was comparable to, or marginally lower than other non-boosted (NBST) results.

- For mixtures with higher cement content (420 kg/m^3), boosted mixtures yielded an expansion of 150% and 50% higher than non-boosted mixtures at 4 and 8 months, but they achieved roughly the same final expansion at 12 months (91%, 94%, and 95% of the final expansion of 1C-420A-S-BST for encapsulated, soaked, and wrapped mixtures, respectively). Although a similar expansion was reached regardless of the testing setup, their final DRI number is significantly different comparing boosted and non-boosted mixtures (i.e., 1475, 1020, 1020, and 1059 for CPT, wrapped, soaked, and encapsulated, respectively).

- The system's alkali content has a significant impact on overall ASR-kinetics. Regardless of the testing protocol selected, mixtures achieved similar final expansions when the total system alkali content is over 3.01 kg/m^3; below this threshold, the alkali from the cement governs the distress features regardless of total system alkalis.

- In terms of crack width, the lower the cement content the smaller the crack width. Moreover, due to the higher system alkali content, boosted mixtures had larger cracks when compared to mixtures with the same cement content.

- The sodium hydroxide addition during concrete fabrication resulted in wider and a higher amount of cracks in mixtures with alkali content as low as 3.01 kg/m^3. However, when the total system alkali content is 3.01 kg/m^3 or less, DRI and distress features are governed by the cement content (that is, alkalis from the cement content).

- Mixtures developed with 1.8 kg/m^3 or lower alkali content (containing cement content lower than 200 kg/m^3) reached similar final expansion (on average 0.08%) regardless of testing setup (boosted vs non-boosted). These mixtures are also classified as prevention level Y (Strong) against ASR-mitigation as per CSA A23.2-27A without any addition of SCMs.

- When compared to Springhill mixtures, Texas sand mixtures presented faster ASR-kinetics. Furthermore, after 8 months of testing, for all boosted mixtures made with Texas sand showed a levelling-off behaviour; thus, cracks may have reached their maximum lengths while widening to continue contributing to expansion.
- Regarding the type of distress features and crack propagation, boosted and non-boosted mixtures developed with alkali content ranging from 5.06 to 1.29 kg/m^3 presented different behaviour. Further study is required to develop a qualitative model of crack propagation of low-alkali system affected by ASR-induced damage.
- Concerns have been expressed about the effect of added sodium hydroxide on crack propagation, highlighting that expansion levels and damage tested under CPT laboratory conditions cannot be directly correlated with field conditions.

8.8 Acknowledgments

The authors gratefully acknowledge the financial support that M. T. de Grazia and C. Trottier benefit from the prestigious Vanier scholarship funded by NSERC (Natural Sciences and Engineering Research Council of Canada). The authors would also like to thank Dr. Gamal Elnabelsya and Dr. Muslim Majeed, technical officers in the Materials and Structures laboratory at the University of Ottawa's Department of Civil Engineering.

8.9 Authors' contributions

Conceptualization, M.T.d.G. and L.F.M.S.; methodology, M.T.d.G., C.T. and L.F.M.S.; formal analysis, M.T.d.G.; data curation, M.T.d.G; writing-original draft preparation, M.T.d.G.; writing – review and editing, C.T. and L.F.M.S; supervision L.F.M.S.

8.10 Competing interests

The authors declare that they have no competing financial interests or personal relationships that could have an impact on the work reported in this paper.

8.11 References

[1] H.F. Campos, N.S. Klein, J. Marques Filho, Proposed mix design method for sustainable high-strength concrete using particle packing optimization, J. Clean. Prod. 265 (2020) 1–15. https://doi.org/10.1016/j.jclepro.2020.121907.

[2] J. Di Filippo, J. Karpman, J.R. Deshazo, J. Di Filippo, J. Karpman, J.R. Deshazo, The impacts of policies to reduce CO2 emissions within the concrete supply chain, Cem. Concr. Compos. 101 (2019) 67–82. https://doi.org/10.1016/j.cemconcomp.2018.08.003.

[3] M.T. De Grazia, L. Sanchez, R.C.O. Romano, R.G. Pileggi, Investigation of Alfred Model Effect on the Fresh and Hardened State Properties of Low-Cement Content (LCC) Systems, Constr. Build. Mater. Accepted (2017) 1–26.

[4] B. Esmaeilkhanian, K.H. Khayat, O.H. Wallevik, Mix design approach for low-powder self-consolidating concrete: Eco-SCC-content optimization and performance, Mater. Struct. 50 (2017) 18. https://doi.org/10.1617/s11527-017-0993-y.

[5] Z.S. Ali, M. Hosseinpoor, A. Yahia, New aggregate grading models for low-binder self-consolidating and semi-self-consolidating concrete (Eco-SCC and Eco-semi-SCC), Constr. Build. Mater. 265 (2020) 120314. https://doi.org/10.1016/j.conbuildmat.2020.120314.

[6] M. T. de Grazia, L. F. M. Sanchez, R. C. O. Romano, R. G. Pileggi, M.T. de Grazia, L. Sanchez, R.C.O. Romano, R.G. Pileggi, M. T. de Grazia, L. F. M. Sanchez, R. C. O. Romano, R. G. Pileggi, Investigation of the use of continuous particle packing models (PPMs) on the fresh and hardened properties of low-cement concrete (LCC) systems, Constr. Build. Mater. 195 (2019) 524–536. https://doi.org/10.1016/j.conbuildmat.2018.11.051.

[7] P.R. de Matos, R.D. Sakata, L.R. Prudêncio, Eco-efficient low binder high-performance self-compacting concretes, Constr. Build. Mater. 225 (2019) 941–955. https://doi.org/10.1016/j.conbuildmat.2019.07.254.

[8] C.S. Shon, S.L. Sarkar, Evaluation of modified ASTM C 1260 accelerated mortar bar test for alkali-silica reactivity, Cem. Concr. Res. 32 (2002) 1981–1987. https://doi.org/10.1016/S0008-8846(02)00903-1.

[9] ASTM C1293, Standard Test Method for Determination of Length Change of Concrete Due to Alkali-Silica Reaction, West Conshohocken, 2018. https://doi.org/10.1520/C1293-18.

[10] M.-A. Berube, J. Frenette, Testing Concrete for AAR in NaOH and NaCl solutions at 38°C and 80°C, Cem. Concr. Compos. 16 (1994) 189–198.

[11] S.U. Einarsdottir, R. Douglas Hooton, Modifications to ASTM C1293 that allow testing of low-Alkali binder systems, ACI Mater. J. 115 (2018) 739–747. https://doi.org/10.14359/51702350.

[12] P. Rivard, M.A. Bérubé, J.P. Ollivier, G. Ballivy, Decrease of pore solution alkalinity in concrete tested for alkali-silica reaction, Mater. Struct. Constr. 40 (2007) 909–921. https://doi.org/10.1617/s11527-006-9191-z.

[13] 106-AAR T.C. Rilem, A – TC 106-2 – Detection of potential alkali-reactivity of aggregates – The ultra-accelerated mortar-bar test B – TC 106-3 – Detection of potential alkali-reactivity of aggregates – Method for aggregate combinations using concrete prisms, Mater. Struct. 33 (2000) 88–93.

[14] J. Lindgård, E.J. Sellevold, M.D.A. Thomas, B. Pedersen, H. Justnes, F. Rønning, Alkali-silica reaction (ASR)-performance testing: Influence of specimen pre-treatment, exposure conditions and prism size on concrete porosity, moisture state and transport properties, Cem. Concr. Res. 53 (2013) 145–167. https://doi.org/10.1016/j.cemconres.2013.05.020.

[15] J. Lindgård, M.D.A. Thomas, E.J. Sellevold, B. Pedersen, Ö. Andiç-Çakır, H. Justnes, T.F. Rønning, Alkali-silica reaction (ASR)-performance testing: Influence of specimen pre-treatment, exposure conditions and prism size on alkali leaching and prism expansion, Cem. Concr. Res. 53 (2013) 68–90. https://doi.org/10.1016/j.cemconres.2013.05.017.

[16] Y. Kawabata, K. Yamada, Y. Sagawa, S. Ogawa, Alkali-Wrapped Concrete Prism Test (AW-CPT) - New testing protocol toward a performance test against alkali-silica reaction, J. Adv. Concr. Technol. 16 (2018) 441–460. https://doi.org/10.3151/jact.16.441.

[17] X.X. Gao, S. Multon, M. Cyr, A. Sellier, Optimising an expansion test for the assessment of alkali-silica reaction in concrete structures, Mater. Struct. 44 (2011) 1641–1653. https://doi.org/10.1617/s11527-011-9724-y.

[18] A. Naranjo, Proposed Test Method for Determining ASR Potential: The Concrete Cylinder Test (CCT), 2012.

[19] S. Stacey, K.J. Folliard, T. Drimalas, M.D.A.A. Thomas, An Accelerated and More Accurate Test Method To ASTM C1293: the Concrete Cylinder Test, 15th Int. Conf. Alkali-Aggregate React. (2016) 11p.

[20] G. Igarashi, K. Yamada, Y. Xu, H. Wong, S. Hirono, S. Ogawa, Image Analysis of Alkali-Aggregate Gel in Concrete Prism Test With Alkali-Wrapping, 15th Int. Conf. Alkali-Aggregate React. Concr. (2016).

[21] K. Yamada, Y. Kawabata, M.R. de Rooij, B.M. Pedersen, R. Brueckner, J.H. Ideker, Recommendation of RILEM TC 258-AAA: RILEM AAR-13: application of alkali-wrapping for concrete prism testing to assess the expansion potential of alkali-silica reaction, Mater. Struct. Constr. 54 (2021) 1–15. https://doi.org/10.1617/s11527-021-01684-z.

[22] C. Trottier, R. Ziapour, A. Zahedi, L. Sanchez, F. Locati, Microscopic characterization of alkali-silica reaction (ASR) affected recycled concrete mixtures induced by reactive coarse and fine aggregates, Cem. Concr. Res. 144 (2021) 106426. https://doi.org/10.1016/j.cemconres.2021.106426.

[23] M. Rashidi, M.C.L. Knapp, A. Hashemi, J.Y. Kim, K.M. Donnell, R. Zoughi, L.J. Jacobs, K.E. Kurtis, Detecting alkali-silica reaction: A multi-physics approach, Cem. Concr. Compos. 73 (2016) 123–135. https://doi.org/10.1016/j.cemconcomp.2016.07.001.

[24] B. Fournier, M.-A. Bérubé, Alkali–aggregate reaction in concrete: a review of basic concepts and engineering implications, Can. J. Civ. Eng. 27 (2000) 167–191.

[25] J. Lindgård, Ö. Andiç-Çakir, I. Fernandes, T.F. Rønning, M.D.A. Thomas, Alkali-silica reactions (ASR): Literature review on parameters influencing laboratory performance testing, Cem. Concr. Res. 42 (2012) 223–243. https://doi.org/10.1016/j.cemconres.2011.10.004.

[26] L.F.M.L.. Sanchez, B.. Fournier, M.. Jolin, J. Duchesne, Reliable quantification of AAR damage through assessment of the Damage Rating Index (DRI), Cem. Concr. Res. 67 (2015) 74–92. https://doi.org/10.1016/j.cemconres.2014.08.002.

[27] L. Sanchez, B. Fournier, M. Jolin, D. Mitchell, J. Bastien, Overall assessment of Alkali-Aggregate Reaction (AAR) in concretes presenting different strengths and incorporating a wide range of reactive aggregate types and natures, Cem. Concr. Res. 93 (2017) 17–31. https://doi.org/10.1016/j.cemconres.2016.12.001.

[28] N. Smaoui, B. Bissonnette, B. Fournier, B. Durand, Mechanical Properties of ASR-Affected Concrete Containing Fine or Coarse Reactive Aggregates, ASTM Int. 3 (2006) 1–16. https://doi.org/10.1520/JAI12010.

[29] L.F.M. Sanchez, T. Drimalas, B. Fournier, D. Mitchell, J. Bastien, Comprehensive damage assessment in concrete affected by different internal swelling reaction (ISR) mechanisms, Cem. Concr. Res. 107 (2018) 284–303.

[30] D.J. De Souza, L.F.M. Sanchez, M.T. De Grazia, Evaluation of a direct shear test setup to quantify AAR-induced expansion and damage in concrete, Constr. Build. Mater. 229 (2019). https://doi.org/10.1016/j.conbuildmat.2019.116806.

[31] R. Ziapour, C. Trottier, L.F.M. Sanchez, Assessment of AAR-induced expansion and damage through the direct shear test, in: Proc. 16th ICAAR, Lisbon, Portugal, 2020.

[32] L.F.M. Sanchez, B. Fournier, M. Jolin, M.A.B. Bedoya, J. Bastien, J. Duchesne, Use of Damage Rating Index to Quantify Alkali-Silica Reaction Damage in Concrete: Fine versus Coarse Aggregate, ACI Mater. J. 113 (2016) 395–407.

[33] V. Villeneuve, B. Fournier, Determination of the damage in concrete affected by ASR–the damage rating index (DRI), in: 14th Int. Conf. Alkali-Aggregate React. Concr., Austin (Texas), 2012: p. electronic.

[34] B. Fournier, J.H. Ideker, K.J. Folliard, M.D.A. Thomas, P.C. Nkinamubanzi, R. Chevrier, Effect of environmental conditions on expansion in concrete due to alkali-silica reaction (ASR), Mater. Charact. 60 (2009) 669–679. https://doi.org/10.1016/j.matchar.2008.12.018.

[35] M. T. de Grazia, N. Goshayeshi, R. Gorga, L. F.M. Sanchez, A.C. Santos, D.J. Souza, Comprehensive semi-empirical approach to describe alkali aggregate reaction (AAR) induced expansion in the laboratory, J. Build. Eng. 40 (2021). https://doi.org/10.1016/j.jobe.2021.102298.

[36] M.-A. Bérubé, J. Duchesne, J.F. Dorion, M. Rivest, Laboratory assessment of alkali contribution by aggregates to concrete and application to concrete structures affected by alkali-silica reactivity, Cem. Concr. Res. 32 (2002) 1215–1227.

[37] A. Leemann, B. Lothenbach, C. Thalmann, Influence of superplasticizers on pore solution composition and on expansion of concrete due to alkali-silica reaction, Constr. Build. Mater. 25 (2011) 344–350. https://doi.org/10.1016/j.conbuildmat.2010.06.019.

[38] ASTM C136, Standard test method for sieve analysis of fine and coarse aggregates., (2016) 8.

[39] C. A23.2-2A, Sieve analysis of fine and coarse aggregate, 2014.

[40] S.A.A.M. Fennis, J.C. Walraven, Using particle packing technology for sustainable concrete mixture design, Heron. 57 (2012) 73–101.

[41] M.N. Mangulkar, S.S. Jamkar, Review of particle packing theories used for concrete mix proportioning, Int. J. Sci. Eng. Res. 4 (2013) 143–148.

[42] S. Kumar, M. Santhanam, S. Kunar, M. Santhanam, Particle packing theories and their application in concrete mixture proportioning : A review, Indian Concr. J. 77 (2003) 1324–1331.

[43] J.E. Funk, D.R. Dinger, Predictive process control of crowded particulate suspensions, 1st ed., New York, 1994. https://doi.org/10.1007/978-1-4615-3118-0.

[44] P. Goltermann, V. Johansen, L. Palbøl, Packing of Aggregates : An Alternative Tool to Determine the Optimal Aggregate Mix, ACI Mater. J. (1997) 435–442.

[45] I. Mehdipour, K.H. Khayat, Understanding the role of particle packing characteristics in rheo-physical properties of cementitious suspensions : A literature review, Constr. Build. Mater. 161 (2018) 340–353.

[46] A. Leemann, B. Lothenbach, The influence of potassium-sodium ratio in cement on concrete expansion due to alkali-aggregate reaction, Cem. Concr. Res. 38 (2008) 1162–1168. https://doi.org/10.1016/j.cemconres.2008.05.004.

[47] U. Costa, T. Mangialardi, A.E. Paolini, Minimizing alkali leaching in the concrete prism expansion test at 38 °C, Constr. Build. Mater. 146 (2017) 547–554. https://doi.org/10.1016/j.conbuildmat.2017.04.116.

[48] C. A23.2-14A, A23.1-14/A23.2-14, Potential expansivity of aggregates (procedure for length change due to alkali-aggregate reaction in concrete prisms at 38 oC), 2014.

[49] R.C.D.O. Romano, D. Dos, R. Torres, R.G. Pileggi, Impact of aggregate grading and air-entrainment on the properties of fresh and hardened mortars, Constr. Build. Mater. 82 (2015) 219–226.

Chapter Nine: Summary and Conclusions

9.1 Summary

Concrete, as the most commonly used construction material in the world, has a significant environmental impact that is rapidly increasing. Yet, high amount of cement, which is the main carbon dioxide (CO_2) emitter, is still used to achieve the required concrete performance, such as rheological, mechanical, and long-term behaviour. Based on the global sustainability goals of concrete net zero, distinct approaches, including enhancement of concrete eco-efficiency and optimization of cement and binder, must be implemented to eliminate CO_2 emissions from concrete production by 2050. Before starting to implement these strategies in the concrete industry, it is necessary to have the knowledge of a feasible material that serves as a substitute for cement exceeding its demand. Furthermore, continuing to use recommended mix-design approaches based on experimental, analytical, or semi-experimental approaches, which typically overestimate cement content and designed compressive strength to account for material variability, will invalidate the progress toward a sustainable material. Although literature shows promising studies developing eco-friendly concrete, no clear procedure has been established indicating ranges of water-to-cement (w/c) ratios to achieve the required fresh and compressive strength properties of low cement mixtures. Moreover, conventional approaches to predicting engineering properties are typically inapplicable to eco-efficient mixtures containing low levels of cement content and a high amount of replacement powders, including industry by-products (i.e., supplementary cementing materials - SCMs and inert fillers). Besides the sustainability benefits of reducing cement and using replacement powders, it may also improve concrete durability and long-term performance. However, the durability of eco-efficient concrete has not been thoroughly studied. Alkali-silica

reaction (ASR), one of the main distress mechanisms in Canada, is highly dependent on the system alkali content, and thus decreasing cement (hence alkalis) content can also be beneficial when the concrete contains reactive aggregates. Although CSA A23.2-27A recommends reducing the total alkali content of the concrete to prevent ASR at various deterioration levels (from mild to very strong), very few studies have evaluated low alkali systems without the use of SCMs. Additionally, the current standardized concrete prism test (CPT), which is an accelerated method for inducing ASR-damage, presents one drawback: leaching. Alkalis are added to the concrete mixture to reduce leaching issues; however, their efficacy on low alkali content mixtures remains questionable. As a result, the effect of ASR-damage in low alkali systems remains less understood leading to inconsistencies when predicting its expansion behaviour on the field.

In this context, this study focused on a detailed and comprehensive laboratory investigation to partially address the aforementioned problems and serve as a starting point for the production of eco-efficient concrete mixtures. The main findings of this extensive investigation are presented hereafter:

9.2 Conclusion

9.2.1 Towards the design of eco-efficient concrete mixtures: An overview

- SCMs are excellent replacements for ordinary Portland cement (OPC), but the only widely available material with annual production equal to or greater than cement is limestone filler. They are also available in distinct PSD that can physically and chemically contribute to concrete short- and long-term performance.

- To achieve global sustainability targets over the next 25 years, concrete mix-design must account for four parameters: rheological, mechanical, durability and sustainability performance (Figure 9.1).

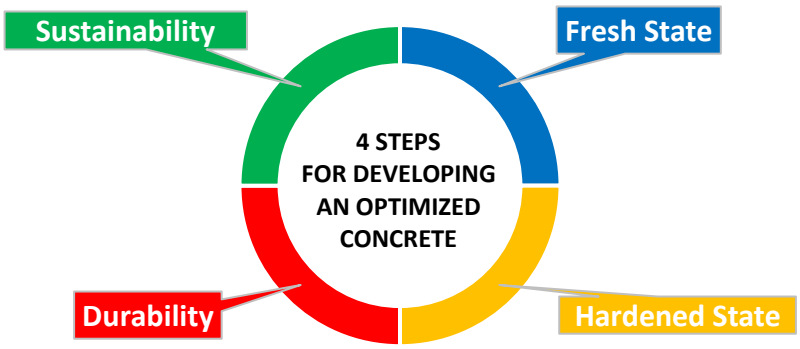

Figure 9.1. Performance parameters for developing optimized concrete mixtures.

- Particle packing models (PPMs), which are advanced mix-design techniques, can be combined with various cement substitute materials to improve the sustainability of concrete and produce concrete with cement content lower than 300 kg/m^3. When the most recent PPMs (i.e., CPM or Alfred model) are used, concrete mixtures achieve better sustainability indicators (i.e., lower global warming potential - GWP and binder intensity index - bi)
- Abrams' law (i.e., w/c) is insufficient for predicting the compressive strength of low cement concrete. Further research is needed to evaluate the effect of water-to-powder (w/p), or even to develop a new method to predict the compressive strength of eco-friendly mixtures designed using PPMs and incorporating considerable levels of powders.

9.2.2 Short-term behaviour of eco-efficient concrete designed through a coupled PPM-MP approach

- The range of slump values (180, 90, and 20 mm) and compressive strength values (18 - 45 MPa) shows the feasibility of producing eco-efficient mixtures for distinct applications and design criteria, which contributes towards Net Zero goals of concrete construction.
- A chart (Figure 9.2) is provided to assist users to develop eco-efficient concrete through PPM-MP design method considering target parameters/performances such as sustainability (cement content), fresh state (slump), and hardened state (compressive strength). It also provides insights into the recommended w/c related to cement content for the pre-selected slump and compressive strength values.

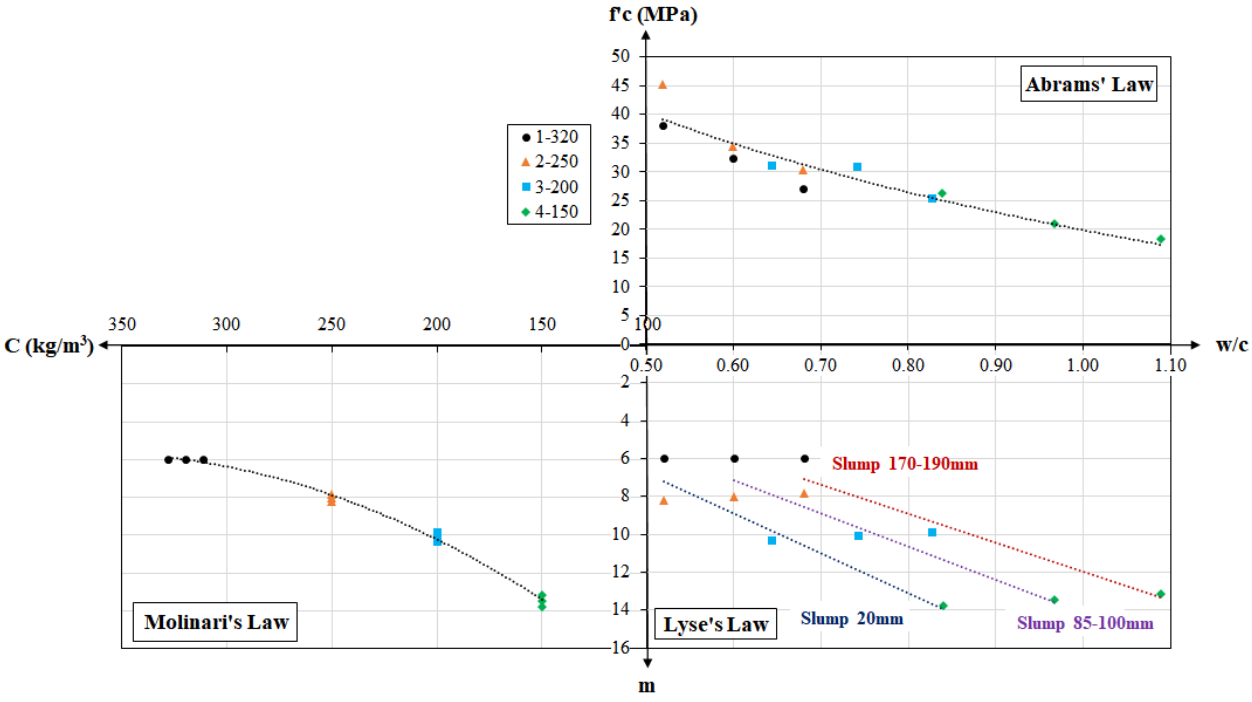

Figure 9.2. Mix-design chart.

- Low cement mixtures developed with LF cannot be fully explained by cement content and w/c, as mixtures with different cement content and w/c, achieved similar compressive strengths, such as 2H-250-0.68 and 3M-200-0.74 (30.7 MPa) or 3H-200-0.83 and 4L-150-0.84 (26 MPa).
- Mobility parameters can be used to aid the development of eco-efficient mixtures to achieve required fresh state properties, yet IPS_{cement} can be applied to predict the compressive strength.

- Four groups of concrete with distinct ranges of cement content (320, 250, 200, 150 kg/m^3) were developed with PPM-MP approach, based on their GWP, they can be classified into distinct Low Carbon Concrete Classes (i.e., Semi-LCC, LCC_{250}, LCC_{200}, and LCC_{150}, respectively). When limestone fillers are applied to the system, GWP can decrease up to 152.85 kg CO_{2eq}, which is around 50% lower than control mixtures developed without limestone fillers.
- The concrete mixtures developed in this study can be considered eco-efficient with ci_{cs} ranging from 10.7 to 5.3 kg/m^{-3}. MPa^{-1}, which are lower than ci_{cs} values of conventional concrete produced worldwide.

9.2.3 Understanding and predicting the hardened state performance of eco-efficient concrete mixtures

- The mixtures 2H-250-0.68 and 3M-200-0.74 had similar apparent porosity, compressive strength, and modulus of elasticity, regardless of cement content or w/c, indicating that up to 36% of limestone filler can be added when a PPM is used to proportion eco-efficient concrete without degrading short-term performance.

- Mixtures developed with similar w/c resulted in higher compressive strength when limestone filler is added. Concrete mixtures incorporating 250 kg/m^3 achieved on average a compressive strength 12% higher than G1; the greatest difference (around 7 MPa) was found on mixtures with low w/c (2L-250-0.52 and 1L-328-0.52).
- The apparent porosity of the mixtures developed without limestone filler is more affected by the w/c than for mixtures containing limestone fillers, illustrating another advantage of using limestone fillers.
- Regarding conventional methods to predict concrete compressive strength, when parameters were adjusted, EN1992-1 was able to better estimate the compressive strength of the eco-friendly mixtures investigated than Abrams law.
- A new method to predict compressive strength of eco-efficient mixtures is proposed, which includes k-factor which is directly proportional to w/p and the α-parameter that assists in the prediction of the compressive strength at different hydration levels (Figure 9.3).

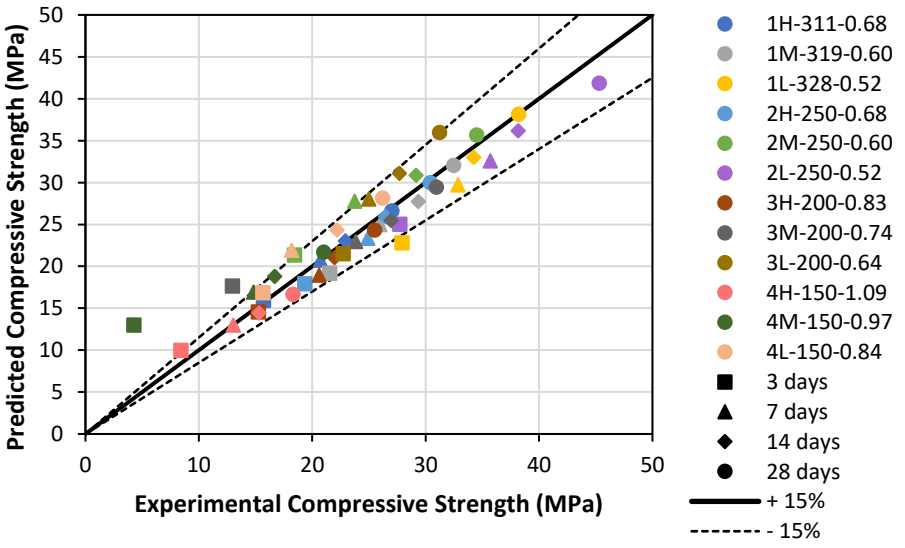

Figure 9.3. Summary compressive strength prediction based on the proposed method.

- All mixtures were classified as eco-efficient based on the bi-index, regardless of cement content, mixtures developed with limestone filler and with high, medium, and low w/c achieved bi-indices of around 8.1, 7.0, and 5.9 kg/m^3. MPa^{-1}, respectively.

9.2.4 Performance appraisal of eco-efficient low-alkali concrete to develop alkali-aggregate reaction (AAR) in the laboratory

- Mixtures incorporating Springhill reactive aggregate show the potential to reduce ASR expansion levels with the sole use of PPM and cement/alkali reduction (Figure 9.4), further improvement can be made using additional measures or materials such as SCMs.

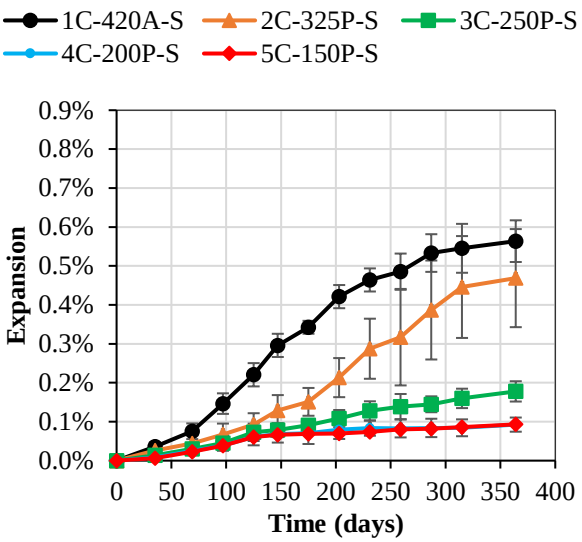

Figure 9.4. Expansion as a function of time for Springhill mixtures.

- The influence of the cement content changes significantly based on the reactive aggregate type. Mixtures developed with limestone filler and lower cement content (≤ 250 kg/m^3) resulted in considerably lower expansion levels, distress features, and DRI number when the highly reactive coarse aggregate (i.e., Springhill – S) is selected, whereas the influence of

cement content is not as significant for the ultra-high reactive fine aggregate (Texas -T) mixtures.

- The DRI numbers obtained can usually be directly correlated with an expansion level, yet a difference is observed between the DRI numbers achieved for sustainable mixtures. Images captured through the stereomicroscope for mixtures incorporating Texas (8 months test) and Springhill (12 months test) show that even though similar DRI number is achieved, the expansion level and crack pattern are considerably different.

9.2.5 Assessment of laboratory test procedures to evaluate ASR-induced expansion and deterioration of eco-efficient concrete

- Comparing different test methods on mixtures developed with higher cement content (420 kg/m^3), boosted mixture yielded higher than non-boosted mixtures at 4 and 8 months, but they achieved roughly the same final expansion at 12 months. Nonetheless, their final DRI number and distress features differ significantly, highlighting the effect of the additional alkalis added in the concrete on the ASR-development and damage.
- Regardless of the testing protocol selected, mixtures achieved similar final expansions when the total system contains similar alkali content and it is over 3.01 kg/m^3; below this threshold, the alkali from the cement governs the distress features regardless of total system alkalis.
- In terms of crack width, the lower the cement content the smaller the crack width. Boosted mixtures had larger cracks than non-boosted mixtures with the same cement content due to the higher alkali content of the system (Figure 9.5).
- Mixtures developed with 1.8 kg/m^3 or lower alkali content (containing cement content lower than 200 kg/m^3) reached similar final expansion (on average 0.08%) regardless of testing

setup (boosted vs non-boosted), being classified as prevention level Y (Strong) against ASR-development as per CSA A23.2-27A without any addition of SCMs.

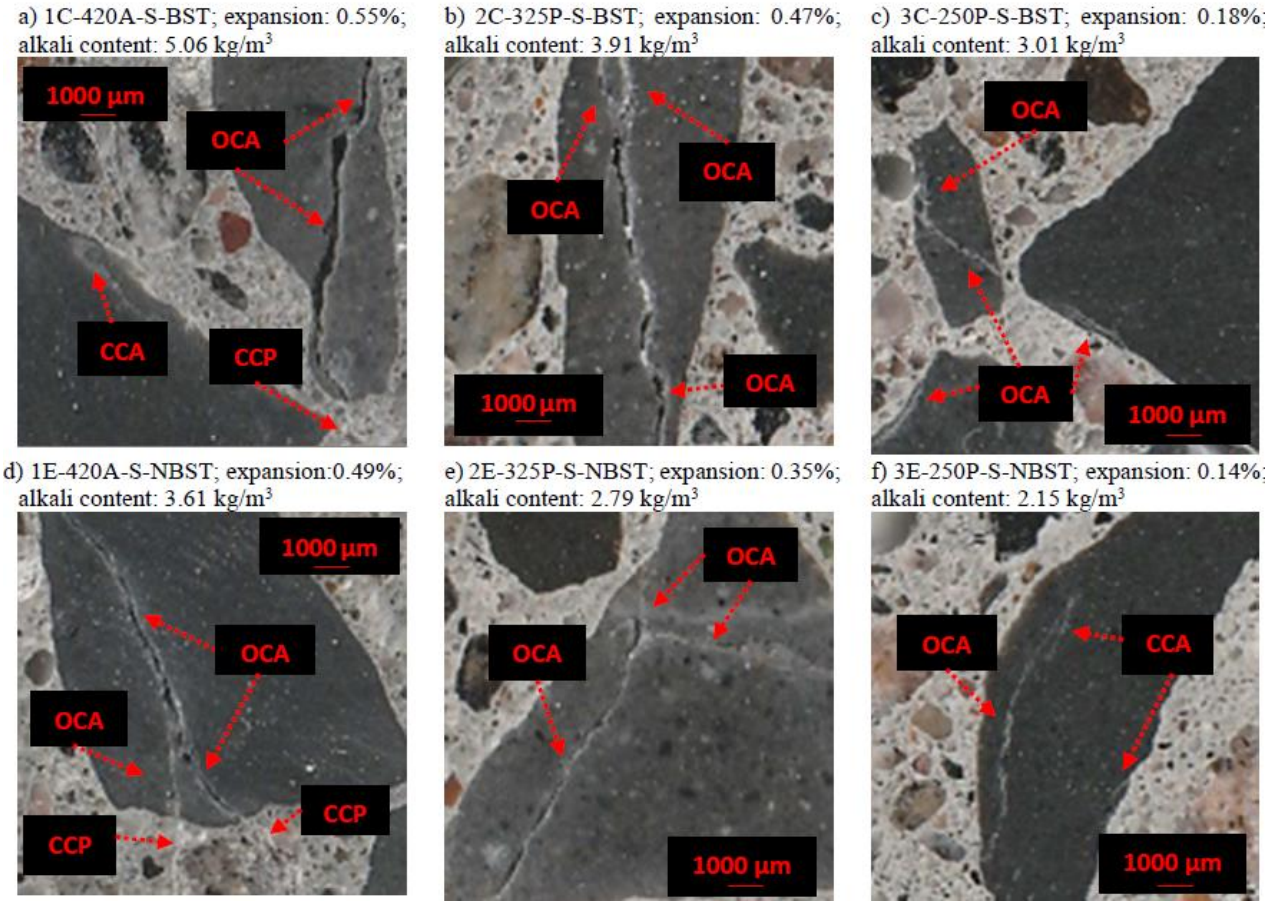

Figure 9.5. Distress features of mixtures evaluated at 12 months: CPT (a-c), Encapsulated (d-f) in order of decreasing cement content.

Chapter Ten: Recommendations for Future Research

After conducting this comprehensive experimental research, further investigations are suggested:

- Assessment of the effect of aggregate and/or inert filler characteristics (such as shape, texture, and hardness) on the short-term performance of concrete.
- Microscopic analysis combined with a further investigation of the stress-strain behaviour of highly packed sustainable mixtures to understand the mechanism of failure of low cement mixtures as it is an integral part towards its use in the industry.
- Microscopic analysis correlated with mechanical properties to determine how mobility parameters, particularly maximum paste thickness (MPT), affect the mechanical properties of concrete.
- Assessing the impact of densely packed systems on aggregate interlock behaviour by evaluating the structural behaviour of eco-efficient concrete, particularly under shear loads.
- Although a low alkali system could reduce ASR expansion for aggregates that were deemed unusable in concrete, further investigations on the losses of mechanical properties of such concrete mixtures correlated to the damage captured through the damage rating index (DRI) are necessary.
- Multi-level assessment of ASR-induced damage development of low cement/alkali mixtures, including the understanding of the mechanical properties' losses (i.e., compressive strength, SDI, modulus of elasticity) and modelling the crack propagation of ASR-development under distinct levels of damage. Compare these results for boosted and non-boosted mixtures to better understand the effect of the alkali boost on the ASR-crack development.

- In terms of damage (i.e., crack propagation vs mechanical property losses), determine which test protocol better represents the damage observed in real structures affected by ASR-damage in terms of damage.
- Conduct a leaching test on the pore solution of concrete mixtures affected by induced ASR-expansion exposed under distinct test conditions (i.e., CPT, wrapped, encapsulated, and soaked).
- Although limestone fillers can be used to produce eco-efficient concrete, one of the main concerns with high amounts of limestone filler in concrete structures is their durability due to sulphate attack, especially thaumasite form of sulphate attack (TSA), thus, future studies on other distress mechanisms are crucial to fully investigate the durability aspects of the eco-efficient mixtures developed in this study.
- Eco-friendly mixtures developed via PPM-MP presented promising results against ASR due to the reduction of alkali content, yet it can decrease decreases the system's pH, which may lessen its ability to control corrosion of steel reinforcement with the passive oxide layer formed at high pH levels. Since the system presents a lower porosity, can they still improve concrete performance against different durability mechanisms (e.g., corrosion, carbonation, freezing and thawing)?
- Suggest durability parameters for inclusion in the PPM-MP model to select the best durability performance-based design.